2001-06

Computational mechanics of the full-scale and model-scale roll-on, roll-off (RORO) stern ramp and experimental modal analysis of the model-scale ramp and support

Buckley, James E.

NAVAL POSTGRADUATE SCHOOL
Monterey, California

THESIS

COMPUTATIONAL MECHANICS OF THE FULL-SCALE AND MODEL-SCALE ROLL-ON, ROLL-OFF (RORO) STERN RAMP AND EXPERIMENTAL MODAL ANALYSIS OF THE MODEL-SCALE RAMP AND SUPPORT

by

James E. Buckley

June 2001

Thesis Advisor: Joshua H. Gordis

REPORT DOCUMENTATION PAGE

Form Approved
OMB No. 0704-0188

1. AGENCY USE ONLY *(Leave blank)*	2. REPORT DATE	3. REPORT TYPE AND DATES COVERED
	June 2001	Master's Thesis

4. TITLE AND SUBTITLE: Computational Mechanics of the Full-Scale and Model-Scale Roll-on, Roll-off (RORO) Stern Ramp and Experimental Modal Analysis of the Model-Scale Ramp and Support

5. FUNDING NUMBERS N0016700WR00366

6. AUTHOR(S)
Buckley, James E.

7. PERFORMING ORGANIZATION NAME(S) AND ADDRESS(ES)
Naval Postgraduate School
Monterey, CA 93943-5000

8. PERFORMING ORGANIZATION REPORT NUMBER

9. SPONSORING / MONITORING AGENCY NAME(S) AND ADDRESS(ES)
N/A

10. SPONSORING / MONITORING AGENCY REPORT NUMBER

11. SUPPLEMENTARY NOTES
The views expressed in this thesis are those of the author and do not reflect the official policy or position of the Department of Defense or the U.S. Government.

12a. DISTRIBUTION / AVAILABILITY STATEMENT	12b. DISTRIBUTION CODE
Approved for public release; distribution is unlimited.	A

13. ABSTRACT *(maximum 200 words)*

It has been determined that current stern ramp designs lack adequate structural integrity during Sea State Three roll-on, roll-off (RORO) operations. Therefore, passive isolation between the stern ramp and the roll-on, roll-off discharge facility (RRDF) is being investigated as a means of reducing ramp stress levels. A coupled hydro-structural simulation model of the combined ship-ramp-RRDF is under development in order to evaluate candidate isolator technologies. This thesis documents a thorough study of several stern ramp finite element models in order to ascertain the suitability of these models for use in the simulation model. Additionally, an experimental facility is being developed to simulate, at model scale, RORO operations. This thesis also documents the finite element analysis and experimental modal analysis of the primary structural components of the facility, specifically the scale model stern ramp and its support.

14. SUBJECT TERMS
Roll-On, Roll-Off, RORO, Stern Ramp, Isolation.

15. NUMBER OF PAGES 176

16. PRICE CODE

17. SECURITY CLASSIFICATION OF REPORT	18. SECURITY CLASSIFICATION OF THIS PAGE	19. SECURITY CLASSIFICATION OF ABSTRACT	20. LIMITATION OF ABSTRACT
Unclassified	Unclassified	Unclassified	UL

NSN 7540-01-280-5500

Standard Form 298 (Rev. 2-89)
Prescribed by ANSI Std. 239-18

THIS PAGE INTENTIONALLY LEFT BLANK

Approved for public release; Distribution is unlimited

COMPUTATIONAL MECHANICS OF THE FULL-SCALE AND MODEL-SCALE ROLL-ON, ROLL-OFF (RORO) STERN RAMP AND EXPERIMENTAL MODAL ANALYSIS OF THE MODEL-SCALE RAMP AND SUPPORT

James E. Buckley
Lieutenant, United States Navy
B.S. Nuclear Engineering, Oregon State University, 1994

Submitted in partial fulfillment of the
requirements for the degree of

MASTER OF SCIENCE IN MECHANICAL ENGINEERING

from the

NAVAL POSTGRADUATE SCHOOL
June 2001

Author: James E. Buckley

Approved by: Joshua H. Gordis, Thesis Advisor

Terry R. McNelley, Chairman
Department of Mechanical Engineering

THIS PAGE INTENTIONALLY LEFT BLANK

ABSTRACT

It has been determined that current stern ramp designs lack adequate structural integrity during Sea State Three roll-on, roll-off (RORO) operations. Therefore, passive isolation between the stern ramp and the RORO discharge facility (RRDF) is being investigated as a means of reducing ramp stress levels. A coupled hydro-structural simulation model of the combined ship-ramp-RRDF is under development in order to evaluate candidate isolator technologies. This thesis documents a thorough study of several stern ramp finite element models in order to ascertain the suitability of these models for use in the simulation model. Additionally, an experimental facility is being developed to simulate, at model scale, RORO operations. This thesis also documents the finite element analysis and experimental modal analysis of the primary structural components of the facility, specifically the scale model stern ramp and its support.

THIS PAGE INTENTIONALLY LEFT BLANK

TABLE OF CONTENTS

THIS PAGE INTENTIONALLY LEFT BLANK

LIST OF FIGURES

LIST OF TABLES

THIS PAGE INTENTIONALLY LEFT BLANK

ACKNOWLEDGMENTS

I would like to thank my family, Melanie, Madeline and Isabel for their understanding and support throughout my time here at the Naval Postgraduate School. I would like to extend my appreciation to Professor Joshua H. Gordis for his assistance and support throughout this project.

THIS PAGE INTENTIONALLY LEFT BLANK

I. INTRODUCTION

The United States Military Sealift Command desires the capability to conduct roll-on, roll-off (RORO) operations in the open ocean. In order to achieve this goal, RORO operations must be able to be performed during Sea State Three. During RORO operations, the offloading vessel is connected to a roll-on, roll-off discharge facility (RRDF) by the vessel's stern ramp. The latest version of such vessels is termed "large, medium speed, roll-on, roll-off" (LMSR), whereas older versions are termed by their particular class, such as "Cape H" or "Cape T". Each of these vessels has a uniquely designed stern ramp.

The limiting condition when conducting RORO operations is the stress induced in the stern ramp due to loading and twist. The stern ramp must have the capability to support two tanks located near its middle while undergoing the twist due to relative motion between the RORO vessel and the RRDF. Because existing stern ramp designs lack adequate structural integrity during Sea State Three RORO operations, modifications must be made to existing RORO equipment to reduce the stress levels in the ramps. One possible method is to employ passive isolation between the stern ramp and the RRDF as a means of reducing ramp stress levels.

A coupled hydro-structural simulation model of the combined ship-ramp-RRDF is under development in order to evaluate candidate isolator technologies. A thorough study of the LMSR, Cape H, and Cape T stern ramp finite element models is necessary in order to ascertain the suitability of these models for use in the simulation model. Additionally, an experimental facility is being developed to simulate, at model scale, wave-induced static and dynamic response of the ramp. Finite element models of the

major components of the experimental facility, specifically the model-scale ramp and its support, have been developed. Correlation of these finite element models with the physical structures must be accomplished for model validation. Experimental modal testing of the model-scale ramp and its support is necessary to update the finite element models.

II. FULL-SCALE RAMP FINITE ELEMENT MODELS

Three finite element models were provided to the Naval Postgraduate School for analysis. Two of the models, the LMSR and Cape H stern ramps, were translated from ANSYS format for use with MSC/NASTRAN. The Cape T stern ramp model was delivered in MSC/NASTRAN format. The Cape H and Cape T models were constructed using metric units whereas the LMSR model was constructed in English units. All results are provided in English units.

Each stern ramp design consists of two sections. Section-One connects to the stern of the RORO vessel for deployment onto the RRDF for RORO operations. Section-Two is connected to Section-One by two, five or eight hinge joints depending on the design, and rests on the RRDF when deployed for RORO operations. Section-Two is designed to be the more flexible portion of the ramp to minimize torsional stresses in the ramp created by the relative motions between the RORO vessel and the RRDF.

A. LARGE, MEDIUM SPEED, ROLL-ON, ROLL-OFF STERN RAMP

Table 1 lists the physical dimensions and material properties of the LMSR ramp.

Length	113.9 ft
Width	24 ft
Weight	105.5 tons
Elastic Modulus	30,000 ksi
Material	Mild steel

Table 1. LMSR Stern Ramp Characteristics

Figure 1 displays the LMSR stern ramp finite element model. Two hinges connect Sections-One and Two allowing for a more flexible coupling than exists in the Cape H or Cape T stern ramp designs.

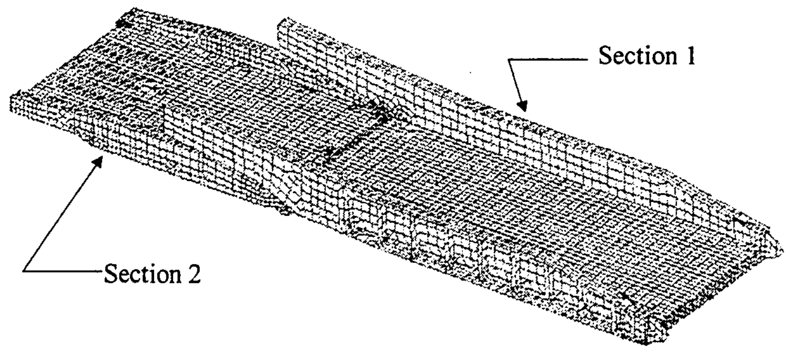

Figure 1. LMSR Stern Ramp Finite Element Model

Five separate boundary condition cases were used for computational modal analysis of the LMSR stern ramp and comparison with results obtained previously from the Cape T stern ramp. Figure 2 displays the grid point locations restrained for each boundary condition case, two each for the ship and RRDF ends and Figures 3 through 7 show the restrained degrees of freedom (DOF) for boundary condition cases one through five.

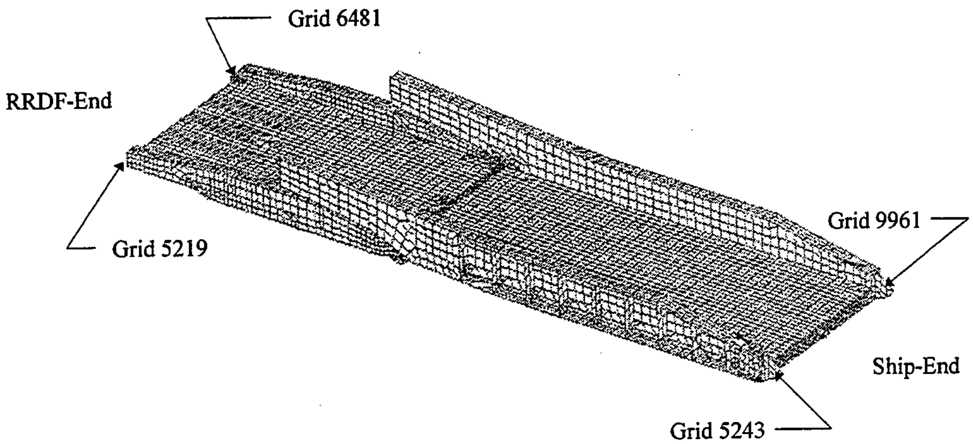

Figure 2. LMSR Boundary Condition Grid Locations

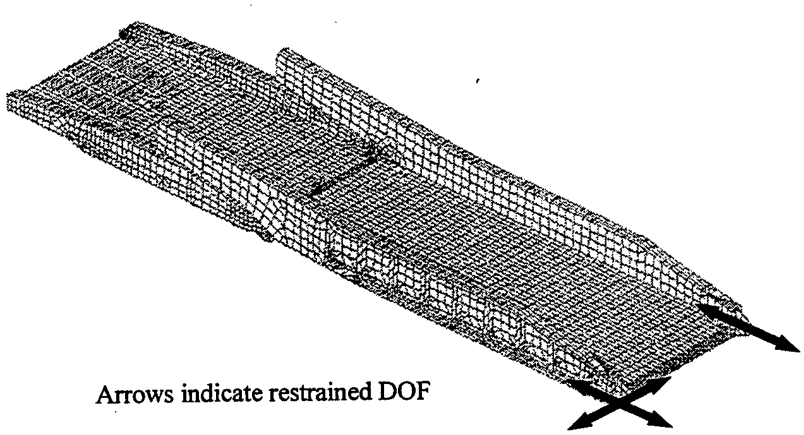

Figure 3. LMSR Boundary Condition Case 1

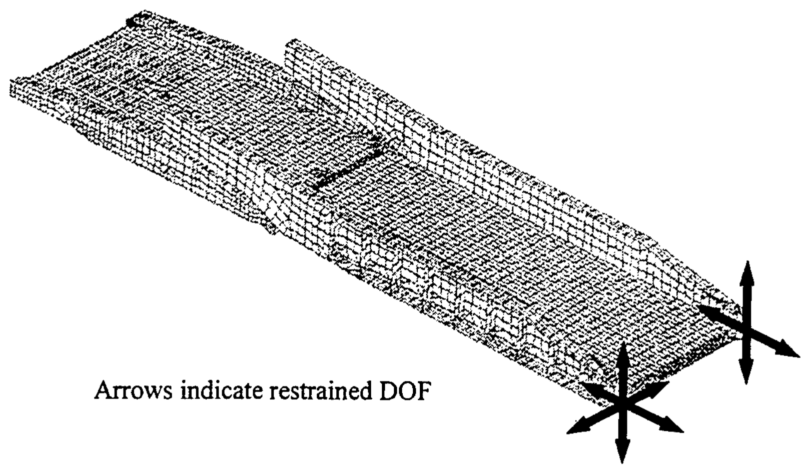

Figure 4. LMSR Boundary Condition Case 2

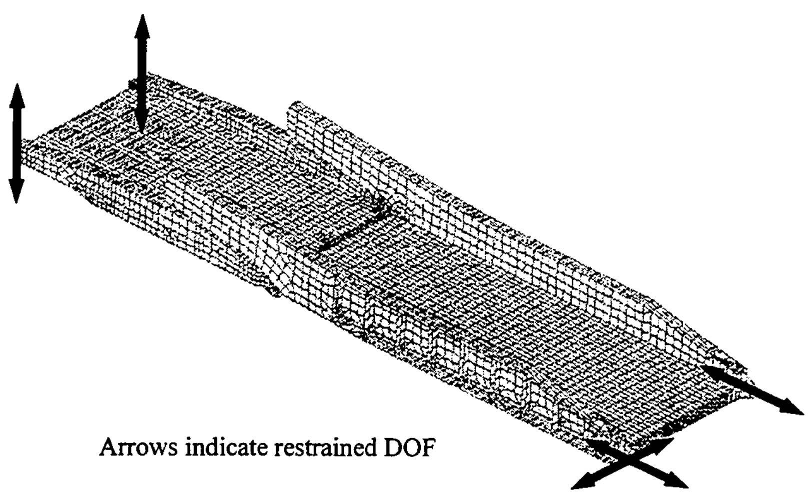

Figure 5. LMSR Boundary Condition Case 3

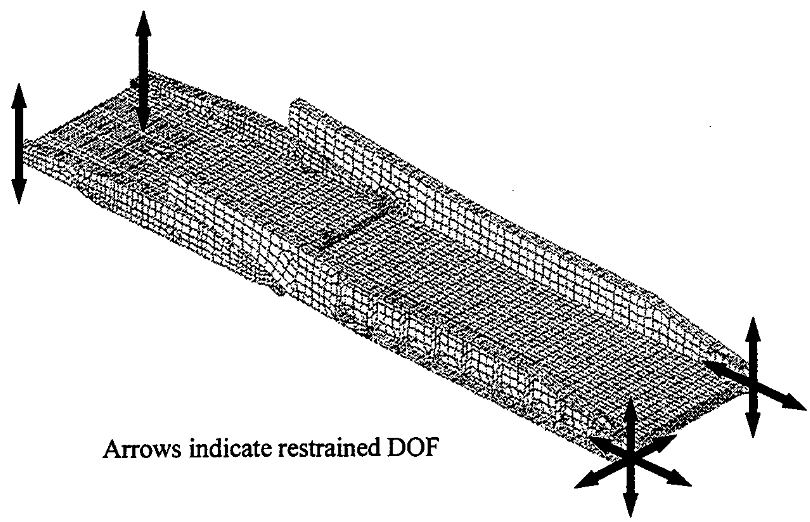

Figure 6. LMSR Boundary Condition Case 4

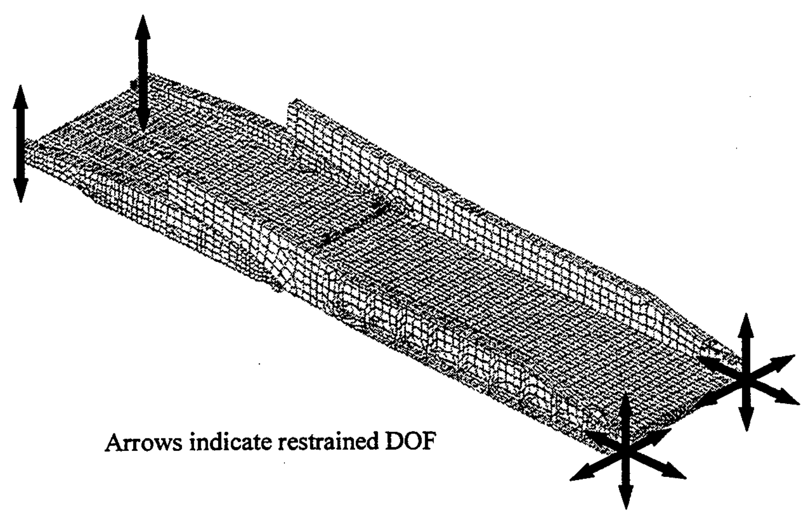

Figure 7. LMSR Boundary Condition Case 5

Case five boundary conditions, shown in Figure 7, were used for all linear static computational analyses of the LMSR stern ramp.

Some modifications were required to be made to the "as delivered" LMSR stern ramp finite element model. The model was originally constructed for the ANSYS finite element software and was translated to MSC/NASTRAN for use at the Naval Postgraduate School. The translation processor was unable to translate an ANSYS element type, MATRIX 27. There were 16 such elements used in the ANSYS version of the LMSR model. These elements modeled a buttressing device used to lock the ramp in the deployed position for RORO operations. The MSC/NASTRAN element type CELAS1 was used to replace the ANSYS MATRIX 27 element and were added to the model. Table 2 contains the grid connection points for the new MSC/NASTRAN elements.

Element Type	Upper Grid	Lower Grid
CELAS1	9101	6786
CELAS1	9106	6787
CELAS1	9107	6788
CELAS1	9105	6782
CELAS1	9126	6799
CELAS1	9131	6800
CELAS1	9129	6801
CELAS1	9127	6798
CELAS1	5336	2320
CELAS1	5338	2325
CELAS1	5337	2324
CELAS1	5332	1809
CELAS1	5358	2332
CELAS1	5360	2334
CELAS1	5362	2333
CELAS1	5357	1852

Table 2. LMSR Stern Ramp Buttressing Device Grid Connection Points

Each CELAS1 element acts in the vertical direction with a stiffness of 24,000,000 lbf/in. Another modification was the construction of lumped mass and rigid element tank models to predict the natural frequencies of a fully loaded (two tanks) LMSR stern ramp. These tank representations were constructed similarly to those that were delivered with the Cape T stern ramp finite element model. Each tank model represented 80.6 tons added mass for a two-tank total of 161.2 tons. The lumped mass and rigid element tank representations were only used with the normal modes analysis of the LMSR stern ramp.

B. CAPE T STERN RAMP

Table 3 lists the physical dimensions and material properties of the Cape T stern ramp.

Length	101.6 ft
Width	25.4 ft
Weight	116.5 tons
Elastic Modulus	30,400 ksi
Material	Mild steel

Table 3. Cape T Stern Ramp Characteristics

Figure 8 displays the Cape T stern ramp finite element model. The Cape T stern ramp differs from the LMSR and Cape H stern ramps in that the buttressing device is modeled engaged in the deployed position. Five hinges are used to connect Sections-One and Two. This results in a somewhat stiffer connection and greater potential to induce torsion stresses in section one due to relative motion between the RRDF and RORO vessel.

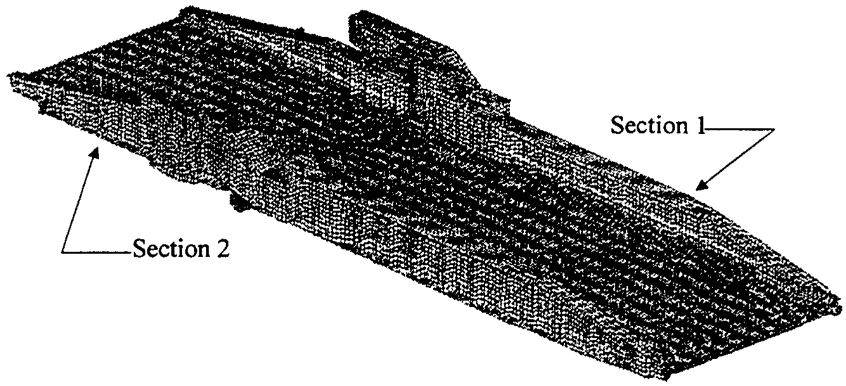

Figure 8. Cape T Stern Ramp Finite Element Model

Figure 9 indicates boundary condition grid locations and Figure 10 displays the restrained DOF used for linear static computational analyses of the Cape T stern ramp model.

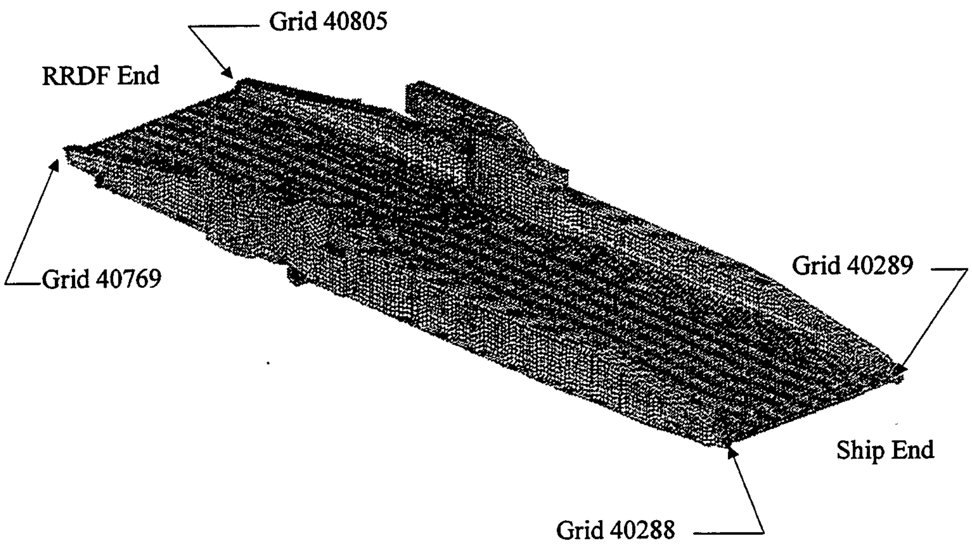

Figure 9. Cape T Boundary Condition Grid Locations

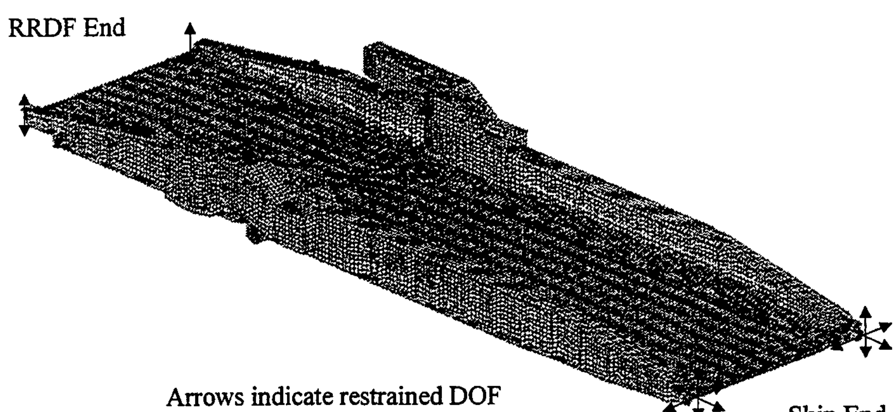

Figure 10. Cape T Boundary Conditions

C. CAPE H STERN RAMP

Table 4 lists the physical dimensions and material properties of the Cape H stern ramp.

Length	143.8 ft
Width RRDF End	44.5 ft
Width Ship End	76.9 ft
Weight	272.9 tons
Elastic Modulus	30,000 ksi
Material	Mild steel

Table 4. Cape H Stern Ramp Characteristics

Figure 11 displays the Cape H stern ramp finite element model. Eight hinges connect

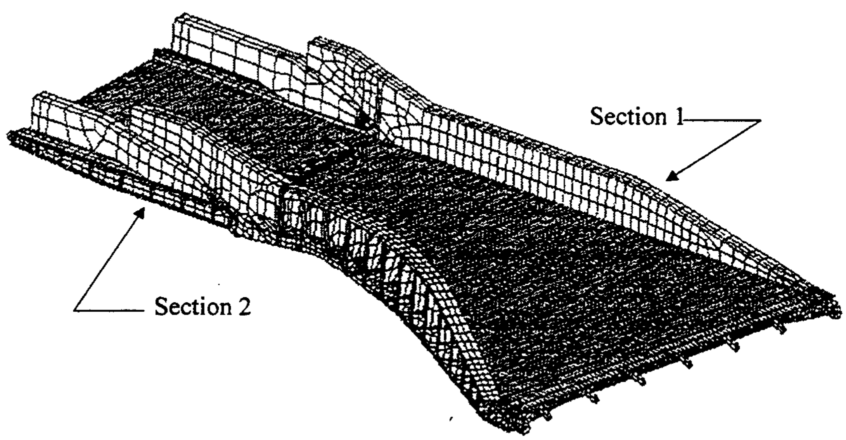

Figure 11. Cape H Stern Ramp Finite Element Model

Sections-One and Two, again this should result in a stiffer coupling than the two-hinge LMSR stern ramp design. The Cape H stern ramp is an asymmetric design unlike both the Cape T and LMSR designs. Also of note are the "split" arms that control the position of Section-Two during operation of the ramp. The split design was necessary

to lower the stowed height of the ramp to allow the Cape H vessel more overhead clearance. The Cape H ramp design has over twice the mass of the other stern ramp designs examined.

The Cape H finite element model provided to the Naval Postgraduate School was an MSC/NASTRAN translation of an ANSYS model. As was the case with the LMSR stern ramp, the MATRIX 27 elements were not converted to MSC/NASTRAN format. CELAS 1 elements were used to replace the MATRIX 27 elements in the MSC/NASTRAN version of the Cape H stern ramp model. Each element acts in the vertical direction only with a stiffness of 97,000,000 lbf/in

Element Type	Upper Grid	Lower Grid
CELAS1	15487	15693
CELAS1	15488	15692
CELAS1	19552	15694
CELAS1	14619	14695
CELAS1	14623	14700
CELAS1	14622	14699
CELAS1	14621	14698
CELAS1	15631	204
CELAS1	14657	16982
CELAS1	20215	20144
CELAS1	20218	20147
CELAS1	20263	20357
CELAS1	20286	20328

Table 5. Cape H Stern Ramp Buttressing Device Grid Connection Points

Figure 12 indicates the boundary condition grid locations and Figure 13 shows the restrained degrees of freedom (DOF) used during the linear static computational analyses of the Cape H stern ramp model.

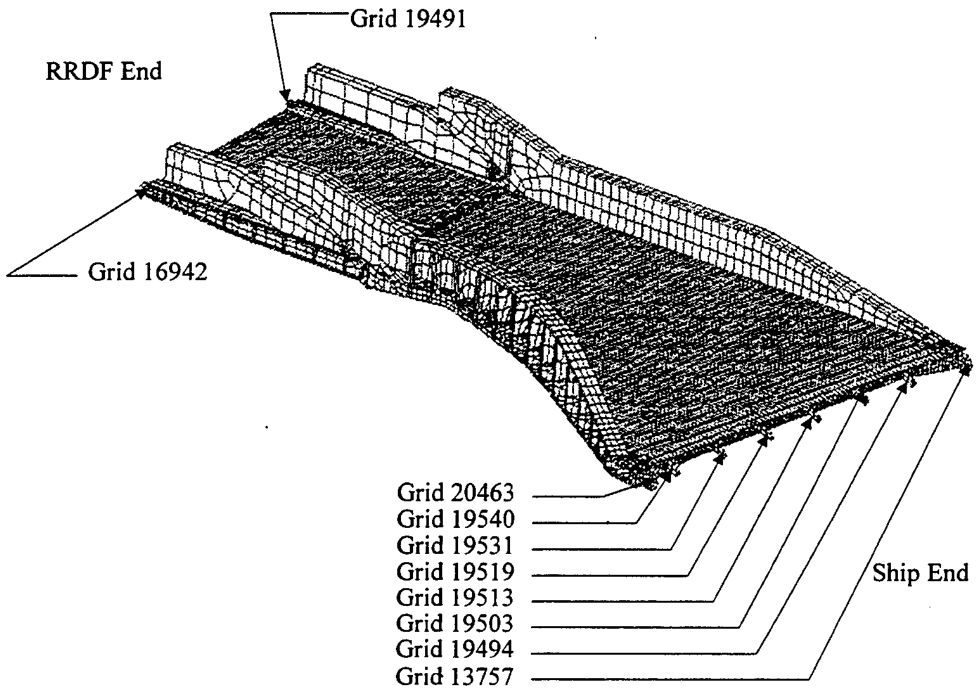

Figure 12. Cape H Boundary Conditions

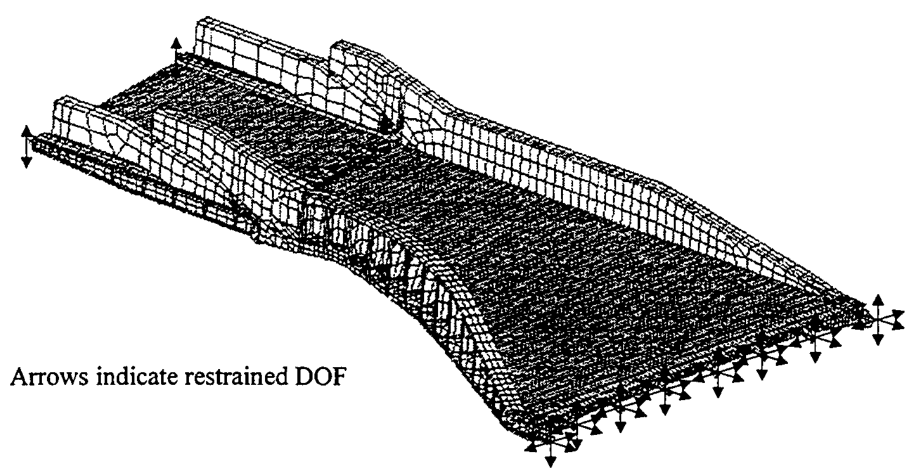

Figure 13. Cape H Boundary Condition Grid Locations

III. MODEL–SCALE RAMP AND SUPPORT FINITE ELEMENT MODELS

The ability to experimentally measure the response characteristics of a ramp with an installed isolator is necessary to ensure the validity of computer models used to predict such responses. Ideally, this would be accomplished on a full-scale ramp. However, a model-scale test facility that exhibits the same response characteristics as a full-scale ramp is better due to ease and reduced cost of experimentation. Through the use of a model-scale facility, many variations of isolator types may be rapidly evaluated and used to update computer simulation models. A computer simulation model that accurately predicts measured behavior at model-scale can easily be adapted to predict response of full-scale ramps with confidence. Figures 14 and 15 show the model-scale ramp and support.

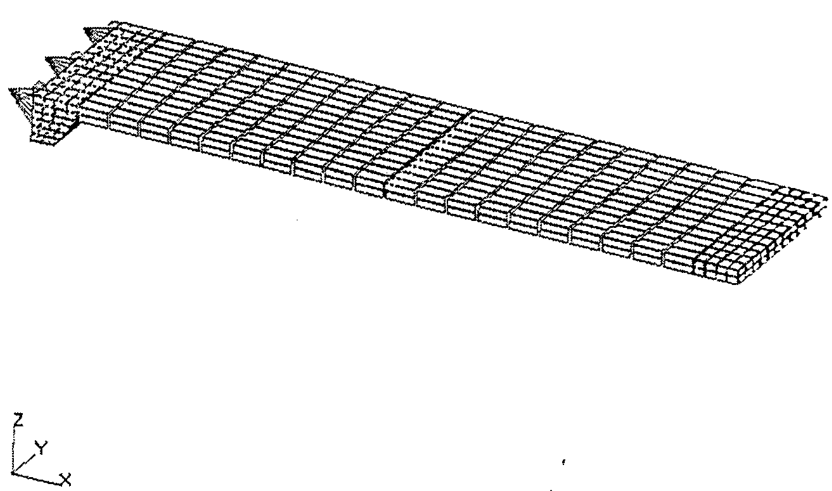

Figure 14. Model-Scale Ramp

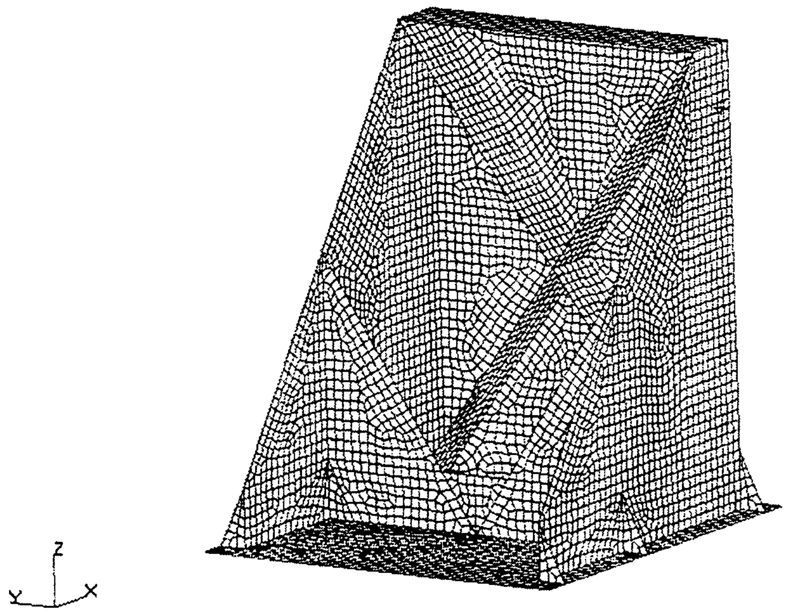

Figure 15. Model-Scale Ramp Support

A. MODEL-SCALE RAMP

MSC/NASTRAN was used to construct a finite element model of the model-scale ramp. The scale-ramp model was designed to have the same aspect ratio and RORO response characteristics as the full-scale Cape T stern ramp. This model was used as a basis for construction of the model-scale ramp to be used with the experimental test facility. Due to requirements for construction and assembly of the model-scale ramp, some minor deviations from the finite element model design were necessary. The model-scale ramp finite element model was updated to reflect these design deviations.

B. MODEL-SCALE RAMP SUPPORT

MSC/NASTRAN was used to construct a finite element model of the model-scale ramp support. This support was designed to minimize excitation of the

experimental test ramp during simulation of RORO operation. Following construction and testing of the scale-ramp support, the model was updated. Specifically, the support was raised above the deck by quarter inch steel shims under the mounting bolts to ease the determination and modeling of boundary conditions. Furthermore, due to inconsistencies in the welded joints of the support, including gaps in welds, the model was updated to reflect these weld gaps.

THIS PAGE INTENTIONALLY LEFT BLANK

IV. RESULTS

A. COMPUTATIONAL MODAL ANALYSIS

1. Large, Medium Speed, Roll-On, Roll-Off, Vessel Stern Ramp

The natural frequencies and mode shapes for all modes below ten hertz were determined using MSC/NASTRAN solution 103. Several boundary condition cases were examined to determine the boundary condition effect on the LMSR stern ramp finite element model's (FEM) natural frequency and mode shape response and to compare with results previously obtained from the Cape T stern ramp. Table 6 contains a natural frequency summary of the five boundary condition cases analyzed.

Mode	Case 1	Case 2	Case 3	Case 4	Case 5
1	0.00	0.00	0.00	1.82	1.82
2	0.00	1.35	1.37	2.53	2.60
3	0.00	2.99	3.04	3.15	3.38
4	2.99	4.13	3.40	6.84	6.85
5	4.25	6.85	5.63	9.32	
6	6.21	8.53	8.80		
7	7.89	9.88	9.36		
8	9.66				
9	9.94				

Table 6. LMSR Boundary Condition Natural Frequency Summary (Hz)

A mode where the natural frequency listed is zero indicates a rigid body mode. Rigid body motion will occur if the structure has fewer that six restraints. Rigid body motion of the LMSR stern ramp will not occur during RORO operation because case 4 and case 5 boundary conditions are used to restrain the stern ramp. PATRAN was used to create Figures 16 through 30 displaying the first three elastic modes.

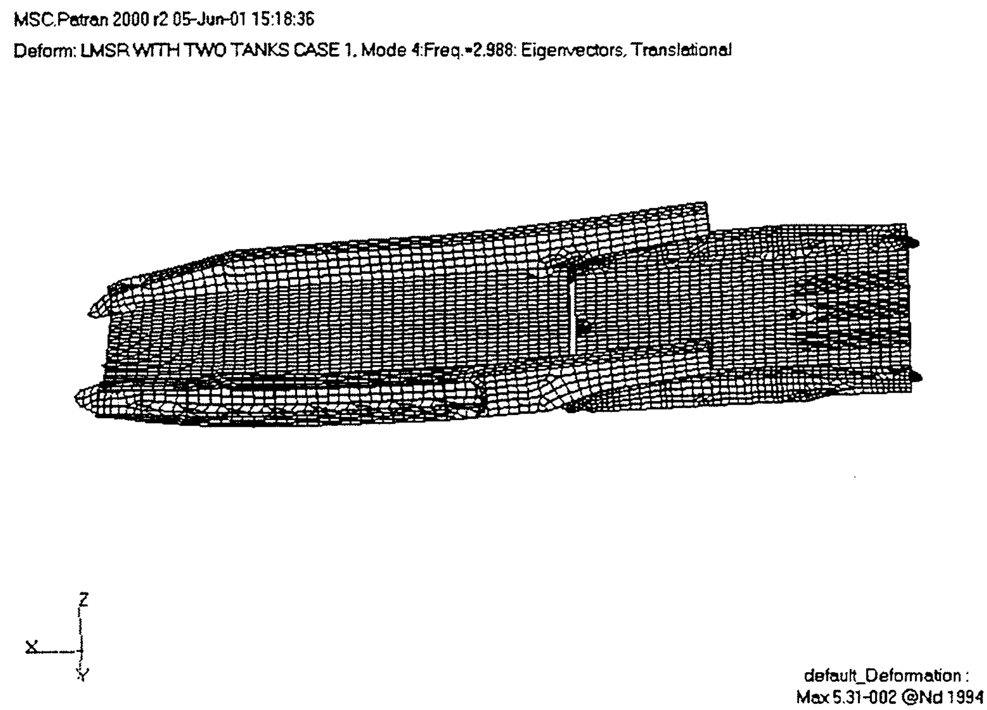

Figure 16. LMSR, Boundary Condition Case 1, Mode 1, Yaw-Torsion

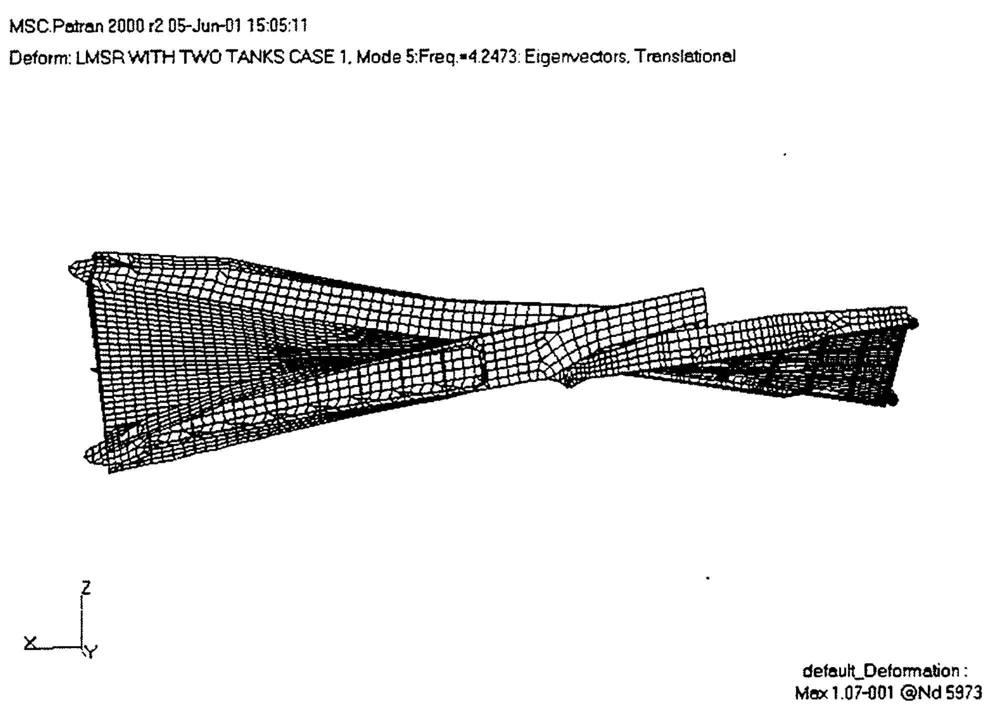

Figure 17. LMSR, Boundary Condition Case 1, Mode 2, Torsion

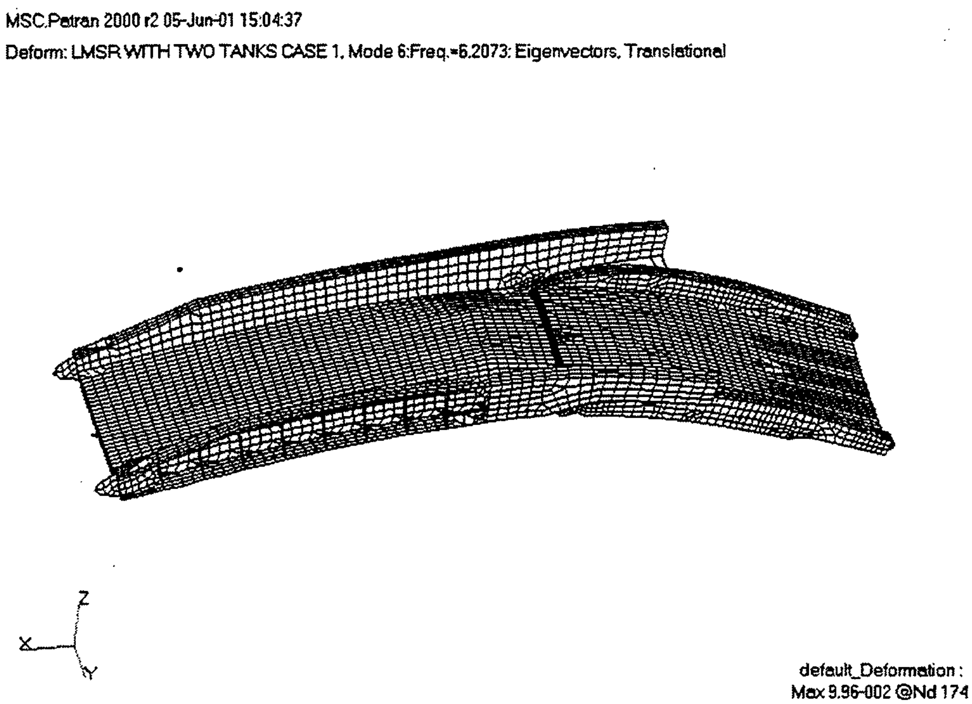

Figure 18. LMSR, Boundary Condition Case 1, Mode 3, Bending

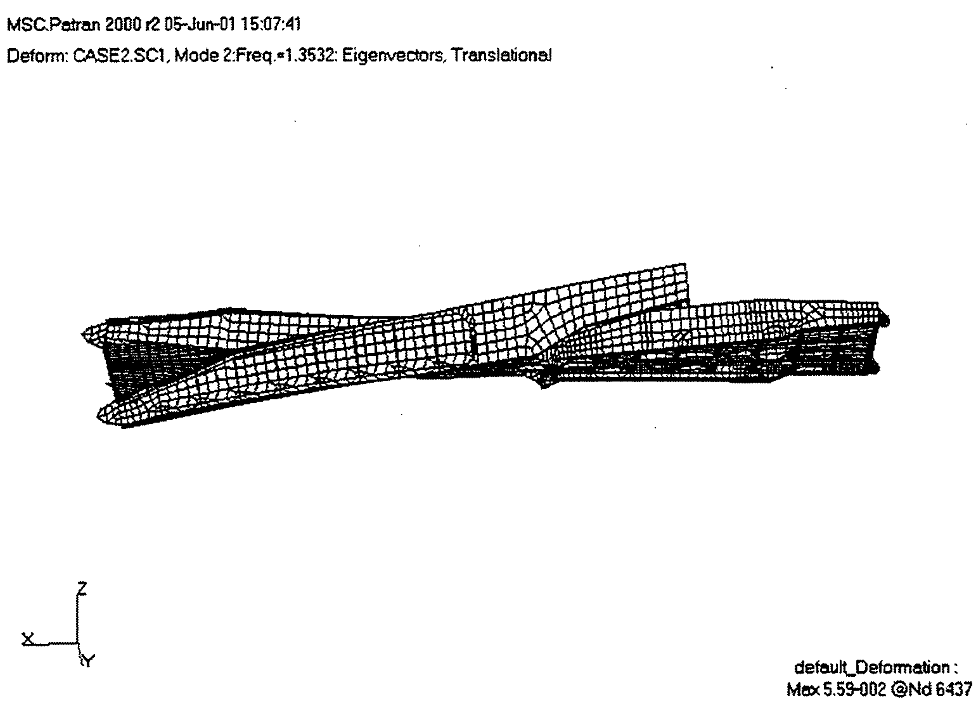

Figure 19. LMSR, Boundary Condition Case 2, Mode 1, Torsion

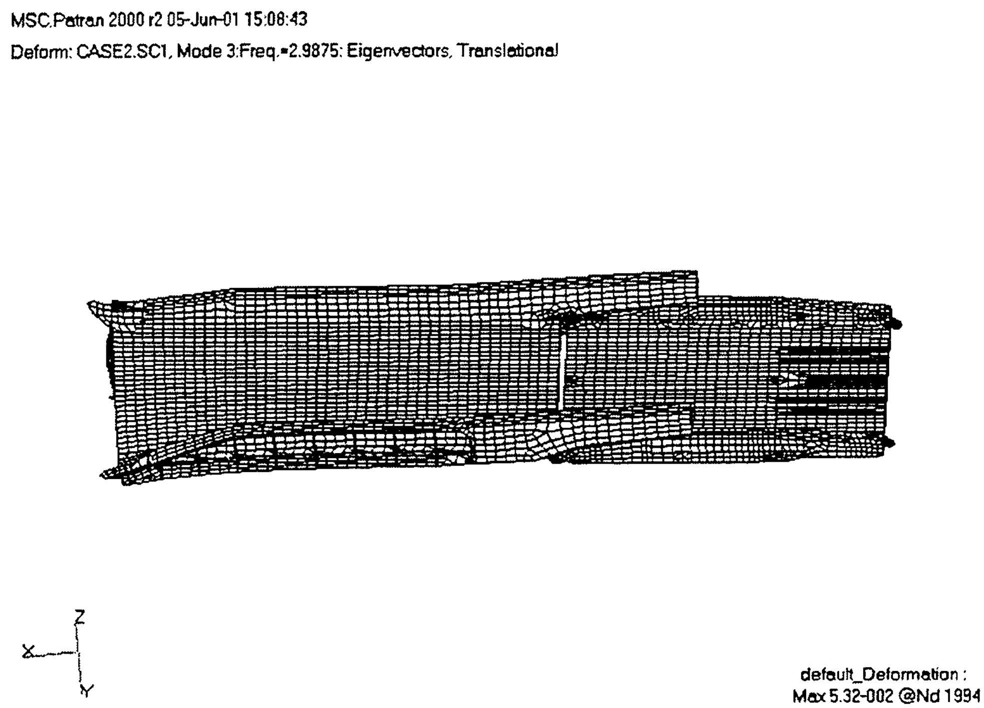

Figure 20. LMSR, Boundary Condition Case 2, Mode 2, Yaw-Torsion

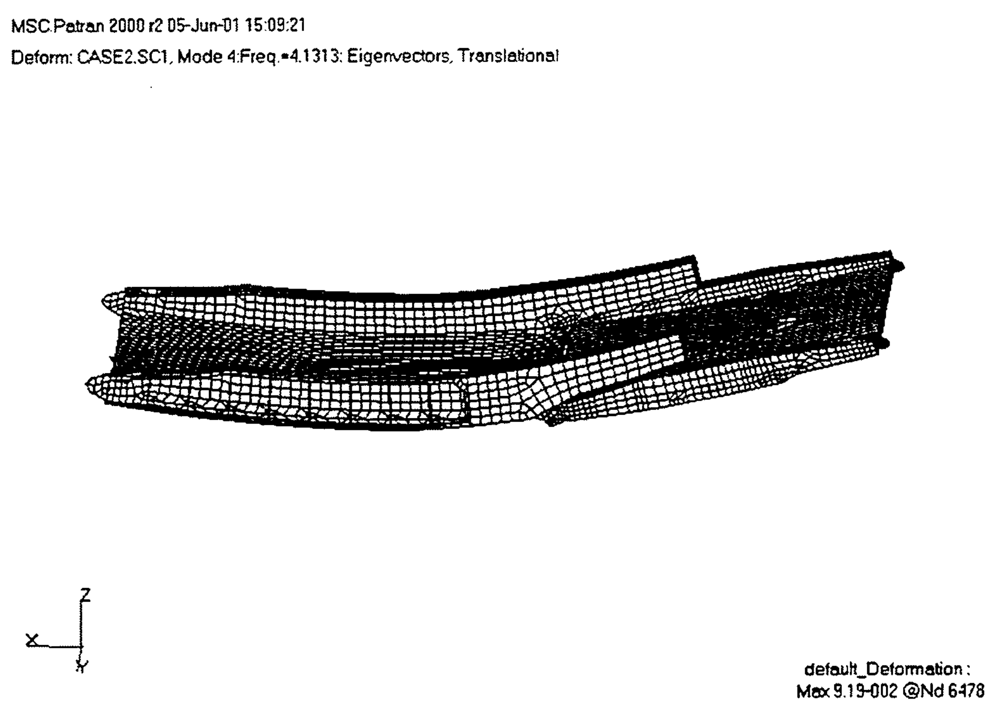

Figure 21. LMSR, Boundary Condition Case 2, Mode 3, Bending

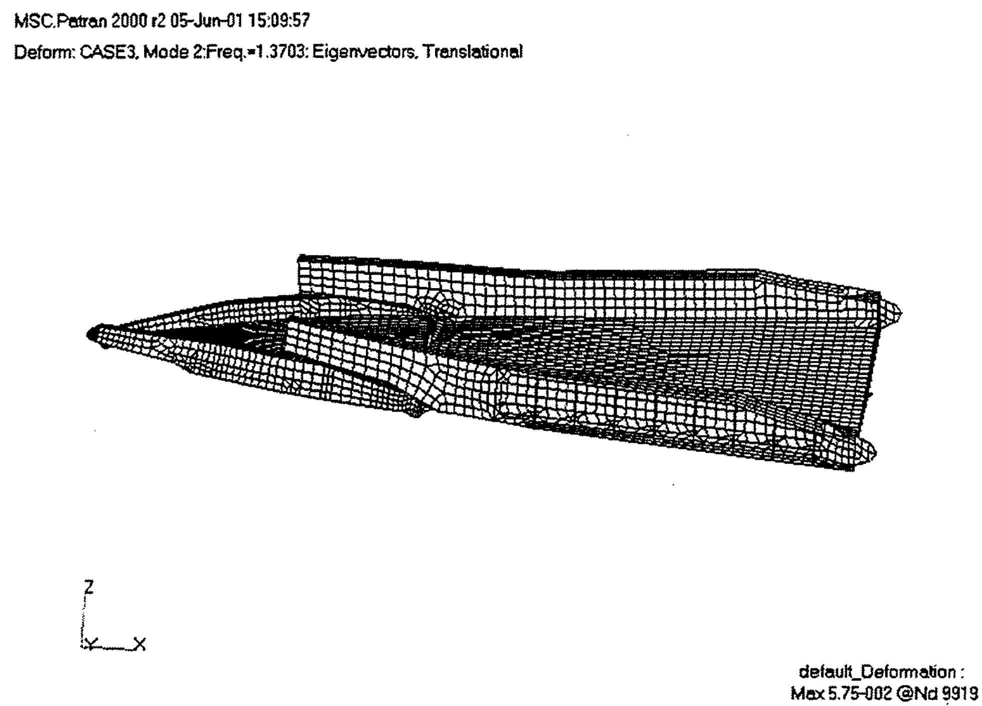

Figure 22. LMSR, Boundary Condition Case 3, Mode 1, Torsion

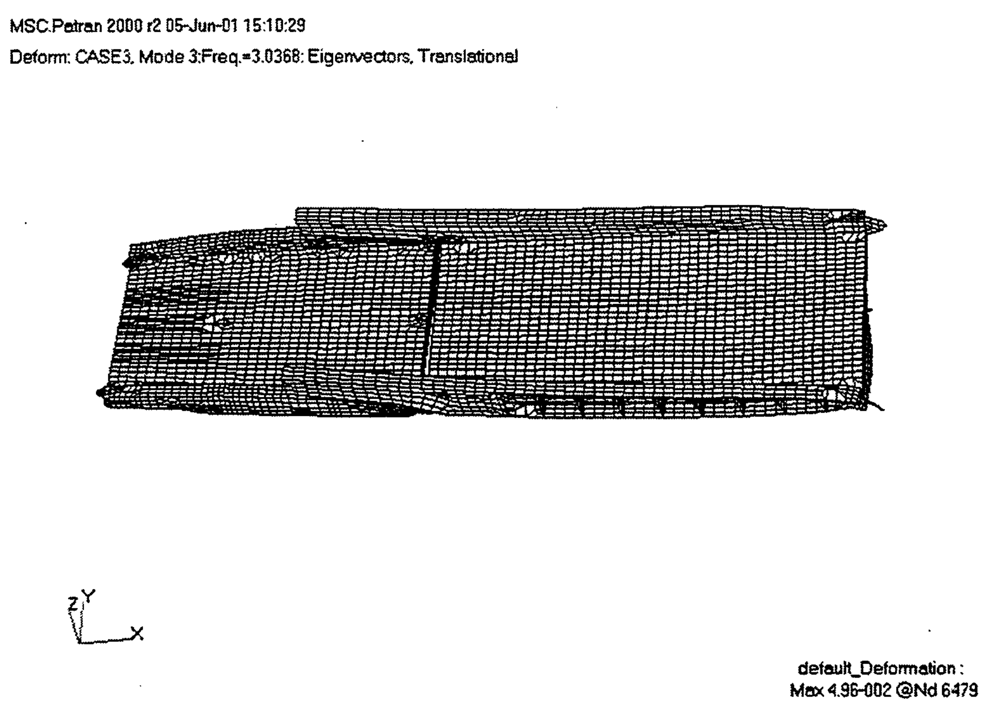

Figure 23. LMSR, Boundary Condition Case 3, Mode 2, Yaw-Torsion

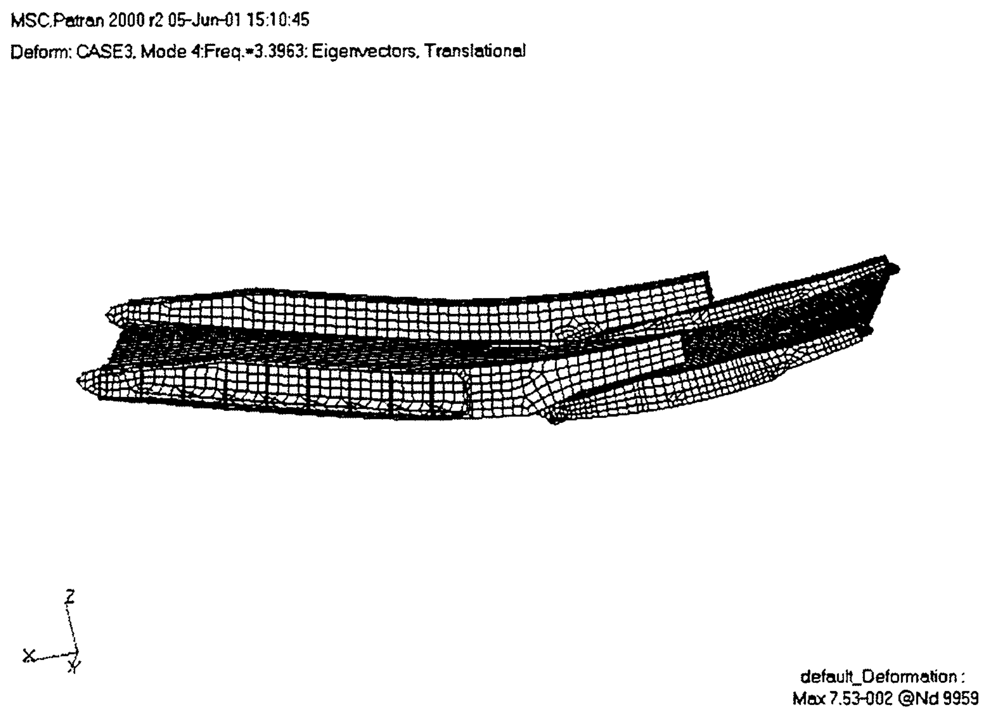

Figure 24. LMSR, Boundary Condition Case 3, Mode 3, Bending

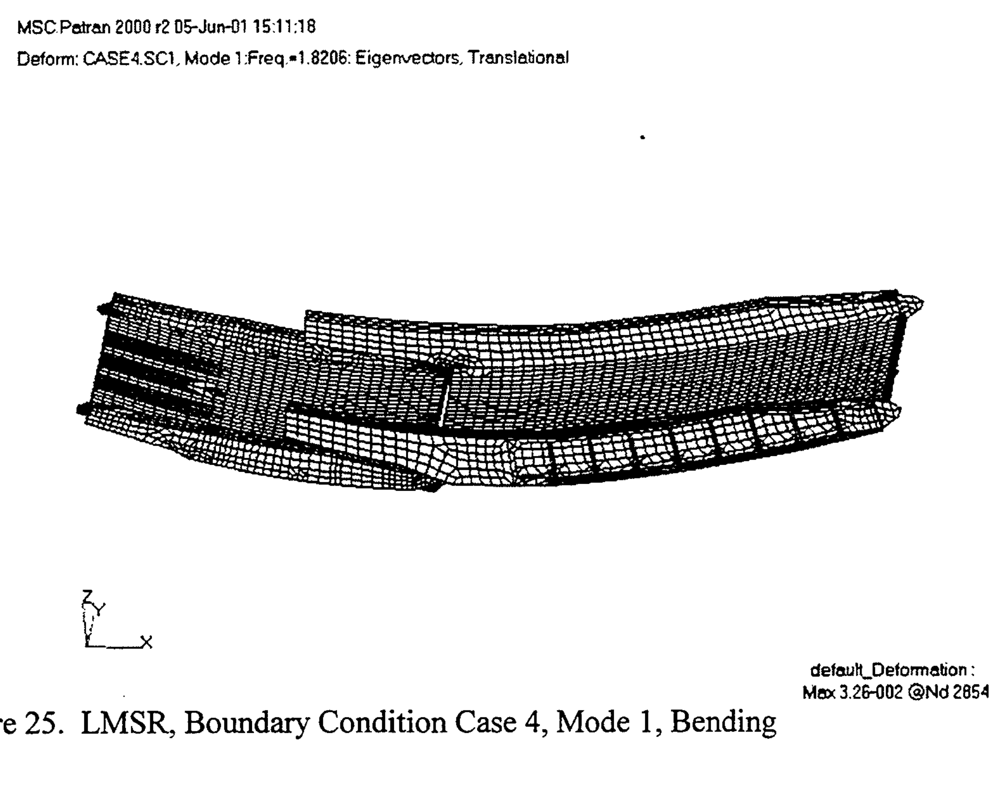

Figure 25. LMSR, Boundary Condition Case 4, Mode 1, Bending

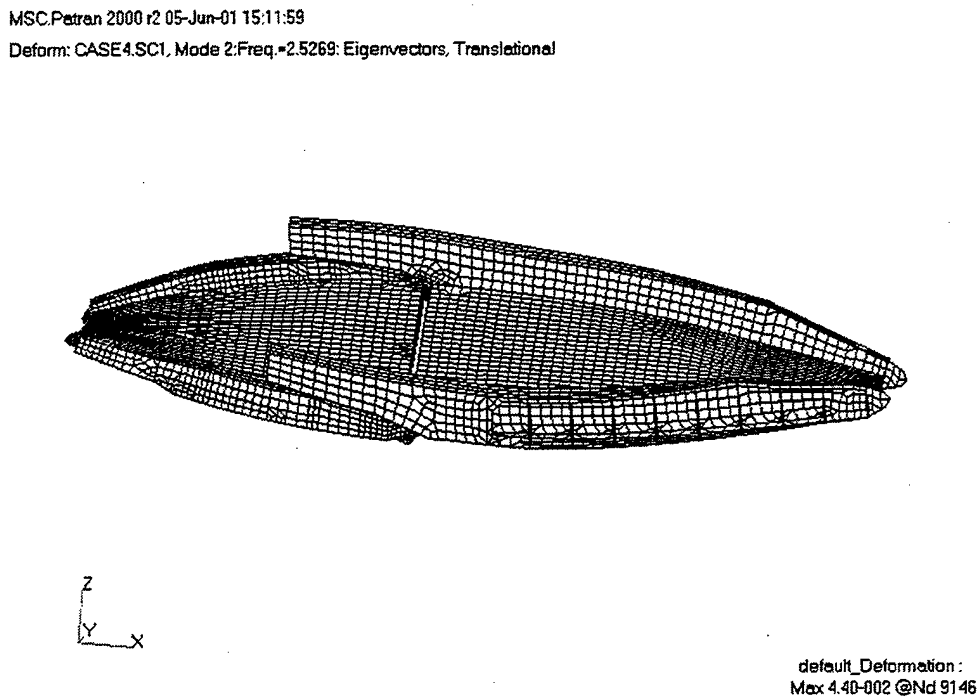

Figure 26. LMSR, Boundary Condition Case 4, Mode 2, Torsion

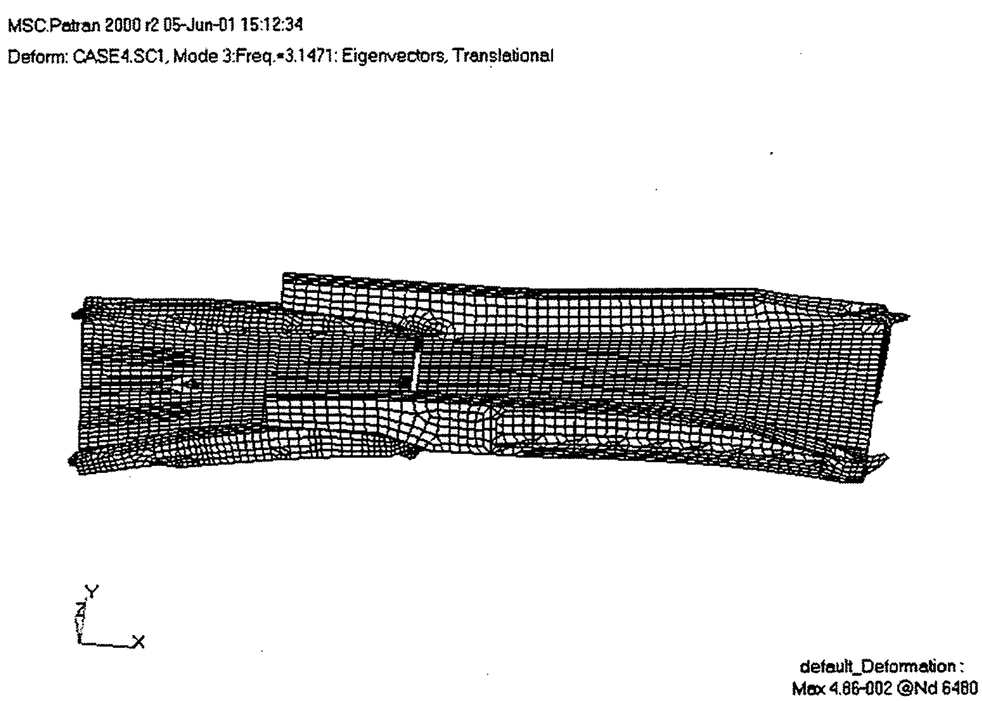

Figure 27. LMSR, Boundary Condition Case 4, Mode 3, Yaw-Torsion

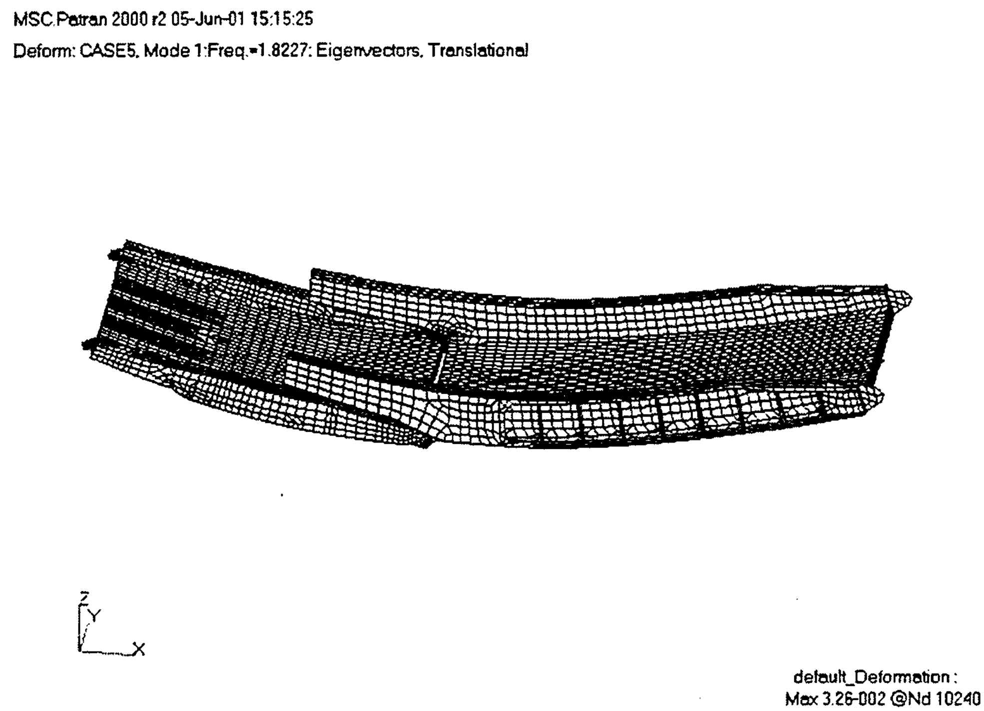

Figure 28. LMSR, Boundary Condition Case 5, Mode 1, Bending

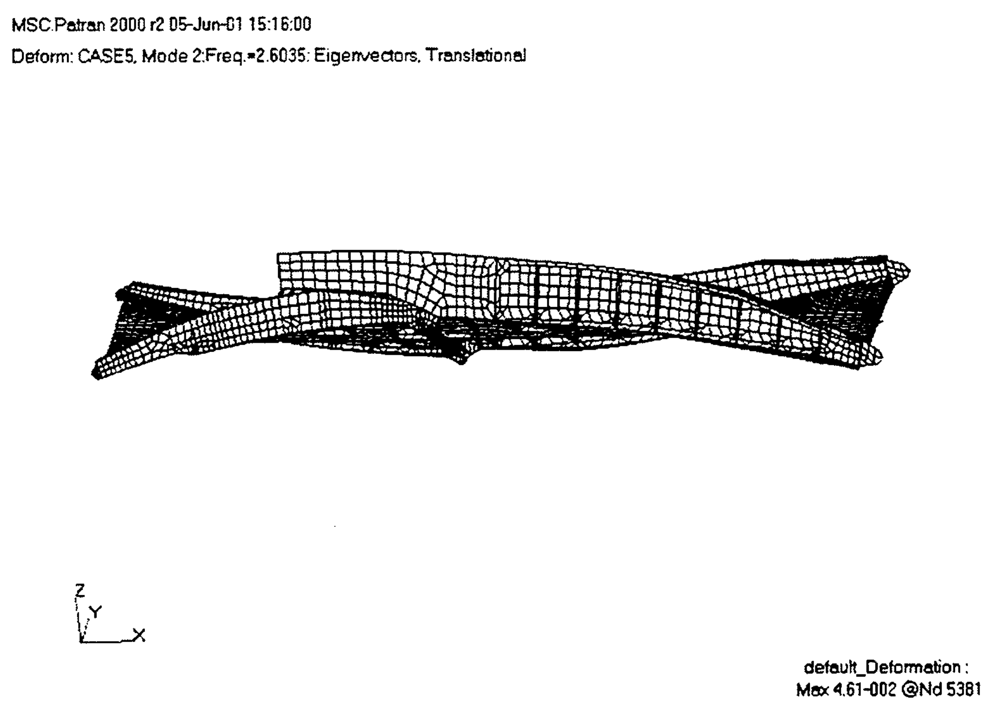

Figure 29. LMSR, Boundary Condition Case 5, Mode 2, Torsion

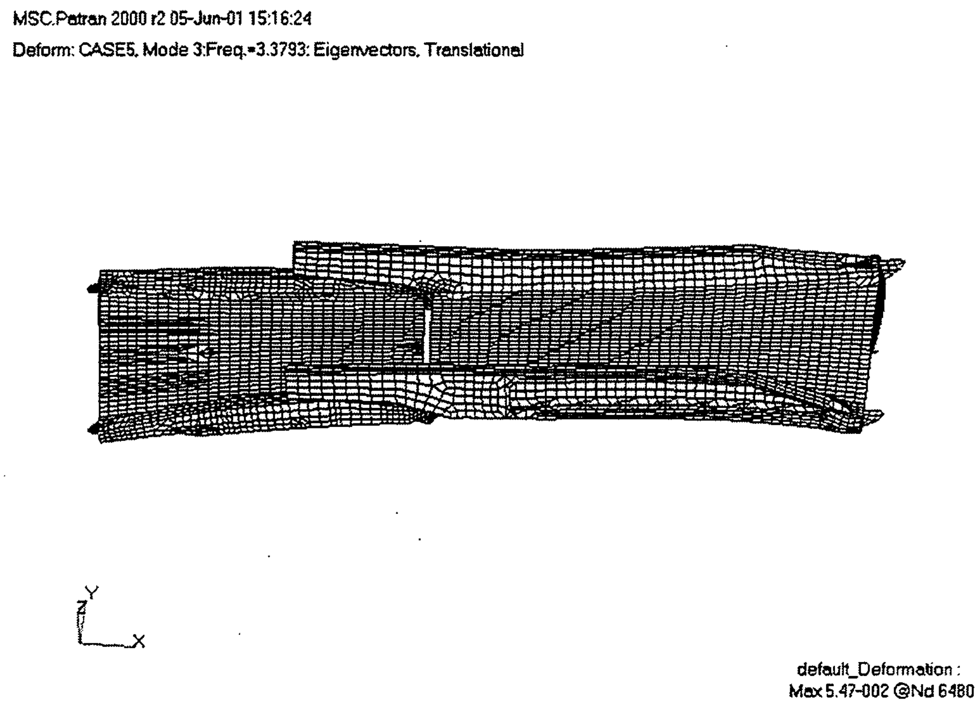

Figure 30. LMSR, Boundary Condition Case 5, Mode 3, Yaw-Torsion

The mode shapes for each boundary condition case were: bending; torsion; and yaw-torsion. The bending and torsion shapes were expected. The yaw-torsion mode is due to the restraints on the RRDF end either being not present (cases 1 and 2) or only in the vertical translational direction (cases 3, 4, and 5). Normal modes analysis results from the LMSR stern ramp are consistent with those from a similar analysis of the Cape T stern ramp. A summary mode shape comparison is included in Table 7.

LMSR Stern Ramp					
Mode	Case 1	Case 2	Case 3	Case 4	Case 5
1	Yaw-Torsion	Torsion	Torsion	Bending	Bending
2	Torsion	Yaw-Torsion	Yaw-Torsion	Torsion	Torsion
3	Bending	Bending	Bending	Yaw-Torsion	Yaw-Torsion
Cape T Stern Ramp					
Mode	Case 1	Case 2	Case 3	Case 4	Case 5
1	Yaw-Torsion	Torsion	Torsion	Bending	Bending
2	Torsion	Yaw-Torsion	Yaw-Torsion	Torsion	Torsion
3	Bending	Bending	Bending	Yaw-Torsion	Yaw-Torsion

Table 7. LMSR and Cape T Stern Ramp Mode Shape Comparison

It has been predicted that the sea state three wave induced motion of the RRDF occurs at 0.35 Hz. As was listed in Table 6, the natural frequency for the first elastic mode of the LMSR stern ramp for all boundary conditions considered is well above 0.35 Hz. Therefore, motion of the LMSR stern ramp may be assumed pseudostatic allowing the use of linear static computational methods for determination of ramp stress levels.

2. Model-Scale Stern Ramp

Finite element models were previously constructed of the major components of the experimental model-scale ramp test facility - specifically the model-scale ramp and it support structure. MSC/NASTRAN was used to predict the first four free-free normal modes of the model-scale stern ramp. Figures 31 through 34 show the first four elastic modes for the model-scale stern ramp.

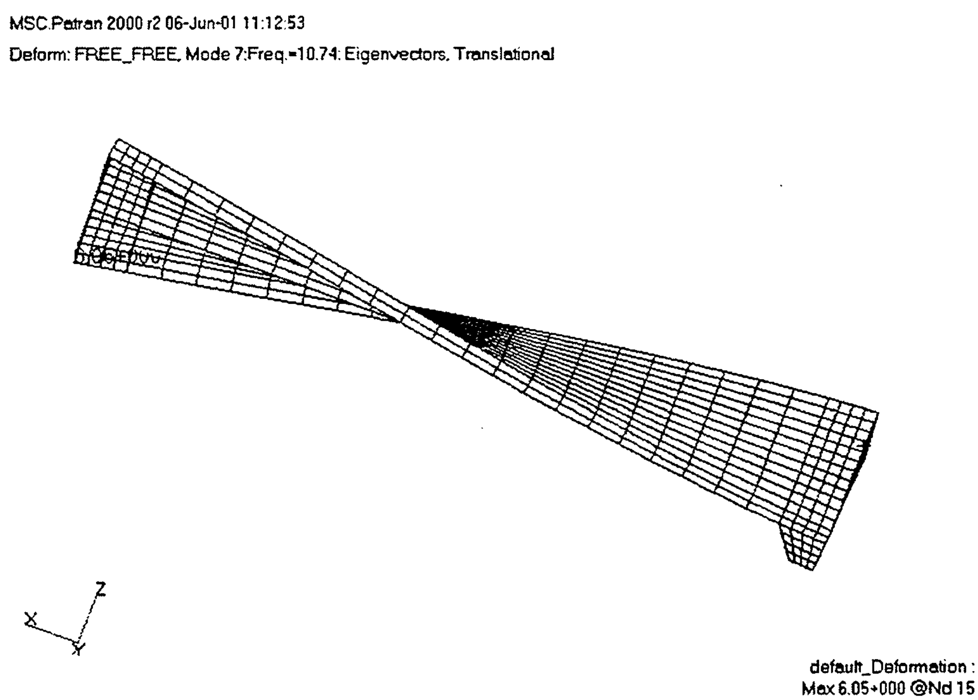

Figure 31. Model Scale Stern Ramp, Mode 1, First Torsion

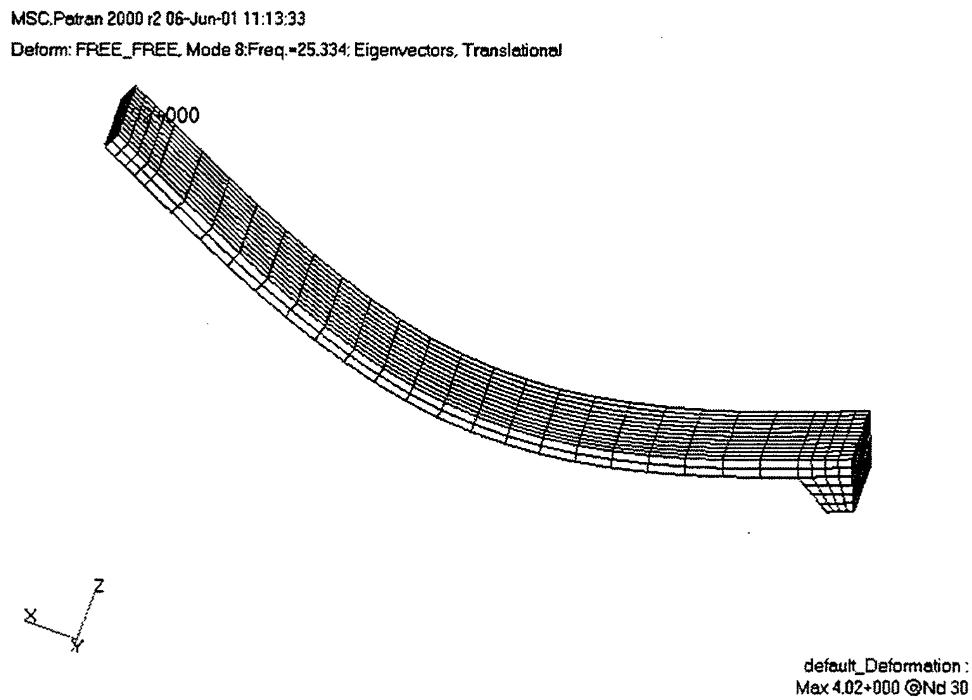

Figure 32. Model Scale Stern Ramp, Mode 2, First Bending

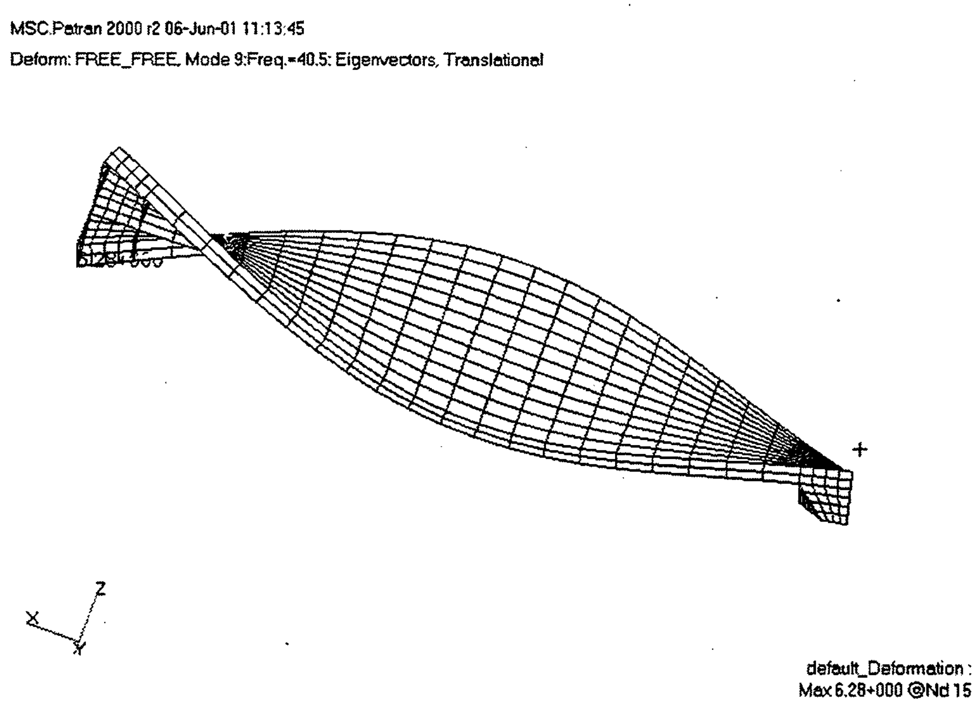

Figure 33. Model Scale Stern Ramp, Mode 3, Second Torsion

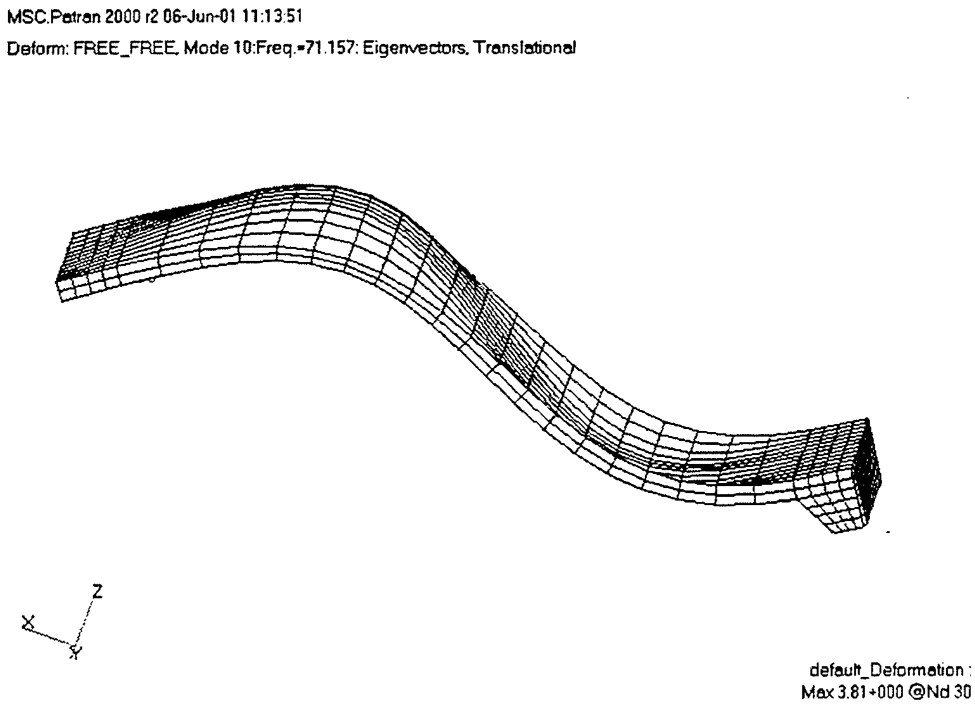

Figure 34. Model Scale Stern Ramp, Mode 4, Second Bending

Some modifications to the finite element model were necessary to accurately reflect the constructed ramp. The first four mode shapes of the model-scale stern ramp correlate with the experimental modal testing of the model-scale stern ramp.

3. Model-Scale Stern Ramp Support

MSC/NASTRAN was used to predict the normal modes of the scale-ramp support structure. The support was analyzed in its mounted condition – six bolts fastened to the deck. The base plate of the support structure was designed to fit flush to the deck, but due to slight bowing of the structure during the fabrication process, the base plate was free to vibrate in the vertical direction. The boundary conditions of the support were set as clamps in the vertical DOF in the regions of the hold down bolts. Figure 35 displays the first vibration mode predicted for the scale-ramp support structure. This mode is

essentially the base plate vibrating in the vertical direction at 51.3 Hz. This mode was correlated with the experimental mode test of the support structure.

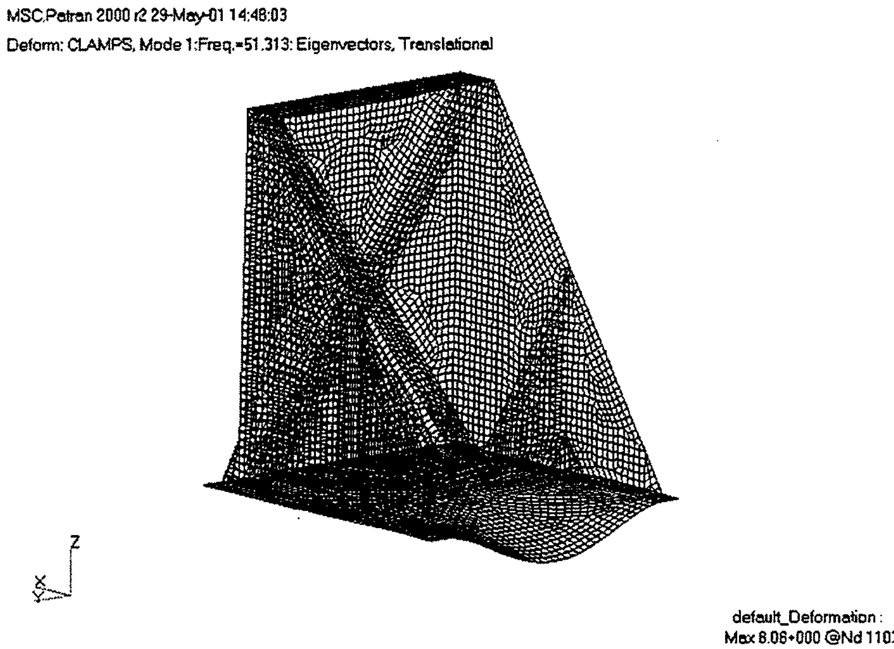

Figure 35. Model-Scale Ramp Support Structure, Mode 1

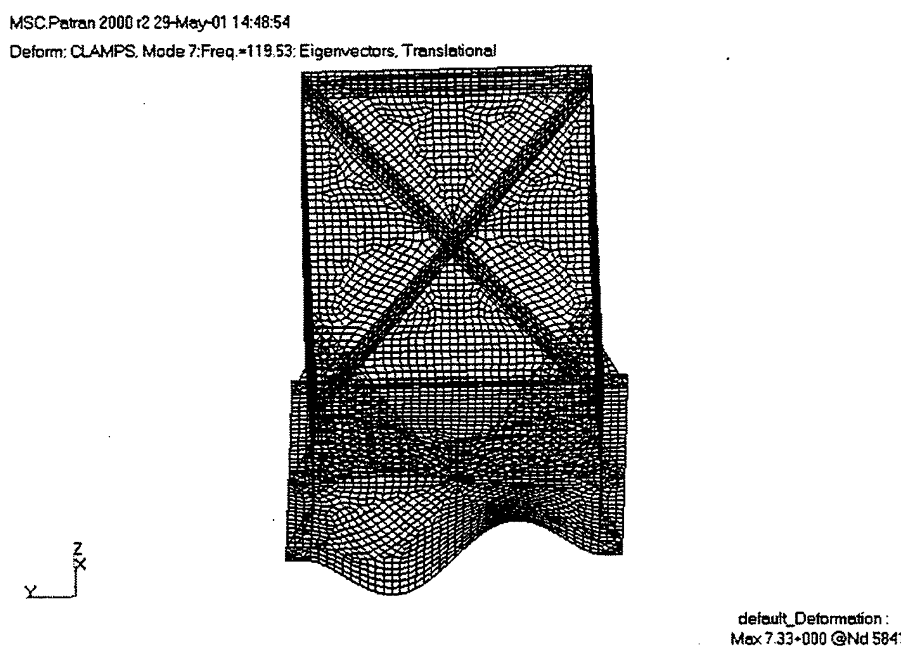

Figure 36. Model-Scale Ramp Support Structure, Mode 7

The only other mode that correlated with the experimental modal testing of the structure was the predicted mode 7, displayed in Figure 36.

Updating the finite element model of the scale-ramp support was approached through several methods. First, the boundary conditions were matched as closely as possible. Second, due to inconsistencies and gaps in the welds of the structure, weld gaps were modeled as an attempt to introduce the asymmetry in the computational modal response that was observed in the vibration test. Third, the mesh of the structure was refined to allow more closely modeling the gaps in the welded joints. This resulted in limited success. The majority of the welds in the structure were right-angled joints between two steel plates. These welds joints were not modeled specifically and thus were not available for updating.

B. COMPUTATIONAL LINEAR STATIC ANALYSIS

Due to the pseudostatic response predicted by normal modes analysis of the LMSR and Cape T stern ramps, linear static analysis was chosen to determine ramp stress levels in each of the three ramp designs (LMSR, Cape T, and Cape H). A thorough study of the stress levels in each ramp under various load condition was necessary to determine the suitability of the particular ramp model for inclusion in the coupled hydro-structural simulation model of the combined ship-ramp-RRDF. A set of load conditions was applied to each ramp design consisting of inertial (gravity) loads and various amounts of twist simulating the wave-induced motion of the RRDF. Additionally, the ramp designs were studied with one and two tank loading configurations as modeled by static pressure loads.

1. Large Medium Speed Roll-On, Roll-Off Vessel Stern Ramp

The LMSR stern ramp analyses were conducted with case 5 boundary conditions (restrained in the three translational DOF at the ship end and the vertical DOF at the RRDF end). Twist angles between the RRDF and ship of zero, one, three, five, and eight degrees were considered. Maximum von Mises stress contour plots were generated with PATRAN and are displayed in Figures 37 through 89.

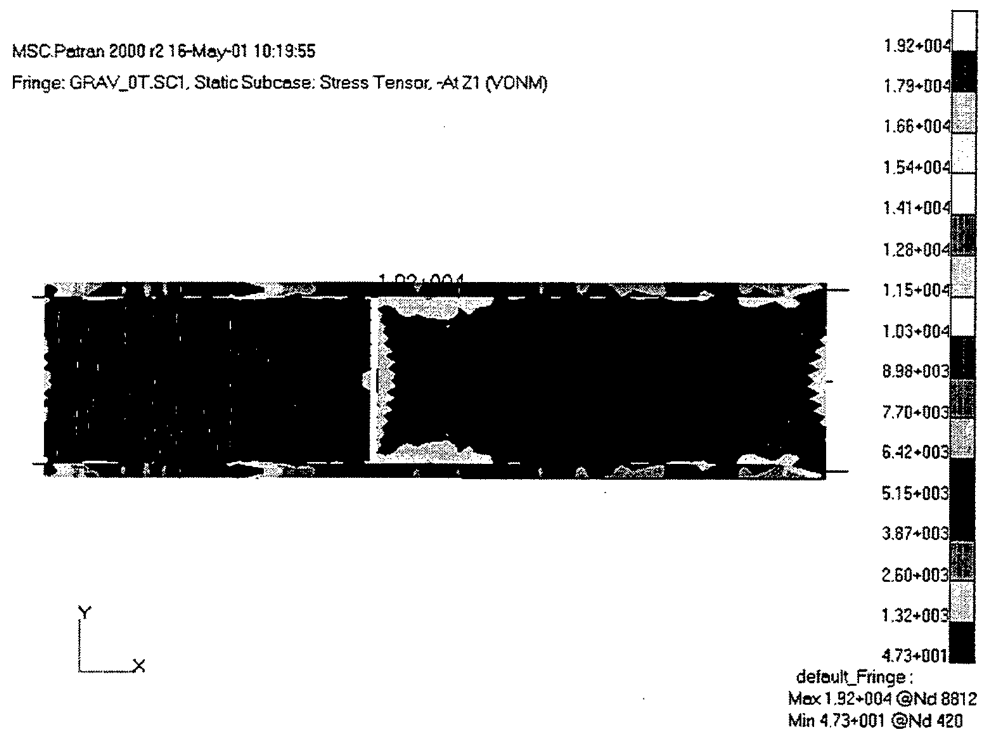

Figure 37. LMSR (top view) von Mises Stress Contour Plot, Max. Stress: 19.2 ksi (Inertia Loading, No Twist, No Tanks)

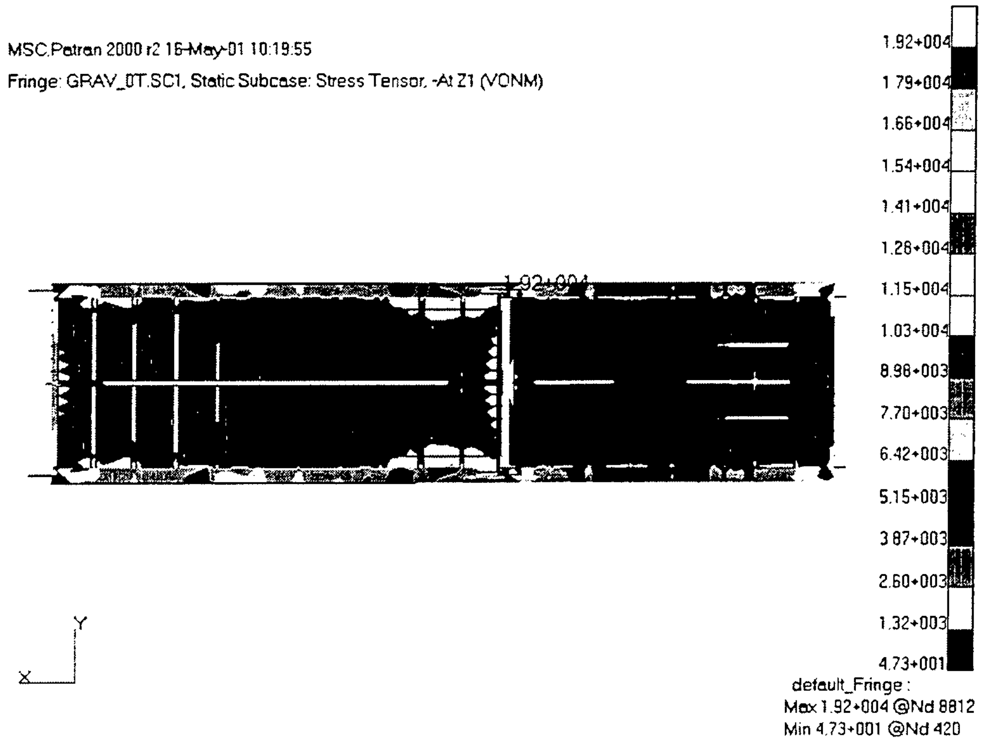

Figure 38. LMSR (bottom view) von Mises Stress Contour Plot, Max. Stress: 19.2 ksi (Inertia Loading, No Twist, No Tanks)

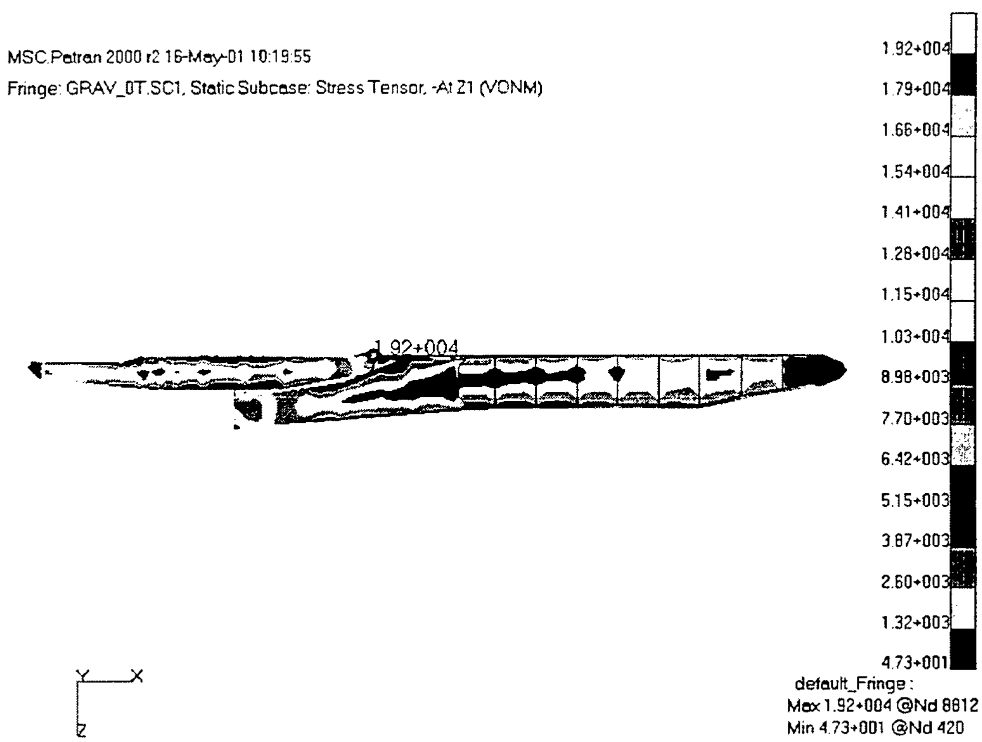

Figure 39. LMSR (right view) von Mises Stress Contour Plot, Max. Stress: 19.2 ksi (Inertia Loading, No Twist, No Tanks)

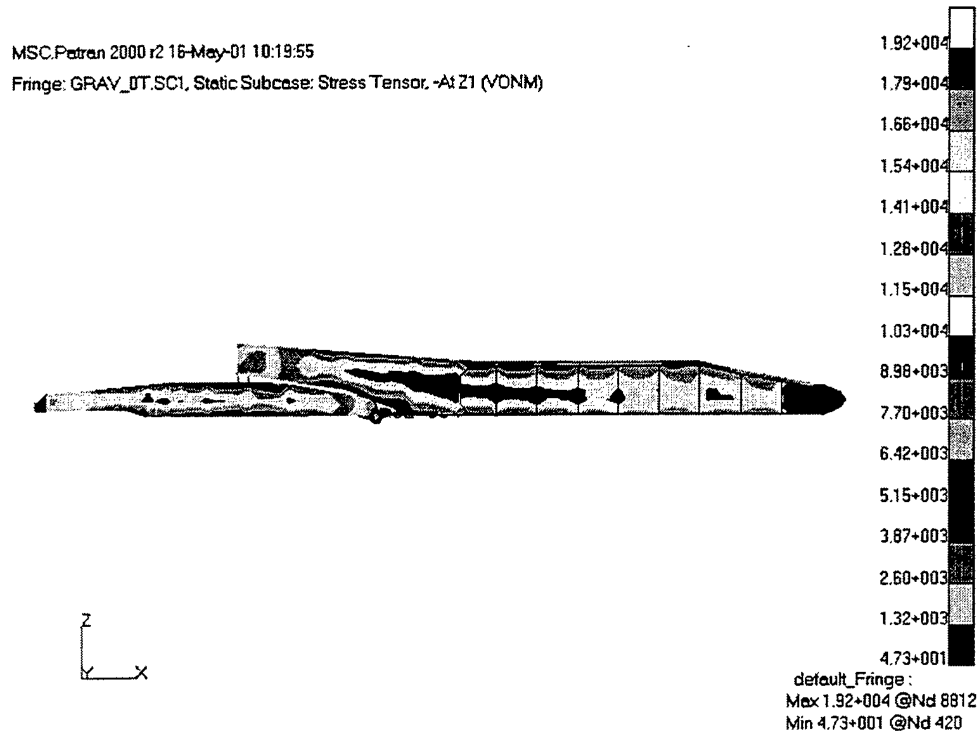

Figure 40. LMSR (left view) von Mises Stress Contour Plot, Max. Stress: 19.2 ksi (Inertia Loading, No Twist, No Tanks)

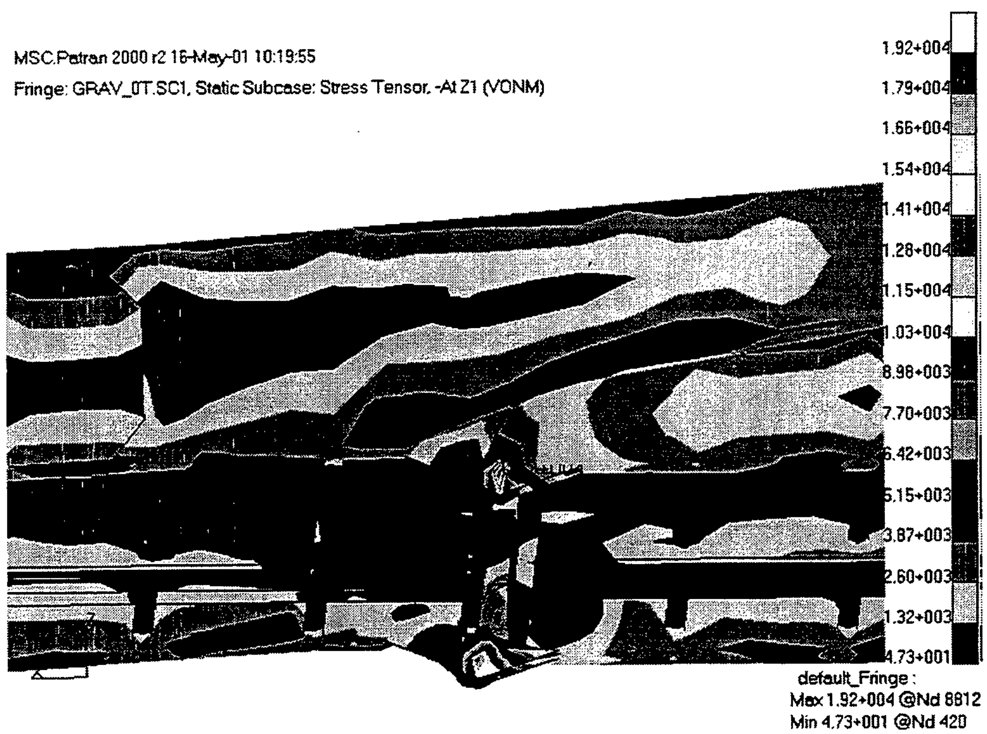

Figure 41. LMSR (close-up) von Mises Stress Contour Plot, Max. Stress: 19.2 ksi (Inertia Loading, No Twist, No Tanks)

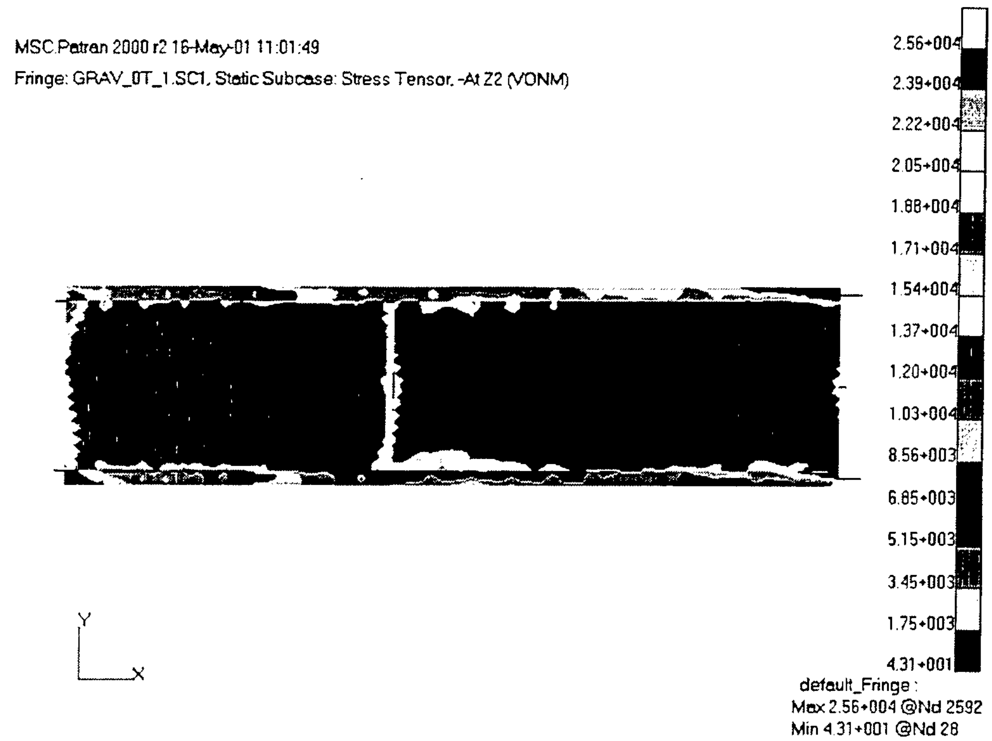

Figure 42. LMSR (top view) von Mises Stress Contour Plot, Max. Stress: 25.6 ksi (Inertia Loading, 1 Degree Twist, No Tanks)

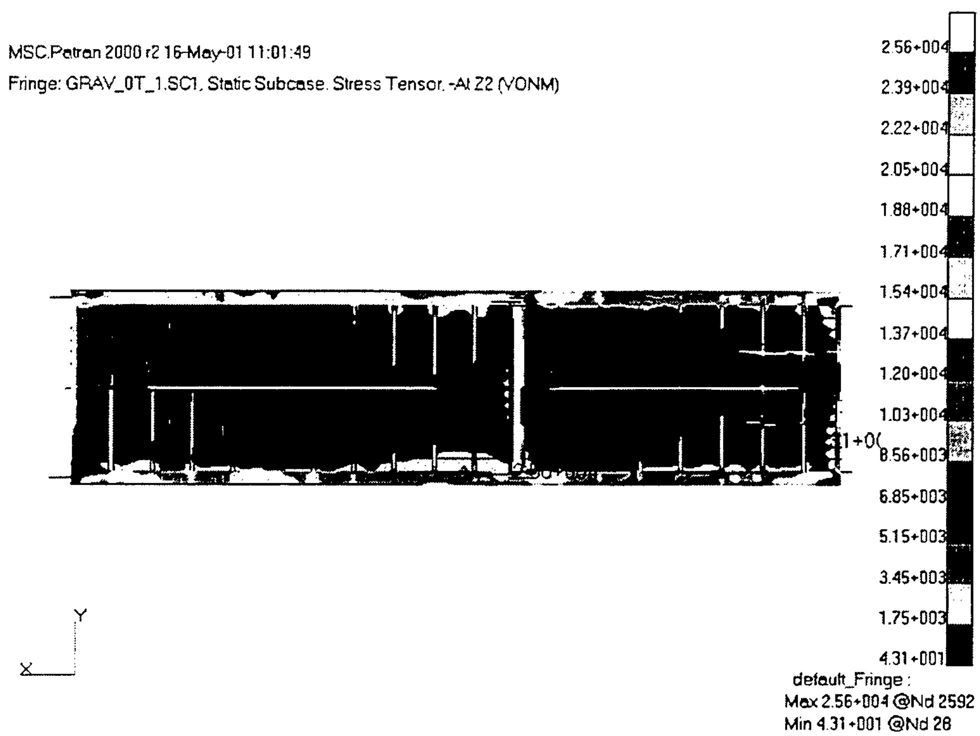

Figure 43. LMSR (bottom view) von Mises Stress Contour Plot, Max. Stress: 25.6 ksi (Inertia Loading, No Twist, One Tank)

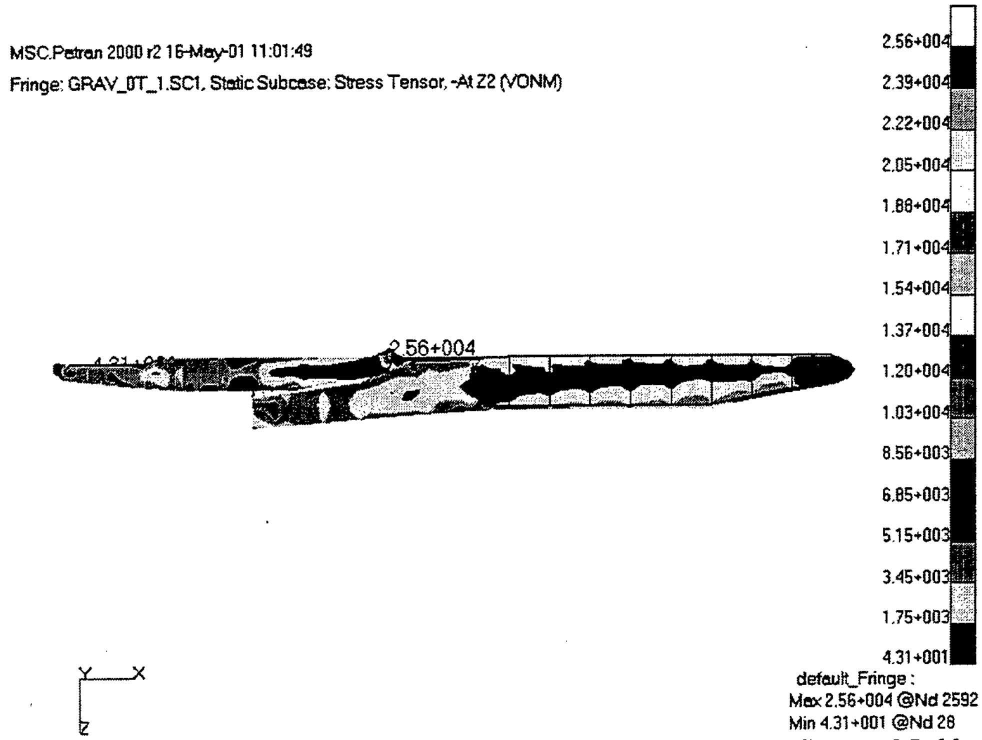

Figure 44. LMSR (right view) von Mises Stress Contour Plot, Max. Stress: 25.6 ksi (Inertia Loading, 1 Degree Twist, No Tanks)

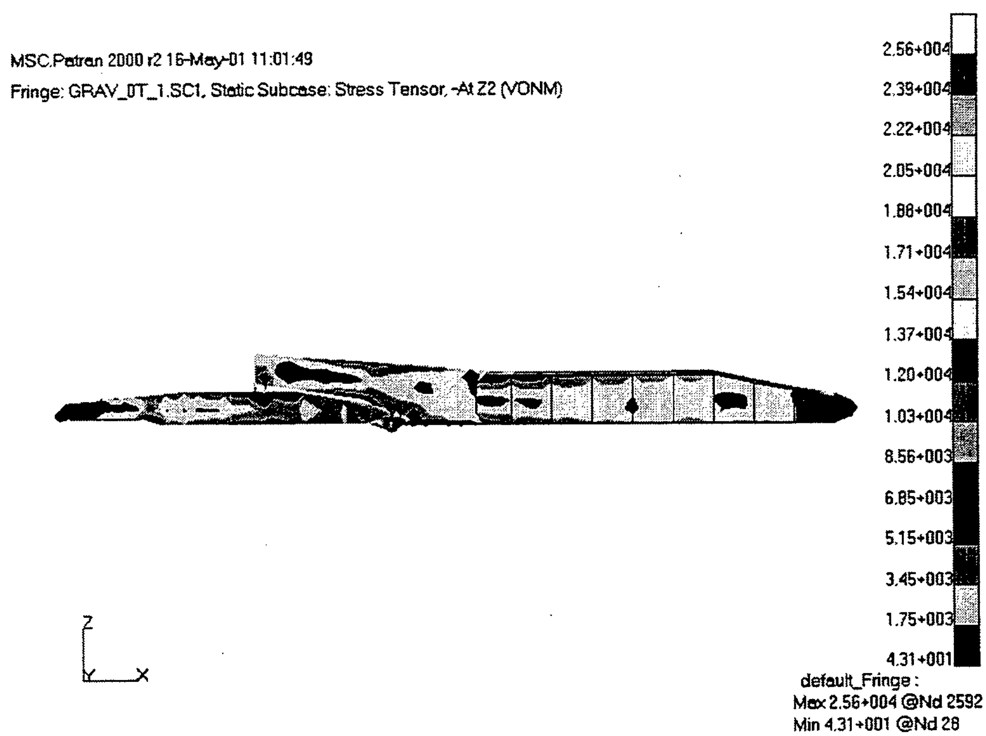

Figure 45. LMSR (left view) von Mises Stress Contour Plot, Max. Stress: 25.6 ksi (Inertia Loading, 1 Degree Twist, No Tanks)

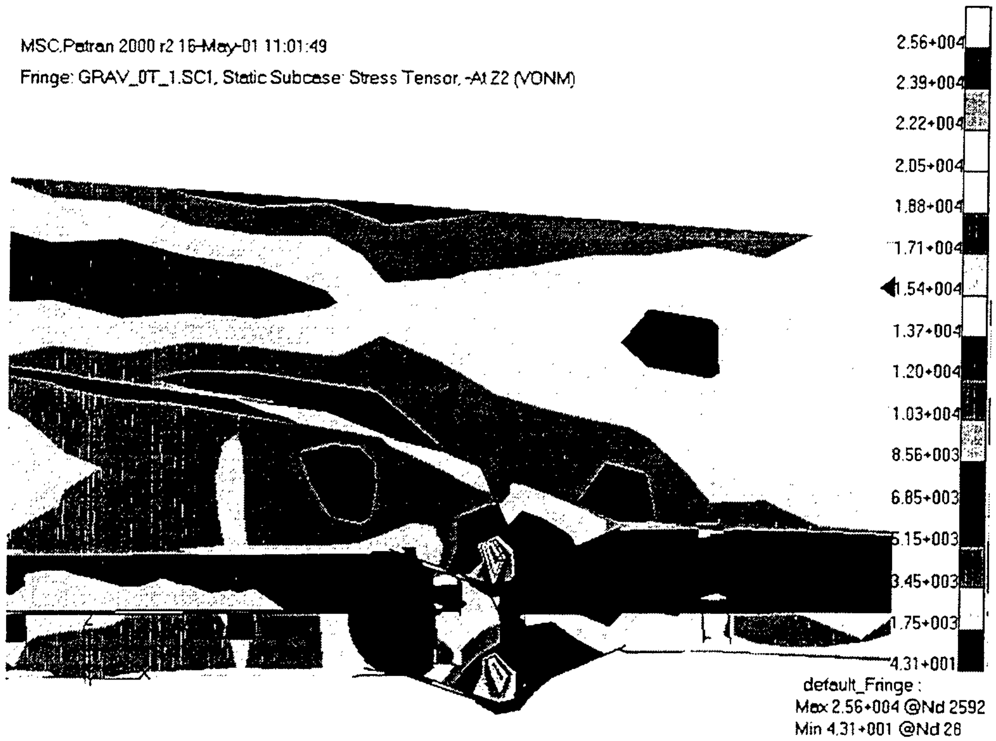

Figure 46. LMSR (close-up) von Mises Stress Contour Plot, Max. Stress: 25.6 ksi (Inertia Loading, 1 Degree Twist, No Tanks)

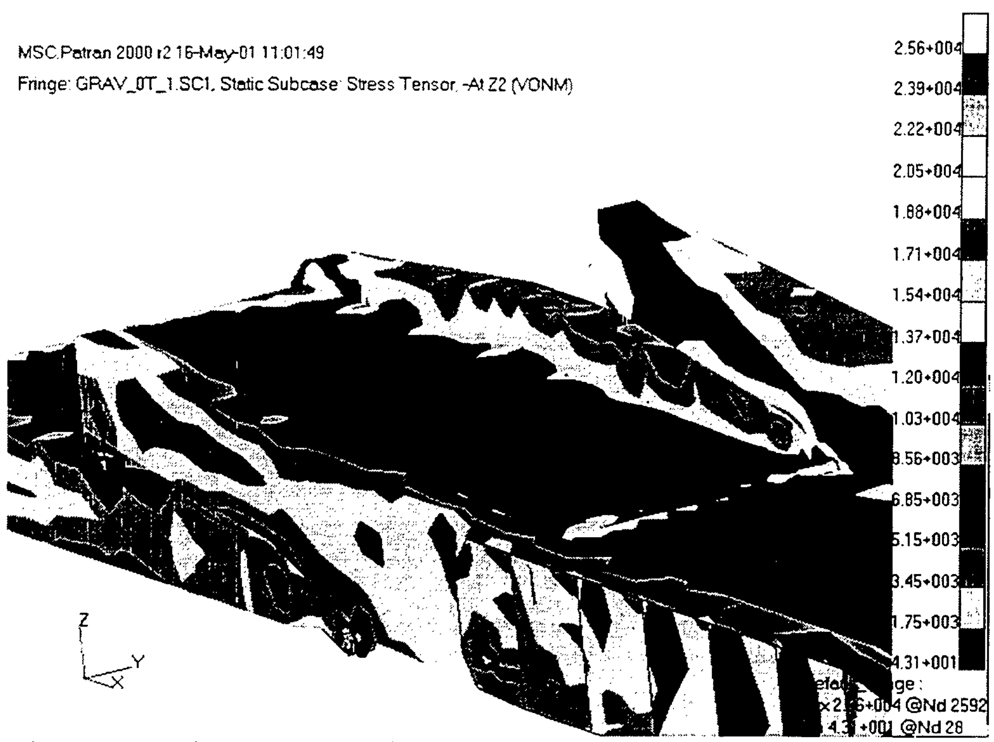

Figure 47. LMSR (close-up) von Mises Stress Contour Plot, Max. Stress: 25.6 ksi (Inertia Loading, 1 Degree Twist, No Tanks)

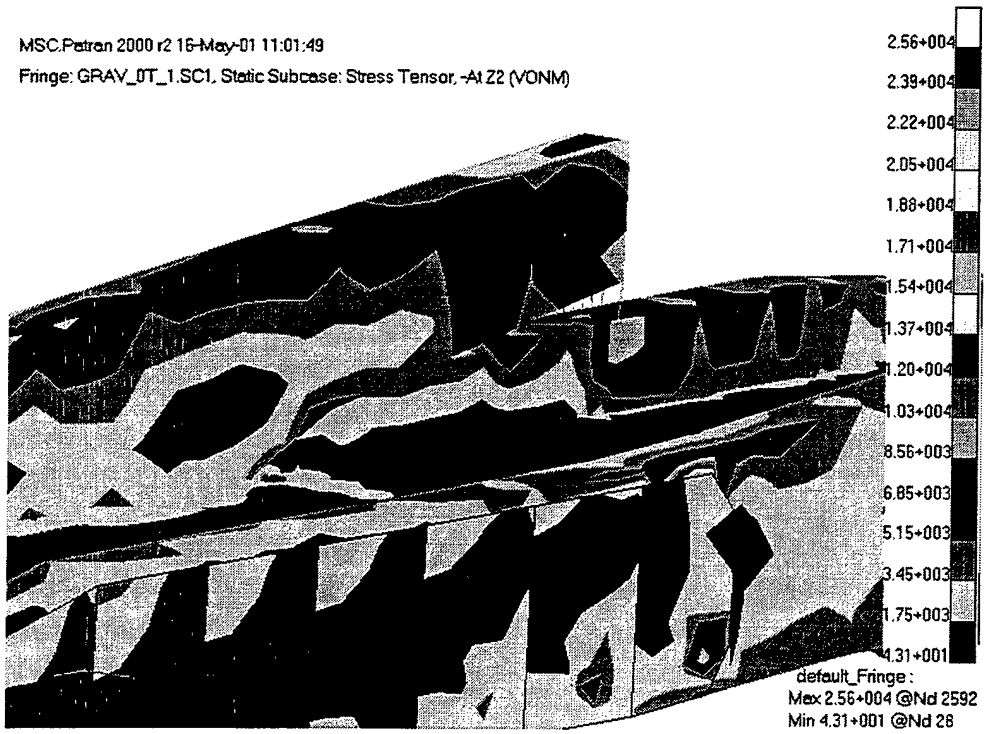

Figure 48. LMSR (close-up) von Mises Stress Contour Plot, Max. Stress: 25.6 ksi (Inertia Loading, 1 Degree Twist, No Tanks)

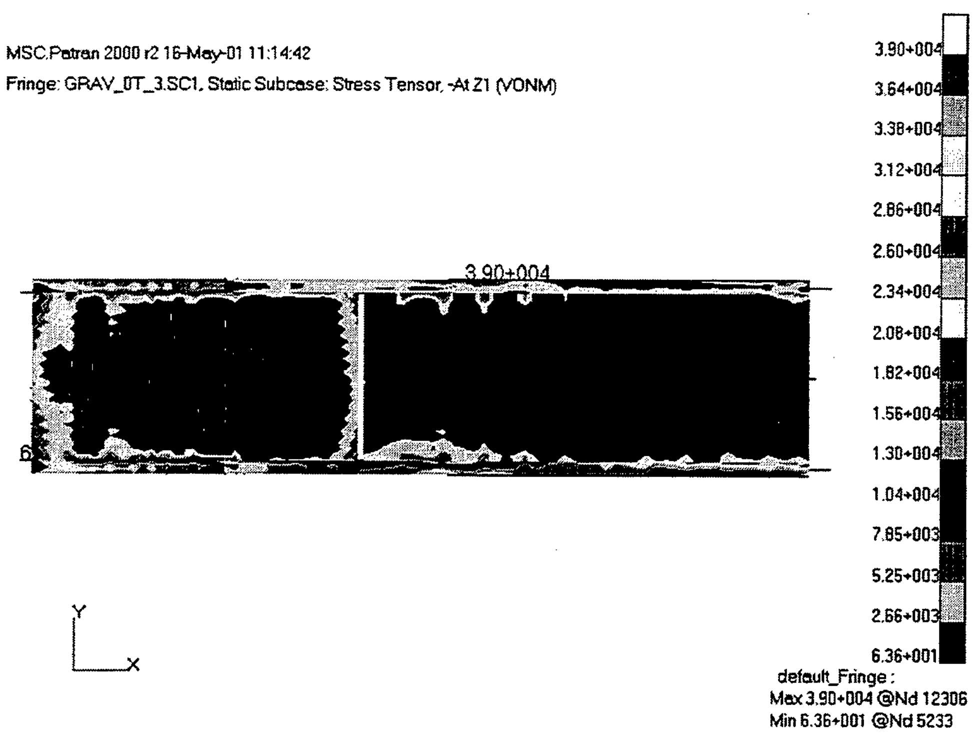

Figure 49. LMSR (top view) von Mises Stress Contour Plot, Max. Stress: 39.0 ksi (Inertia Loading, 3 Degree Twist, No Tanks)

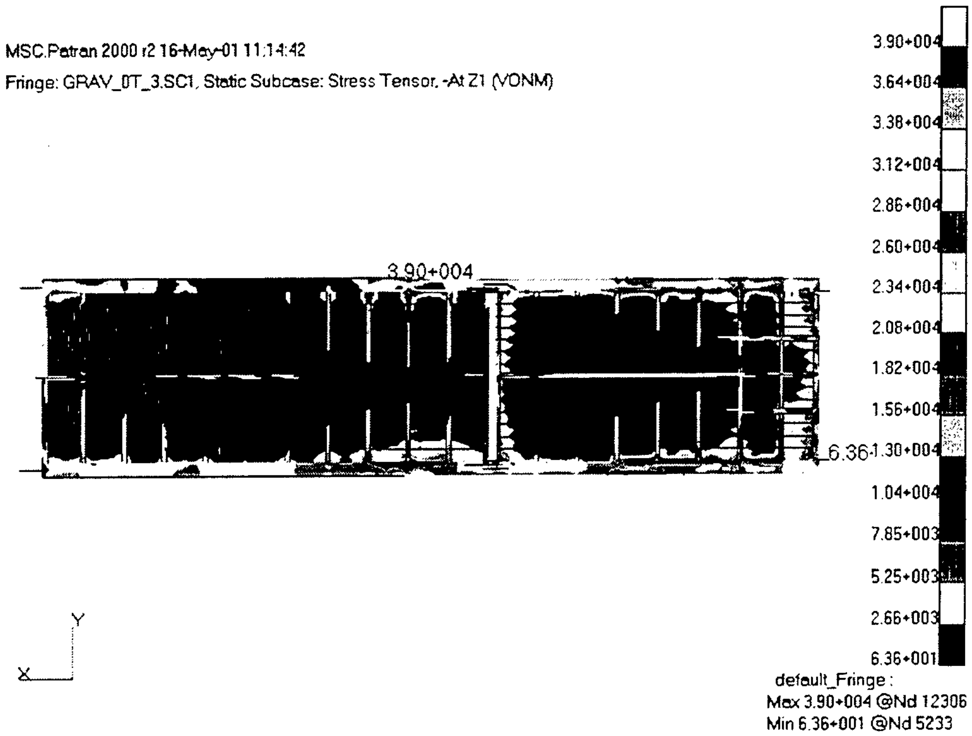

Figure 50. LMSR (bottom view) von Mises Stress Contour Plot, Max. Stress: 39.0 ksi (Inertia Loading, 3 Degree Twist, No Tanks)

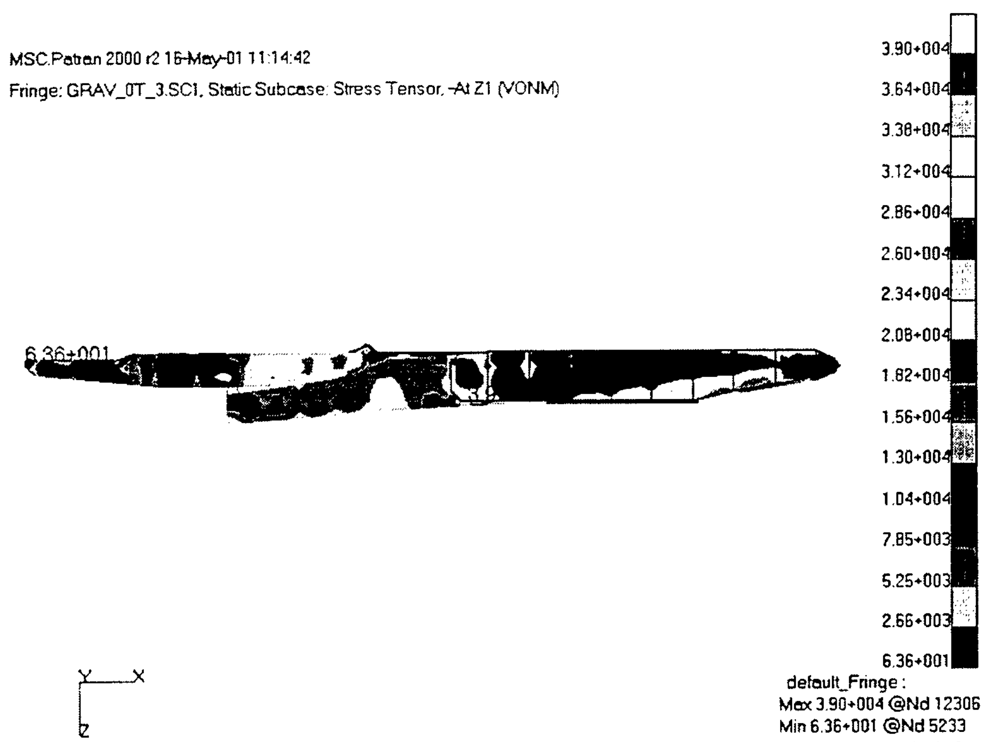

Figure 51. LMSR (right view) von Mises Stress Contour Plot, Max. Stress: 39.0 ksi (Inertia Loading, 3 Degree Twist, No Tanks)

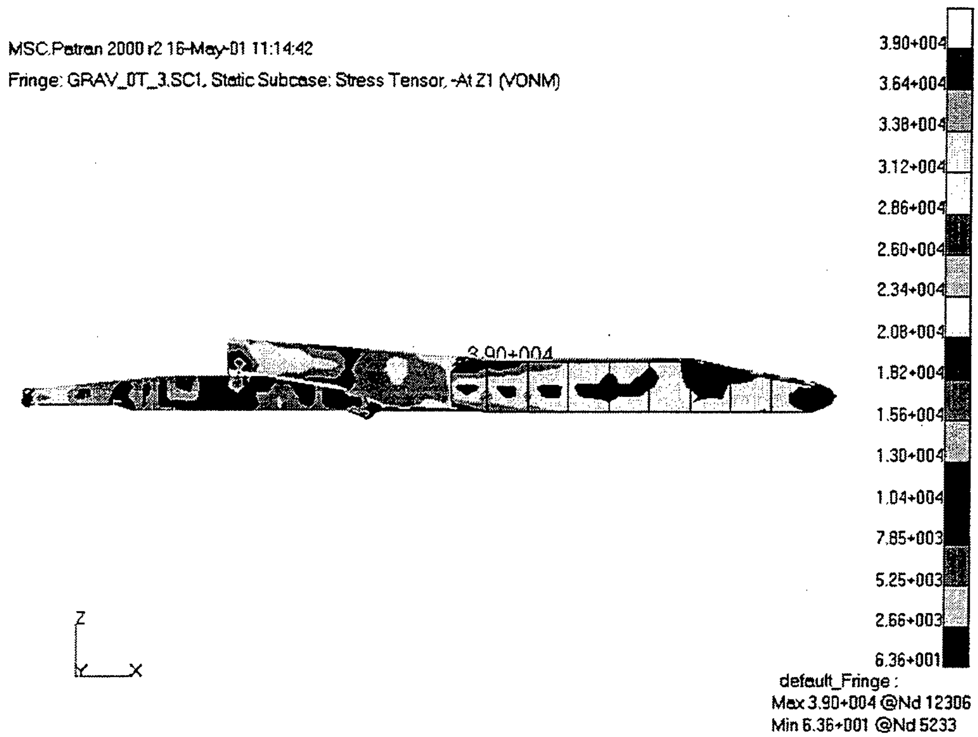

Figure 52. LMSR (left view) von Mises Stress Contour Plot, Max. Stress: 39.0 ksi (Inertia Loading, 3 Degree Twist, No Tanks)

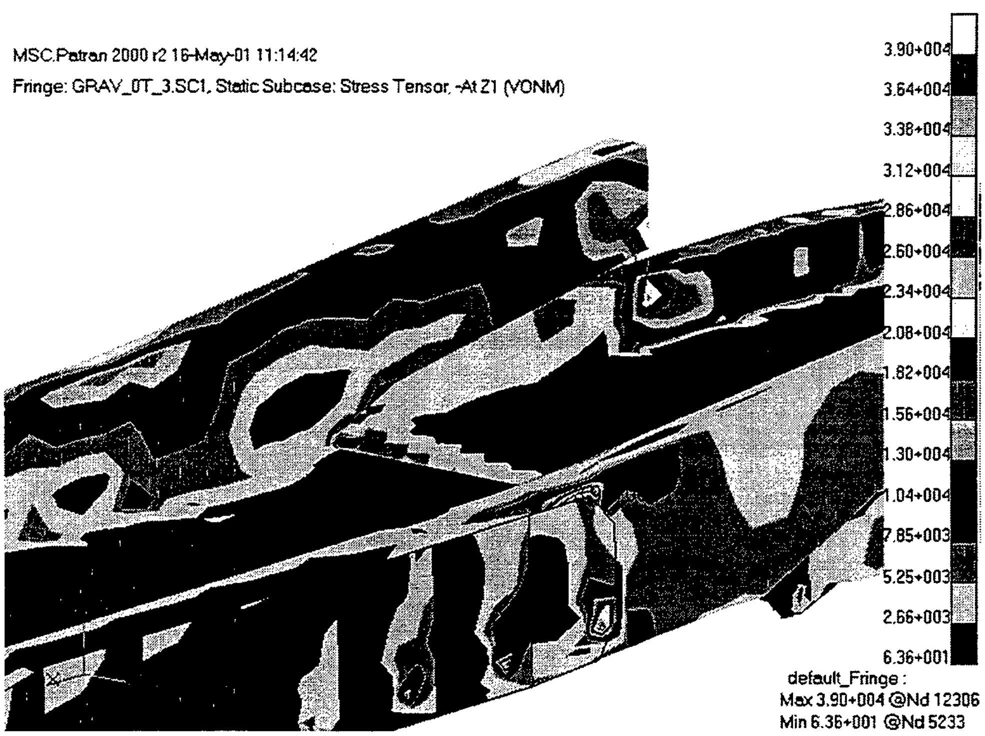

Figure 53. LMSR (close-up) von Mises Stress Contour Plot, Max. Stress: 39.0 ksi (Inertia Loading, 3 Degree Twist, No Tanks)

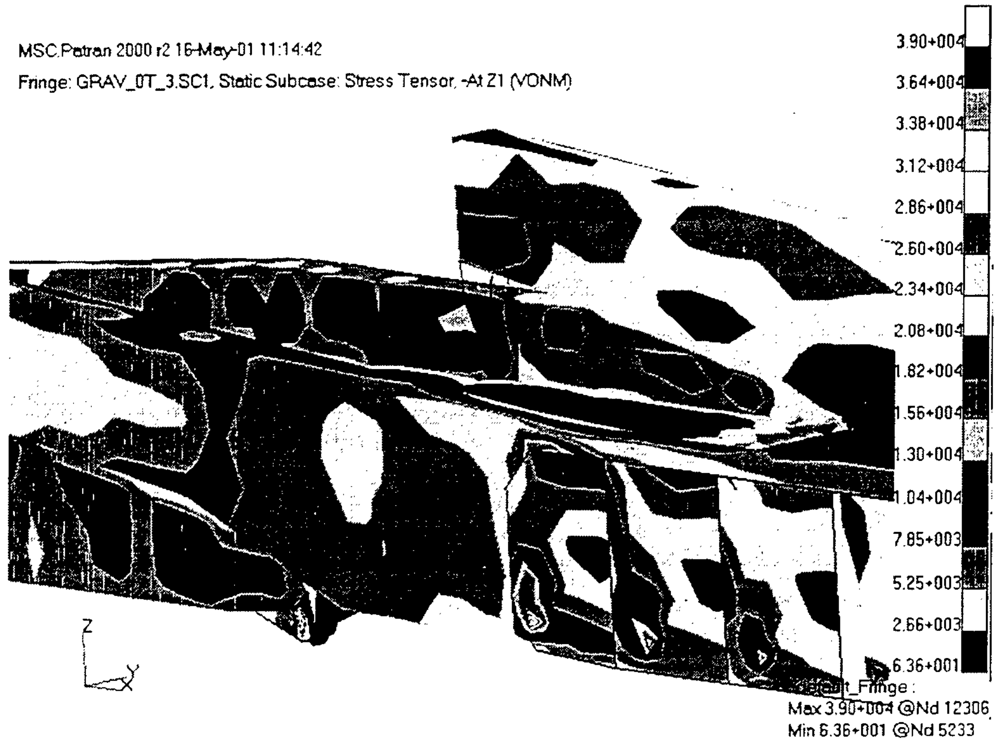

Figure 54. LMSR (close-up) von Mises Stress Contour Plot, Max. Stress: 39.0 ksi (Inertia Loading, 3 Degree Twist, No Tanks)

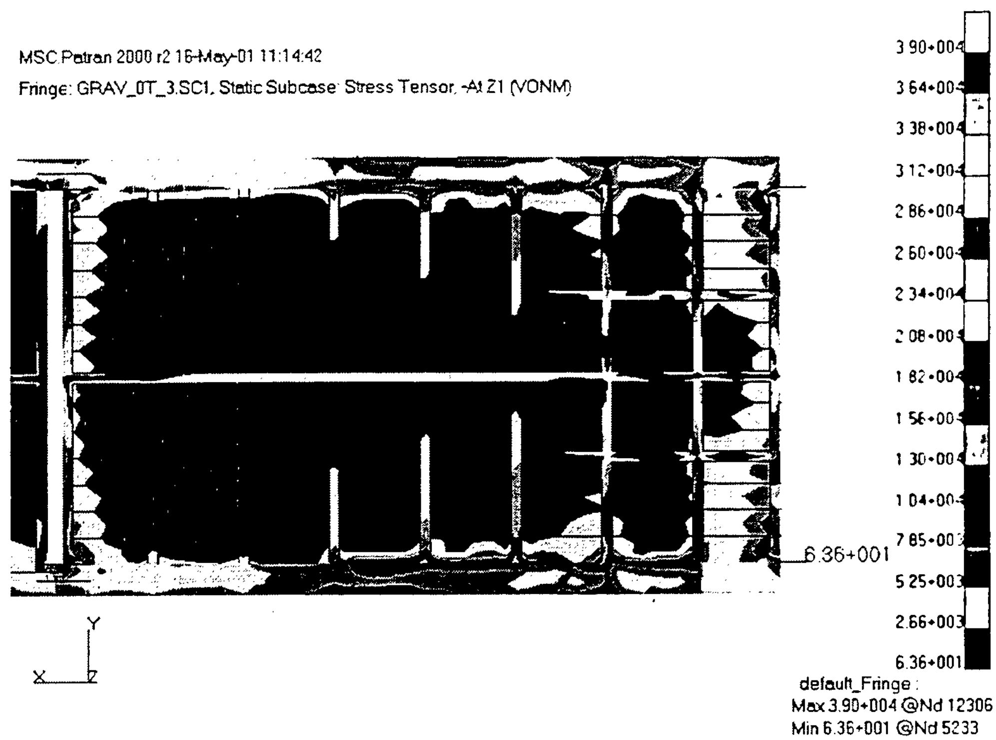

Figure 55. LMSR (close-up) von Mises Stress Contour Plot, Max. Stress: 39.0 ksi (Inertia Loading, 3 Degree Twist, No Tanks)

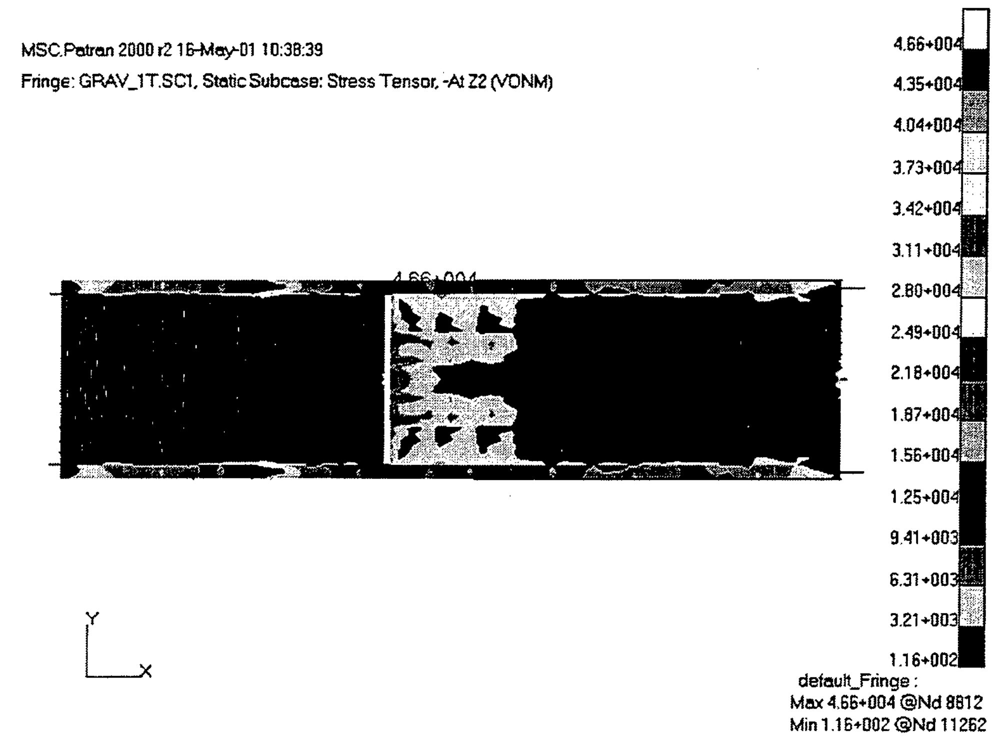

Figure 56. LMSR (top view) von Mises Stress Contour Plot, Max. Stress: 46.6 ksi (Inertia Loading, No Twist, One Tank)

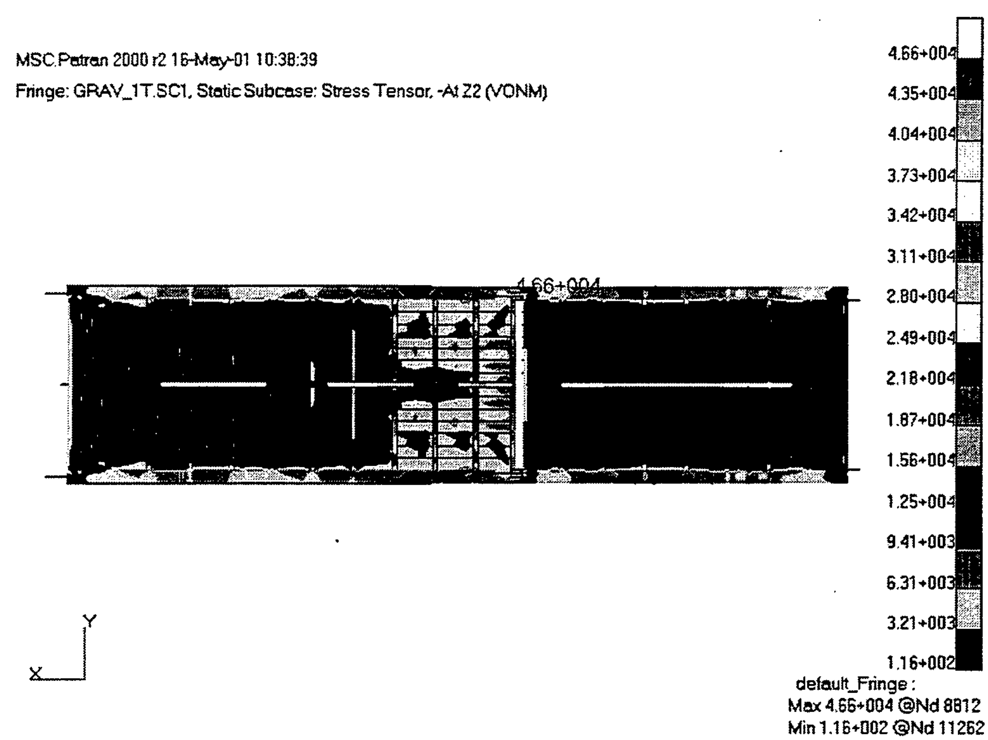

Figure 57. LMSR (bottom view) von Mises Stress Contour Plot, Max. Stress: 46.6 ksi (Inertia Loading, No Twist, One Tank)

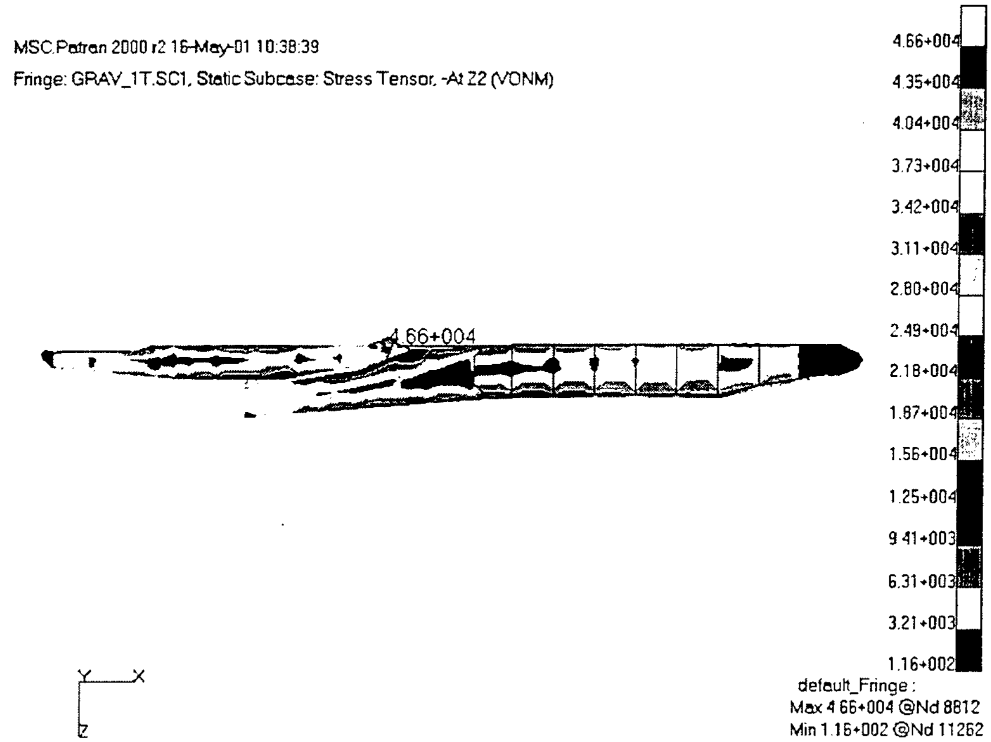

Figure 58. LMSR (right view) von Mises Stress Contour Plot, Max. Stress: 46.6 ksi (Inertia Loading, No Twist, One Tank)

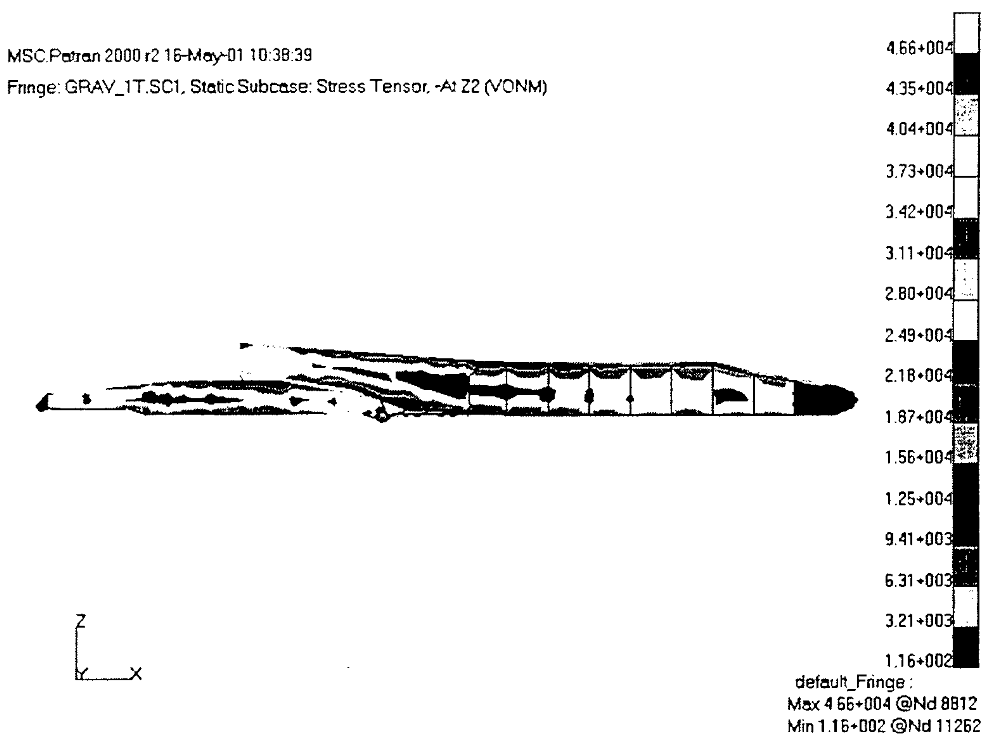

Figure 59. LMSR (left view) von Mises Stress Contour Plot, Max. Stress: 46.6 ksi (Inertia Loading, No Twist, One Tank)

Figure 60. LMSR (close-up) von Mises Stress Contour Plot, Max. Stress: 46.6 ksi (Inertia Loading, No Twist, One Tank)

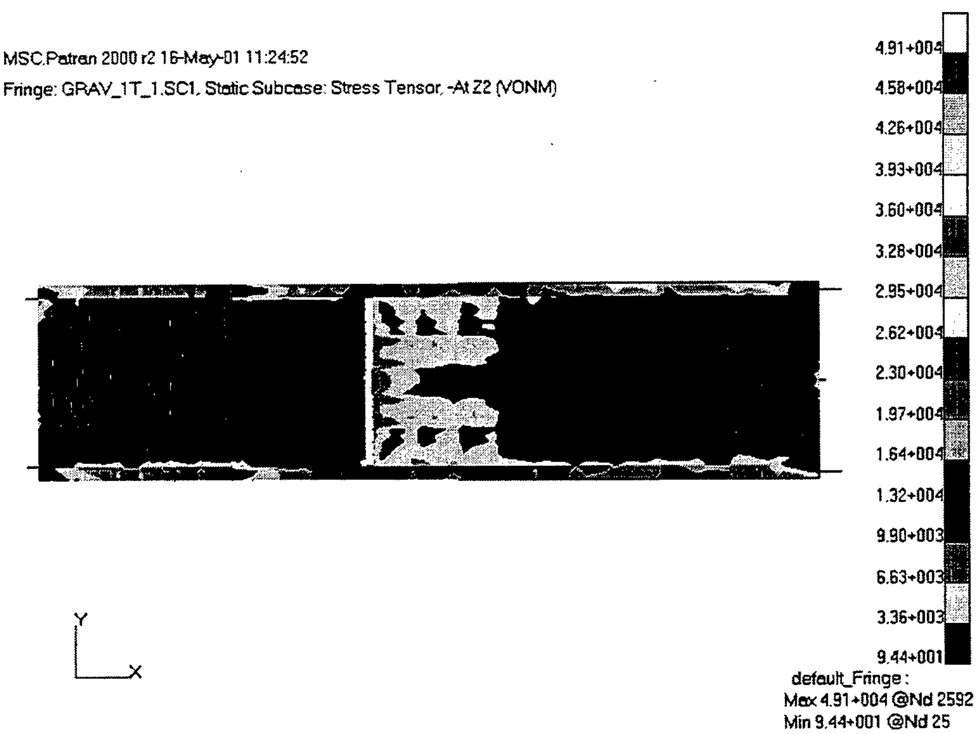

Figure 61. LMSR (top view) von Mises Stress Contour Plot, Max. Stress: 49.1 ksi (Inertia Loading, 1 Degree Twist, One Tank)

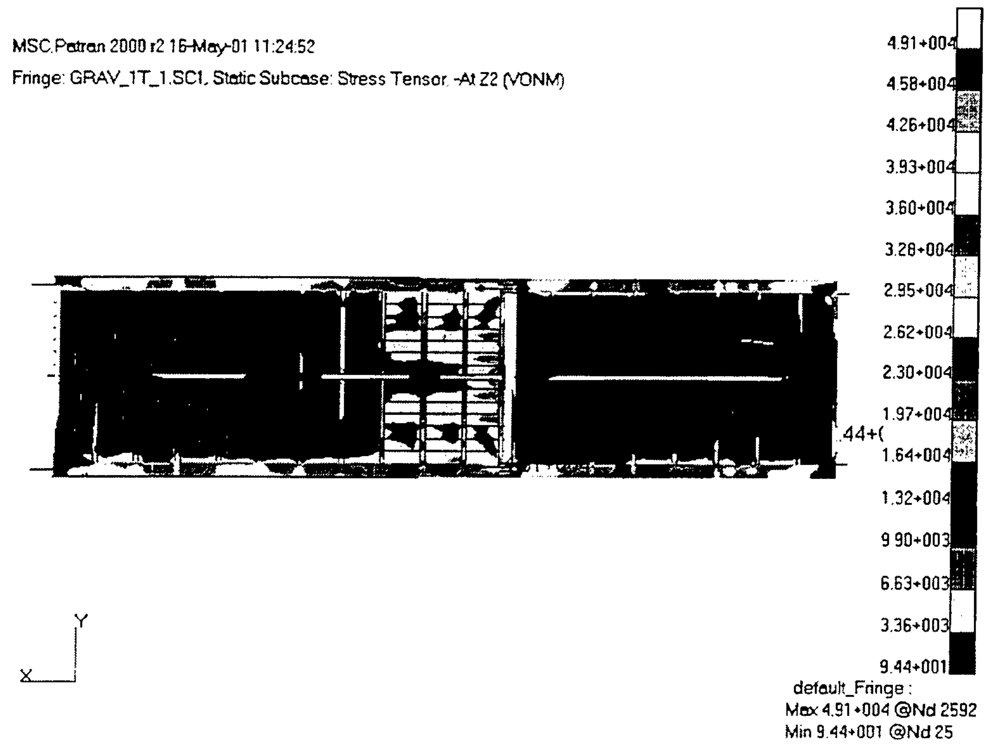

Figure 62. LMSR (bottom view) von Mises Stress Contour Plot, Max. Stress: 49.1 ksi (Inertia Loading, 1 Degree Twist, One Tank)

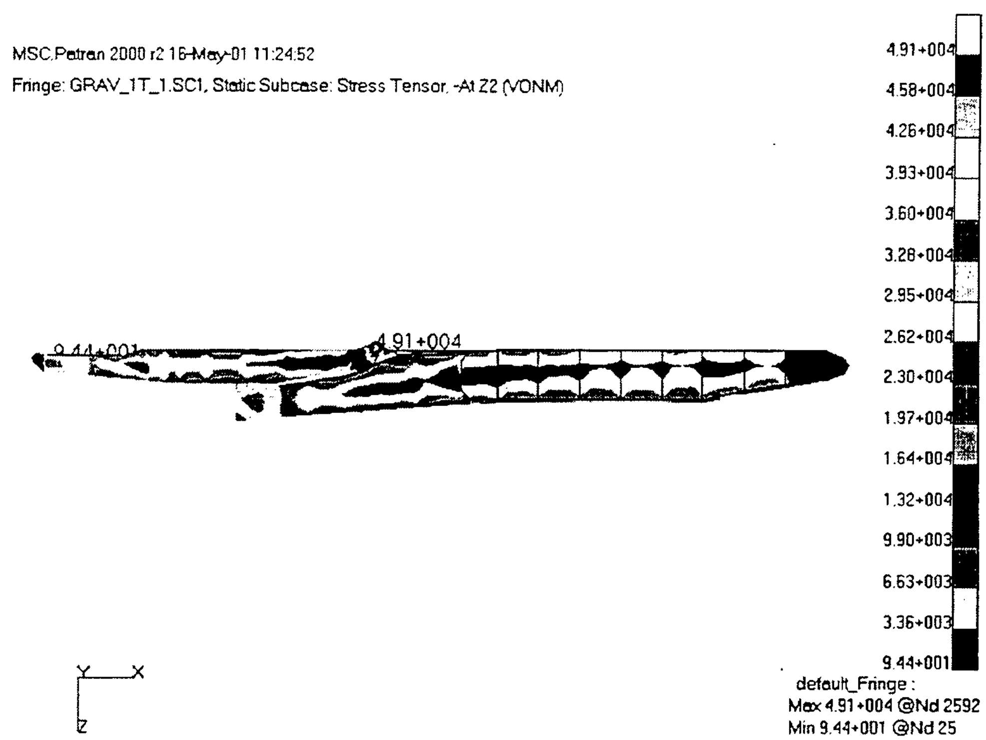

Figure 63. LMSR (right view) von Mises Stress Contour Plot, Max. Stress: 49.1 ksi (Inertia Loading, 1 Degree Twist, One Tank)

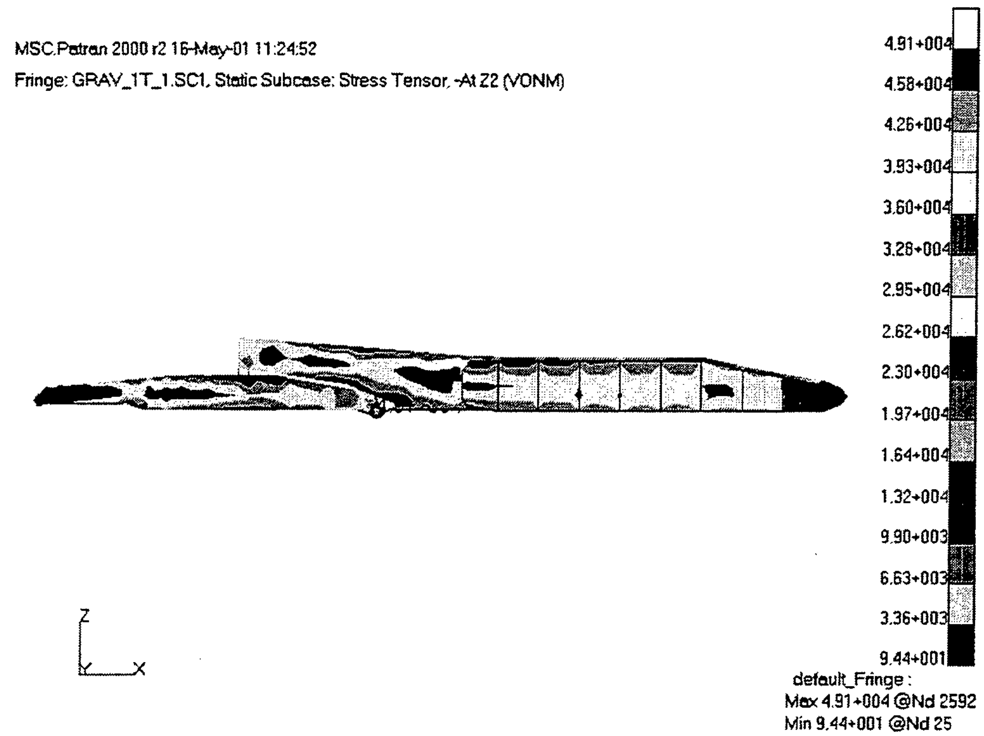

Figure 64. LMSR (left view) von Mises Stress Contour Plot, Max. Stress: 49.1 ksi (Inertia Loading, 1 Degree Twist, One Tank)

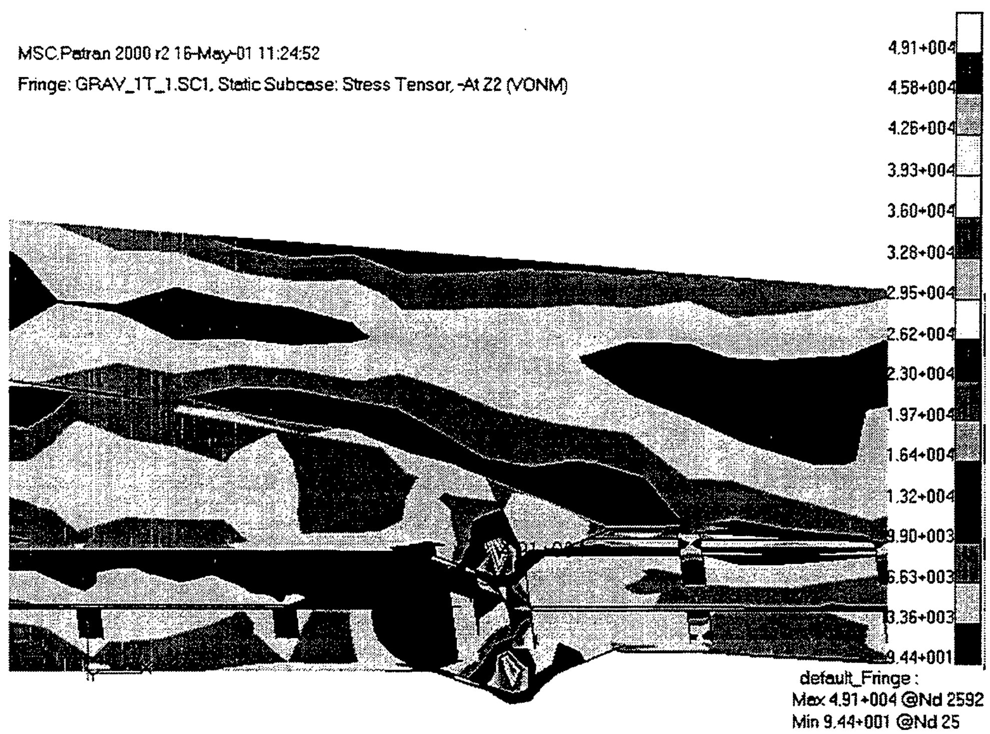

Figure 65. LMSR (close-up) von Mises Stress Contour Plot, Max. Stress: 49.1 ksi (Inertia Loading, 1 Degree Twist, One Tank)

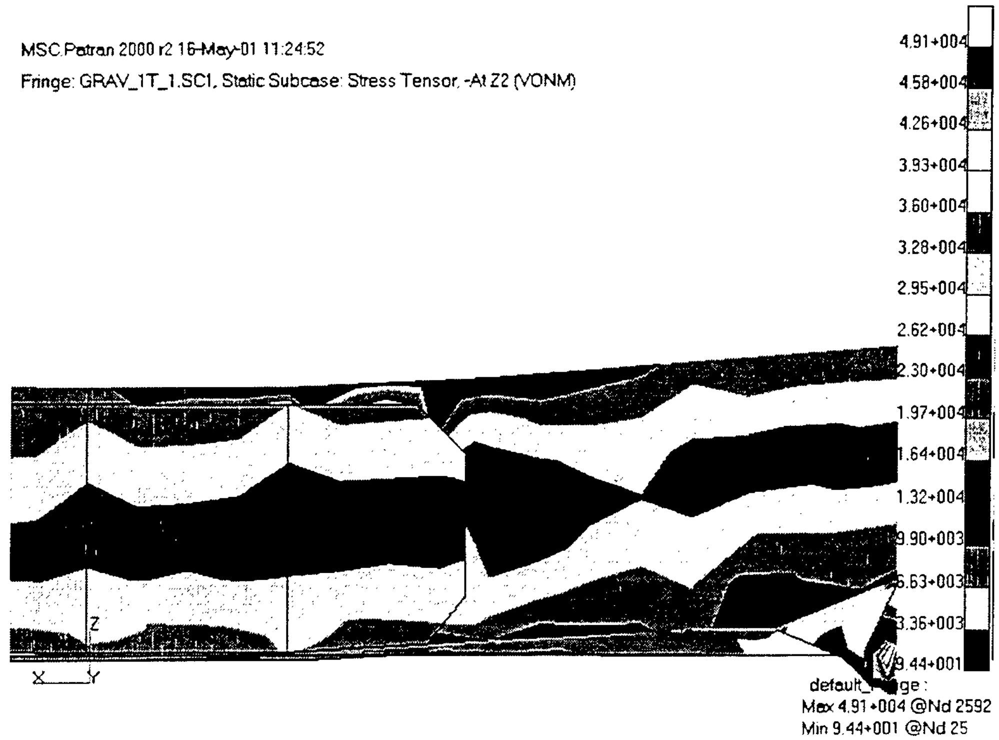

Figure 66. LMSR (close-up) von Mises Stress Contour Plot, Max. Stress: 49.1 ksi (Inertia Loading, 1 Degree Twist, One Tank)

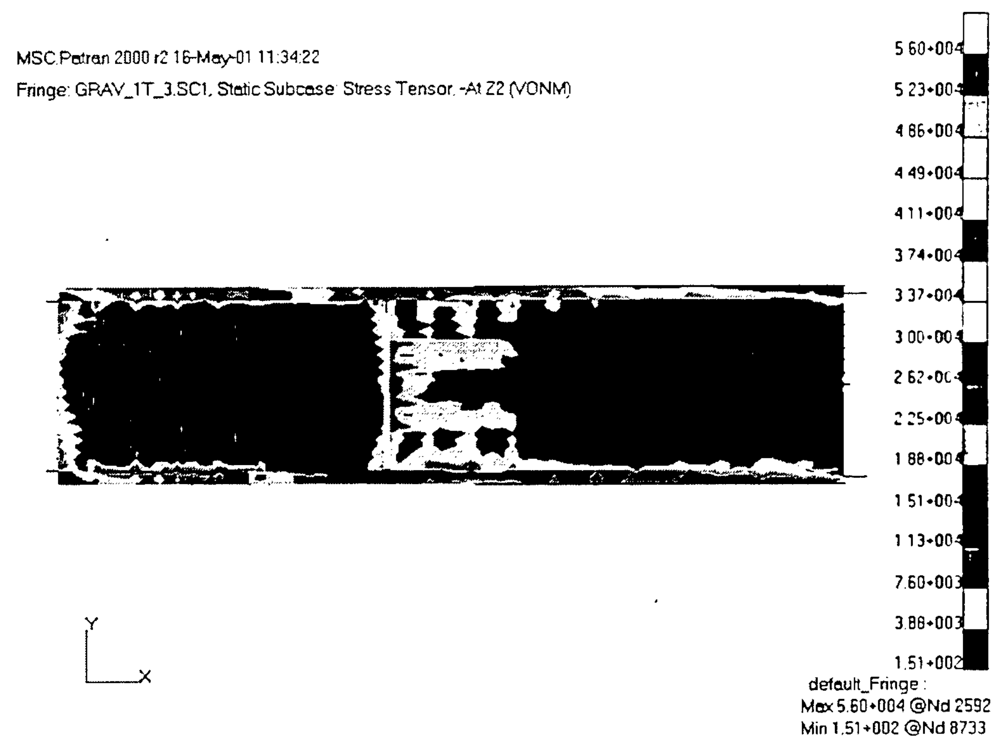

Figure 67. LMSR (top view) von Mises Stress Contour Plot, Max. Stress: 56.0 ksi (Inertia Loading, 3 Degree Twist, One Tank)

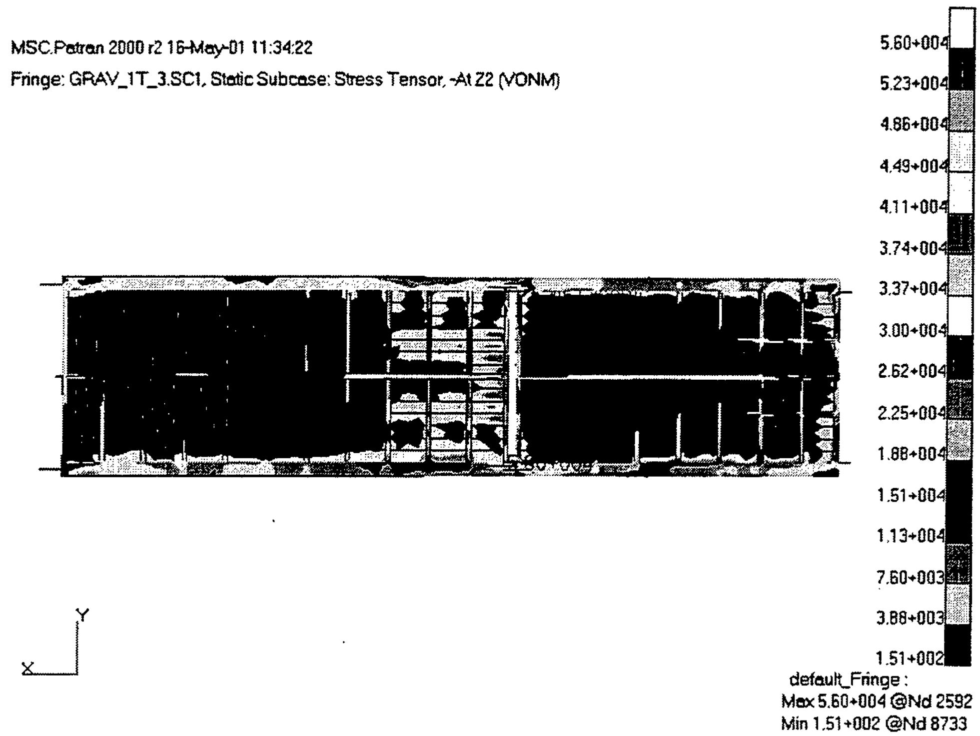

Figure 68. LMSR (bottom view) von Mises Stress Contour Plot, Max. Stress: 56.0 ksi (Inertia Loading, 3 Degree Twist, One Tank)

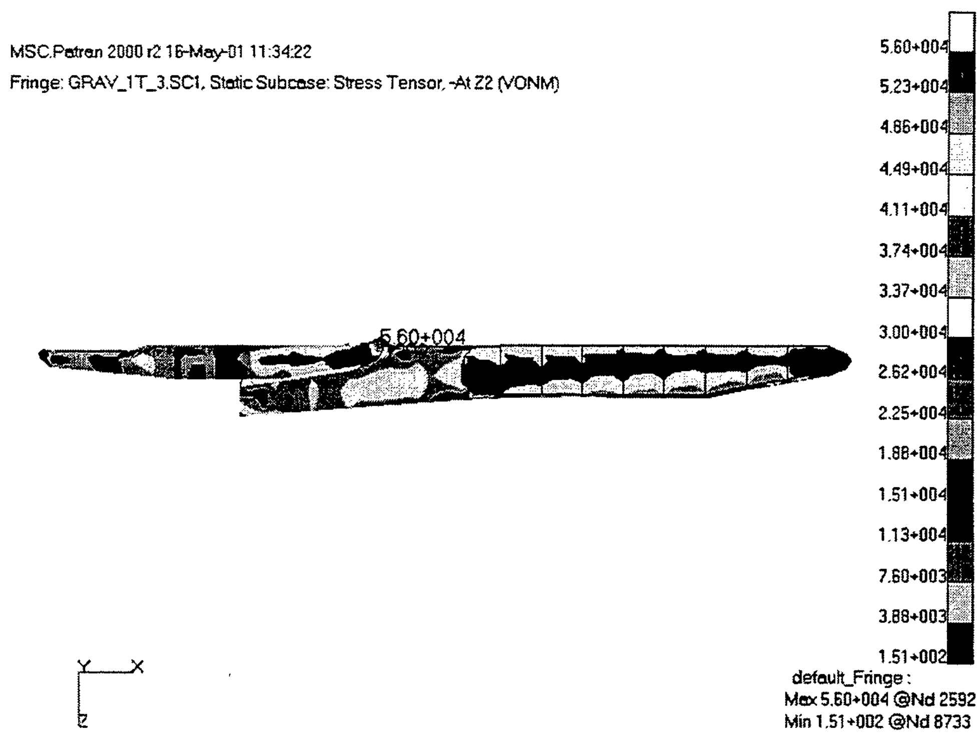

Figure 69. LMSR (right view) von Mises Stress Contour Plot, Max. Stress: 56.0 ksi (Inertia Loading, 3 Degree Twist, One Tank)

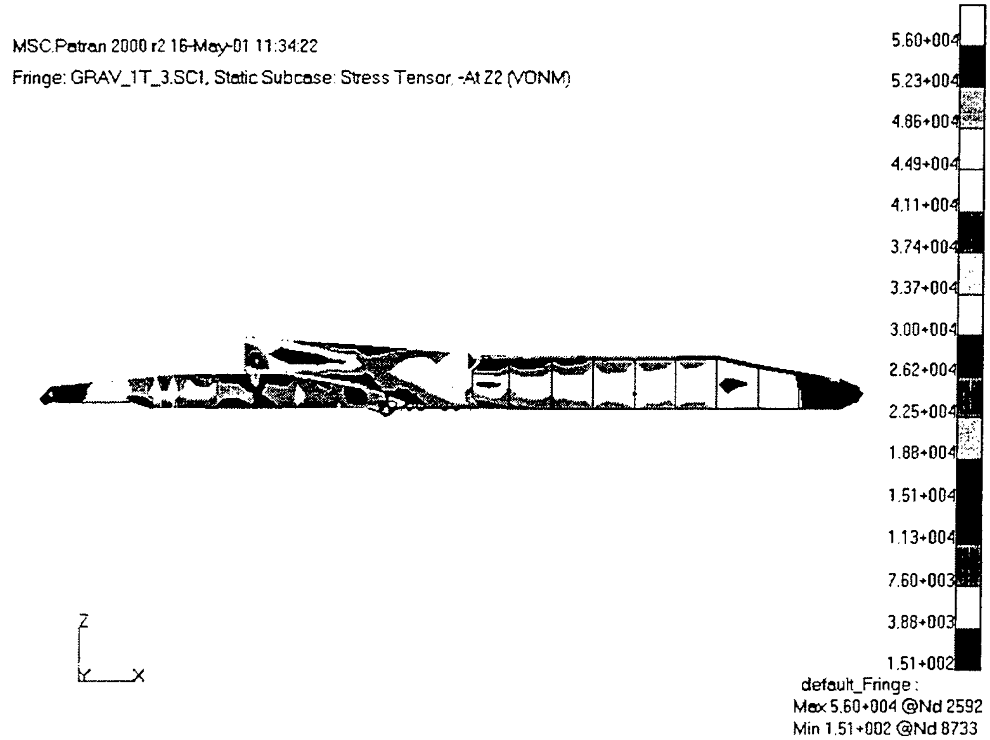

Figure 70. LMSR (left view) von Mises Stress Contour Plot, Max. Stress: 56.0 ksi (Inertia Loading, 3 Degree Twist, One Tank)

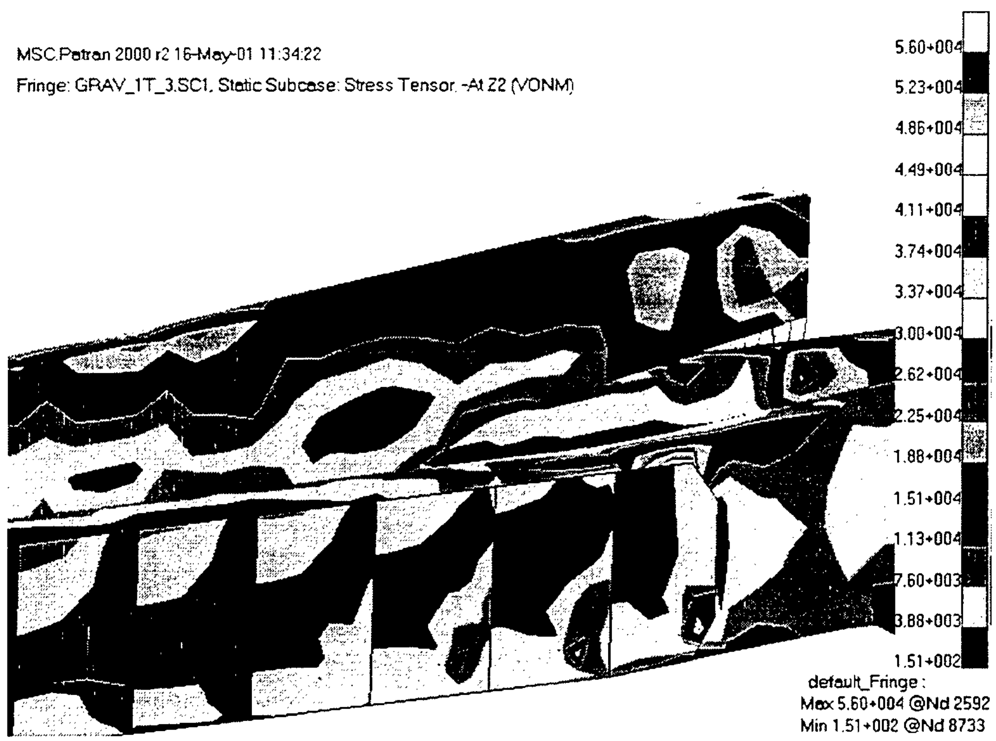

Figure 71. LMSR (close-up) von Mises Stress Contour Plot, Max. Stress: 56.0 ksi (Inertia Loading, 3 Degree Twist, One Tank)

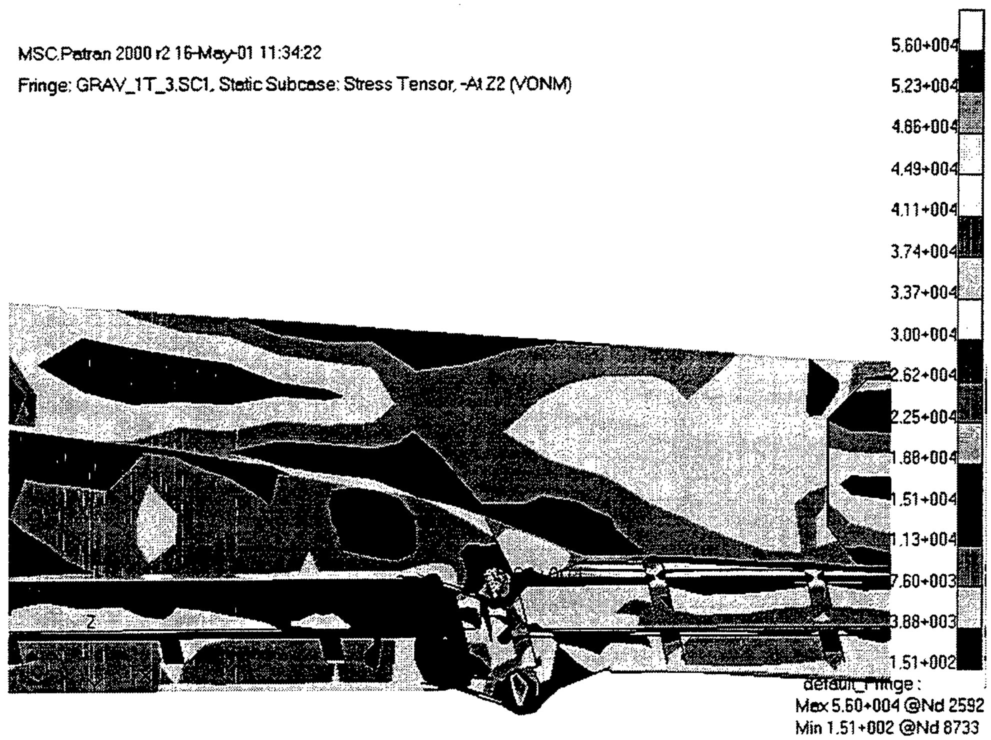

Figure 72. LMSR (close-up) von Mises Stress Contour Plot, Max. Stress: 56.0 ksi (Inertia Loading, 3 Degree Twist, One Tank)

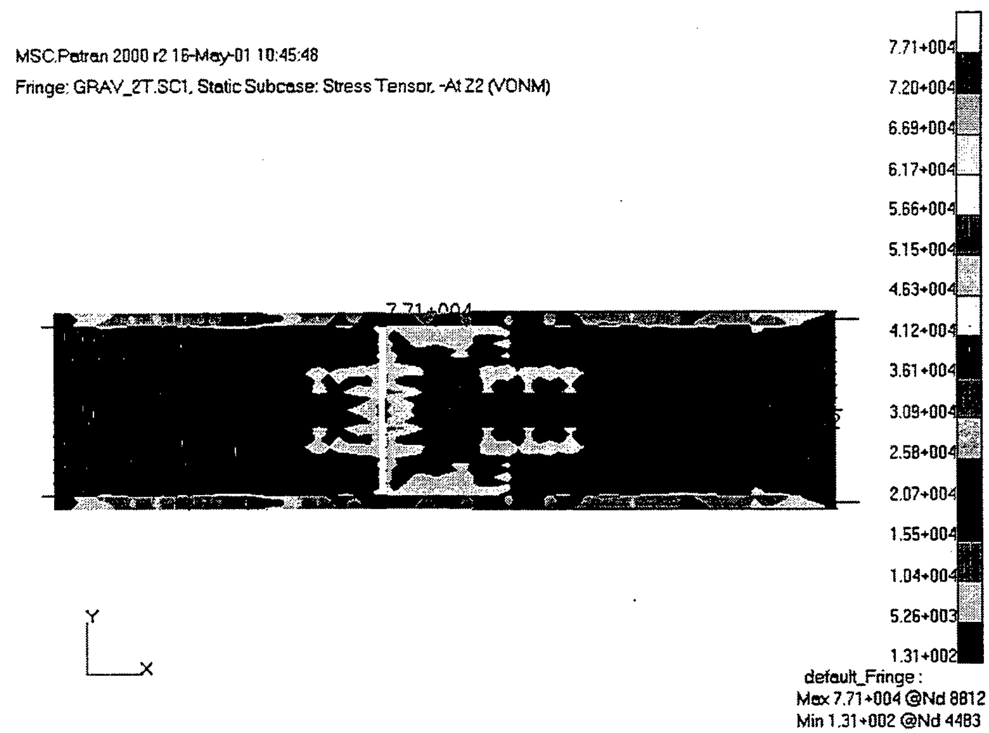

Figure 73. LMSR (top view) von Mises Stress Contour Plot, Max. Stress: 77.1 ksi (Inertia Loading, No Twist, Two Tanks)

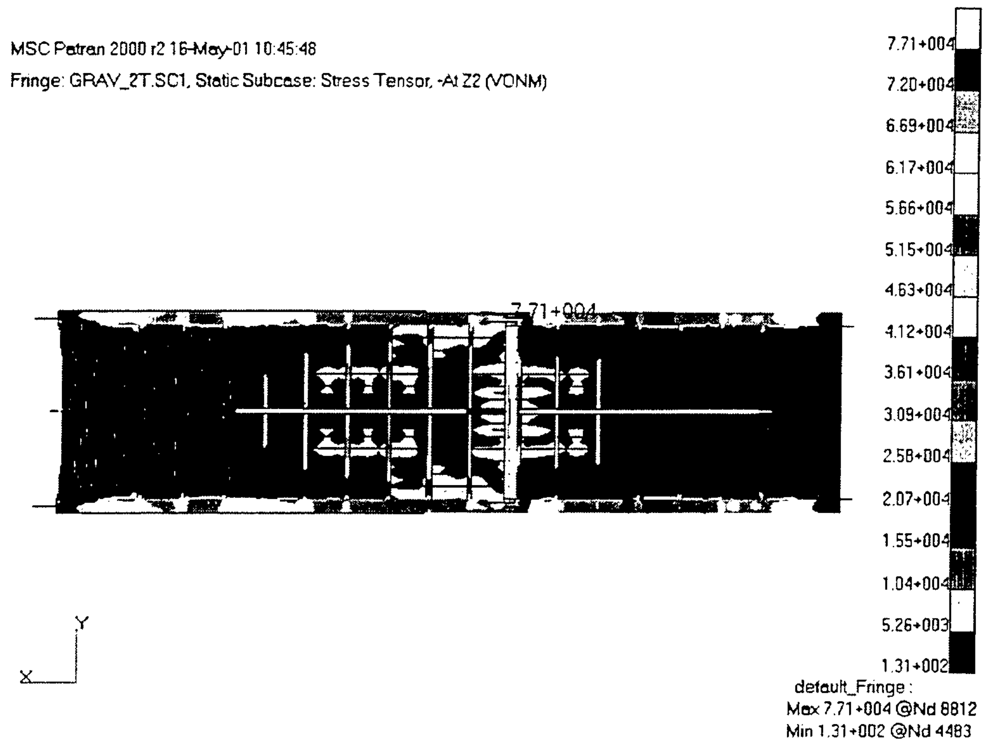

Figure 74. LMSR (bottom view) von Mises Stress Contour Plot, Max. Stress: 77.1 ksi (Inertia Loading, No Twist, Two Tanks)

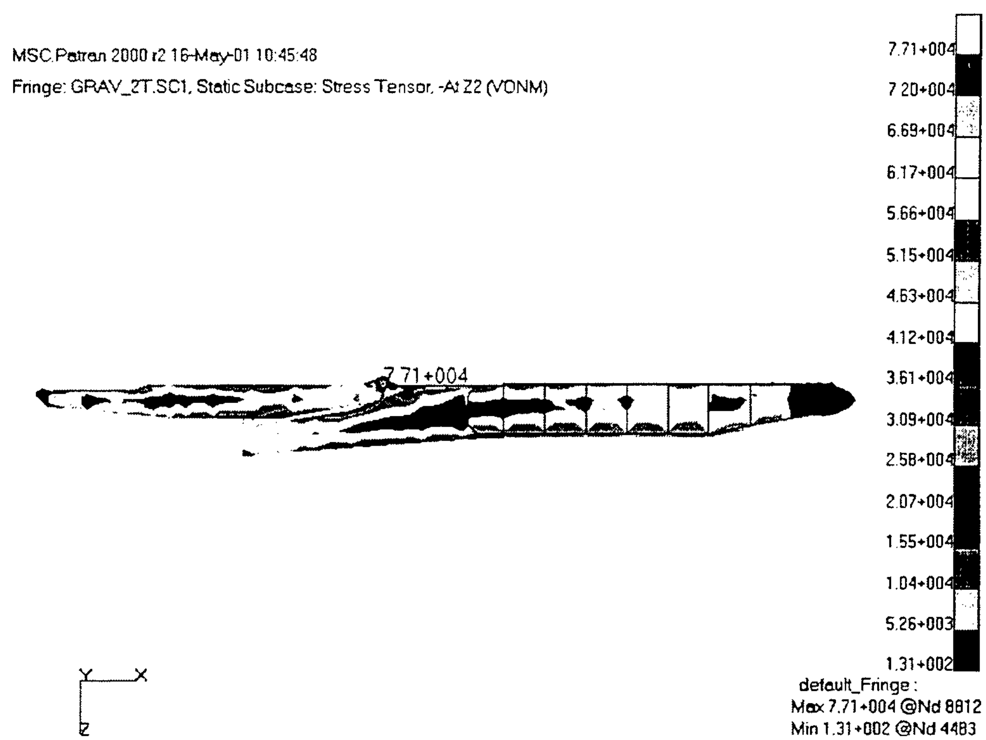

Figure 75. LMSR (right view) von Mises Stress Contour Plot, Max. Stress: 77.1 ksi (Inertia Loading, No Twist, Two Tanks)

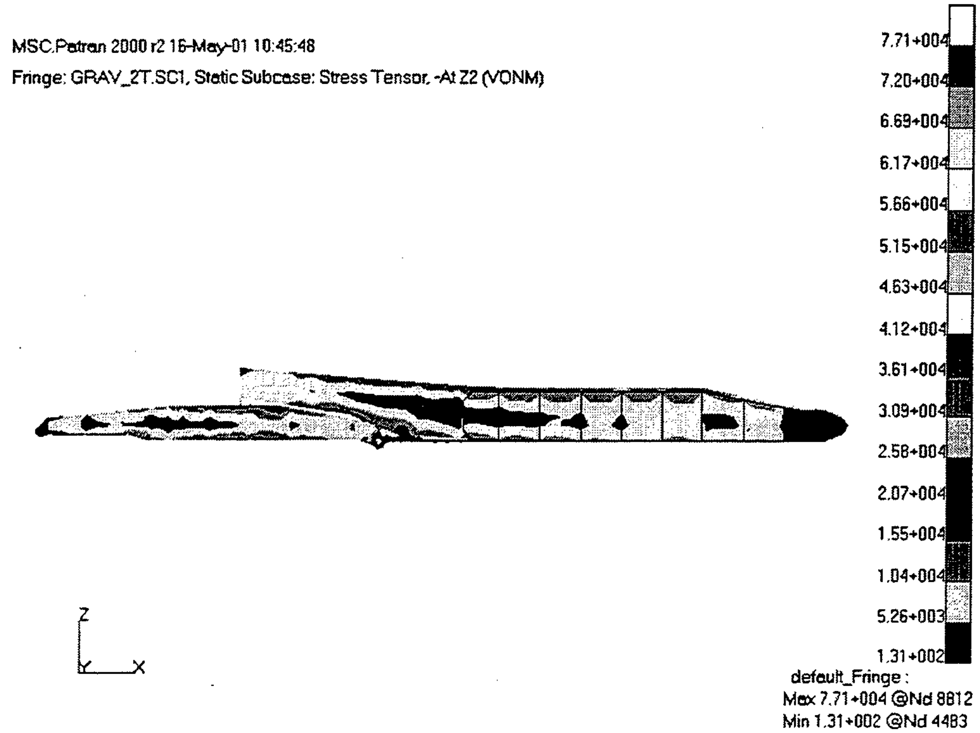

Figure 76. LMSR (left view) von Mises Stress Contour Plot, Max. Stress: 77.1 ksi (Inertia Loading, No Twist, Two Tanks)

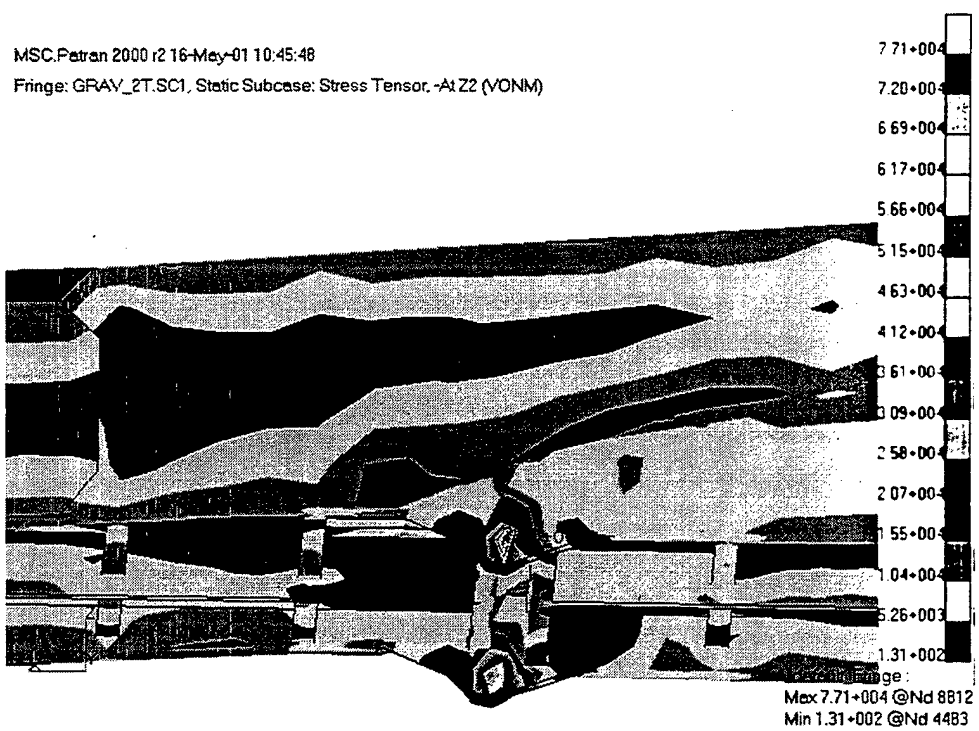

Figure 77. LMSR (close-up) von Mises Stress Contour Plot, Max. Stress: 77.1 ksi (Inertia Loading, No Twist, Two Tanks)

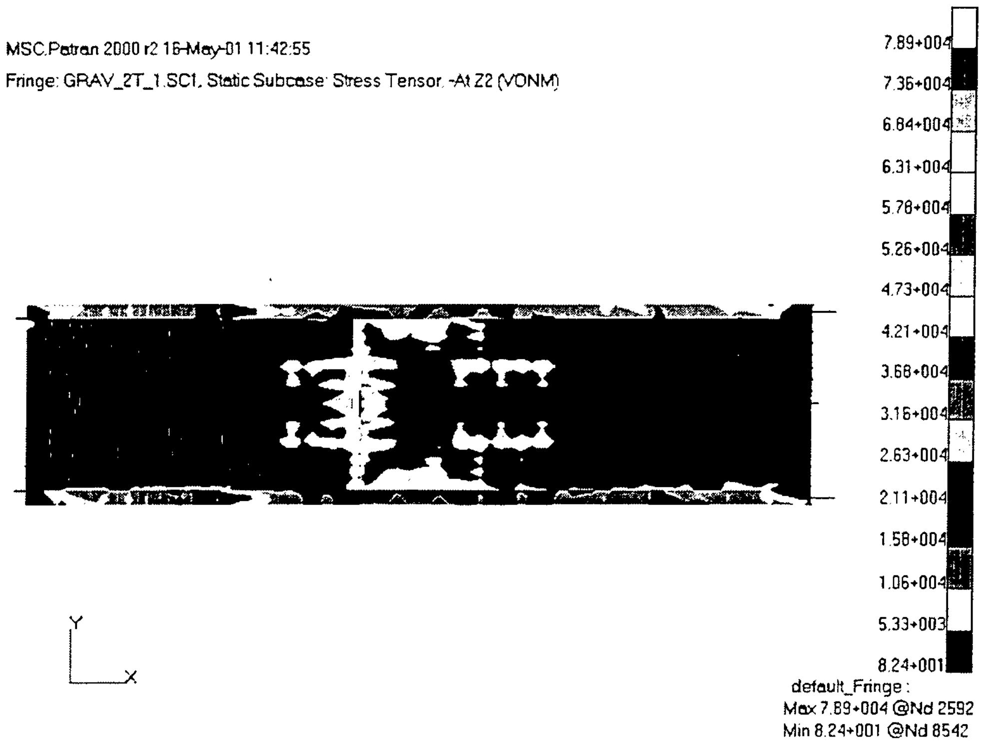

Figure 78. LMSR (top view) von Mises Stress Contour Plot, Max. Stress: 78.9 ksi (Inertia Loading, 1 Degree Twist, Two Tanks)

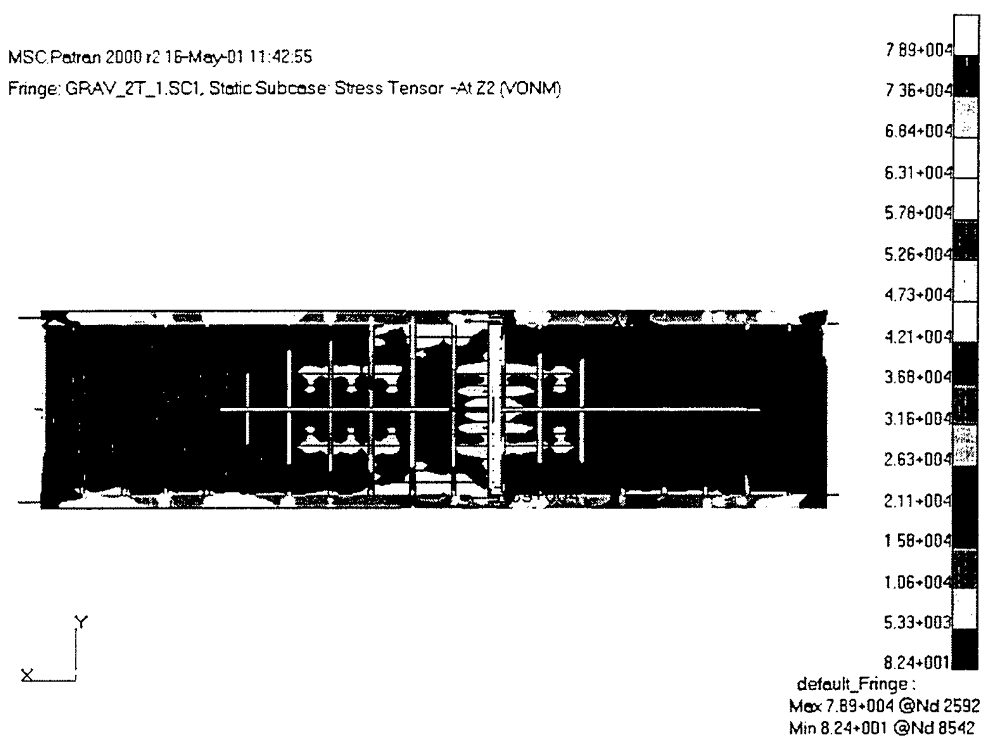

Figure 79. LMSR (bottom view) von Mises Stress Contour Plot, Max. Stress: 78.9 ksi (Inertia Loading, 1 Degree Twist, Two Tanks)

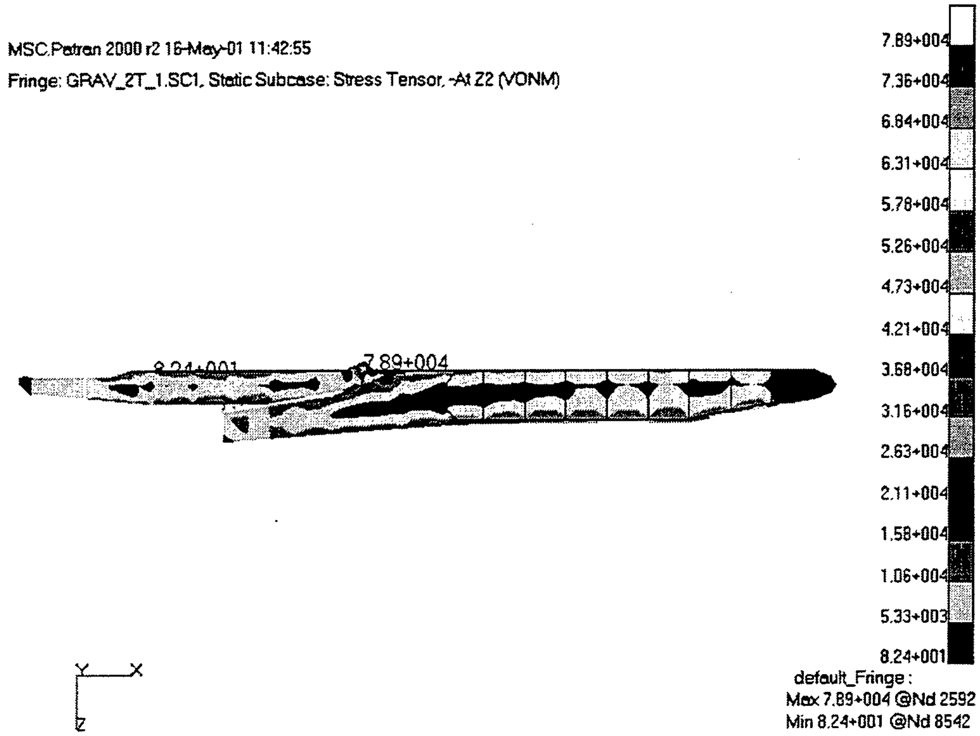

Figure 80. LMSR (right view) von Mises Stress Contour Plot, Max. Stress: 78.9 ksi (Inertia Loading, 1 Degree Twist, Two Tanks)

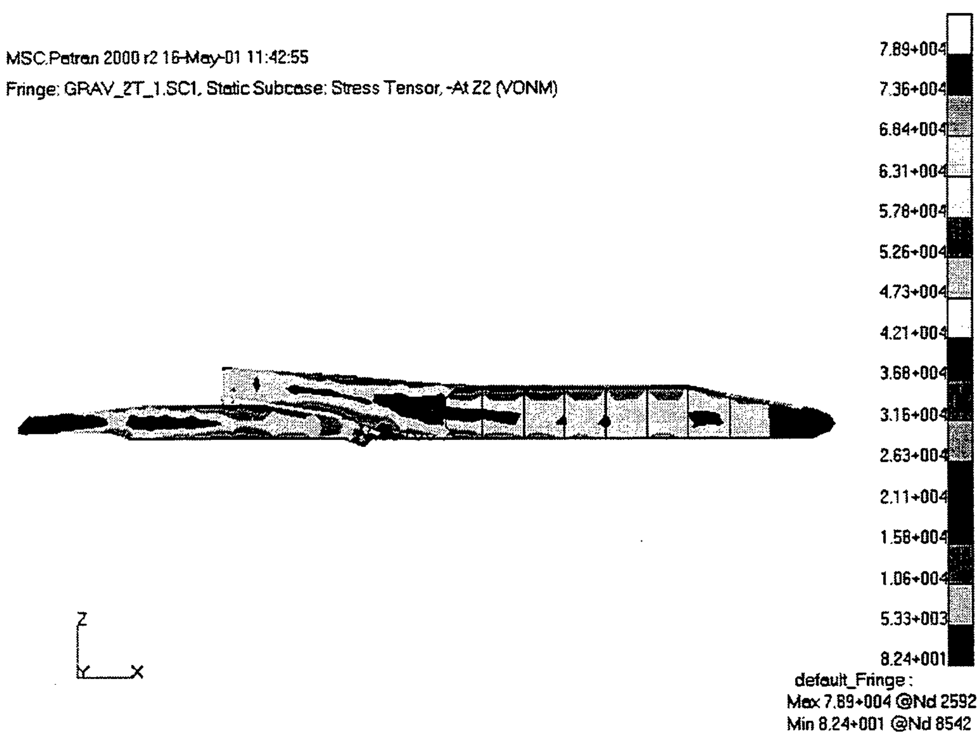

Figure 81. LMSR (left view) von Mises Stress Contour Plot, Max. Stress: 78.9 ksi (Inertia Loading, 1 Degree Twist, Two Tanks)

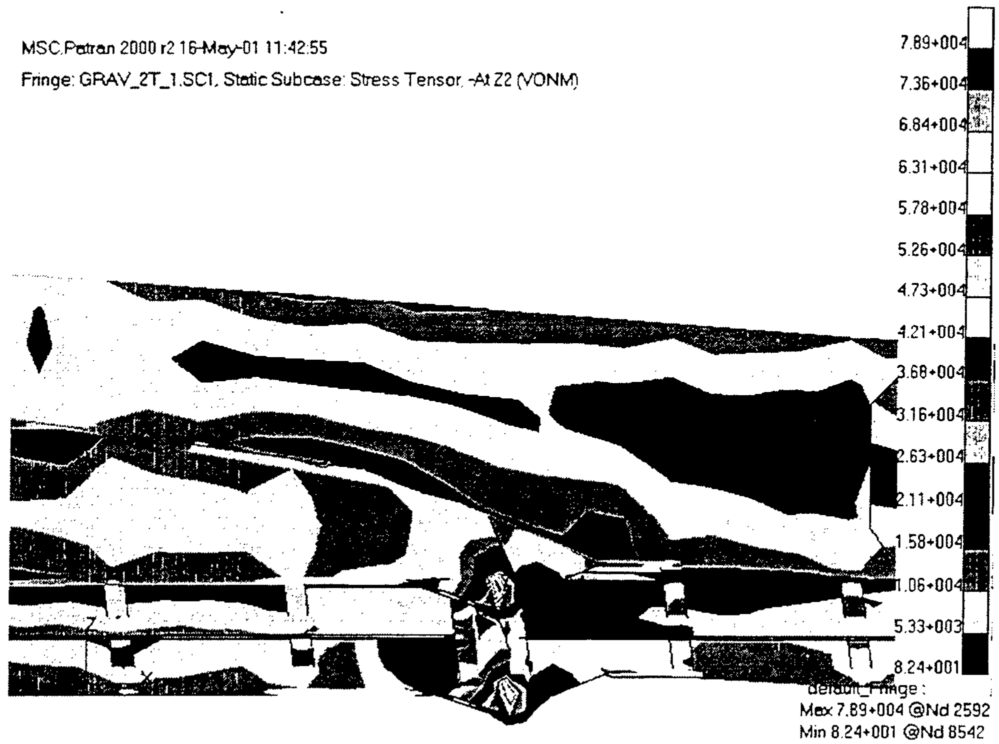

Figure 82. LMSR (close-up) von Mises Stress Contour Plot, Max. Stress: 78.9 ksi (Inertia Loading, 1 Degree Twist, Two Tanks)

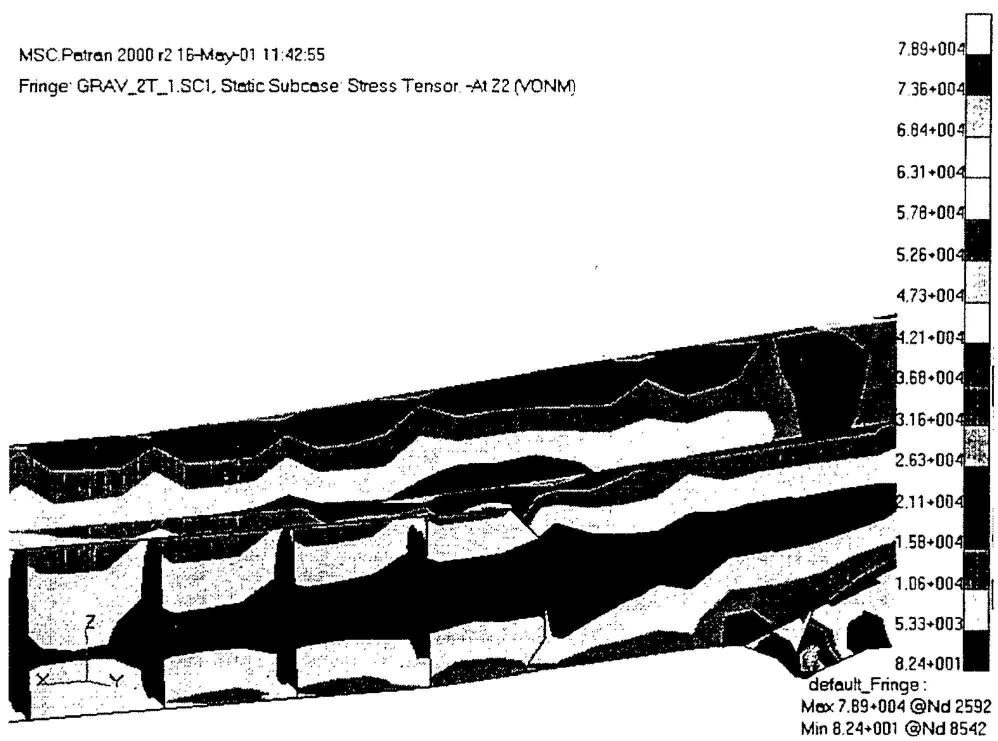

Figure 83. LMSR (close-up) von Mises Stress Contour Plot, Max. Stress: 78.9 ksi (Inertia Loading, 1 Degree Twist, Two Tanks)

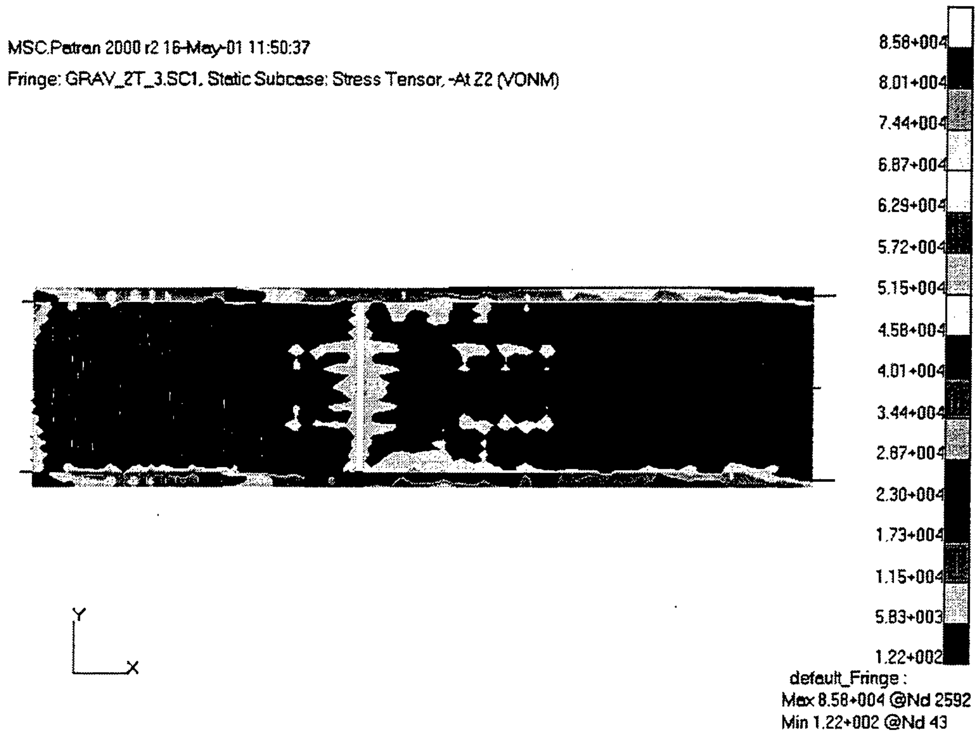

Figure 84. LMSR (top view) von Mises Stress Contour Plot, Max. Stress: 85.8 ksi (Inertia Loading, 3 Degree Twist, Two Tanks)

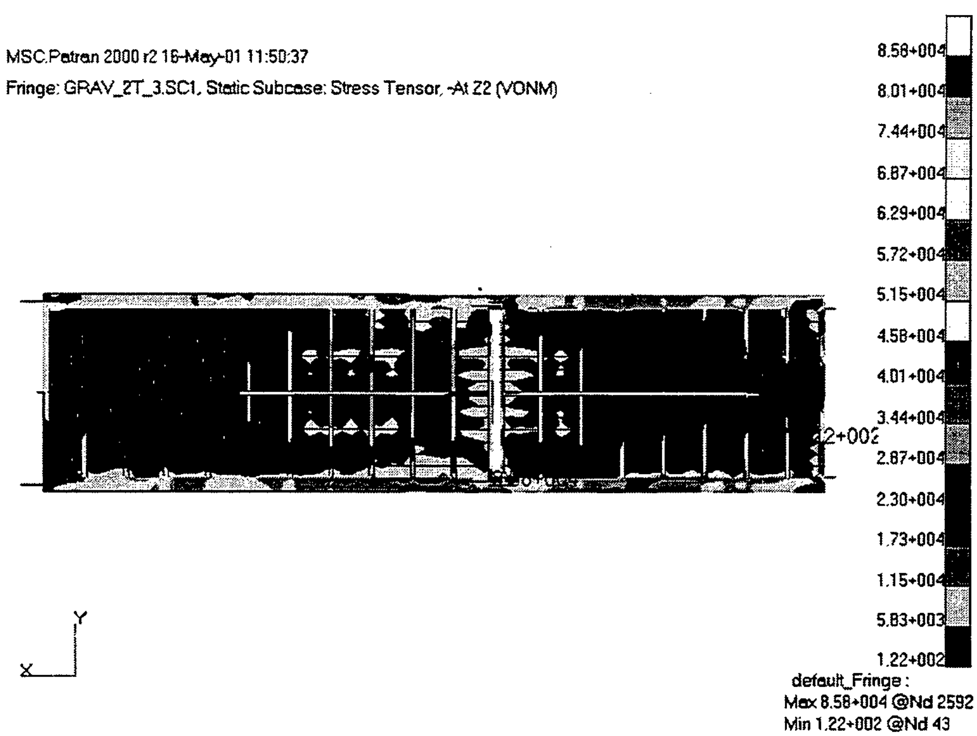

Figure 85. LMSR (bottom view) von Mises Stress Contour Plot, Max. Stress: 85.8 ksi (Inertia Loading, 3 Degree Twist, Two Tanks)

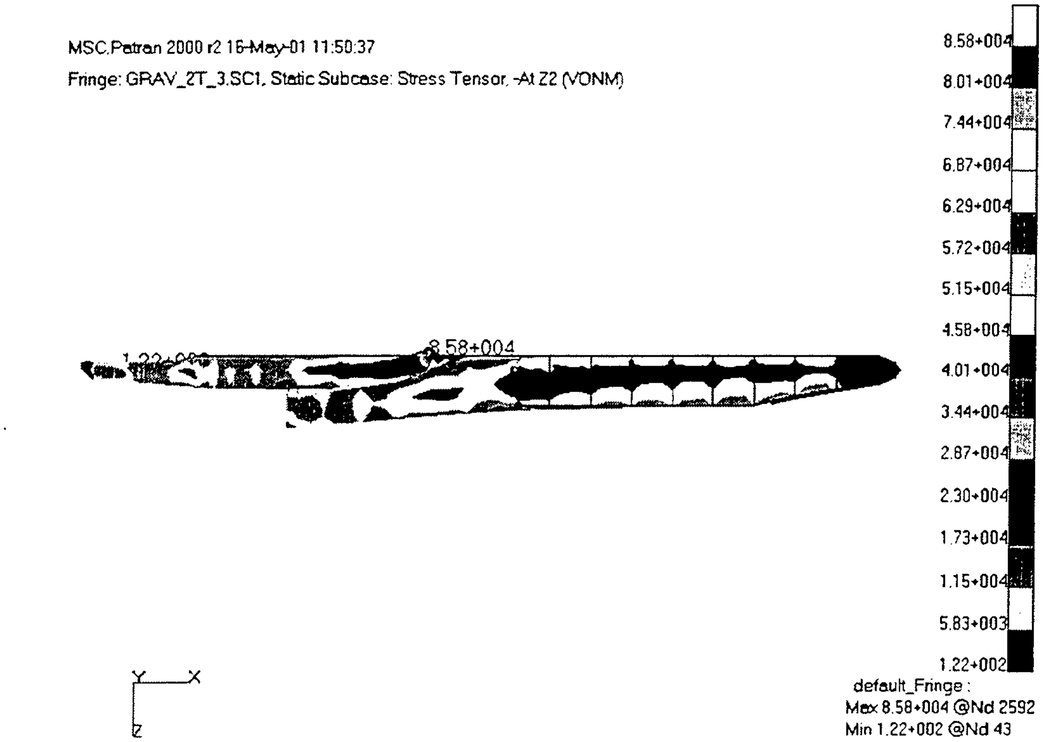

Figure 86. LMSR (right view) von Mises Stress Contour Plot, Max. Stress: 85.8 ksi (Inertia Loading, 3 Degree Twist, Two Tanks)

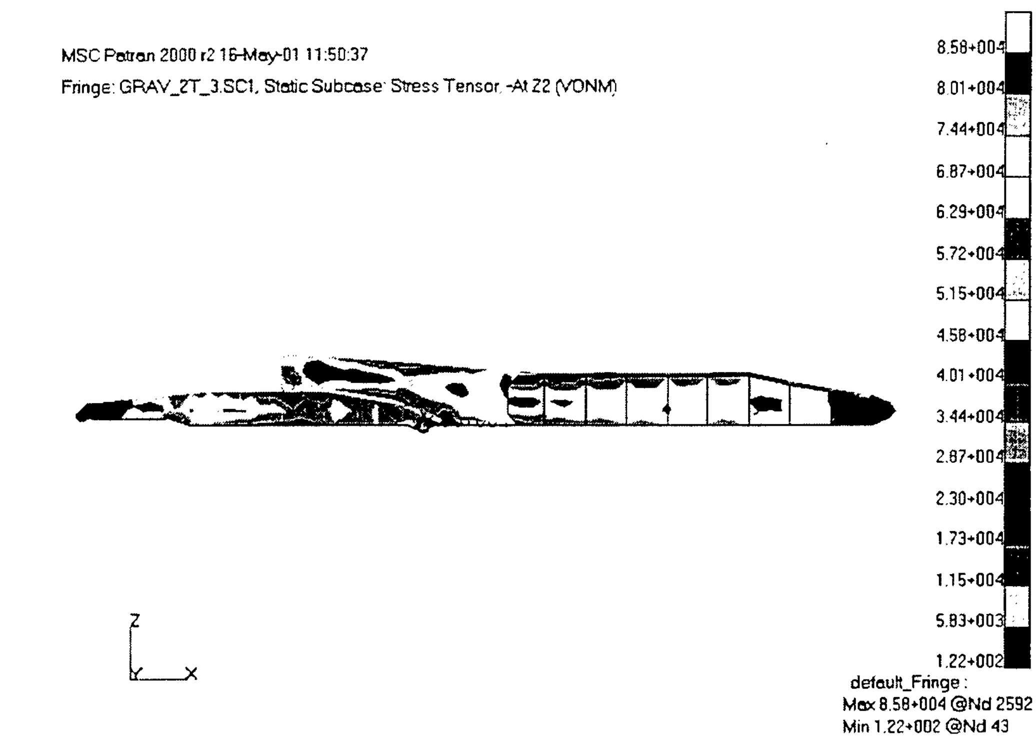

Figure 87. LMSR (left view) von Mises Stress Contour Plot, Max. Stress: 85.8 ksi (Inertia Loading, 3 Degree Twist, Two Tanks)

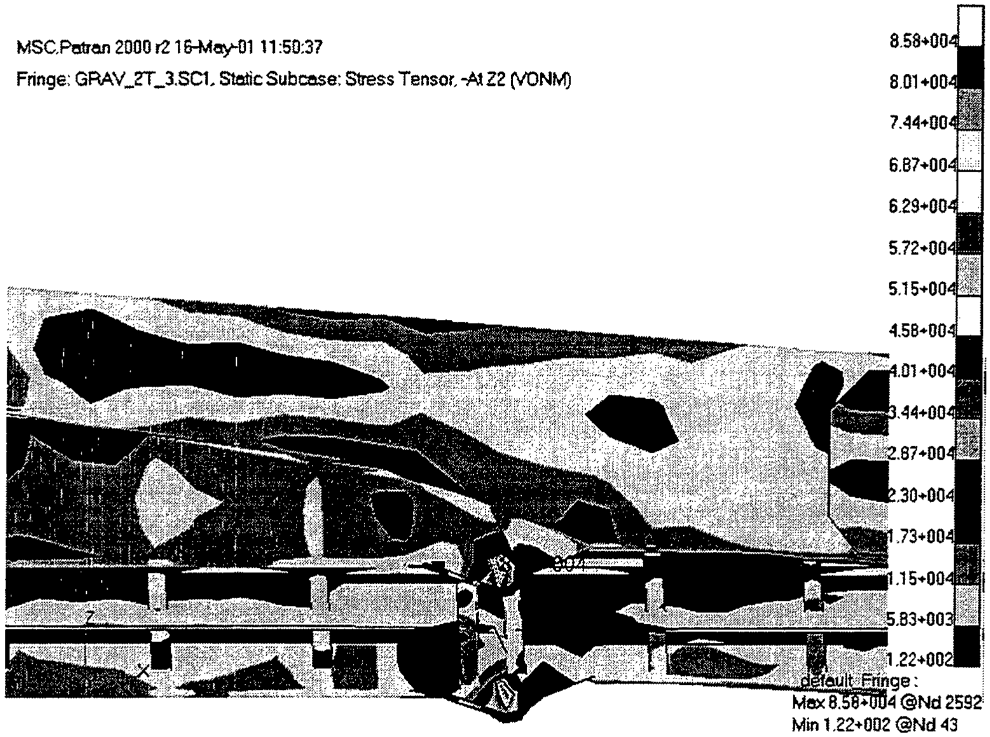

Figure 88. LMSR (close-up) von Mises Stress Contour Plot, Max. Stress: 85.8 ksi (Inertia Loading, 3 Degree Twist, Two Tanks)

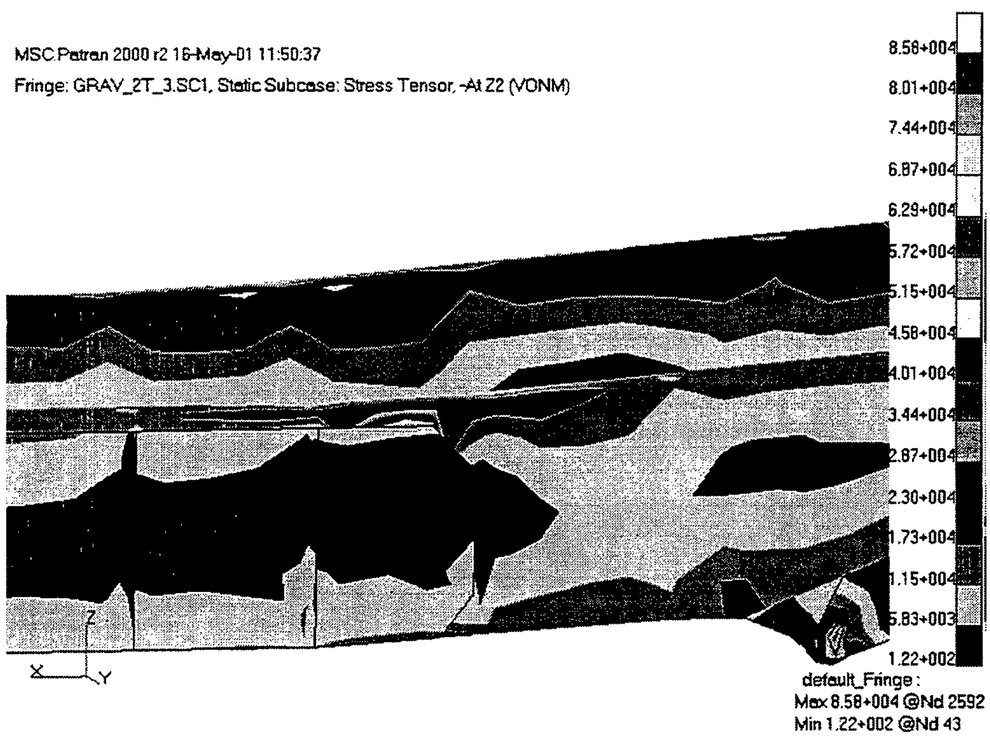

Figure 89. LMSR (close-up) von Mises Stress Contour Plot, Max. Stress: 85.8 ksi (Inertia Loading, 3 Degree Twist, Two Tanks)

2. Cape T Stern Ramp

The Cape T stern ramp analyses were conducted with the same boundary conditions as the LMSR stern ramp (restrained in the three translational DOF at the ship end and the vertical DOF at the RRDF end). Twist angles between the RRDF and ship of zero, one, and three degrees were considered. Maximum von Mises stress contour plots were generated with PATRAN and are displayed in Figures 90 through 140.

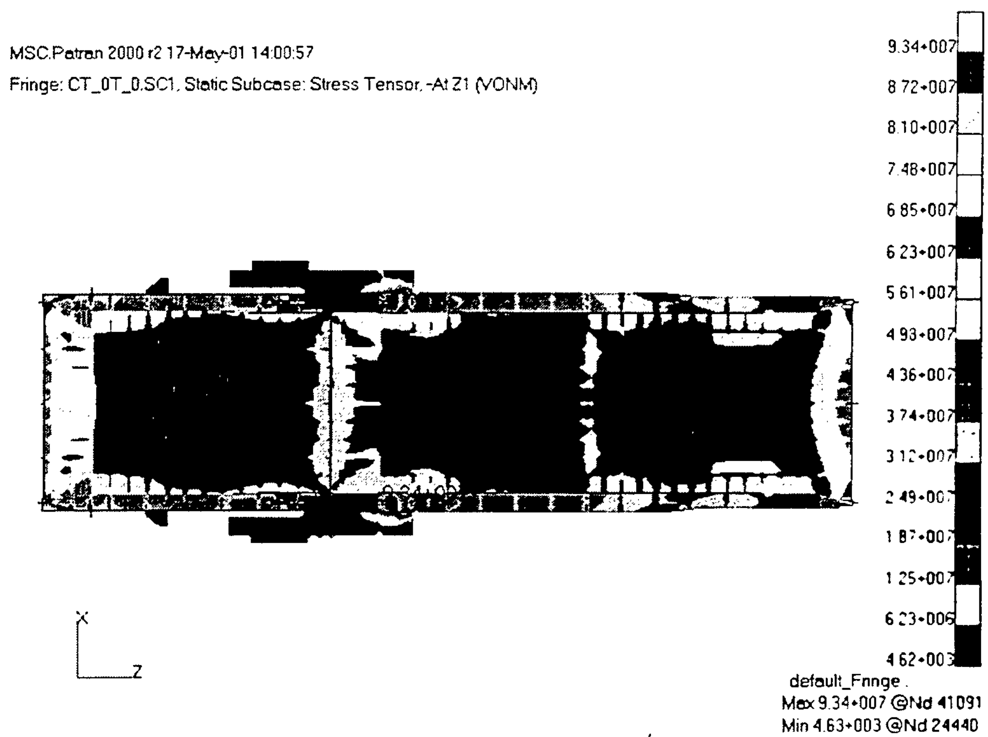

Figure 90. Cape T (top view) von Mises Stress Contour Plot, Max. Stress: 13.5 ksi (Inertia Loading, No Twist, No Tanks)

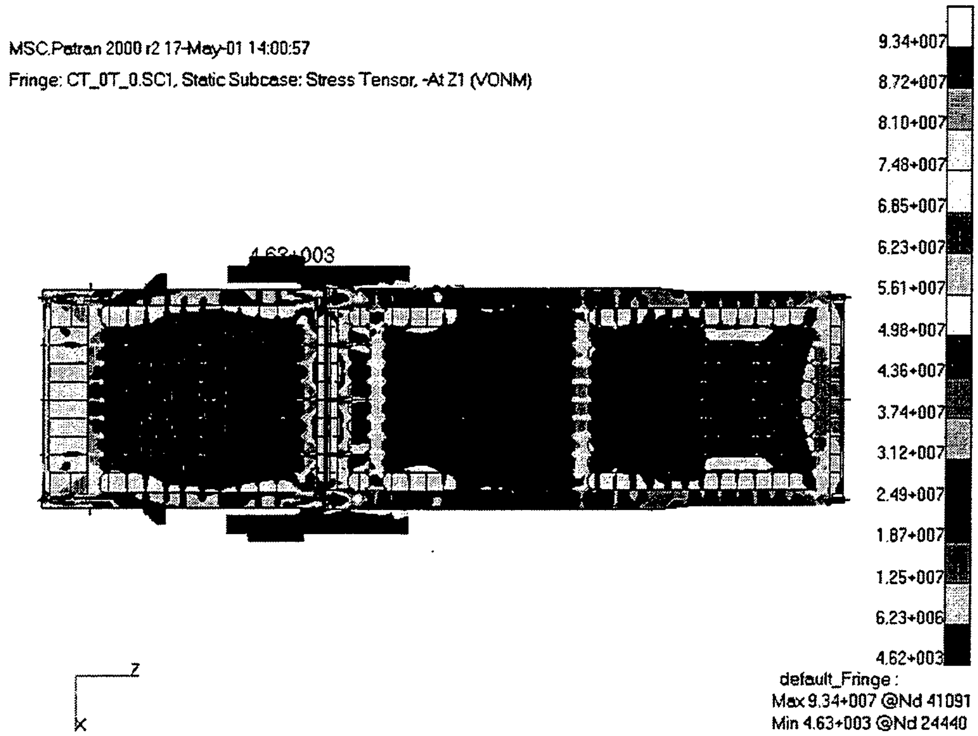

Figure 91. Cape T (bottom view) von Mises Stress Contour Plot, Max. Stress: 13.5 ksi (Inertia Loading, No Twist, No Tanks)

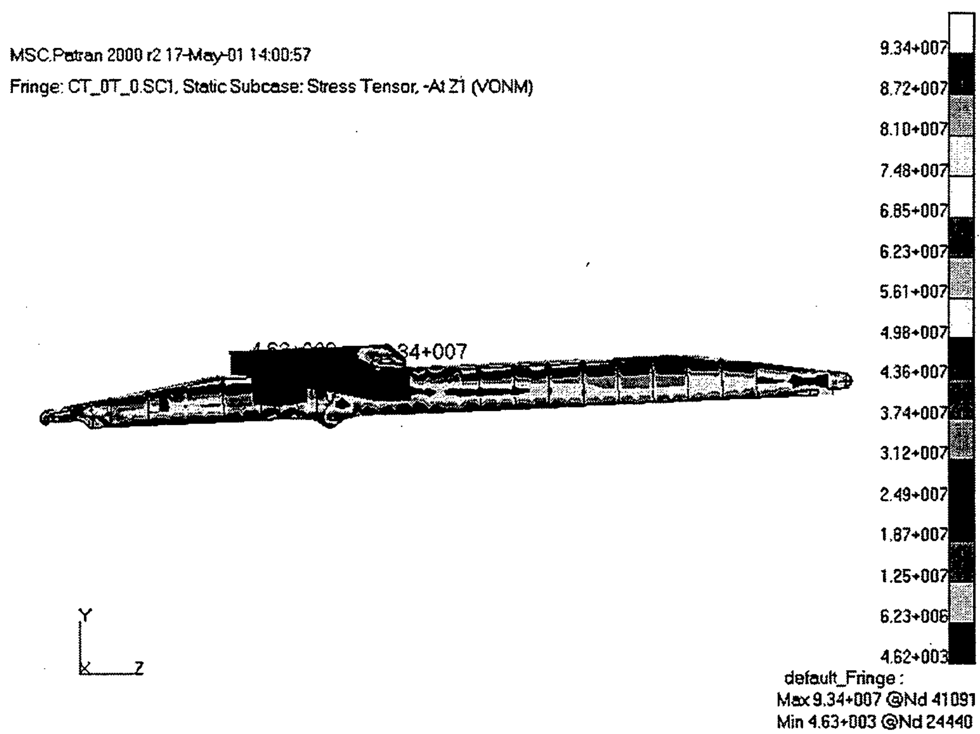

Figure 92. Cape T (left view) von Mises Stress Contour Plot, Max. Stress: 13.5 ksi (Inertia Loading, No Twist, No Tanks)

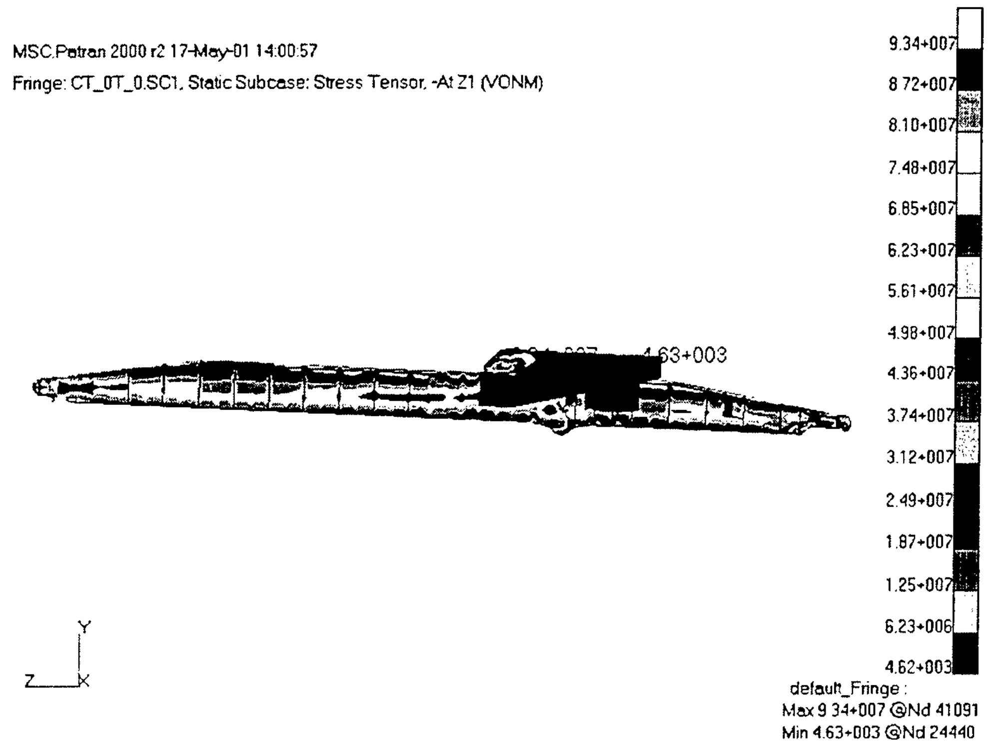

Figure 93. Cape T (right view) von Mises Stress Contour Plot, Max. Stress: 13.5 ksi (Inertia Loading, No Twist, No Tanks)

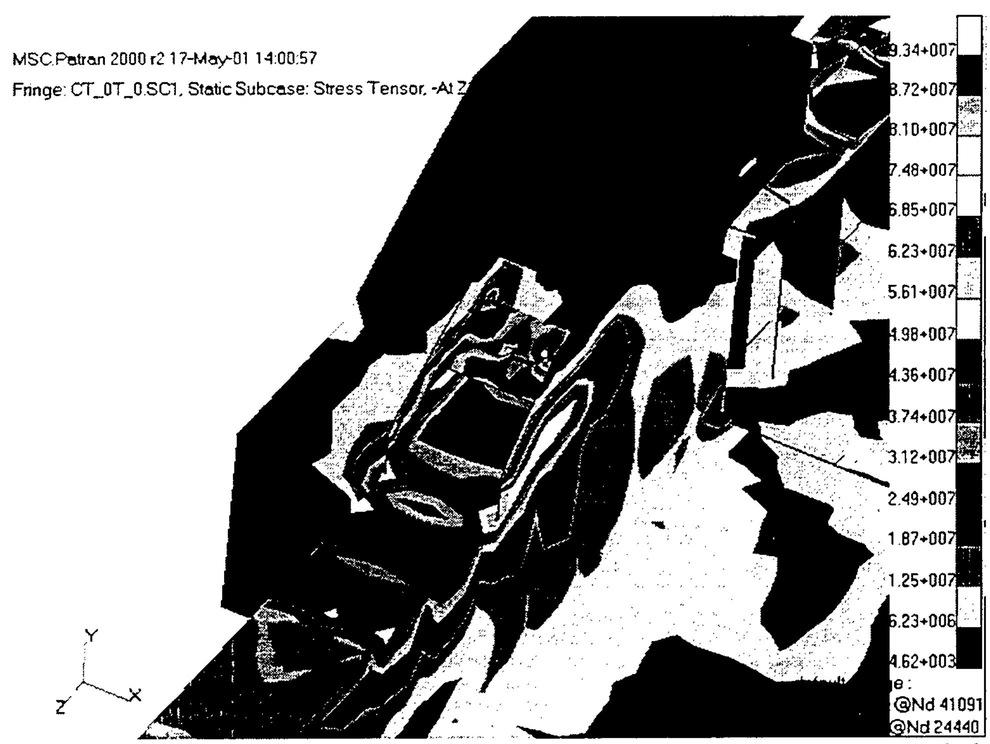

Figure 94. Cape T (close-up) von Mises Stress Contour Plot, Max. Stress: 13.5 ksi (Inertia Loading, No Twist, No Tanks)

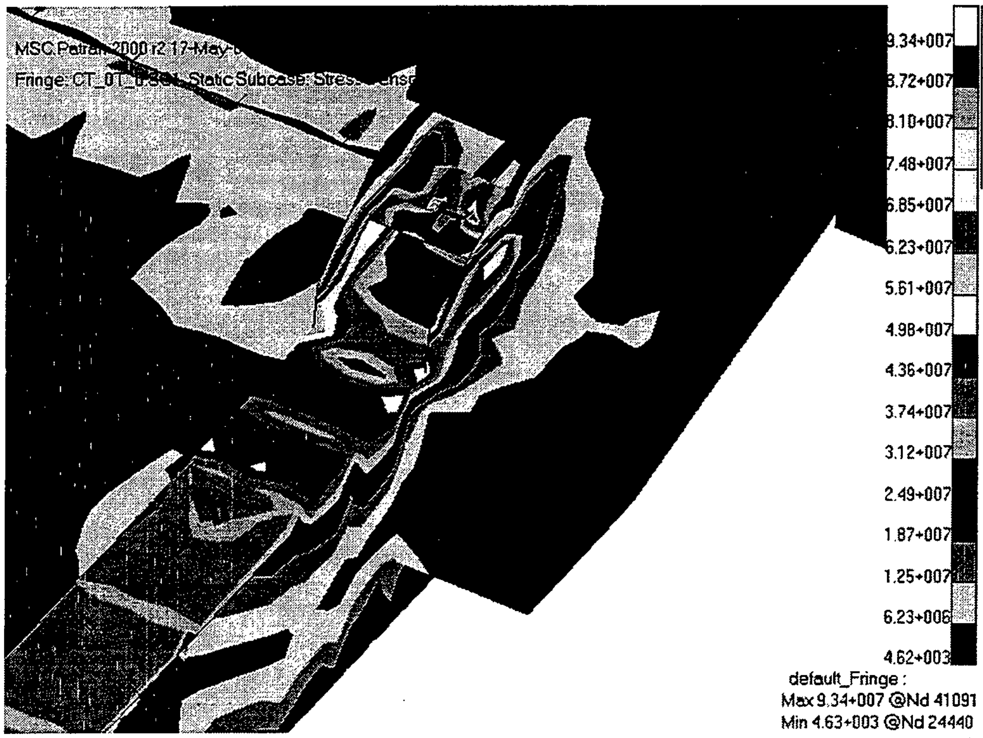

Figure 95. Cape T (close-up) von Mises Stress Contour Plot, Max. Stress: 13.5 ksi (Inertia Loading, No Twist, No Tanks)

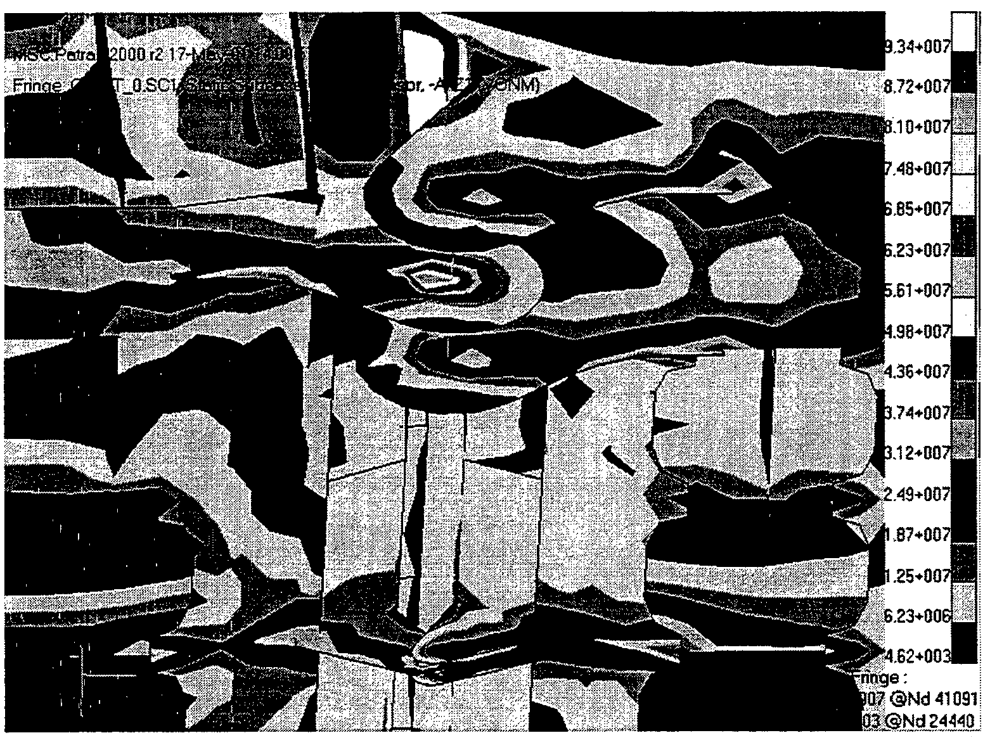

Figure 96. Cape T (close-up) von Mises Stress Contour Plot, Max. Stress: 13.5 ksi (Inertia Loading, No Twist, No Tanks)

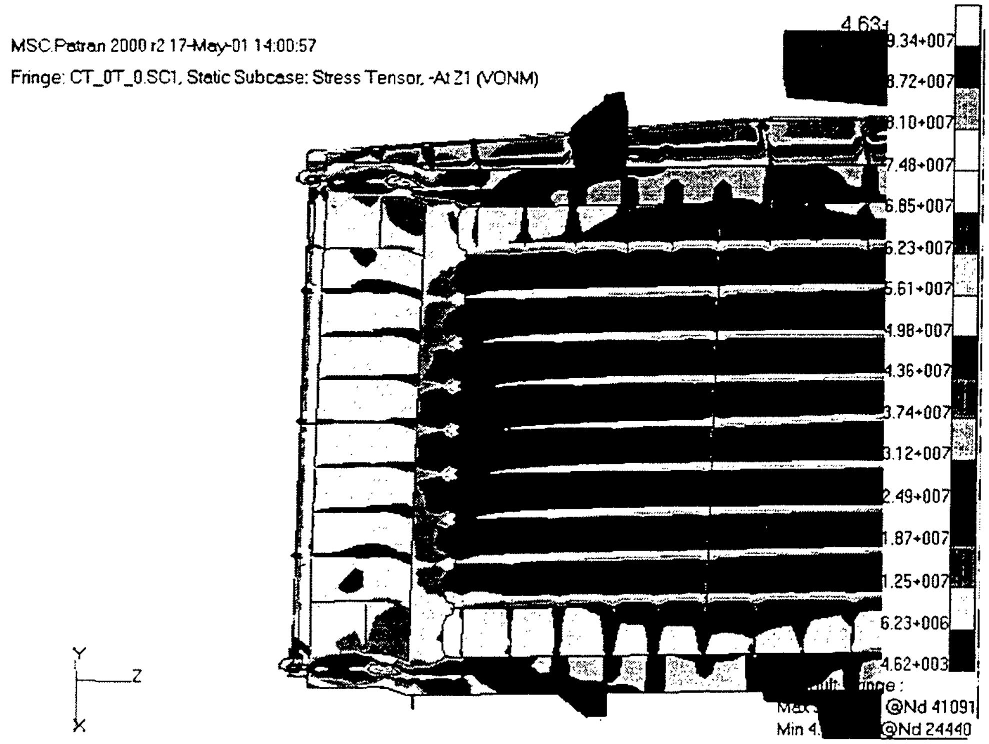

Figure 97. Cape T (close-up) von Mises Stress Contour Plot, Max. Stress: 13.5 ksi (Inertia Loading, No Twist, No Tanks)

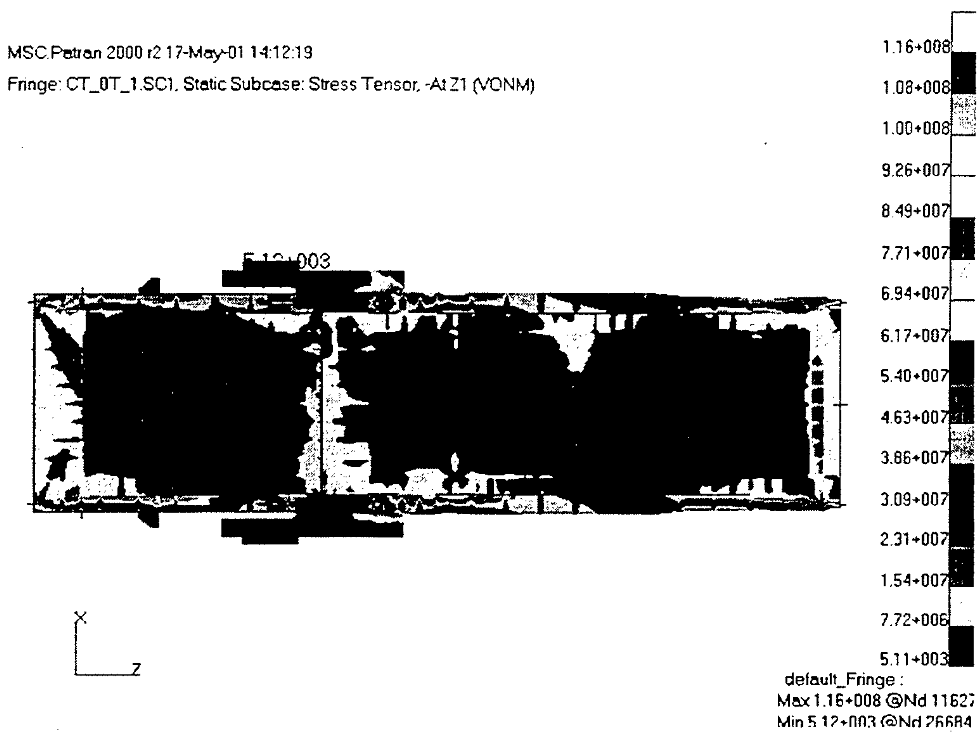

Figure 98. Cape T (top view) von Mises Stress Contour Plot, Max. Stress: 16.8 ksi (Inertia Loading, 1 Degree Twist, No Tanks)

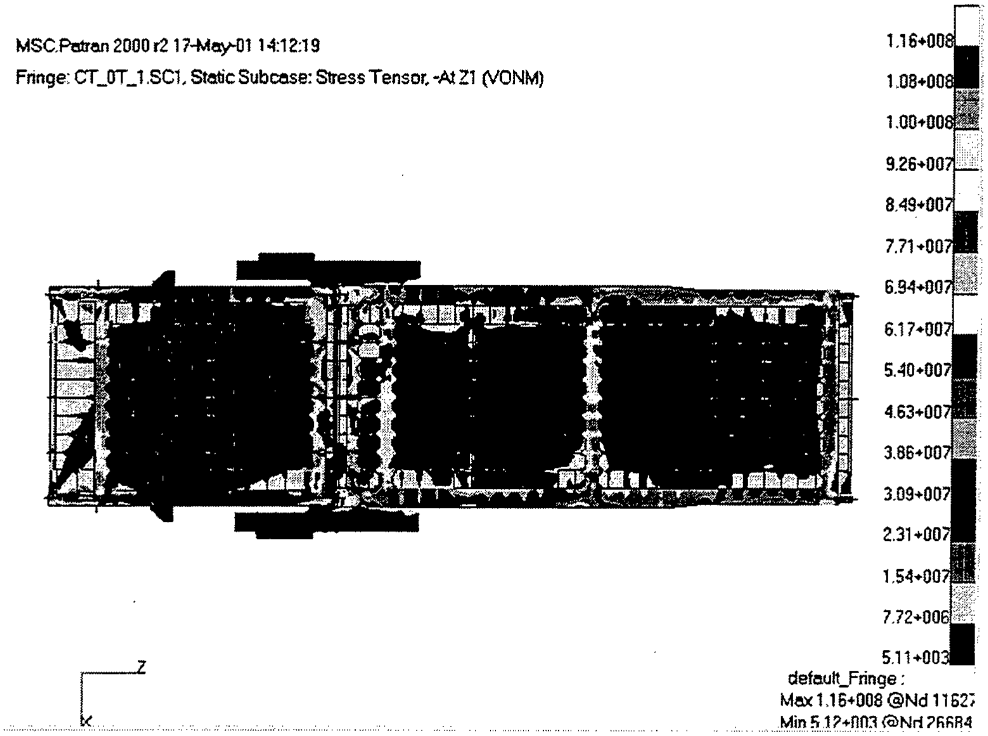

Figure 99. Cape T (bottom view) von Mises Stress Contour Plot, Max. Stress: 16.8 ksi (Inertia Loading, 1 Degree Twist, No Tanks)

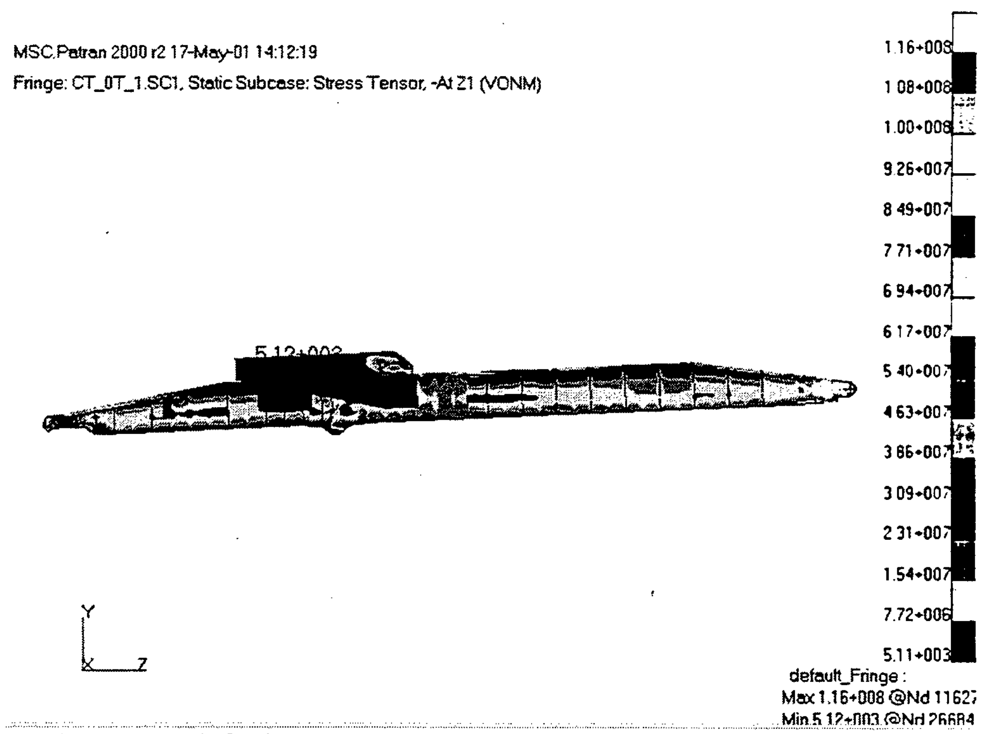

Figure 100. Cape T (left view) von Mises Stress Contour Plot, Max. Stress: 16.8 ksi (Inertia Loading, 1 Degree Twist, No Tanks)

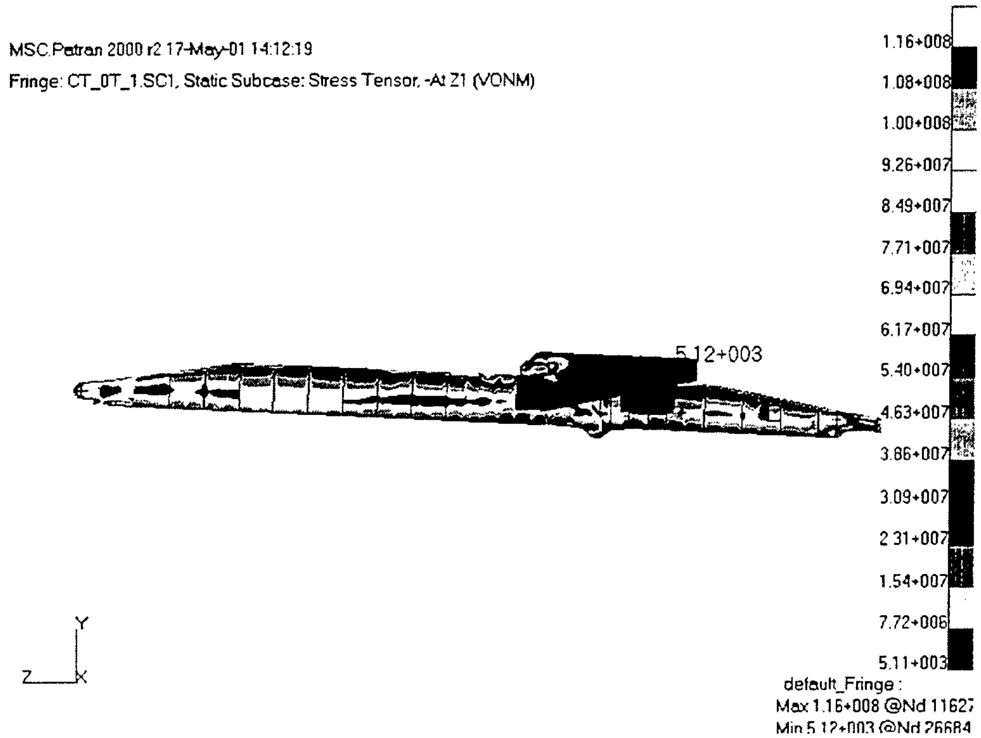

Figure 101. Cape T (right view) von Mises Stress Contour Plot, Max. Stress: 16.8 ksi (Inertia Loading, 1 Degree Twist, No Tanks)

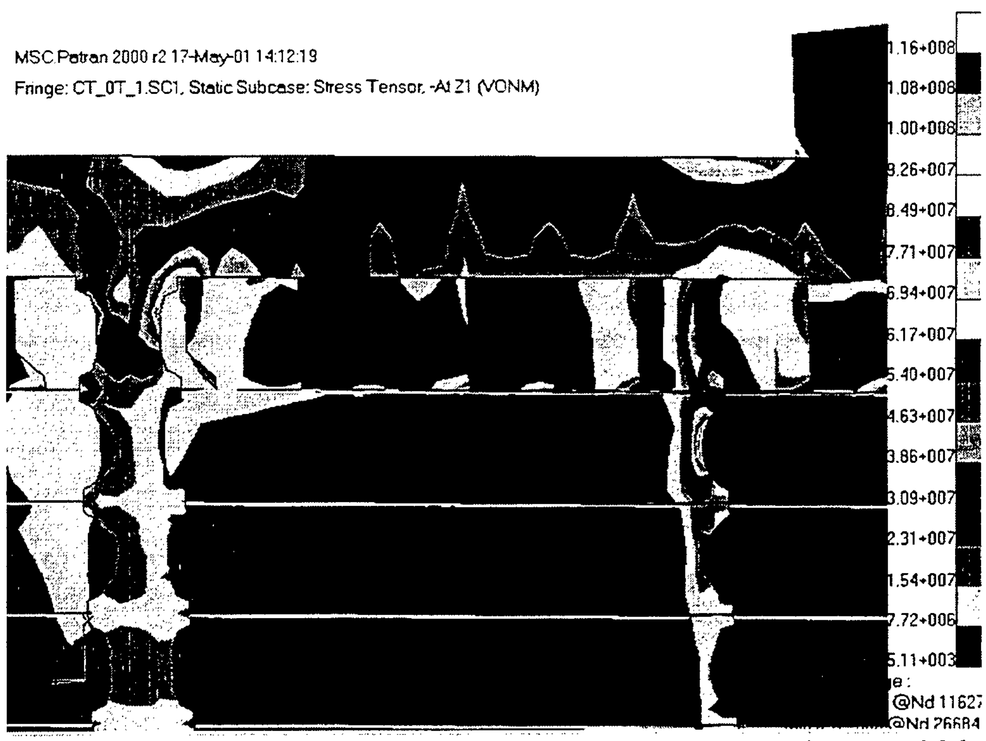

Figure 102. Cape T (close-up) von Mises Stress Contour Plot, Max. Stress: 16.8 ksi (Inertia Loading, 1 Degree Twist, No Tanks)

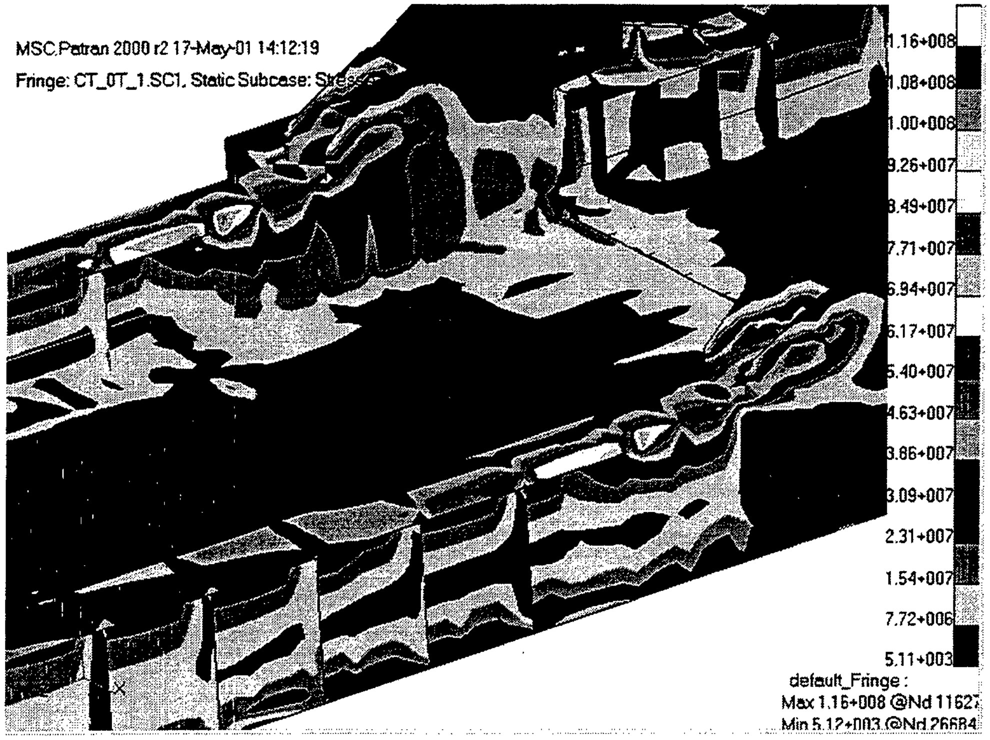

Figure 103. Cape T (close-up) von Mises Stress Contour Plot, Max. Stress: 16.8 ksi (Inertia Loading, 1 Degree Twist, No Tanks)

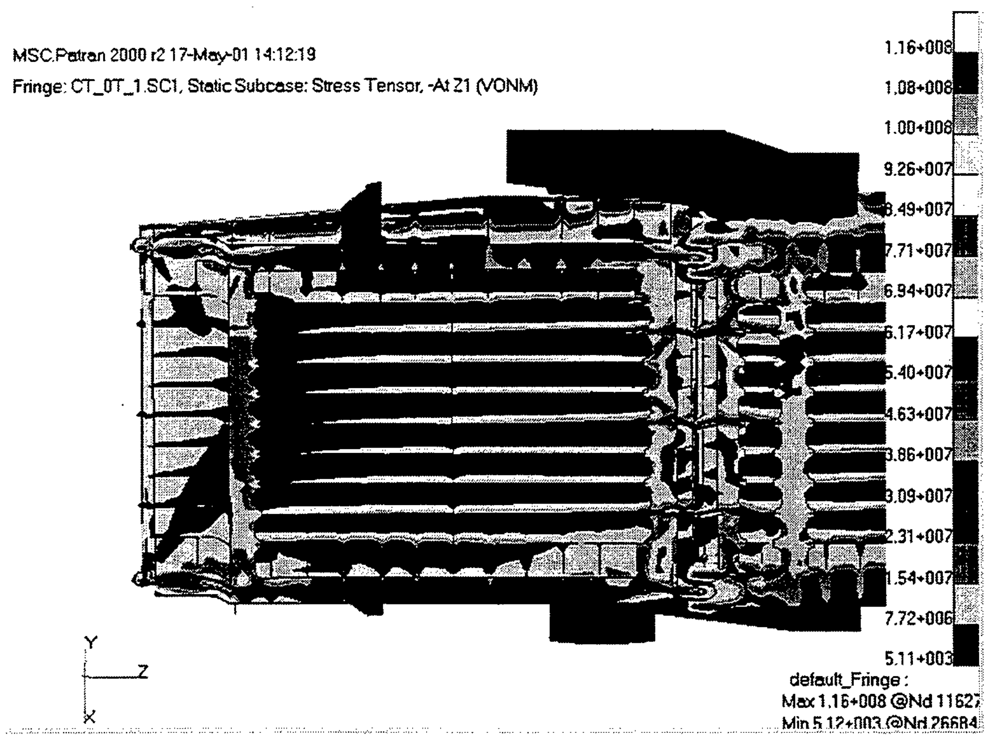

Figure 104. Cape T (close-up) von Mises Stress Contour Plot, Max. Stress: 16.8 ksi (Inertia Loading, 1 Degree Twist, No Tanks)

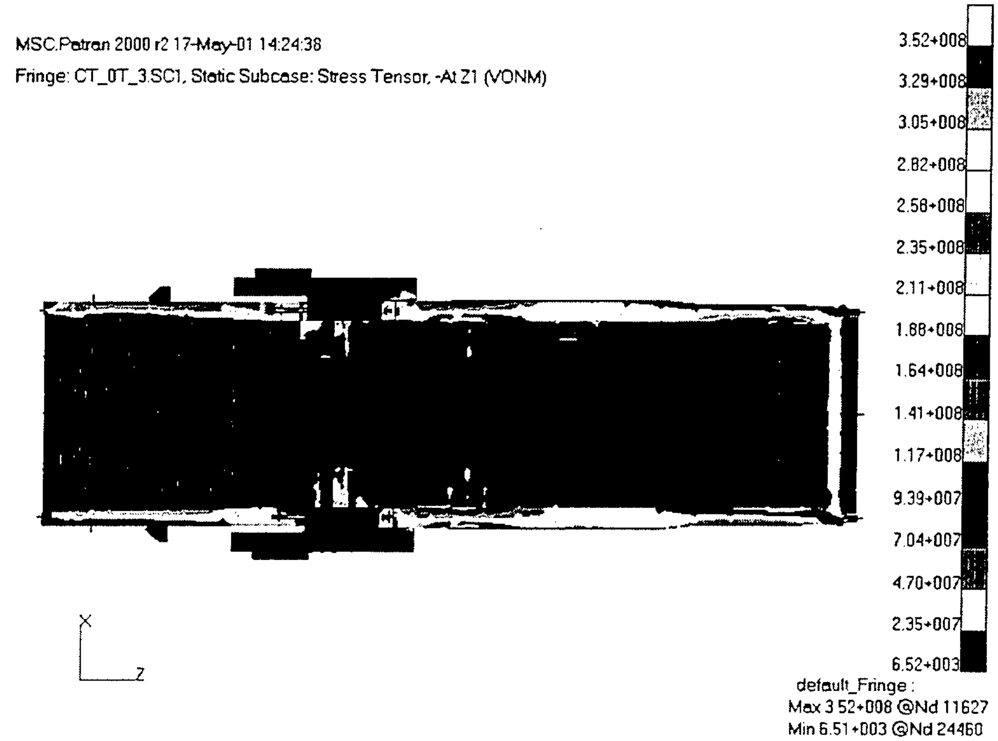

Figure 105. Cape T (top view) von Mises Stress Contour Plot, Max. Stress: 51.1 ksi (Inertia Loading, 3 Degree Twist, No Tanks)

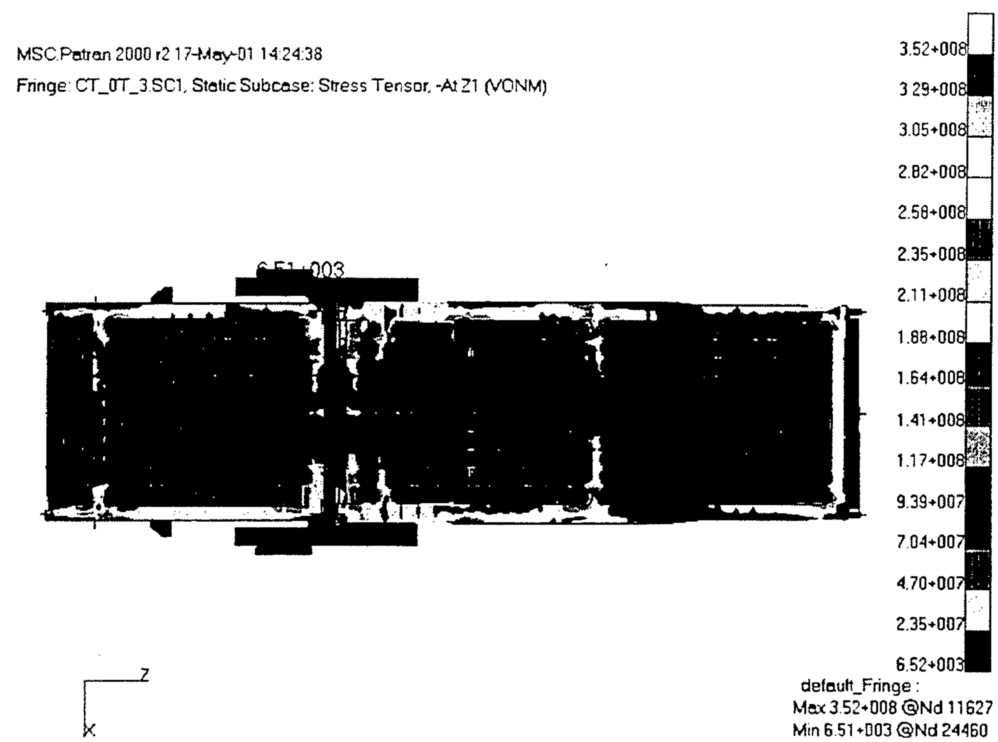

Figure 106. Cape T (bottom view) von Mises Stress Contour Plot, Max. Stress: 51.1 ksi (Inertia Loading, 3 Degree Twist, No Tanks)

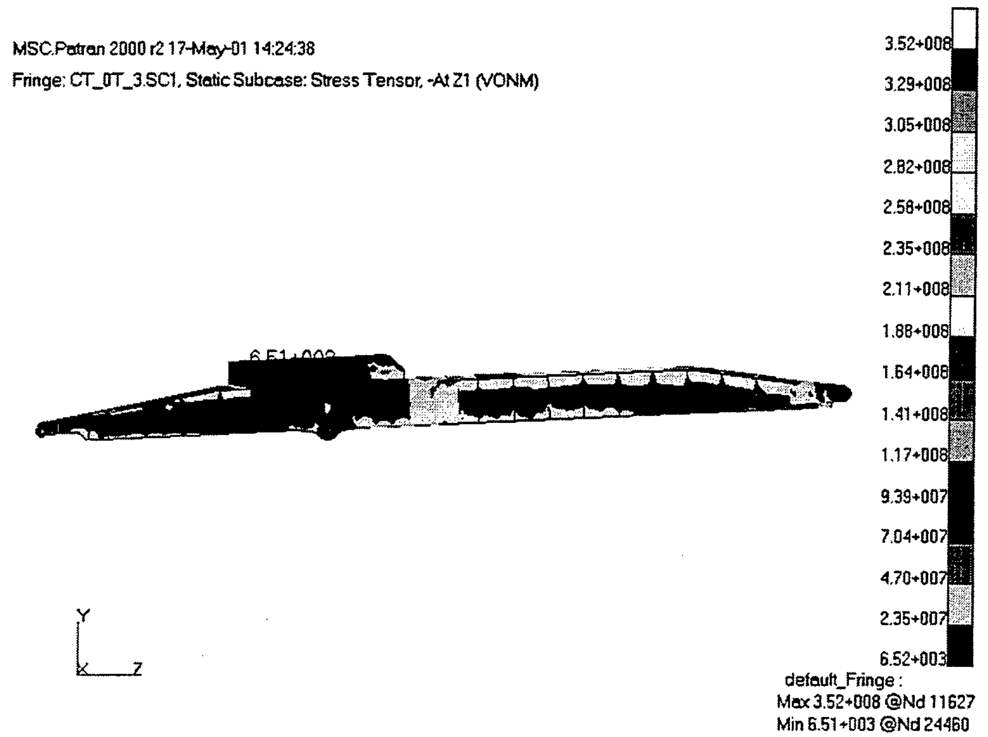

Figure 107. Cape T (left view) von Mises Stress Contour Plot, Max. Stress: 51.1 ksi (Inertia Loading, 3 Degree Twist, No Tanks)

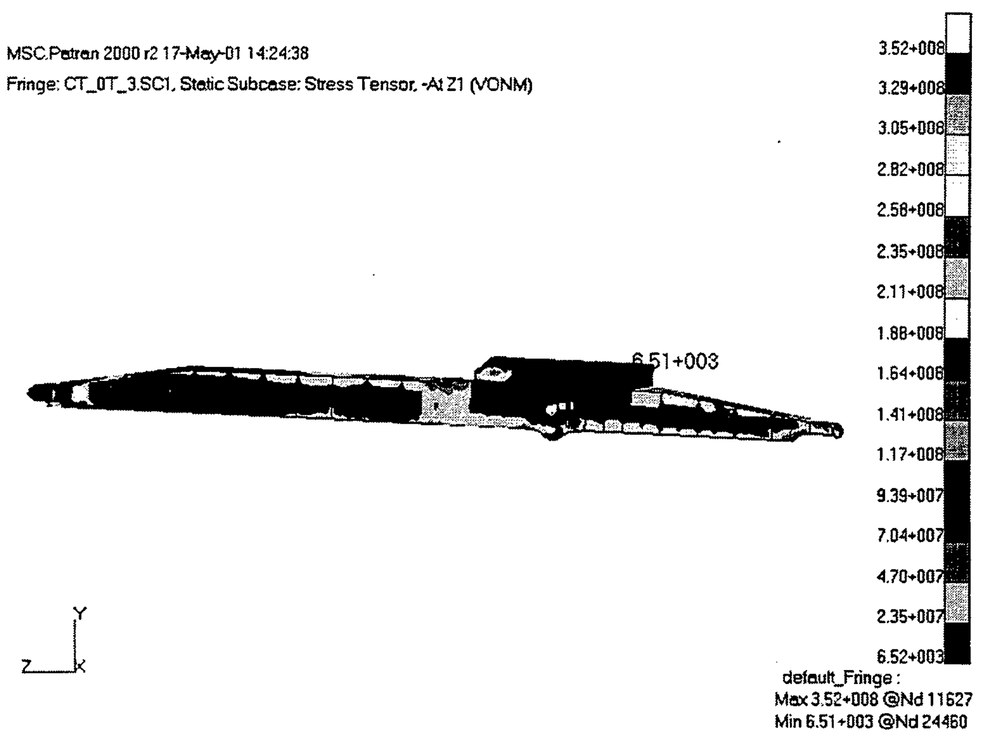

Figure 108. Cape T (right view) von Mises Stress Contour Plot, Max. Stress: 51.1 ksi (Inertia Loading, 3 Degree Twist, No Tanks)

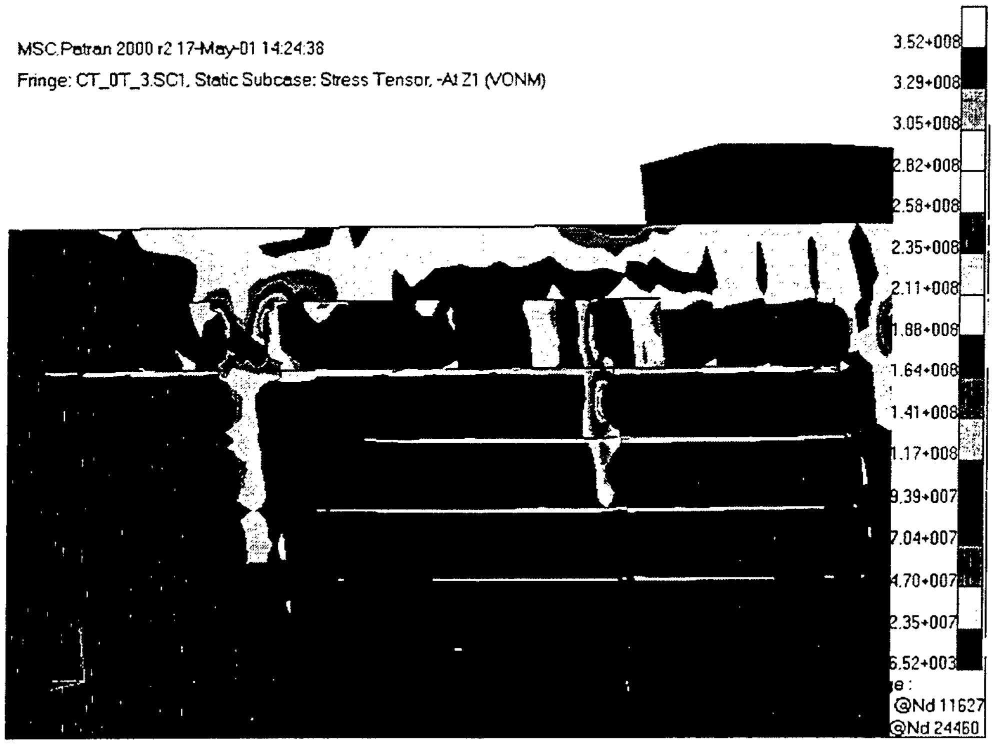

Figure 109. Cape T (close-up) von Mises Stress Contour Plot, Max. Stress: 51.1 ksi (Inertia Loading, 3 Degree Twist, No Tanks)

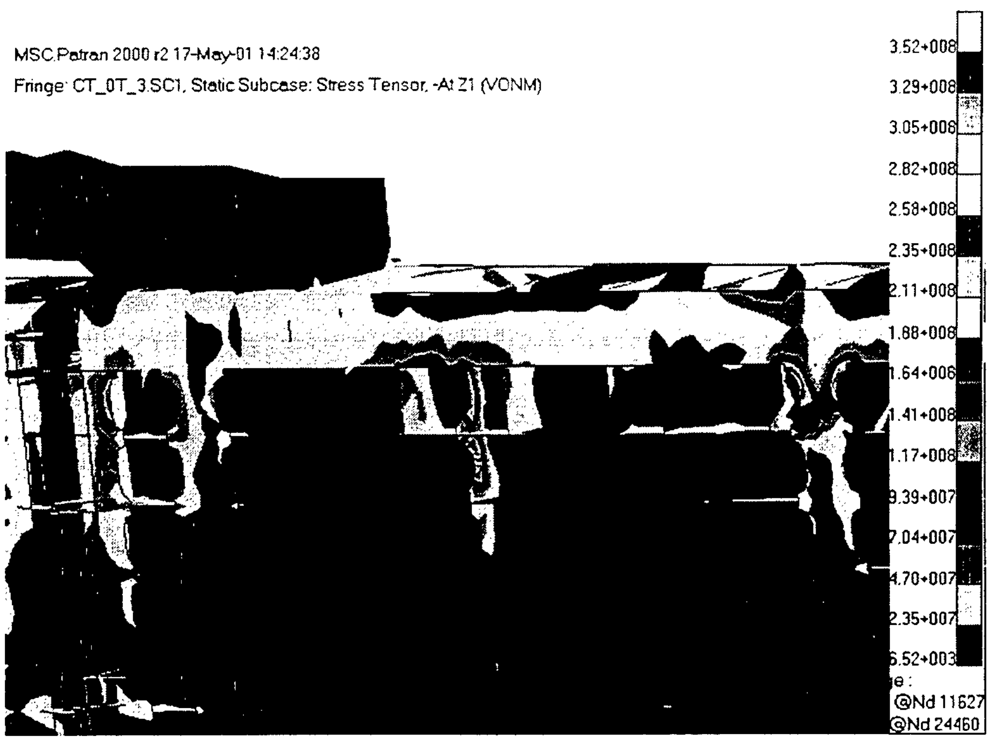

Figure 110. Cape T (close-up) von Mises Stress Contour Plot, Max. Stress: 51.1 ksi (Inertia Loading, 3 Degree Twist, No Tanks)

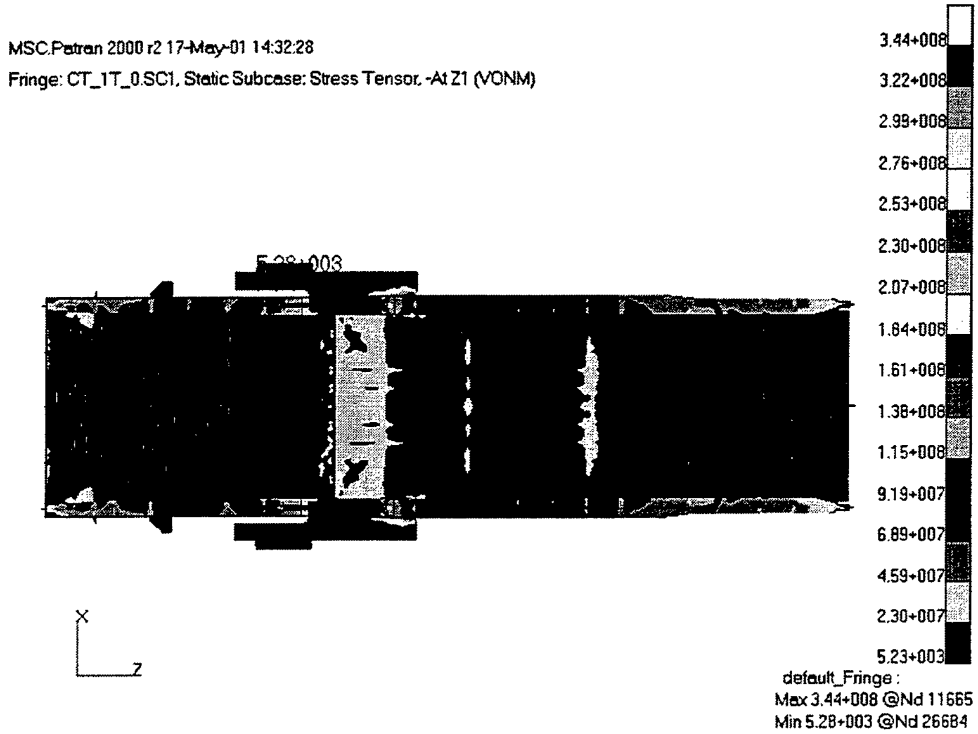

Figure 111. Cape T (top view) von Mises Stress Contour Plot, Max. Stress: 49.9 ksi (Inertia Loading, No Twist, One Tank)

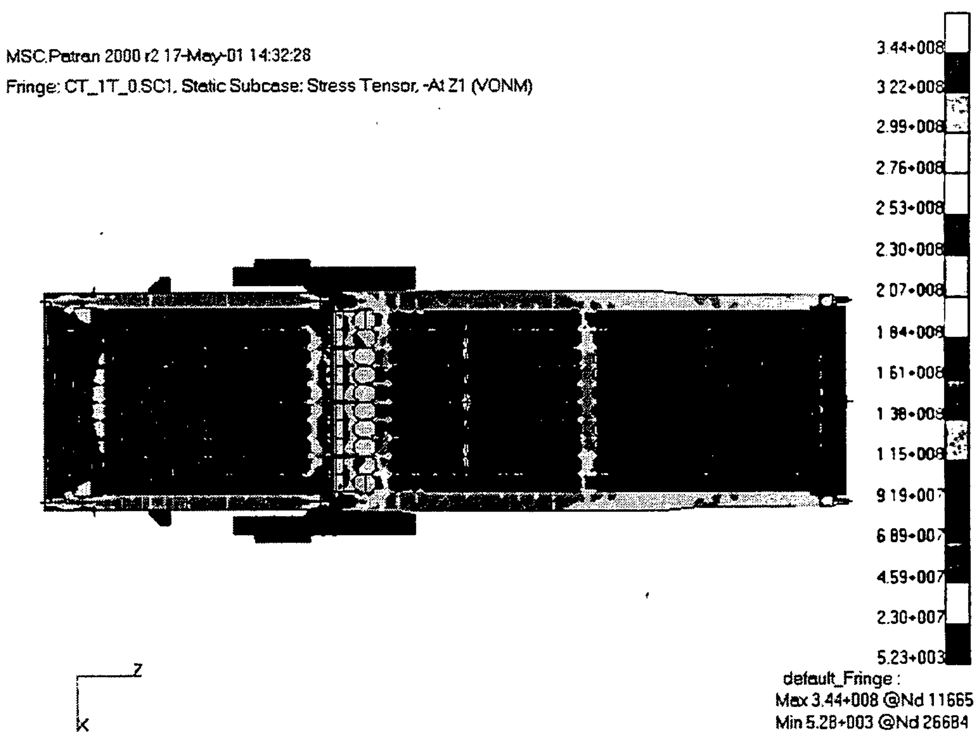

Figure 112. Cape T (bottom view) von Mises Stress Contour Plot, Max. Stress: 49.9 ksi (Inertia Loading, No Twist, One Tank)

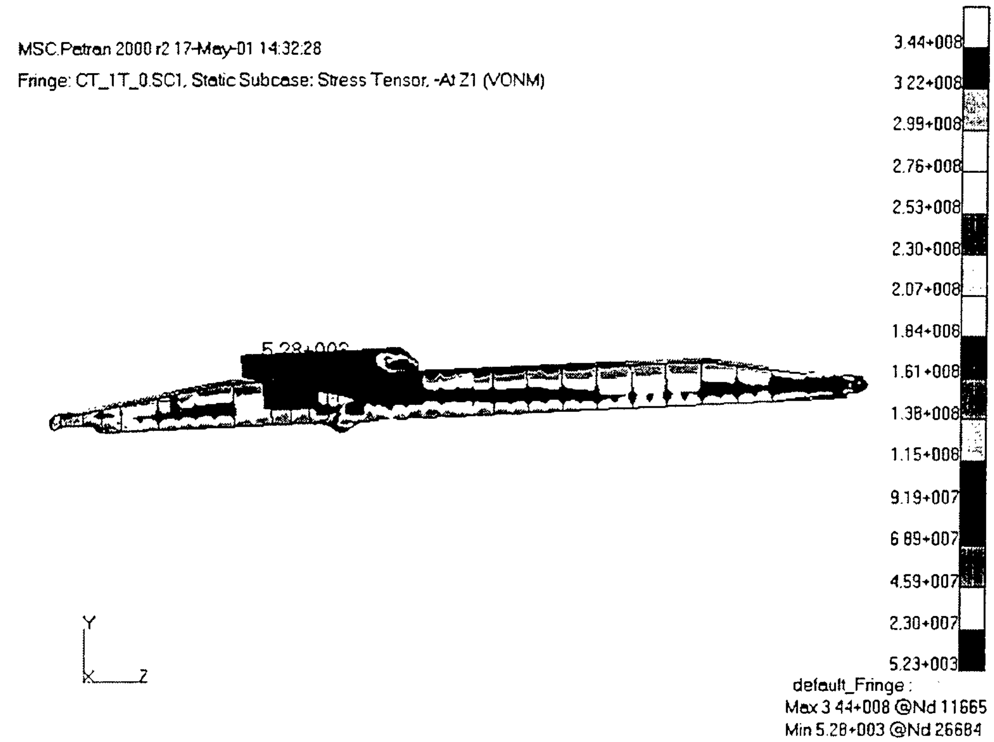

Figure 113. Cape T (left view) von Mises Stress Contour Plot, Max. Stress: 49.9 ksi (Inertia Loading, No Twist, One Tank)

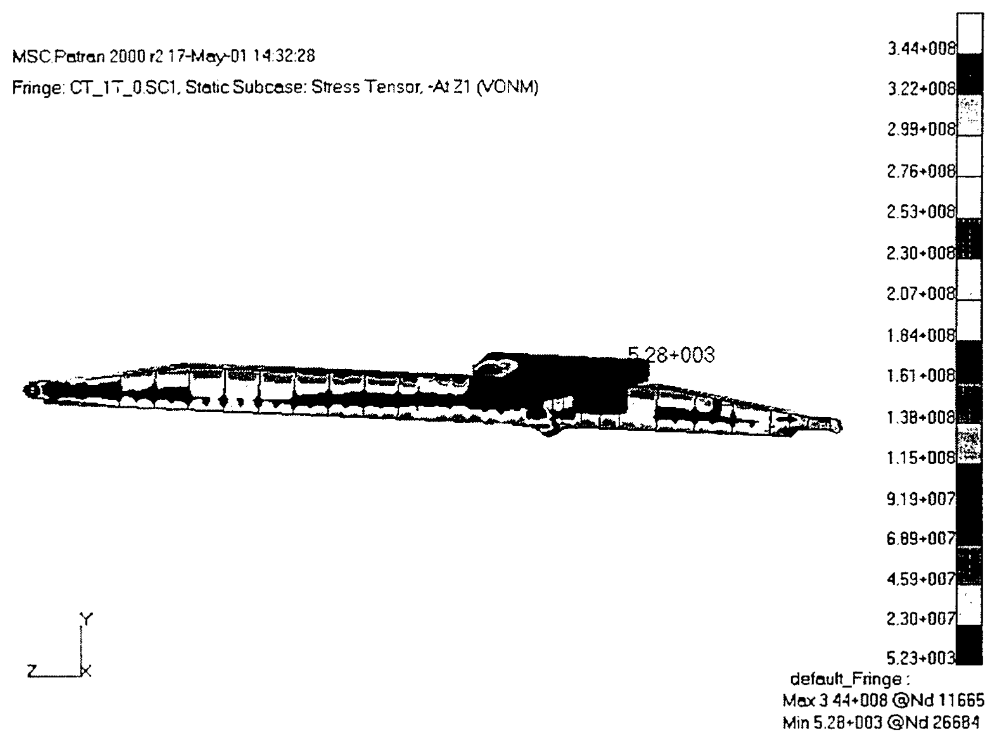

Figure 114. Cape T (right view) von Mises Stress Contour Plot, Max. Stress: 49.9 ksi (Inertia Loading, No Twist, One Tank)

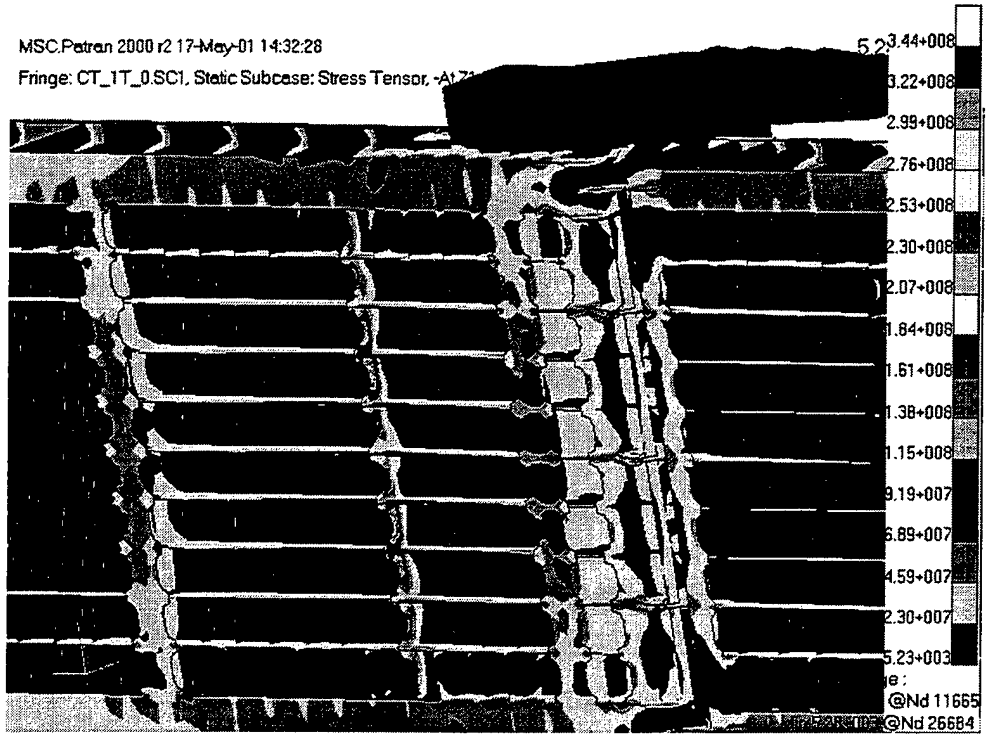

Figure 115. Cape T (close-up) von Mises Stress Contour Plot, Max. Stress: 49.9 ksi (Inertia Loading, No Twist, One Tank)

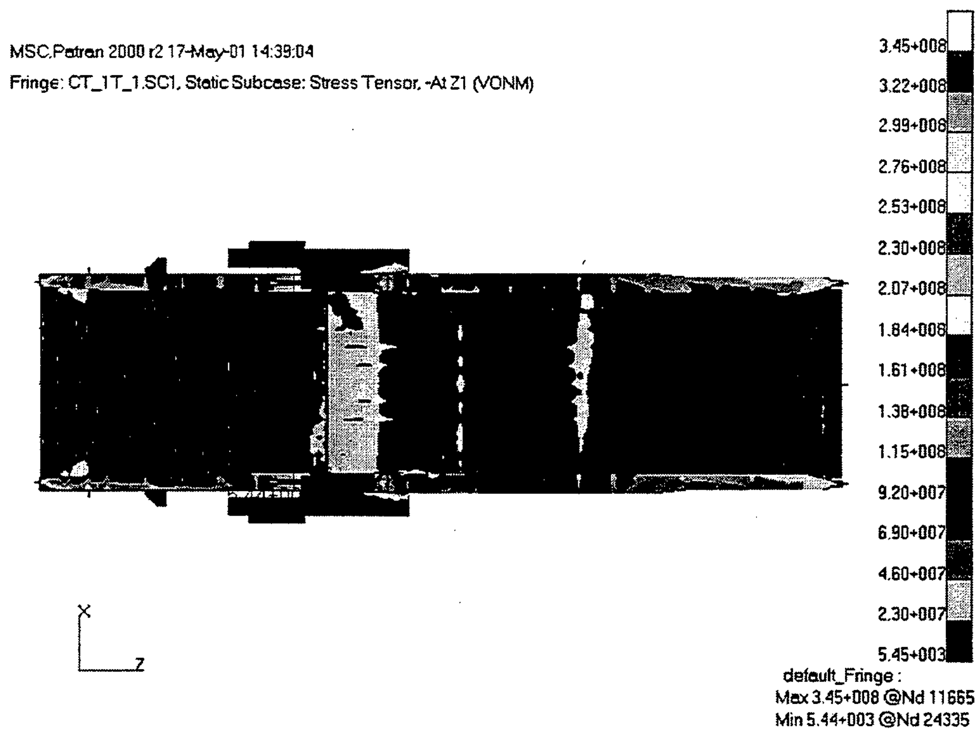

Figure 116. Cape T (top view) von Mises Stress Contour Plot, Max. Stress: 50.1 ksi (Inertia Loading, 1 Degree Twist, One Tank)

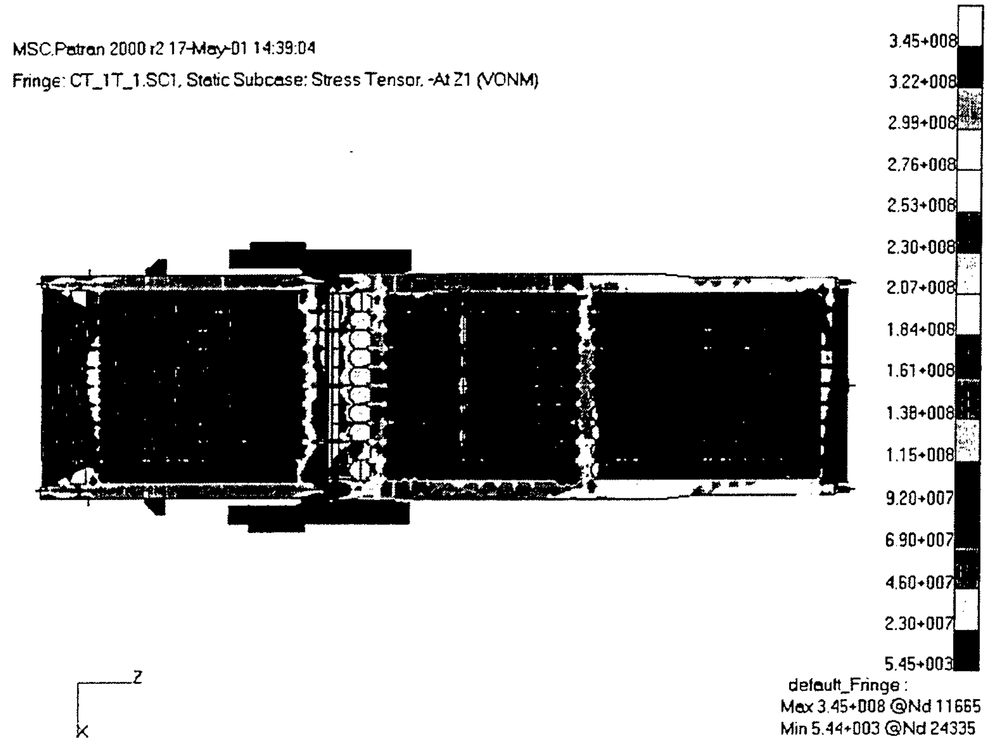

Figure 117. Cape T (bottom view) von Mises Stress Contour Plot, Max. Stress: 50.1 ksi (Inertia Loading, 1 Degree Twist, One Tank)

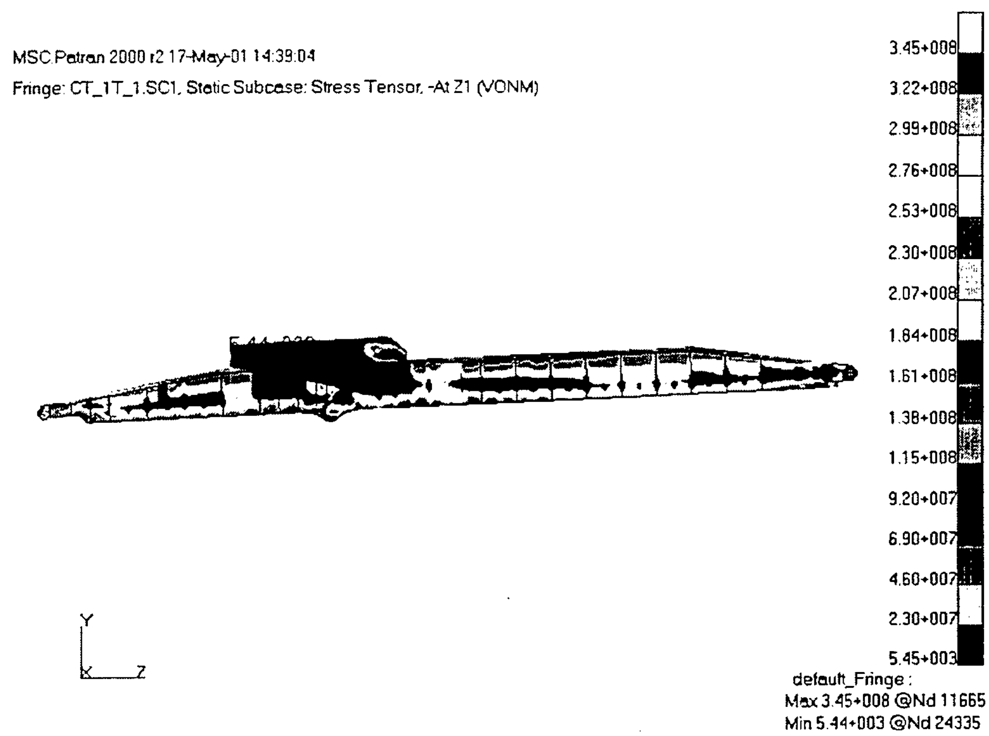

Figure 118. Cape T (left view) von Mises Stress Contour Plot, Max. Stress: 50.1 ksi (Inertia Loading, 1 Degree Twist, One Tank)

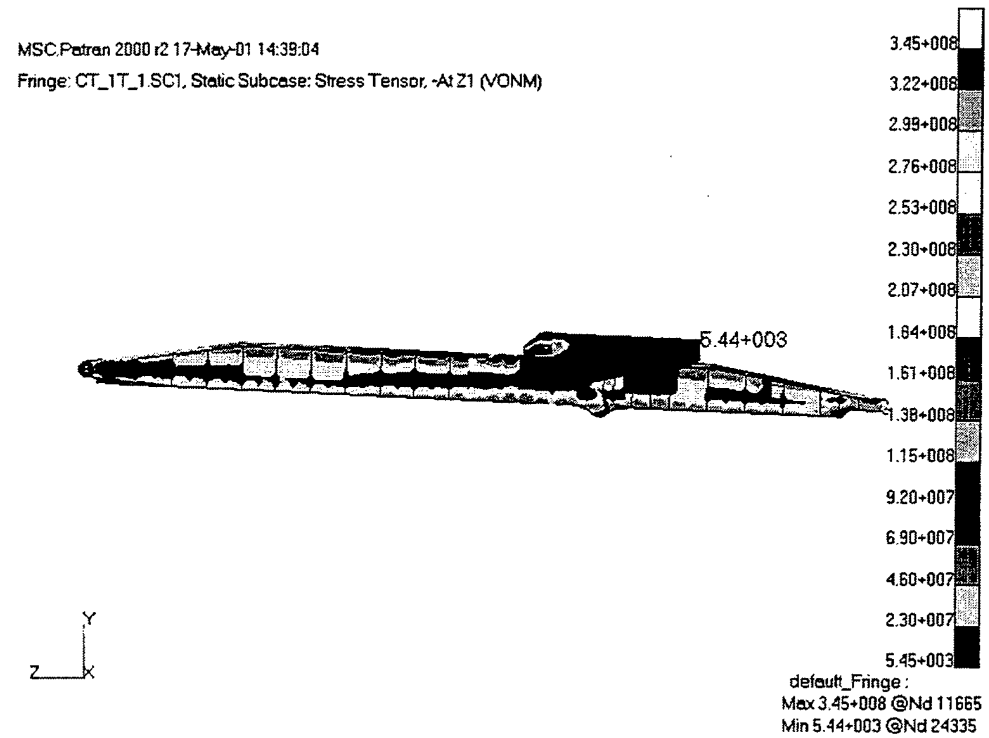

Figure 119. Cape T (right view) von Mises Stress Contour Plot, Max. Stress: 50.1 ksi (Inertia Loading, 1 Degree Twist, One Tank)

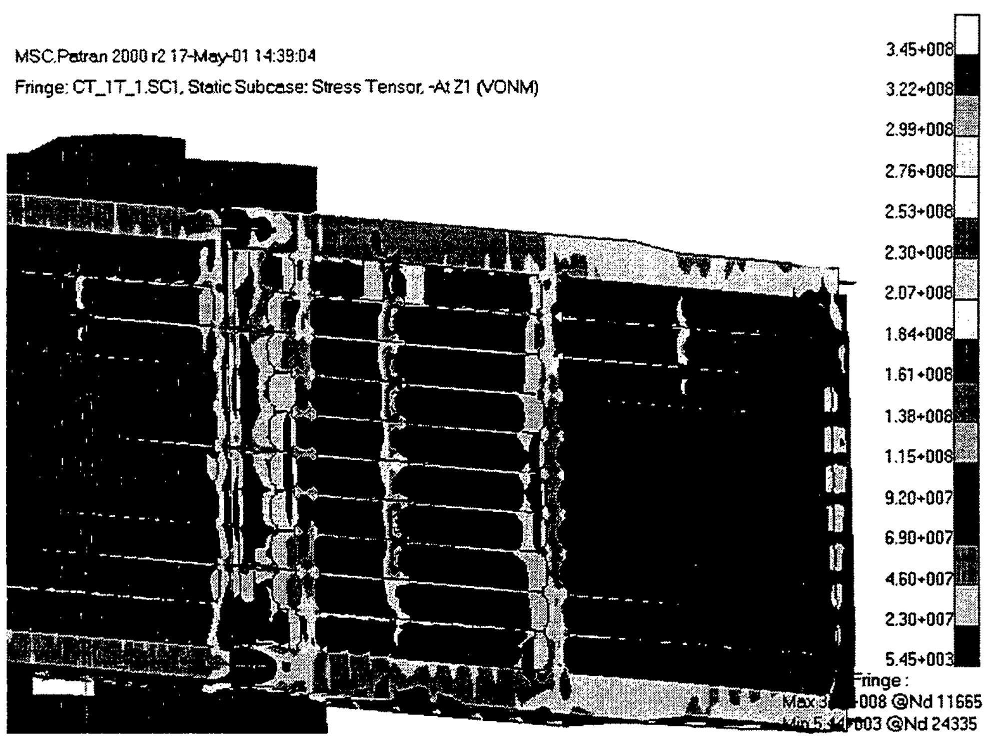

Figure 120. Cape T (close-up) von Mises Stress Contour Plot, Max. Stress: 50.1 ksi (Inertia Loading, 1 Degree Twist, One Tank)

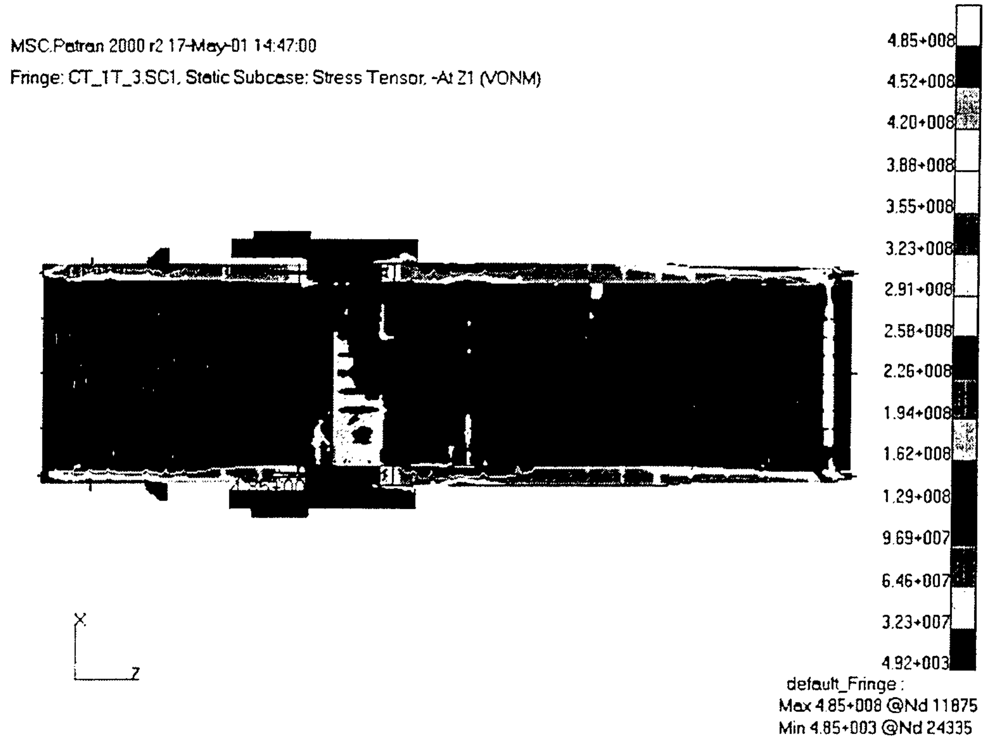

Figure 121. Cape T (top view) von Mises Stress Contour Plot, Max. Stress: 70.3 ksi (Inertia Loading, 3 Degree Twist, One Tank)

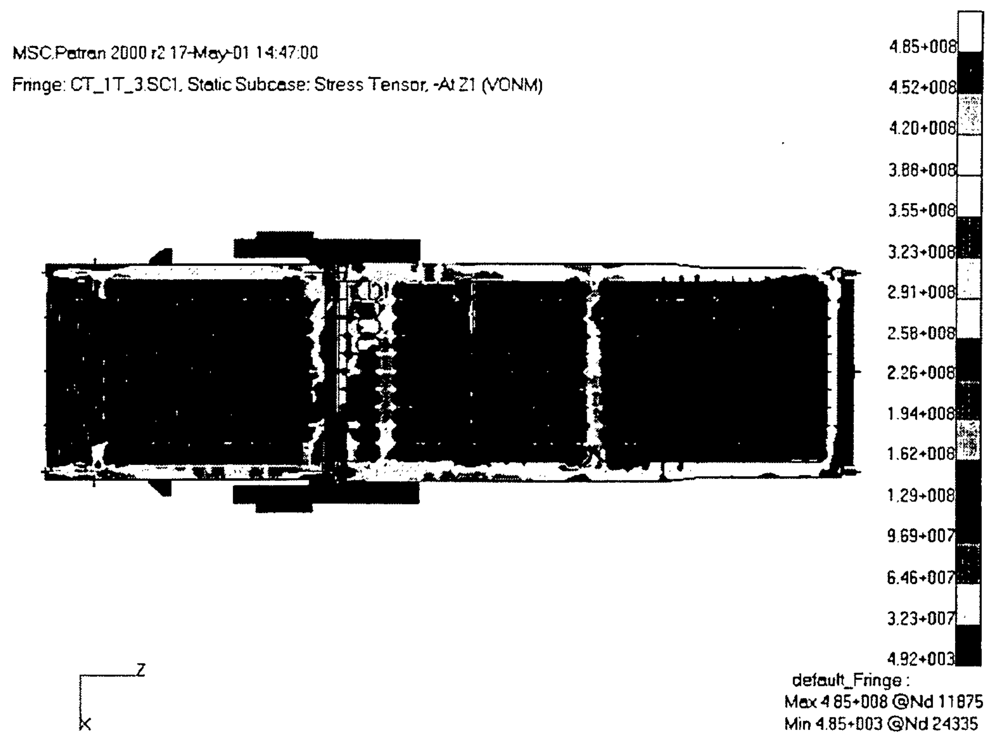

Figure 122. Cape T (bottom view) von Mises Stress Contour Plot, Max. Stress: 70.3 ksi (Inertia Loading, 3 Degree Twist, One Tank)

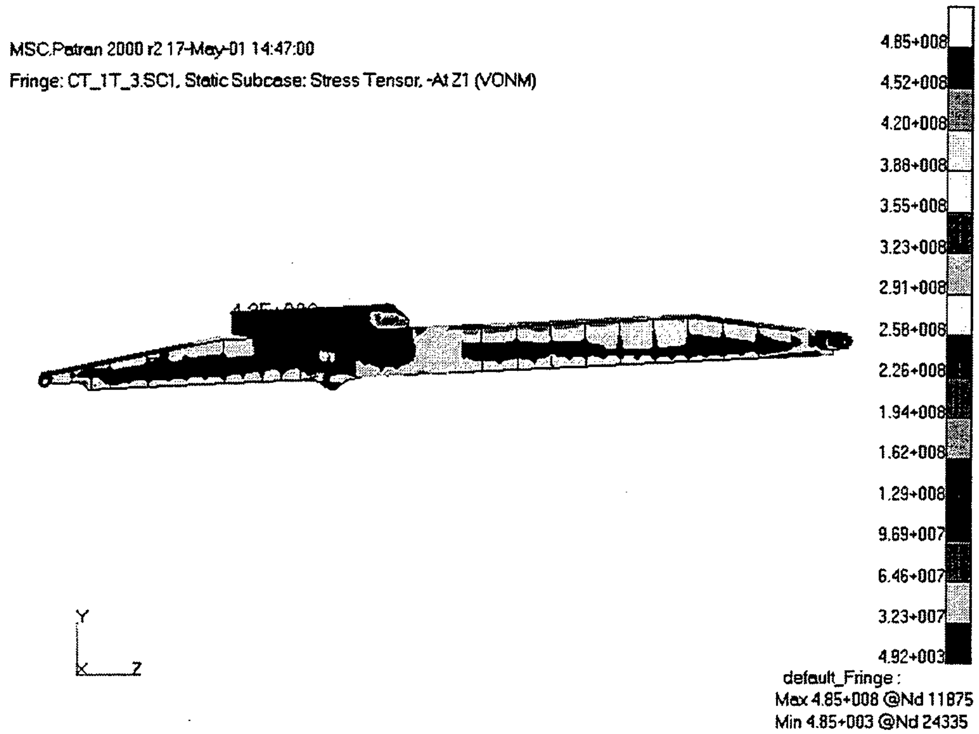

Figure 123. Cape T (left view) von Mises Stress Contour Plot, Max. Stress: 70.3 ksi (Inertia Loading, 3 Degree Twist, One Tank)

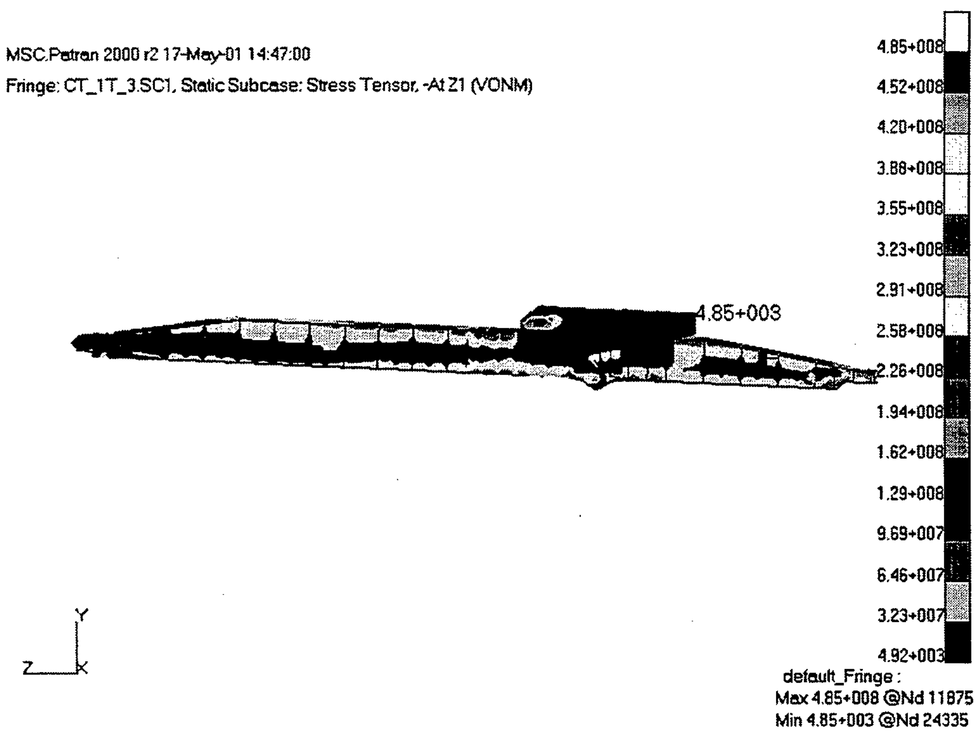

Figure 124. Cape T (right view) von Mises Stress Contour Plot, Max. Stress: 70.3 ksi (Inertia Loading, 3 Degree Twist, One Tank)

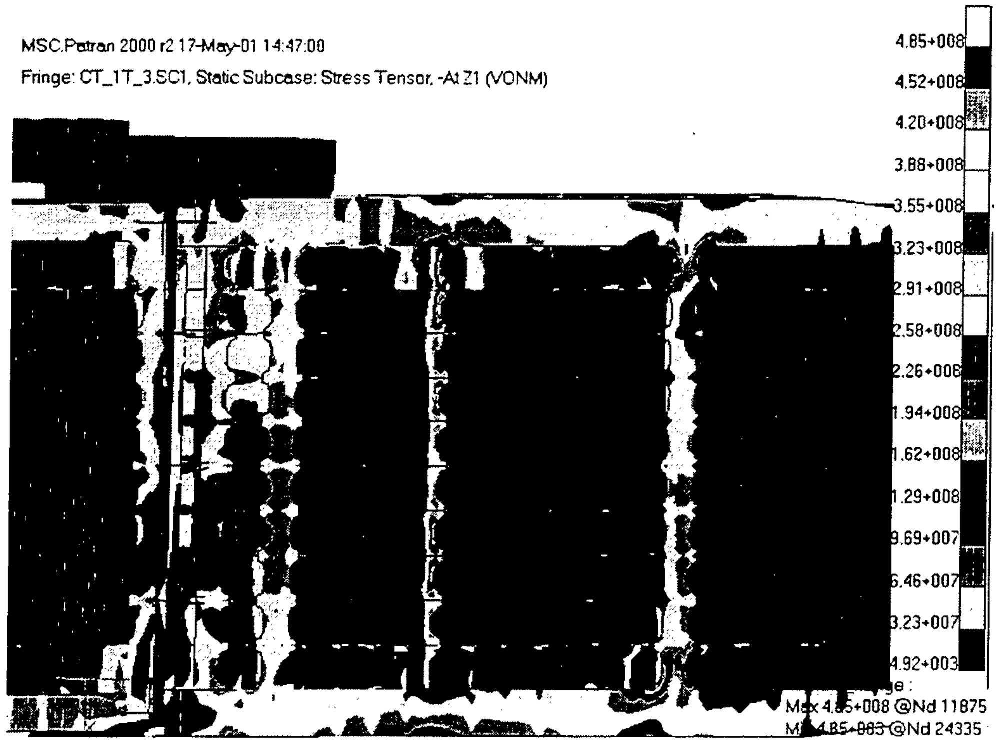

Figure 125. Cape T (close-up) von Mises Stress Contour Plot, Max. Stress: 70.3 ksi (Inertia Loading, 3 Degree Twist, One Tank)

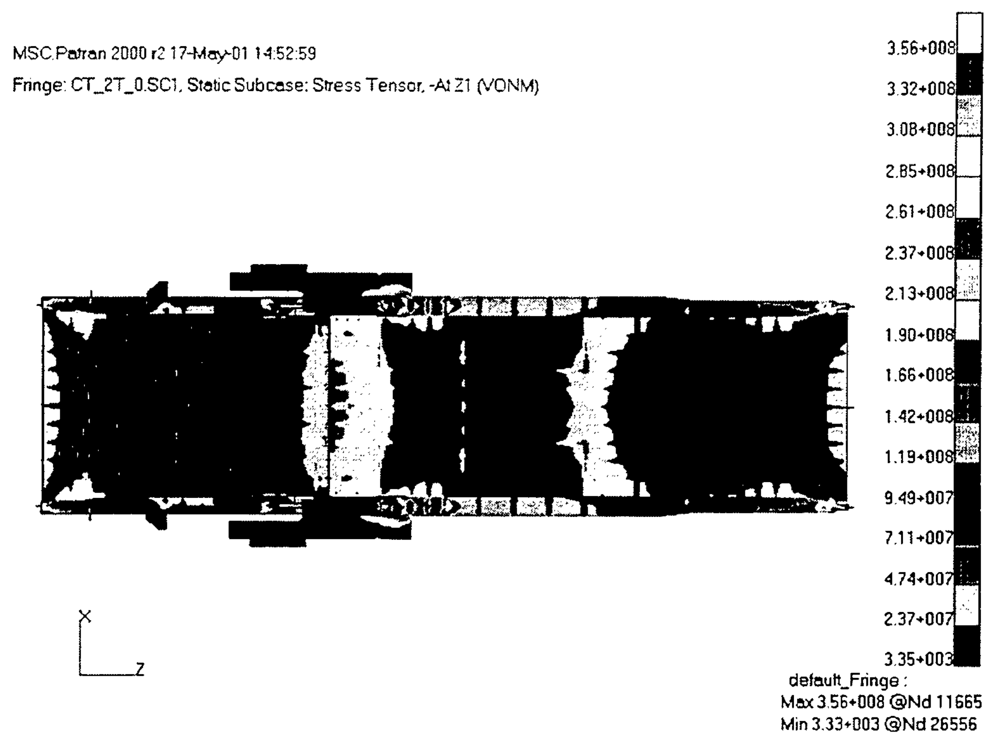

Figure 126. Cape T (top view) von Mises Stress Contour Plot, Max. Stress: 51.6 ksi (Inertia Loading, No Twist, Two Tanks)

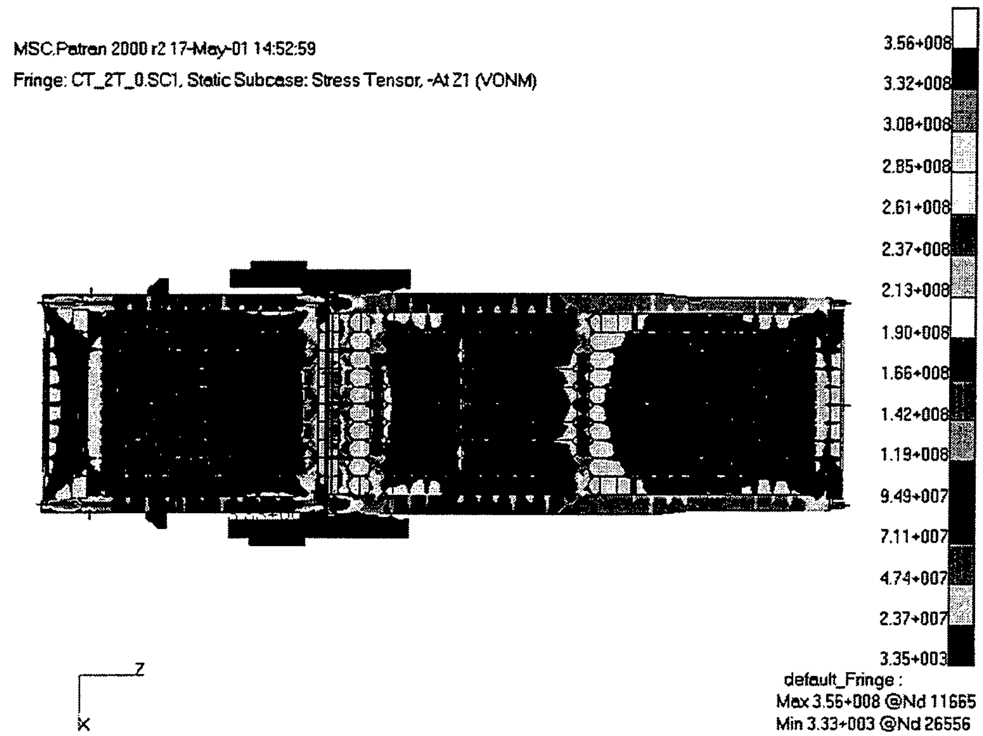

Figure 127. Cape T (bottom view) von Mises Stress Contour Plot, Max. Stress: 51.6 ksi (Inertia Loading, No Twist, Two Tanks)

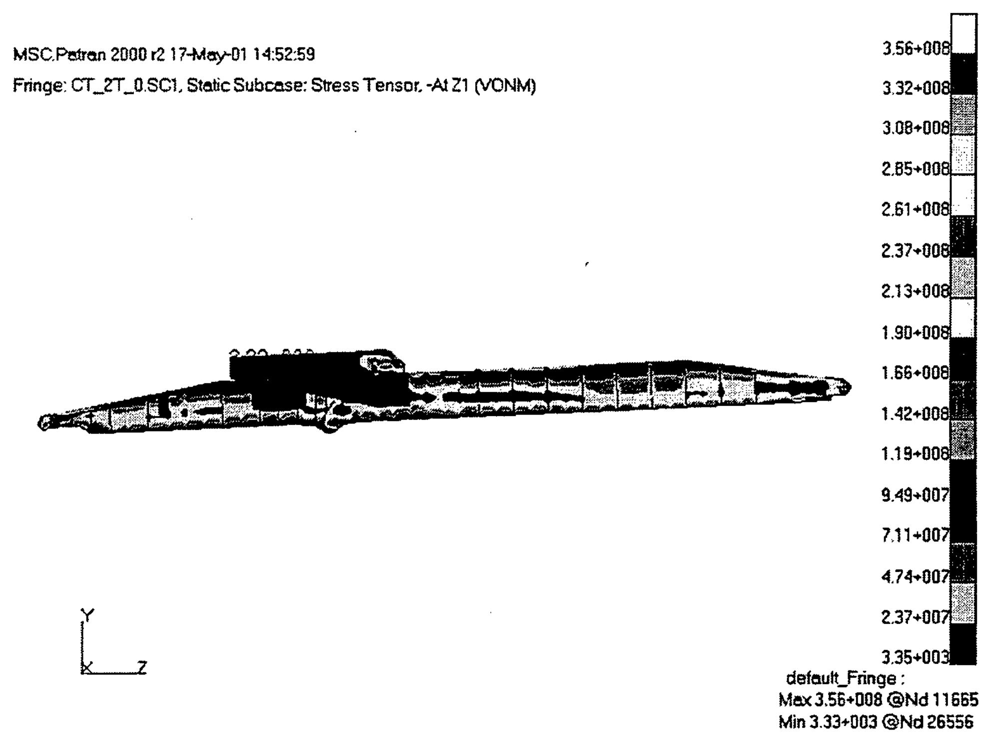

Figure 128. Cape T (left view) von Mises Stress Contour Plot, Max. Stress: 51.6 ksi (Inertia Loading, No Twist, Two Tanks)

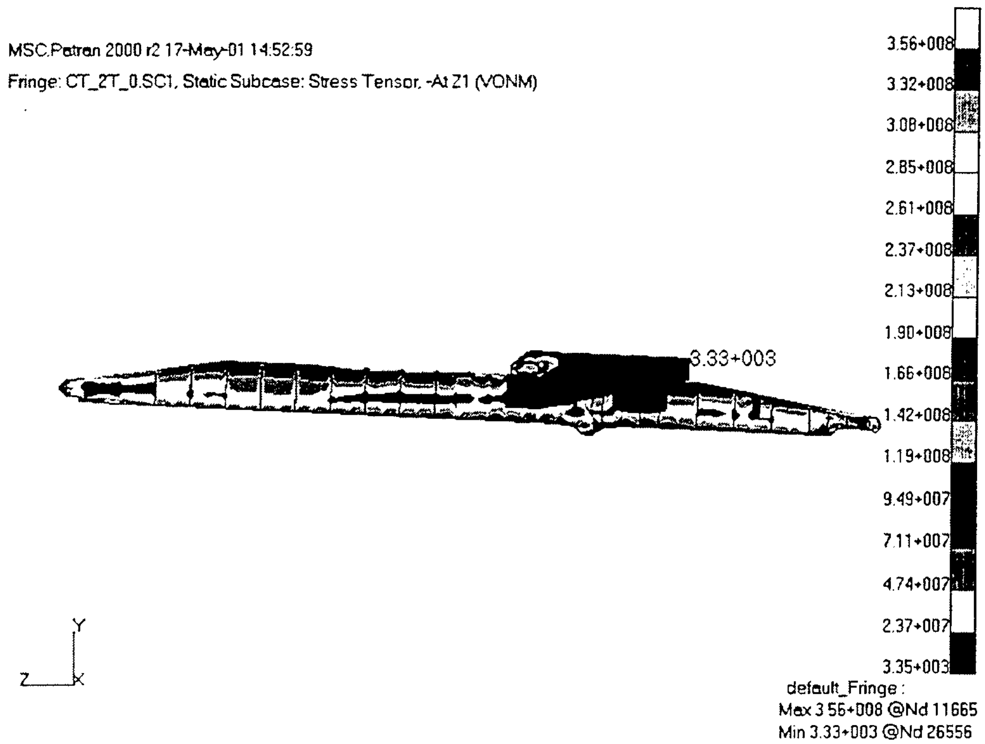

Figure 129. Cape T (right view) von Mises Stress Contour Plot, Max. Stress: 51.6 ksi (Inertia Loading, No Twist, Two Tanks)

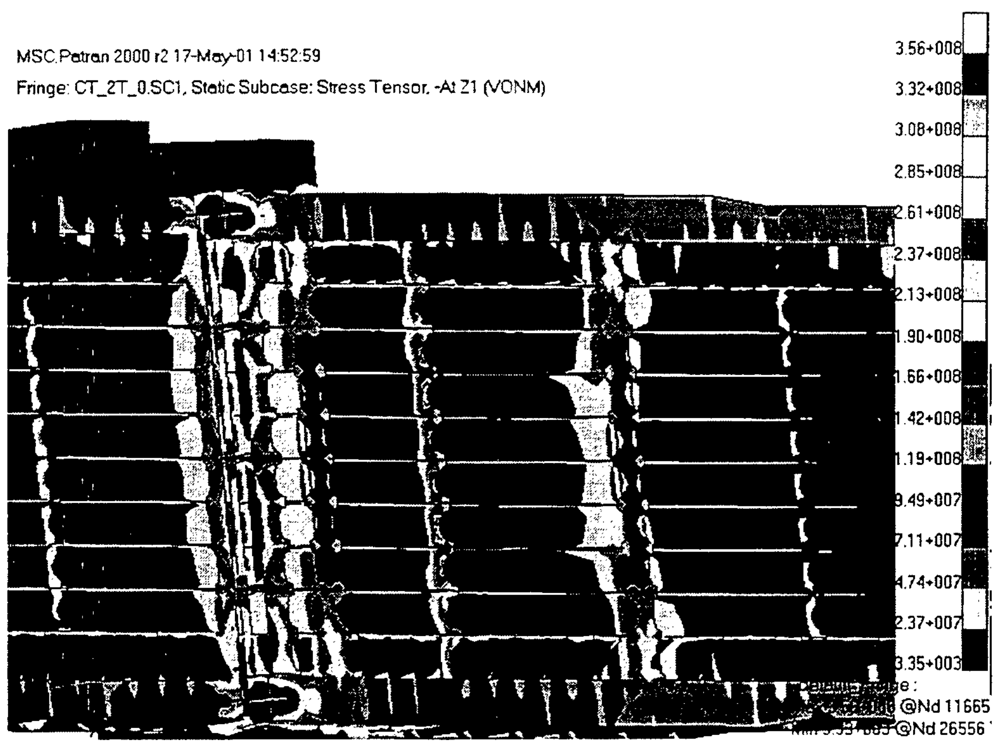

Figure 130. Cape T (close-up) von Mises Stress Contour Plot, Max. Stress: 51.6 ksi (Inertia Loading, No Twist, Two Tanks)

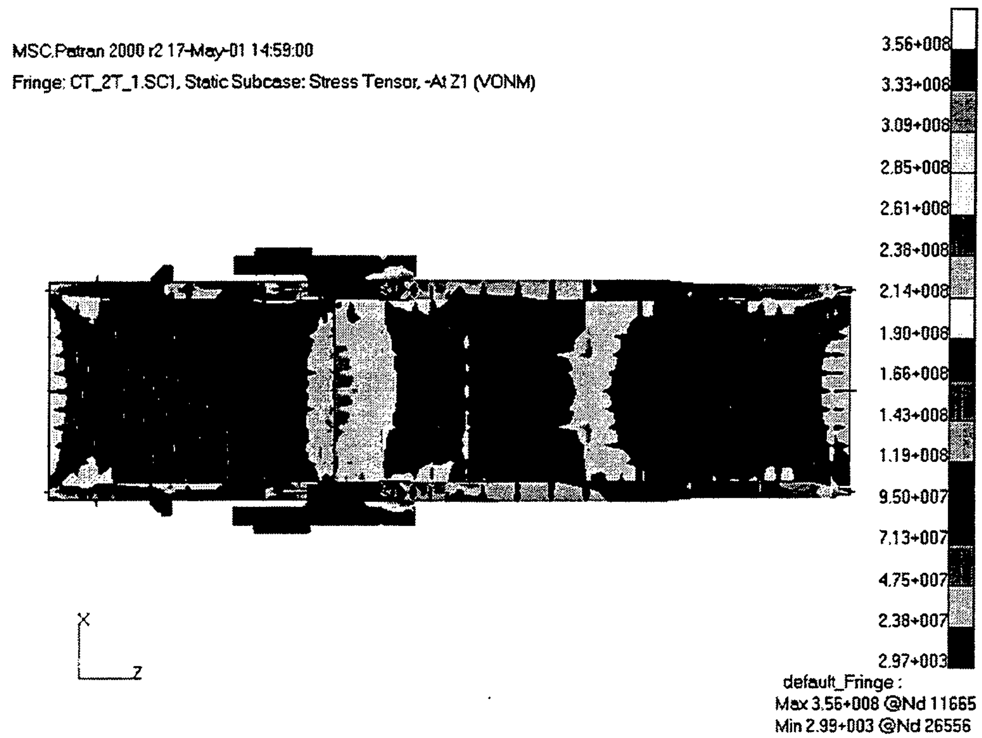

Figure 131. Cape T (top view) von Mises Stress Contour Plot, Max. Stress: 51.6 ksi (Inertia Loading, 1 Degree Twist, Two Tanks)

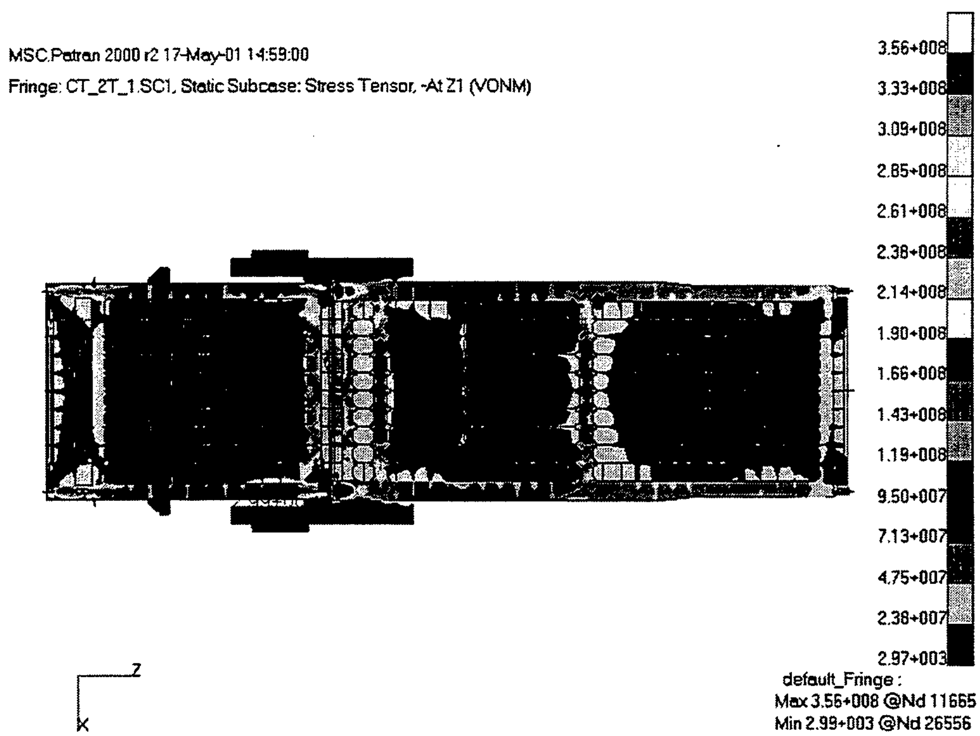

Figure 132. Cape T (bottom view) von Mises Stress Contour Plot, Max. Stress: 51.6 ksi (Inertia Loading, 1 Degree Twist, Two Tanks)

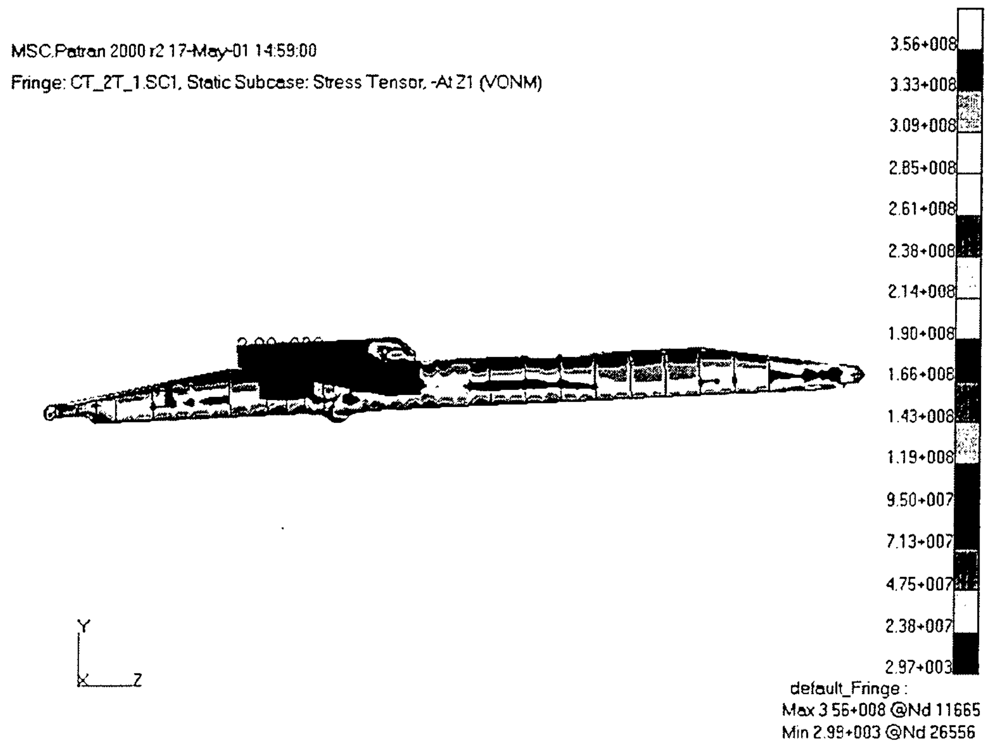

Figure 133. Cape T (left view) von Mises Stress Contour Plot, Max. Stress: 51.6 ksi (Inertia Loading, 1 Degree Twist, Two Tanks)

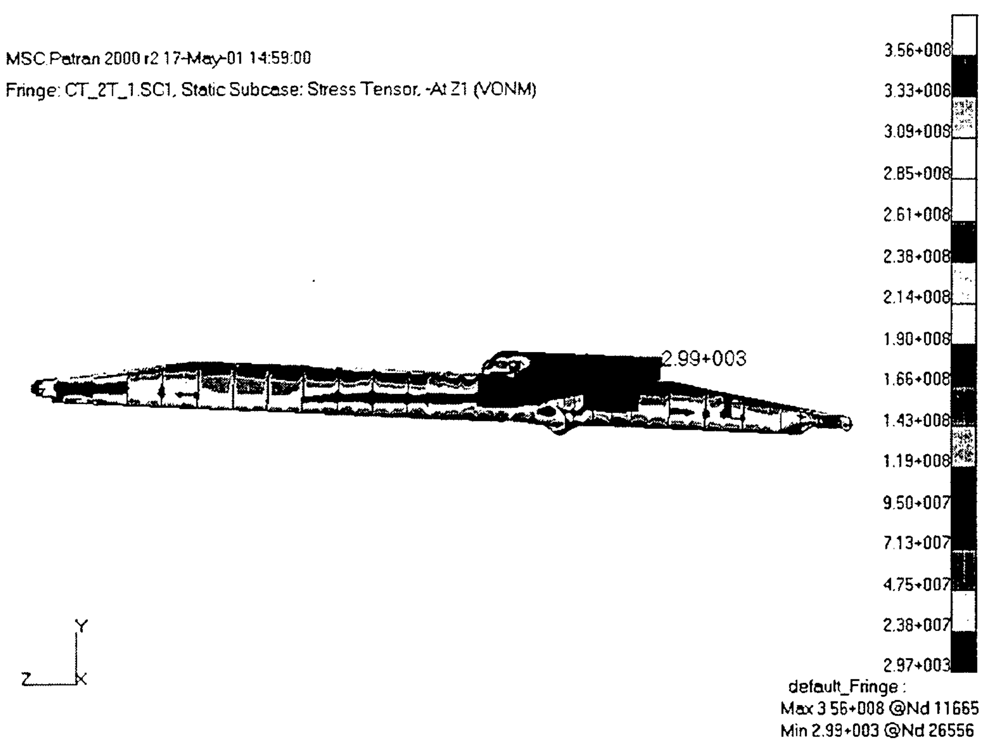

Figure 134. Cape T (right view) von Mises Stress Contour Plot, Max. Stress: 51.6 ksi (Inertia Loading, 1 Degree Twist, Two Tanks)

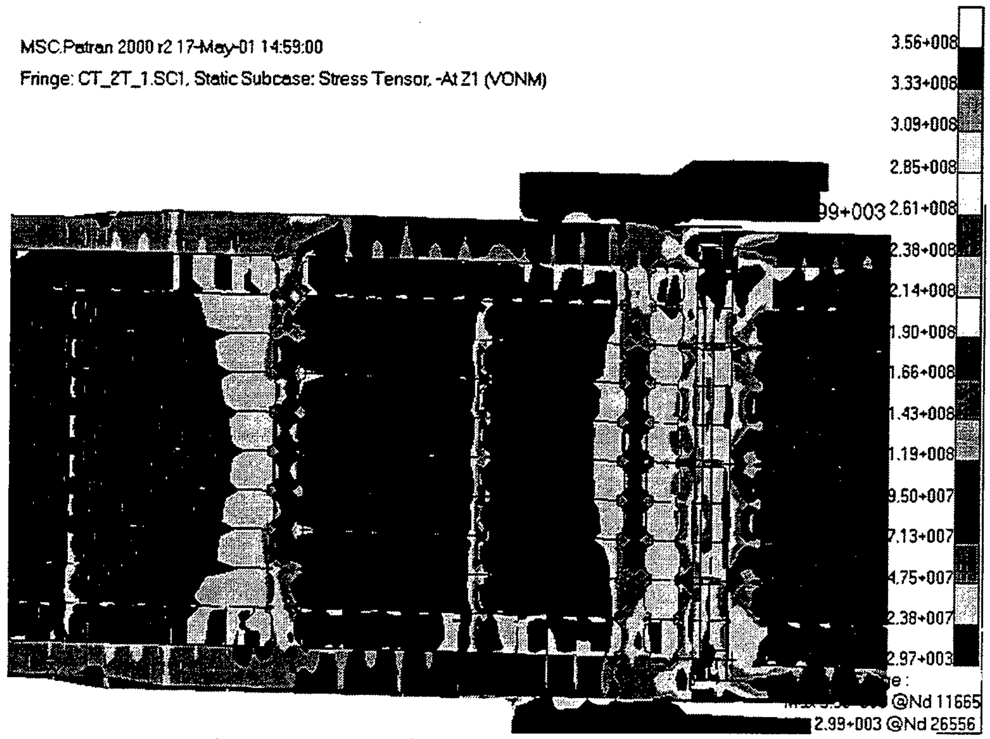

Figure 135. Cape T (close-up) von Mises Stress Contour Plot, Max. Stress: 51.6 ksi (Inertia Loading, 1 Degree Twist, Two Tanks)

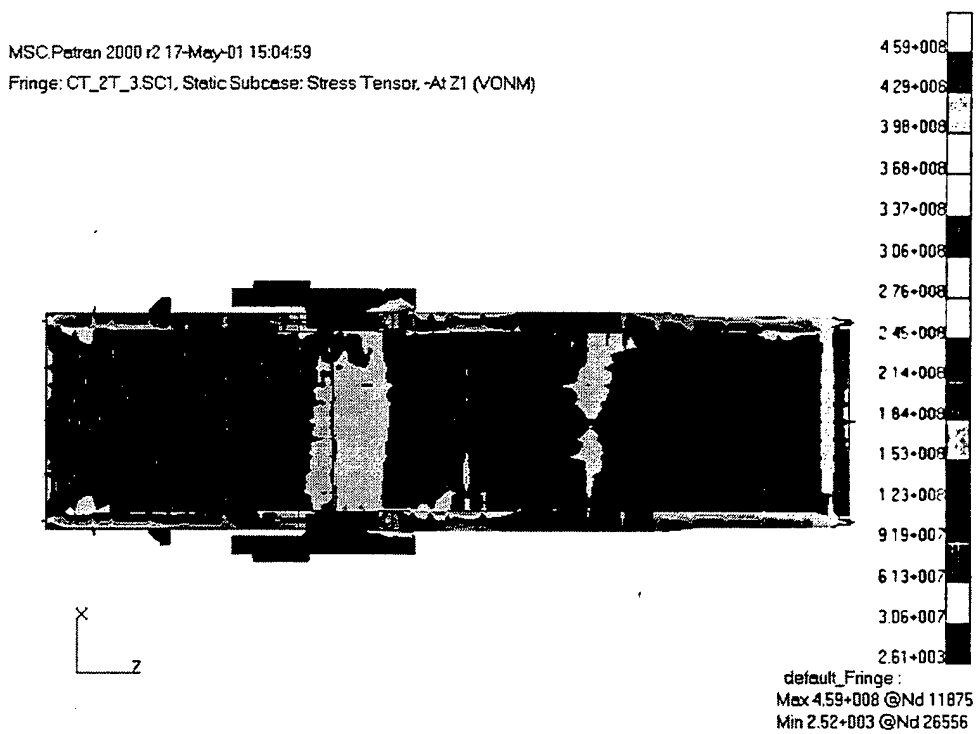

Figure 136. Cape T (top view) von Mises Stress Contour Plot, Max. Stress: 66.6 ksi (Inertia Loading, 3 Degree Twist, Two Tanks)

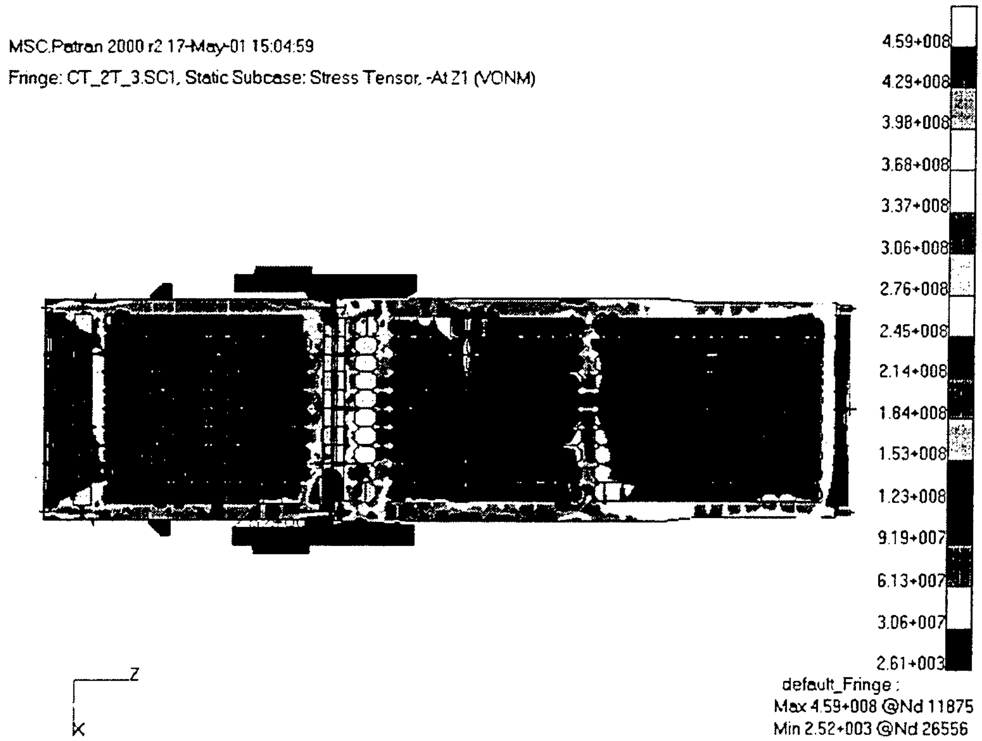

Figure 137. Cape T (bottom view) von Mises Stress Contour Plot, Max. Stress: 66.6 ksi (Inertia Loading, 3 Degree Twist, Two Tanks)

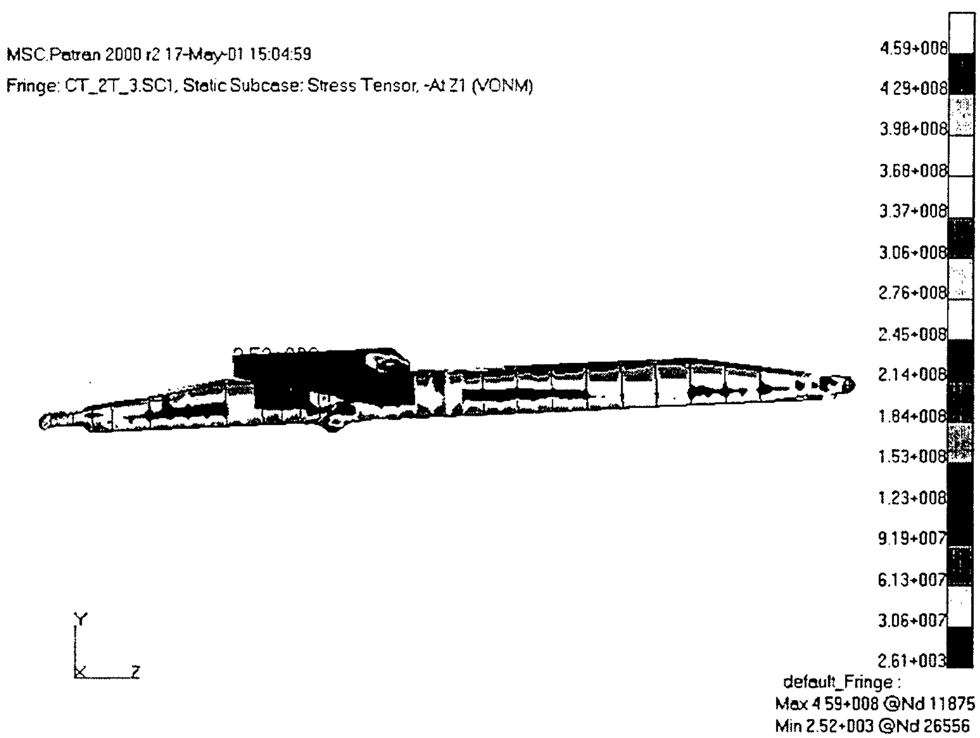

Figure 138. Cape T (left view) von Mises Stress Contour Plot, Max. Stress: 66.6 ksi (Inertia Loading, 3 Degree Twist, Two Tanks)

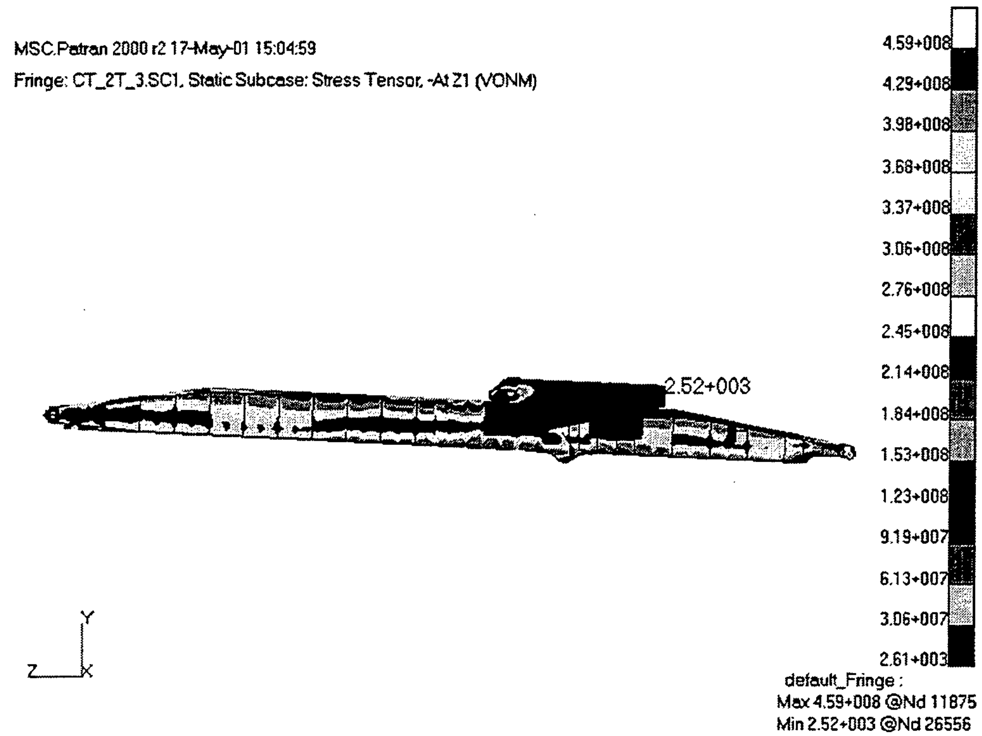

Figure 139. Cape T (right view) von Mises Stress Contour Plot, Max. Stress: 66.6 ksi (Inertia Loading, 3 Degree Twist, Two Tanks)

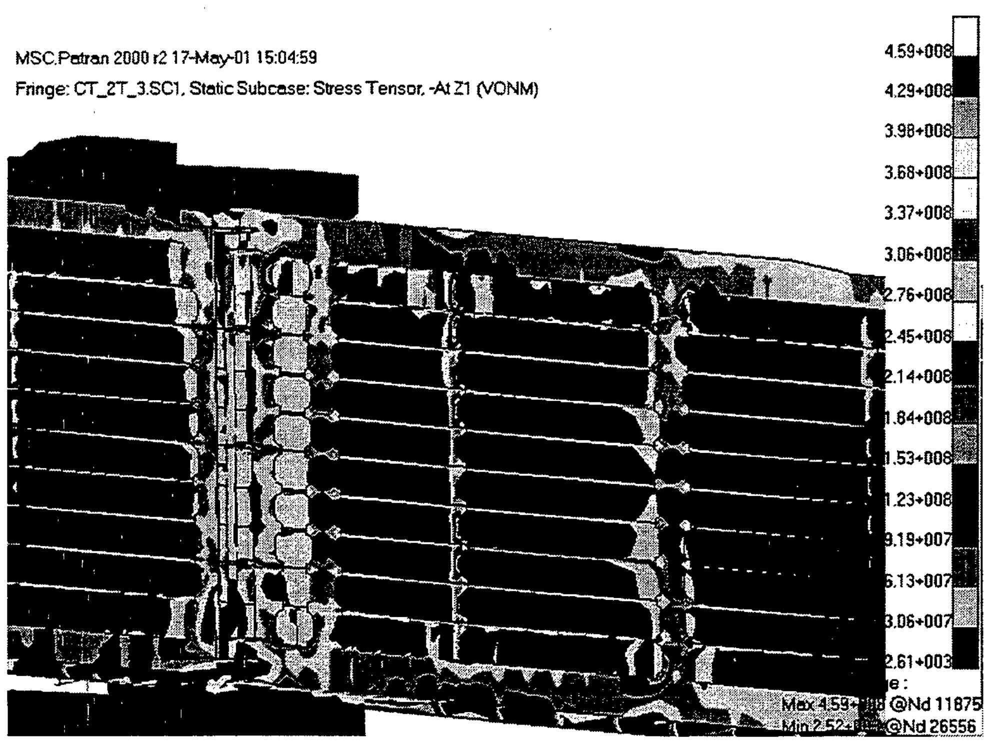

Figure 140. Cape T (close-up) von Mises Stress Contour Plot, Max. Stress: 66.6 ksi (Inertia Loading, 3 Degree Twist, Two Tanks)

3. Cape H Stern Ramp

The Cape H stern ramp analyses were conducted with boundary conditions similar to the Cape T and LMSR stern ramps (restrained in the three translational DOF at the ship end and the vertical DOF at the RRDF end). The Cape H ramp is an asymmetric design that is angled when deployed for RORO operations. Twist angles between the RRDF and ship of zero, one, and three degrees were considered. Maximum von Mises stress contour plots were generated with PATRAN and are displayed in Figures 141 through 192.

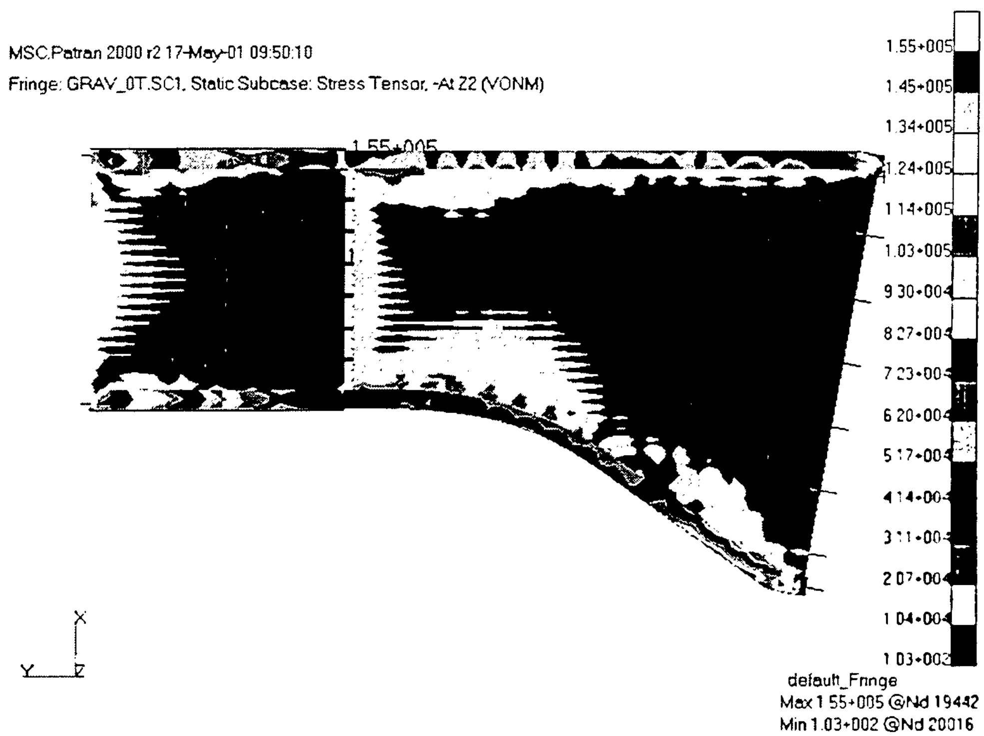

Figure 141. Cape H (top view) von Mises Stress Contour Plot, Max. Stress: 22.5 ksi (Inertia Loading, No Twist, No Tanks)

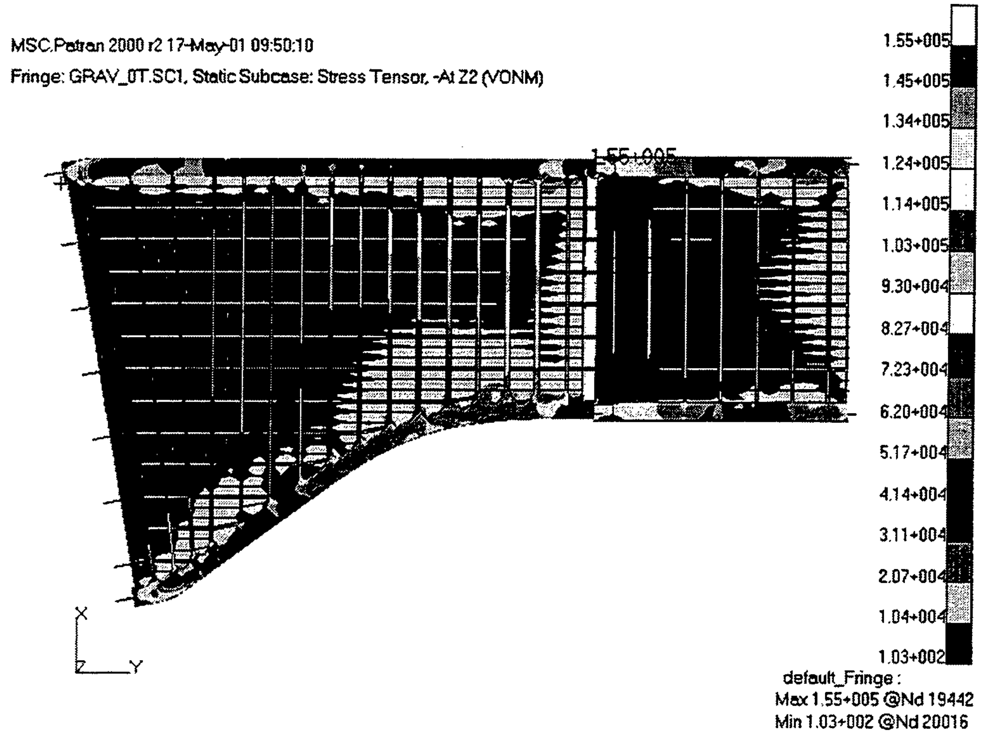

Figure 142. Cape H (bottom view) von Mises Stress Contour Plot, Max. Stress: 22.5 ksi (Inertia Loading, No Twist, No Tanks)

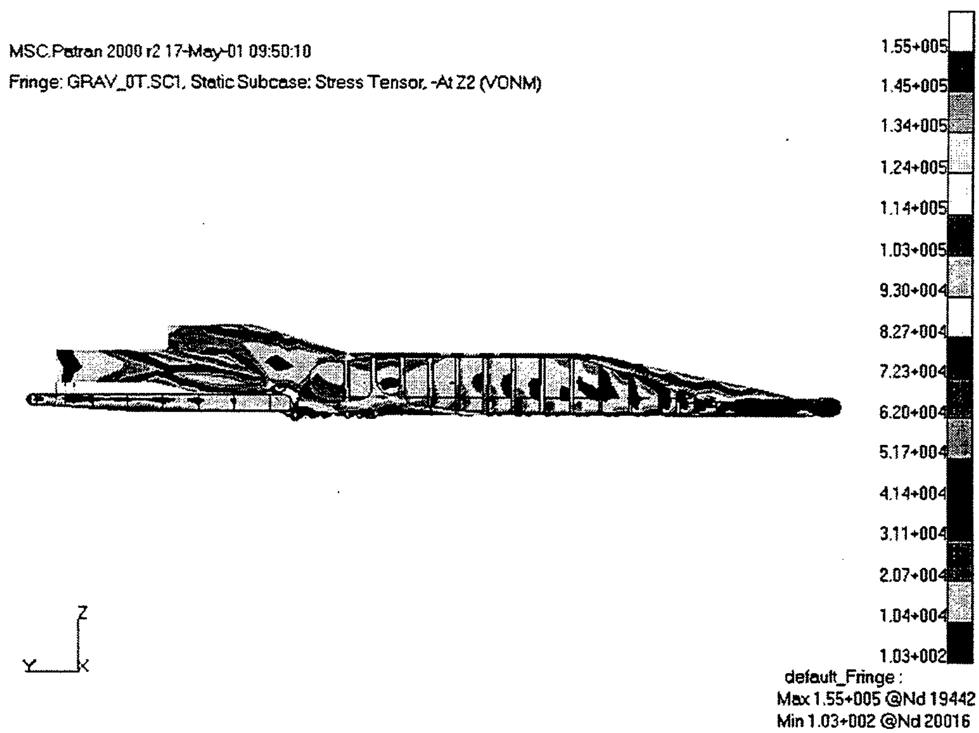

Figure 143. Cape H (left view) von Mises Stress Contour Plot, Max. Stress: 22.5 ksi (Inertia Loading, No Twist, No Tanks)

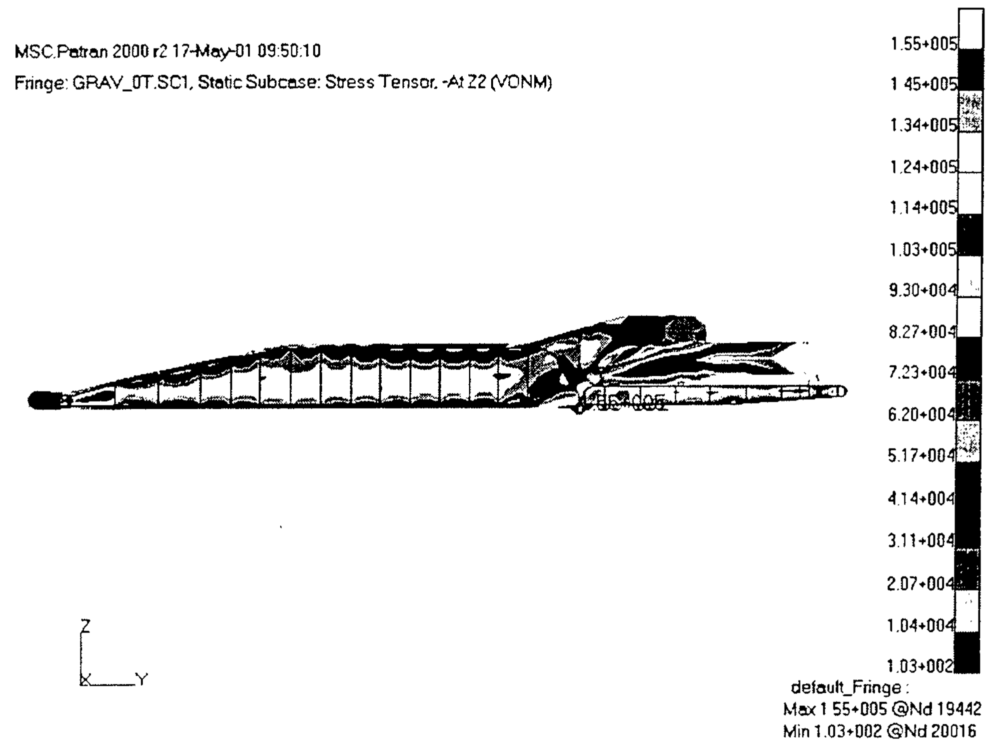

Figure 144. Cape H (right view) von Mises Stress Contour Plot, Max. Stress: 22.5 ksi (Inertia Loading, No Twist, No Tanks)

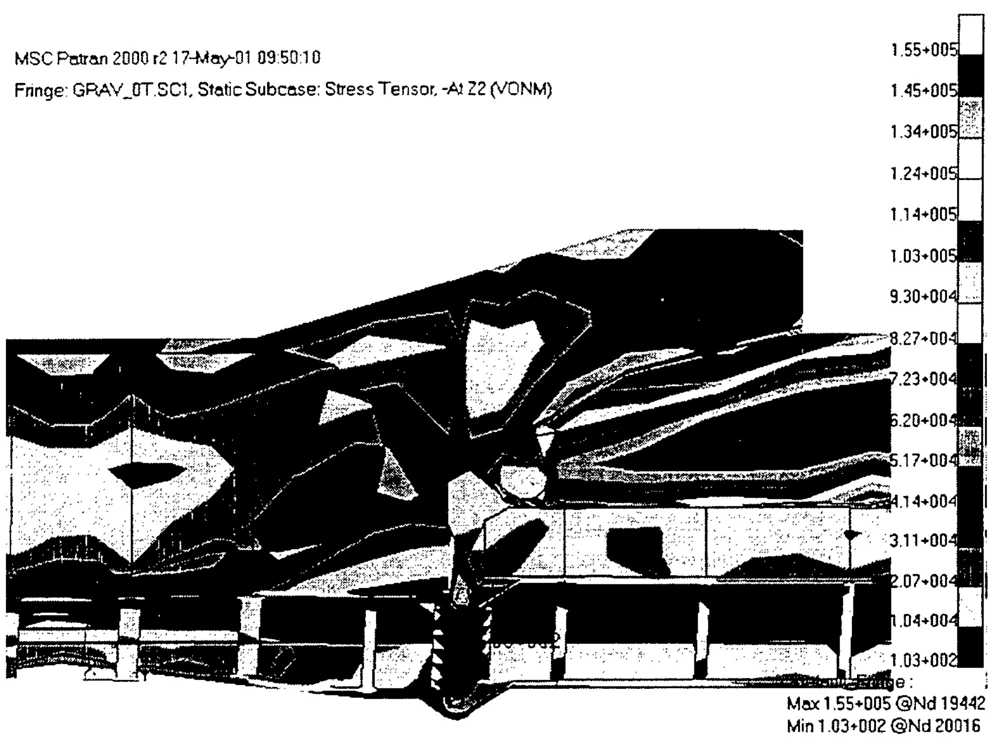

Figure 145. Cape H (close-up) von Mises Stress Contour Plot, Max. Stress: 22.5 ksi (Inertia Loading, No Twist, No Tanks)

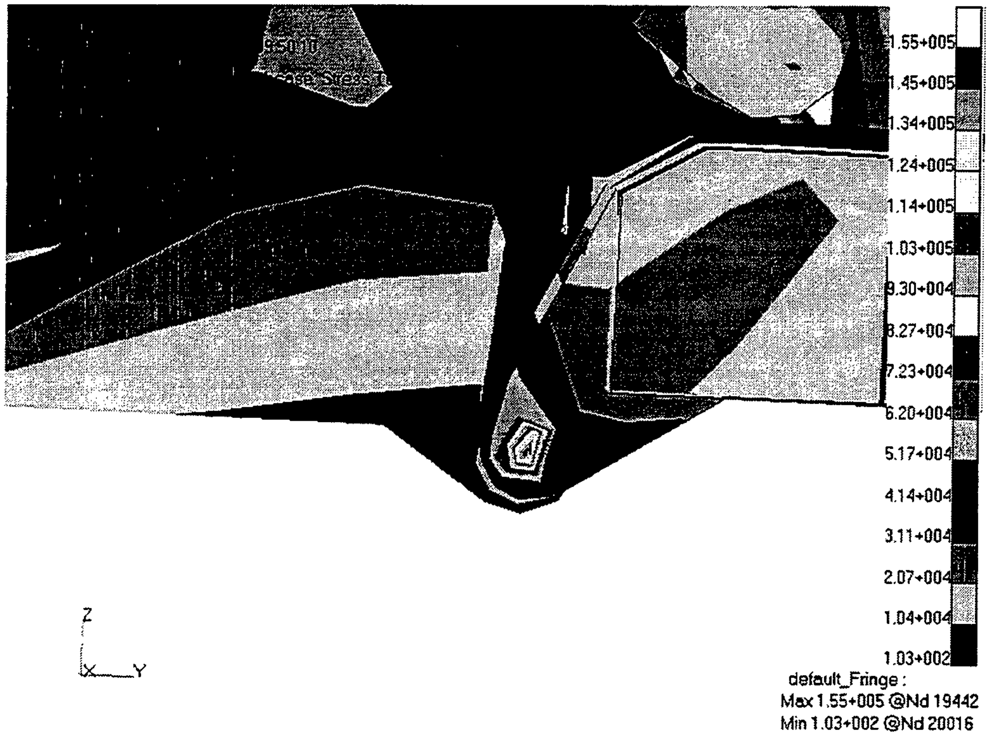

Figure 146. Cape H (close-up) von Mises Stress Contour Plot, Max. Stress: 22.5 ksi (Inertia Loading, No Twist, No Tanks)

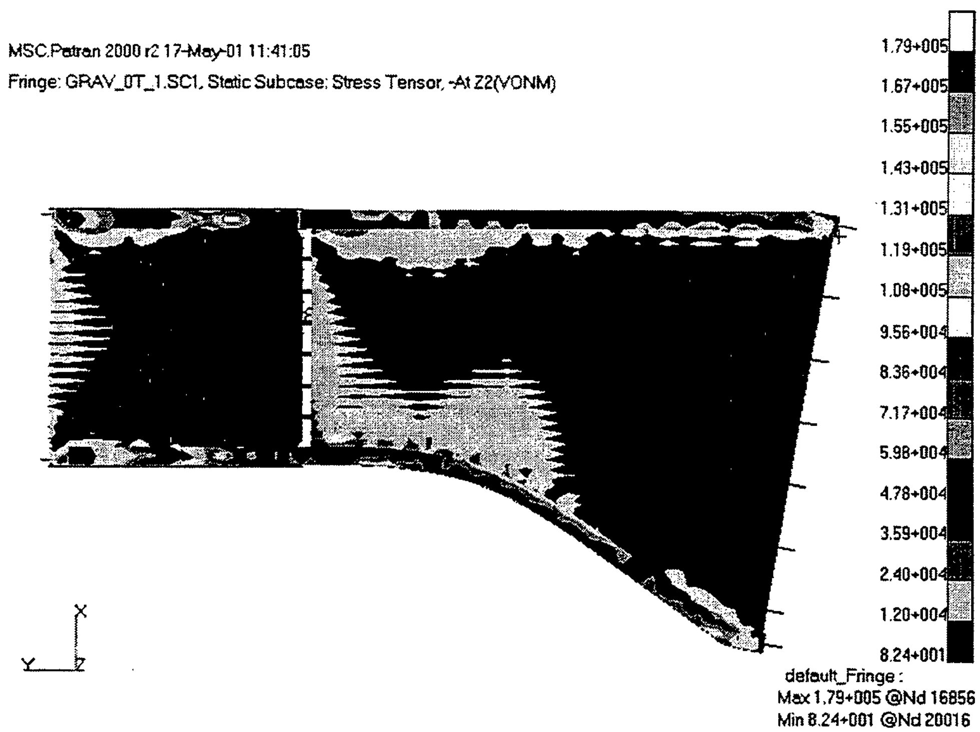

Figure 147. Cape H (top view) von Mises Stress Contour Plot, Max. Stress: 26.0 ksi (Inertia Loading, 1 Degree Twist, No Tanks)

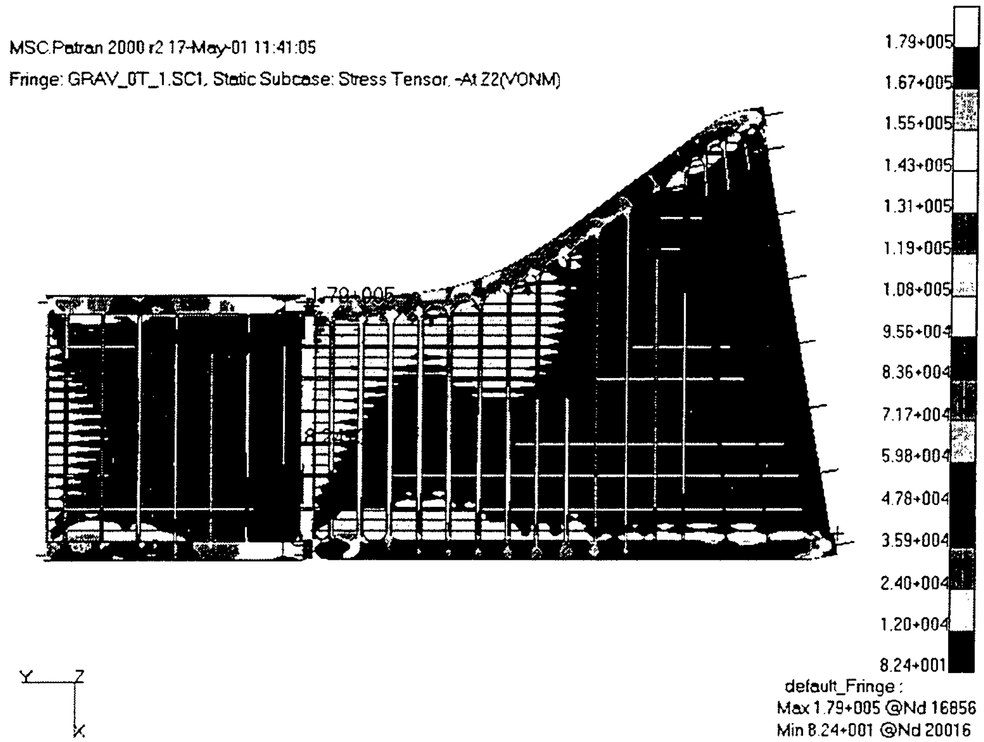

Figure 148. Cape H (bottom view) von Mises Stress Contour Plot, Max. Stress: 26.0 ksi (Inertia Loading, 1 Degree Twist, No Tanks)

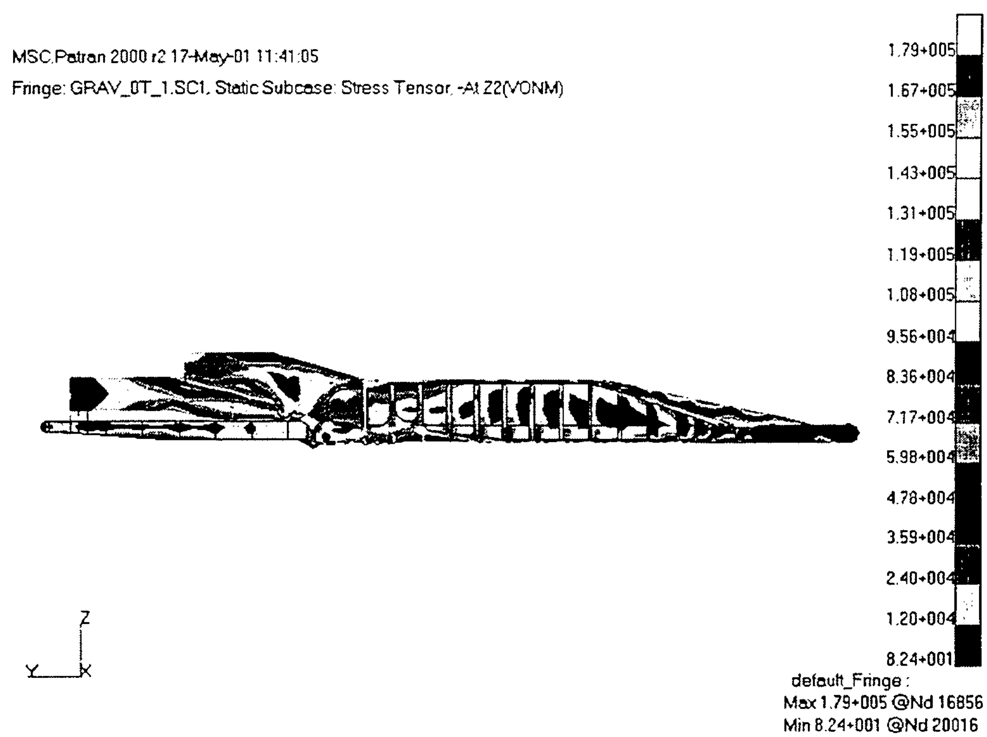

Figure 149. Cape H (left view) von Mises Stress Contour Plot, Max. Stress: 26.0 ksi (Inertia Loading, 1 Degree Twist, No Tanks)

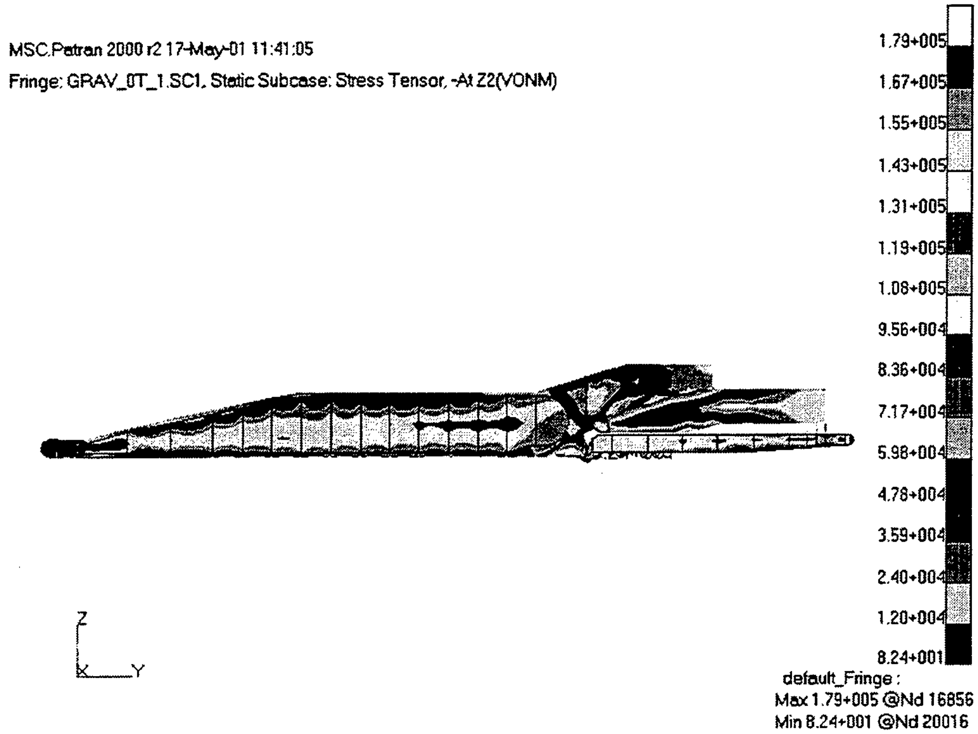

Figure 150. Cape H (right view) von Mises Stress Contour Plot, Max. Stress: 26.0 ksi (Inertia Loading, 1 Degree Twist, No Tanks)

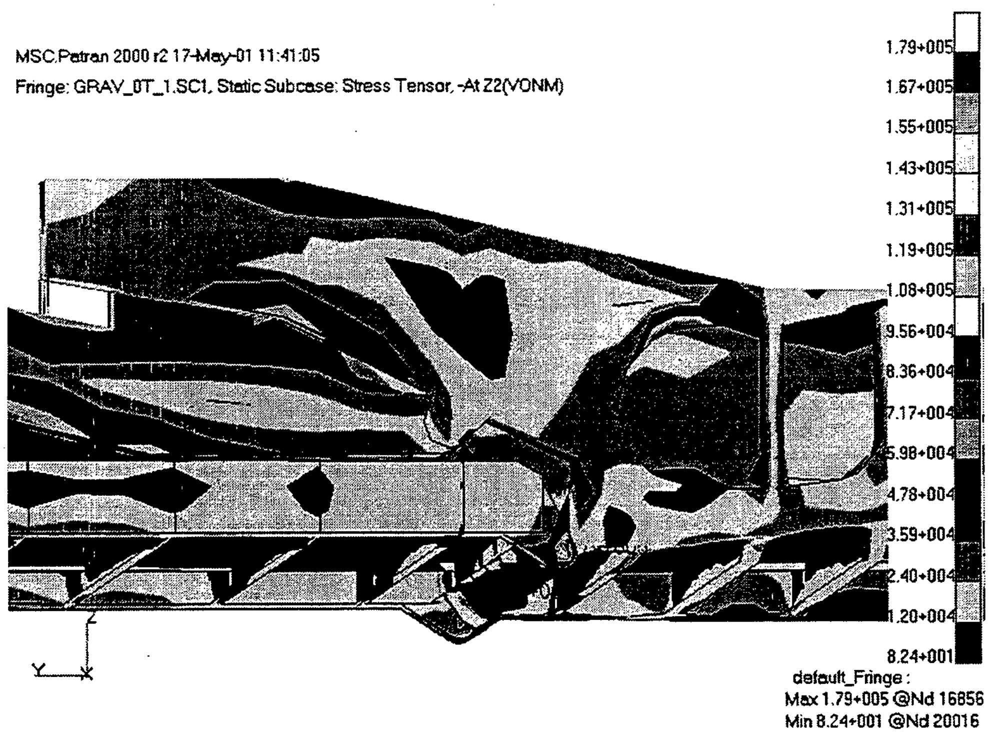

Figure 151. Cape H (close-up) von Mises Stress Contour Plot, Max. Stress: 26.0 ksi (Inertia Loading, 1 Degree Twist, No Tanks)

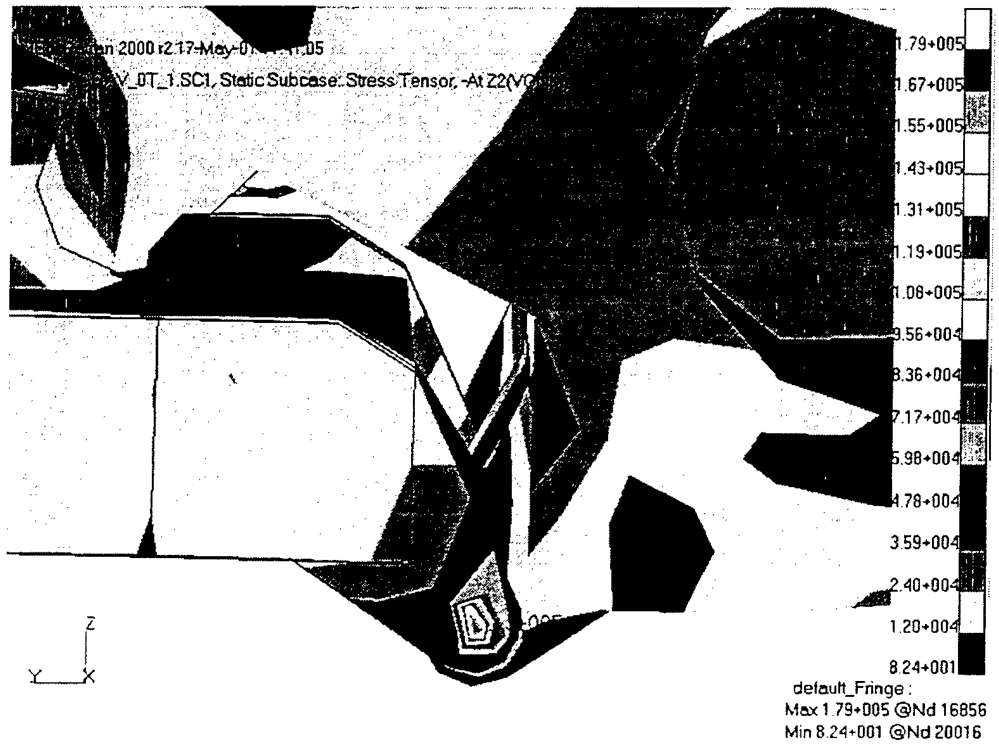

Figure 152. Cape H (close-up) von Mises Stress Contour Plot, Max. Stress: 26.0 ksi (Inertia Loading, 1 Degree Twist, No Tanks)

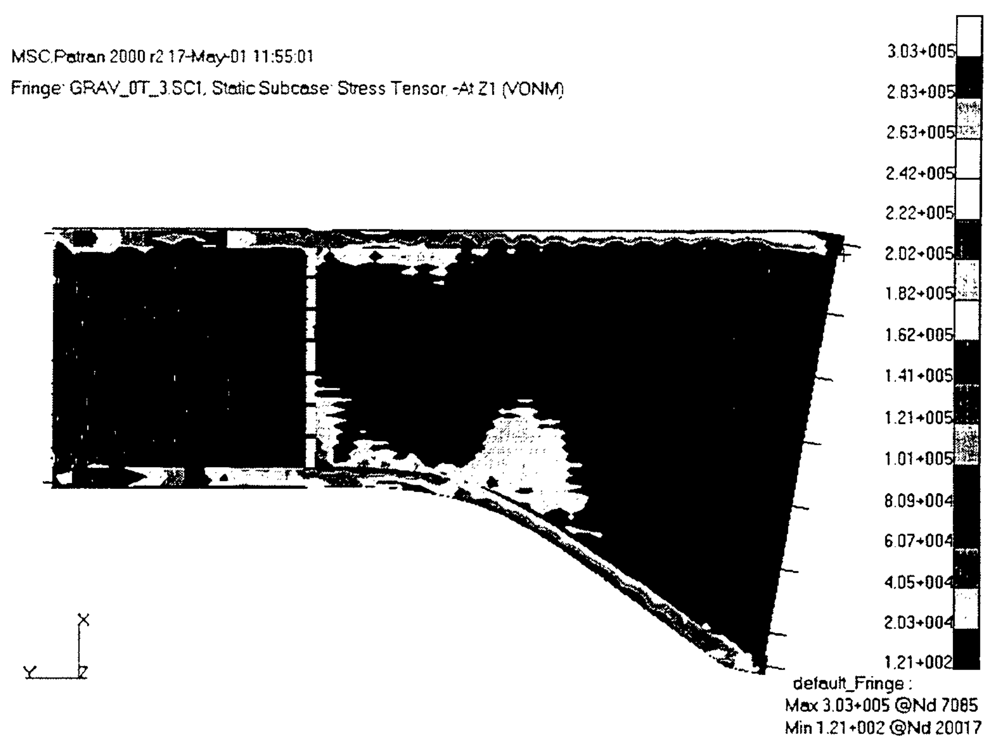

Figure 153. Cape H (top view) von Mises Stress Contour Plot, Max. Stress: 44.7 ksi (Inertia Loading, 3 Degree Twist, No Tanks)

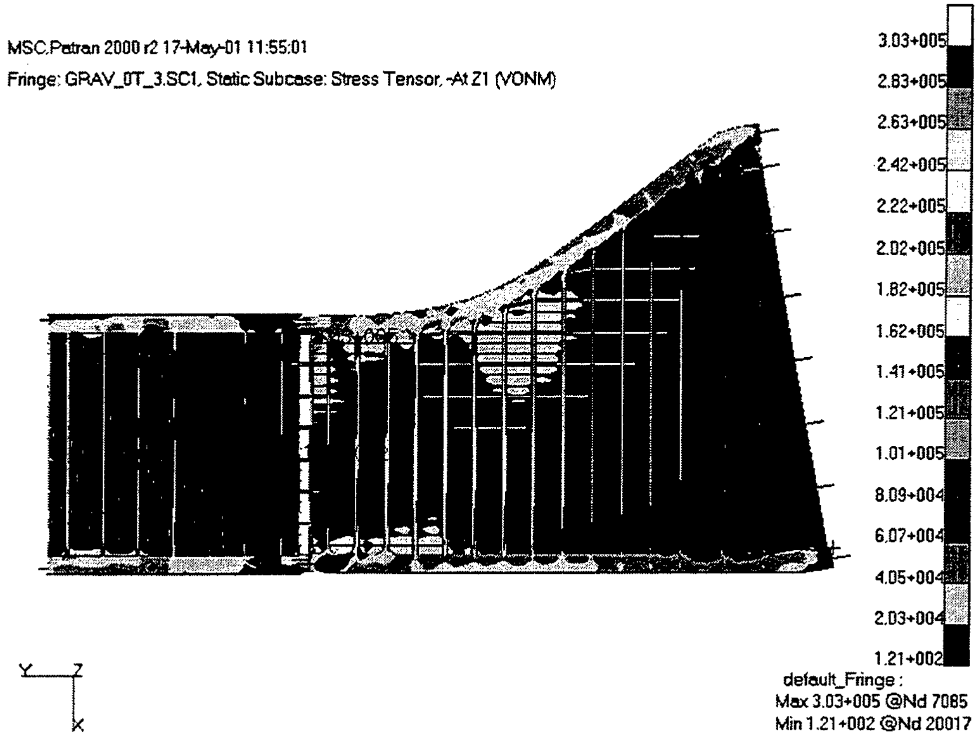

Figure 154. Cape H (bottom view) von Mises Stress Contour Plot, Max. Stress: 44.7 ksi (Inertia Loading, 3 Degree Twist, No Tanks)

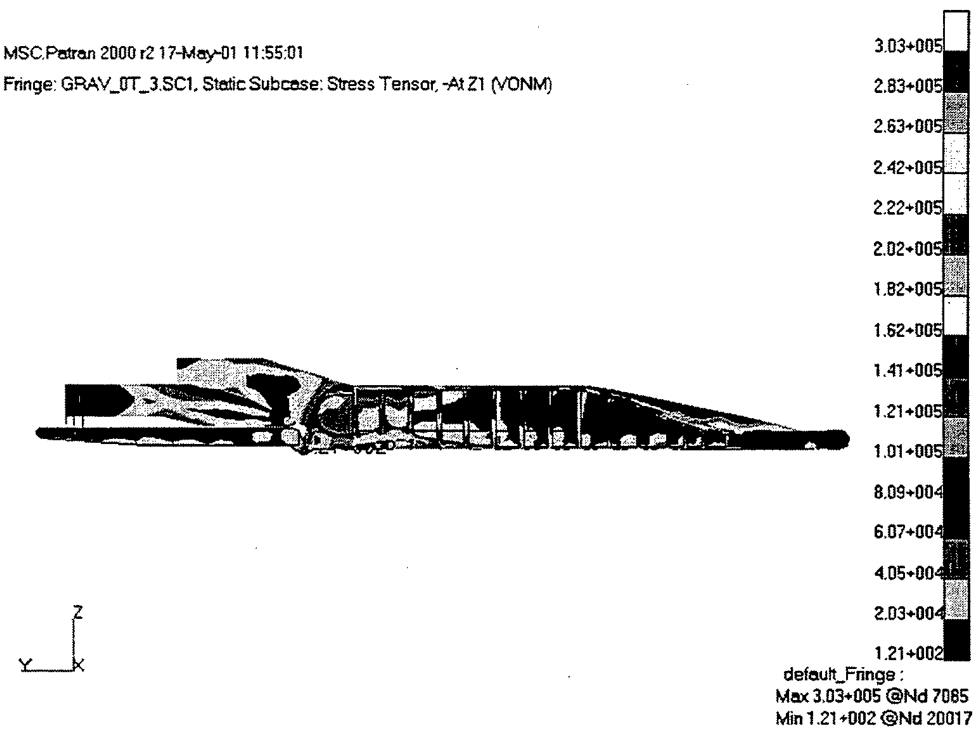

Figure 155. Cape H (left view) von Mises Stress Contour Plot, Max. Stress: 44.7 ksi (Inertia Loading, 3 Degree Twist, No Tanks)

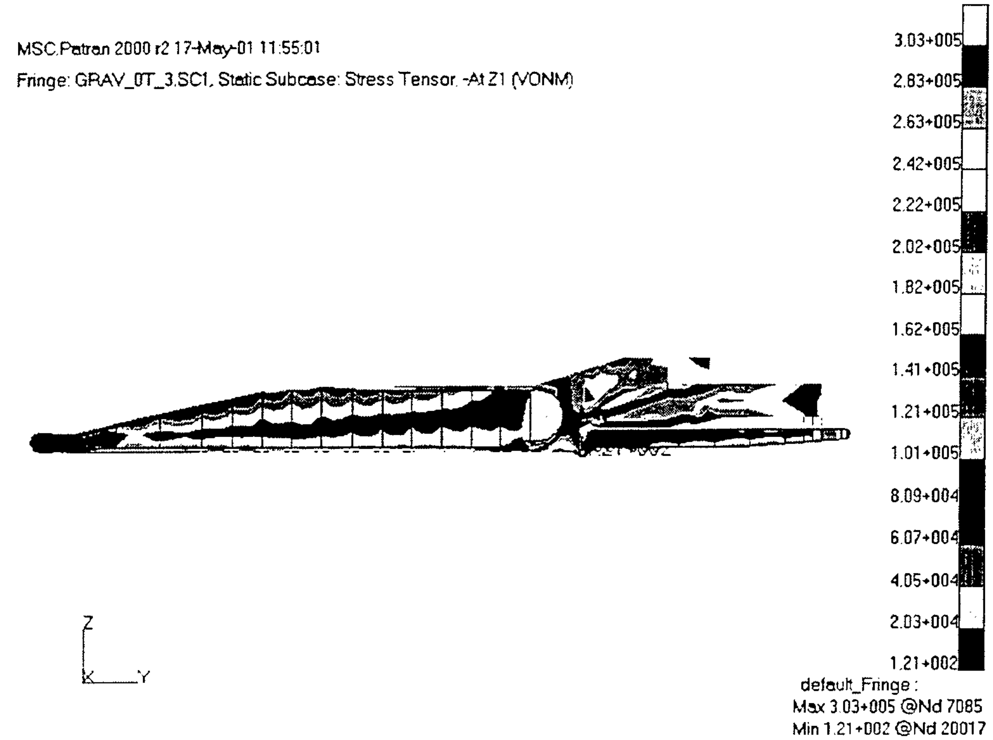

Figure 156. Cape H (right view) von Mises Stress Contour Plot, Max. Stress: 44.7 ksi (Inertia Loading, 3 Degree Twist, No Tanks)

Figure 157. Cape H (close-up) von Mises Stress Contour Plot, Max. Stress: 44.7 ksi (Inertia Loading, 3 Degree Twist, No Tanks)

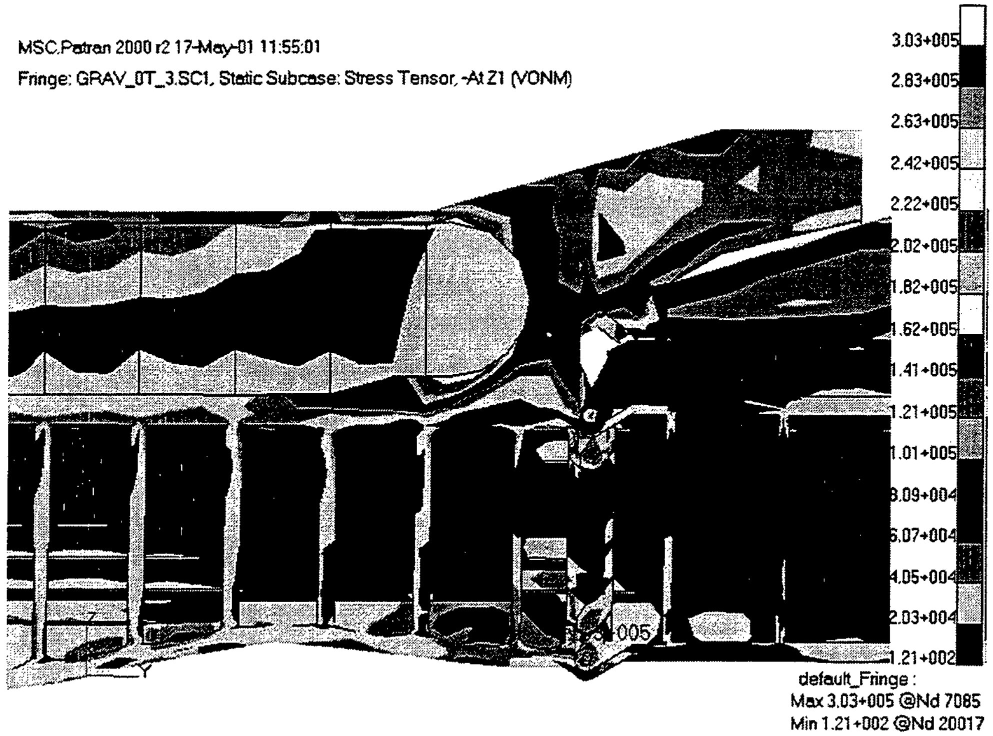

Figure 158. Cape H (close-up) von Mises Stress Contour Plot, Max. Stress: 44.7 ksi (Inertia Loading, 3 Degree Twist, No Tanks)

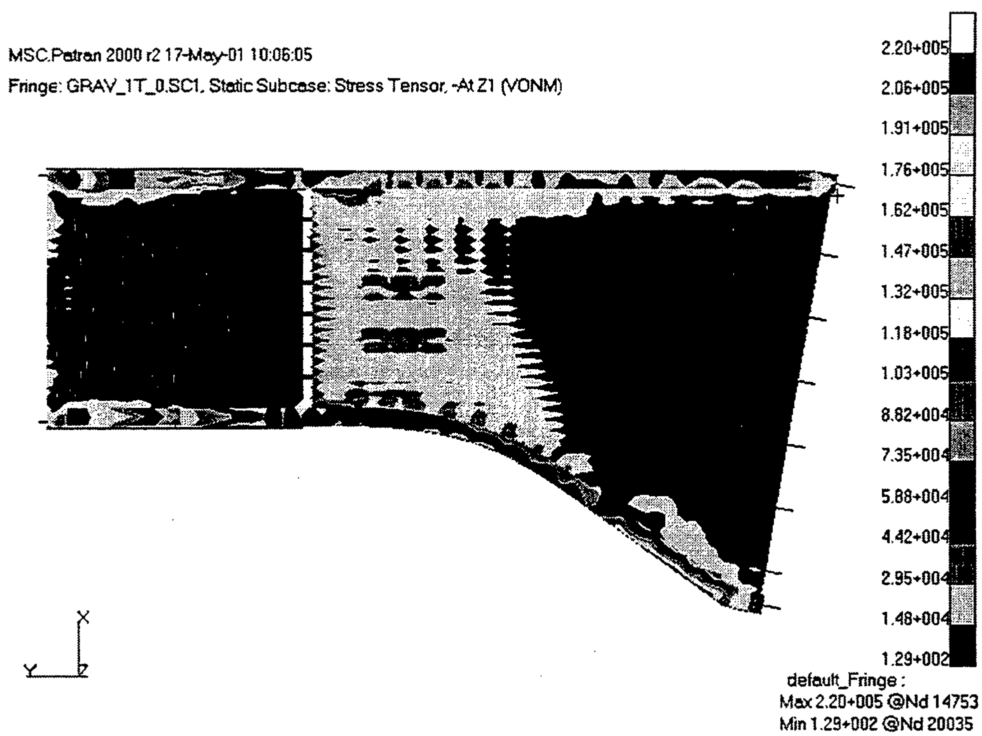

Figure 159. Cape H (top view) von Mises Stress Contour Plot, Max. Stress: 31.9 ksi (Inertia Loading, No Twist, One Tank)

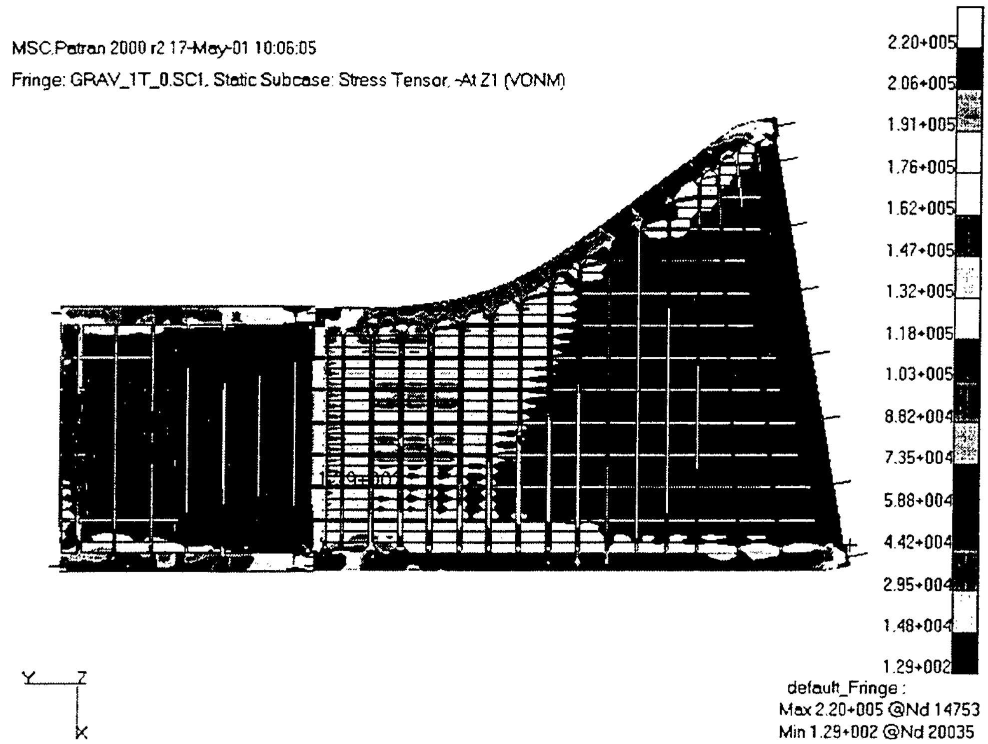

Figure 160. Cape H (bottom view) von Mises Stress Contour Plot, Max. Stress: 31.9 ksi (Inertia Loading, No Twist, One Tank)

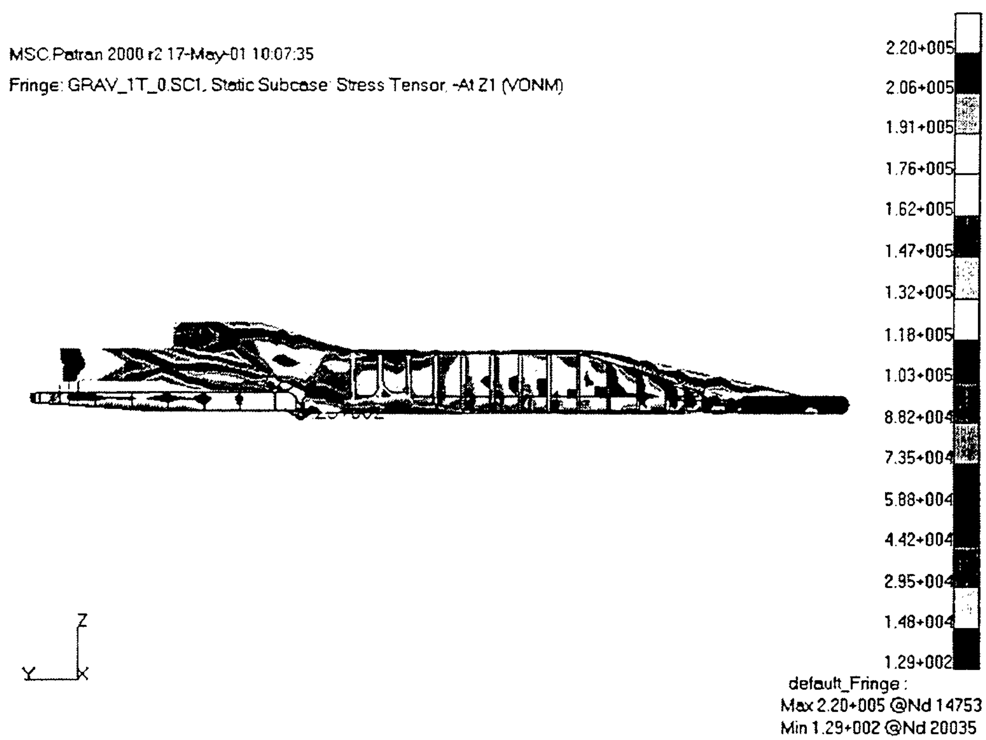

Figure 161. Cape H (left view) von Mises Stress Contour Plot, Max. Stress: 31.9 ksi (Inertia Loading, No Twist, One Tank)

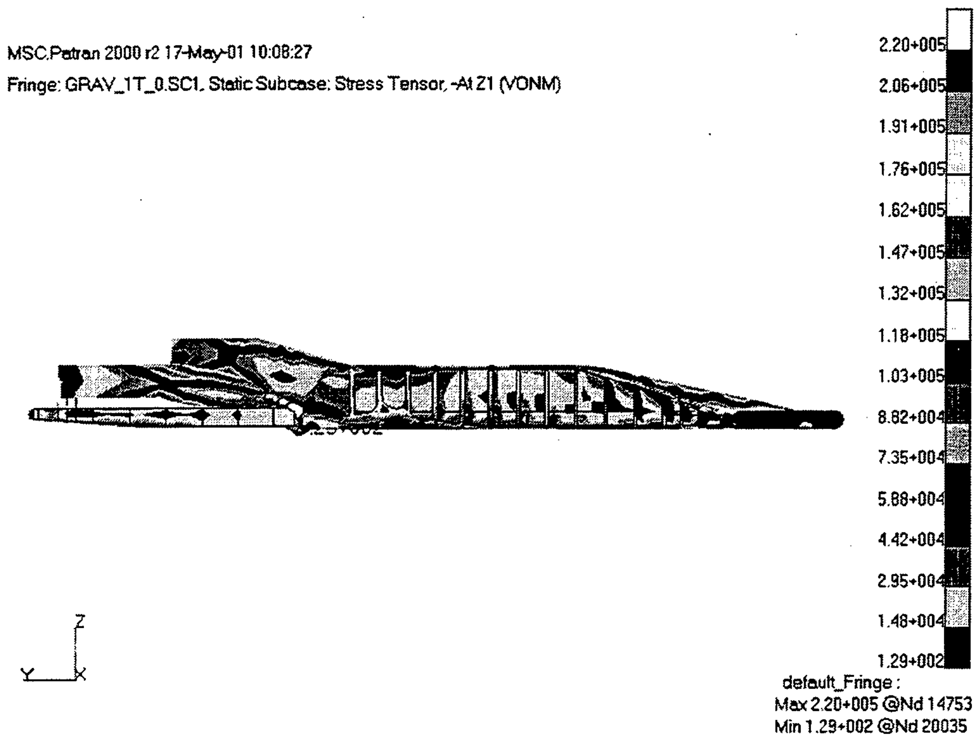

Figure 162. Cape H (right view) von Mises Stress Contour Plot, Max. Stress: 31.9 ksi (Inertia Loading, No Twist, One Tank)

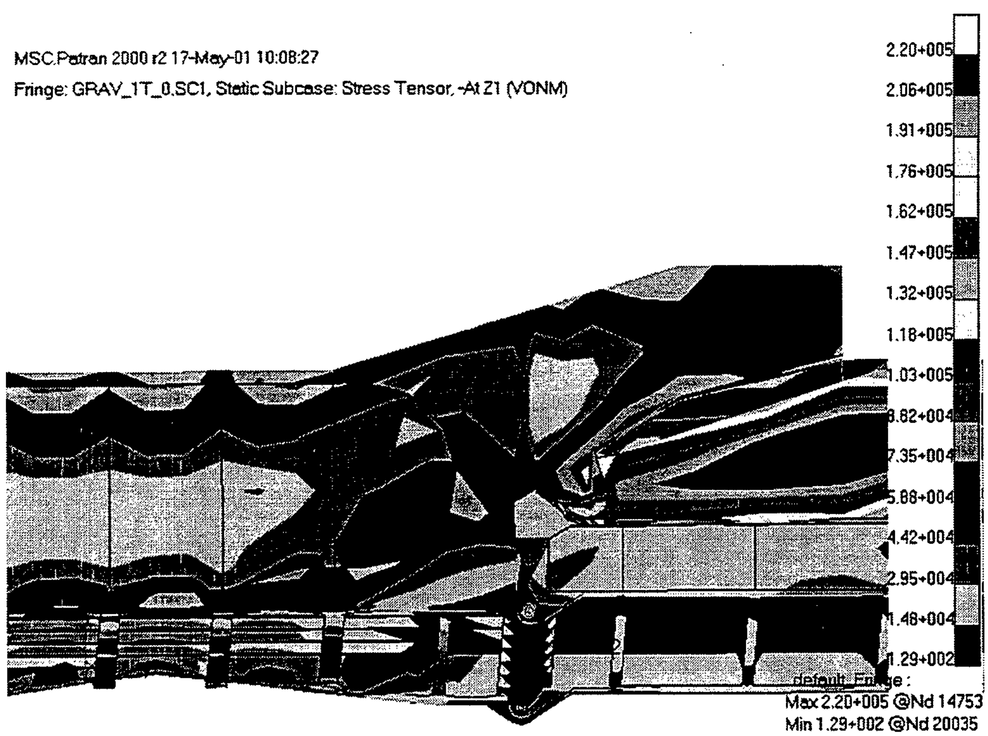

Figure 163. Cape H (close-up) von Mises Stress Contour Plot, Max. Stress: 31.9 ksi (Inertia Loading, No Twist, One Tank)

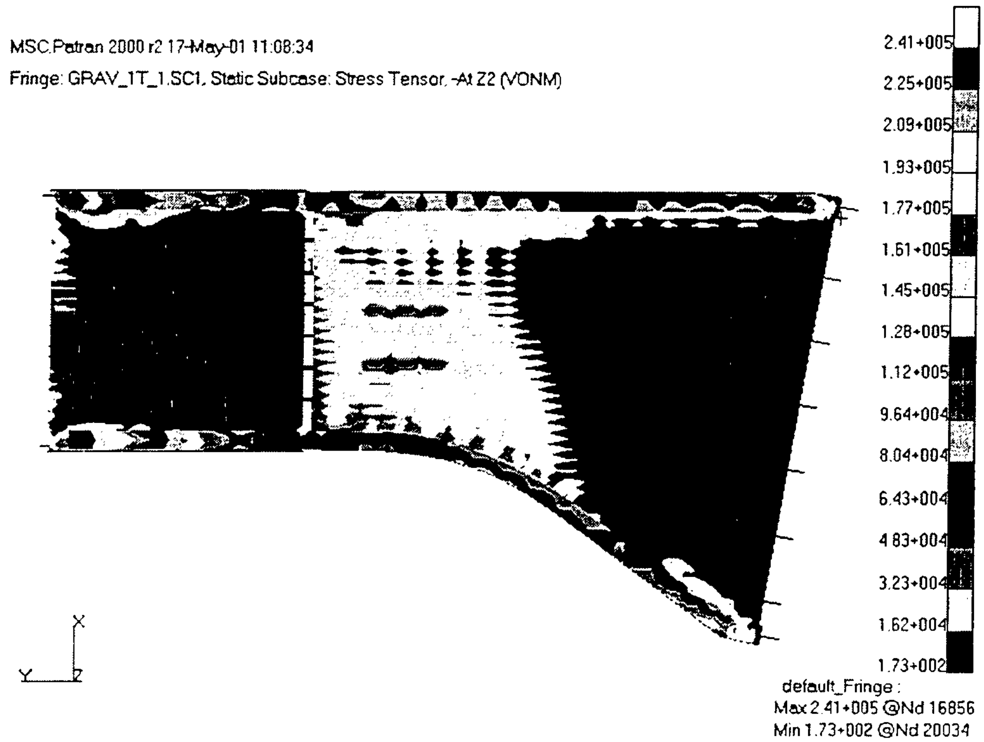

Figure 164. Cape H (top view) von Mises Stress Contour Plot, Max. Stress: 35.0 ksi (Inertia Loading, 1 Degree Twist, One Tank)

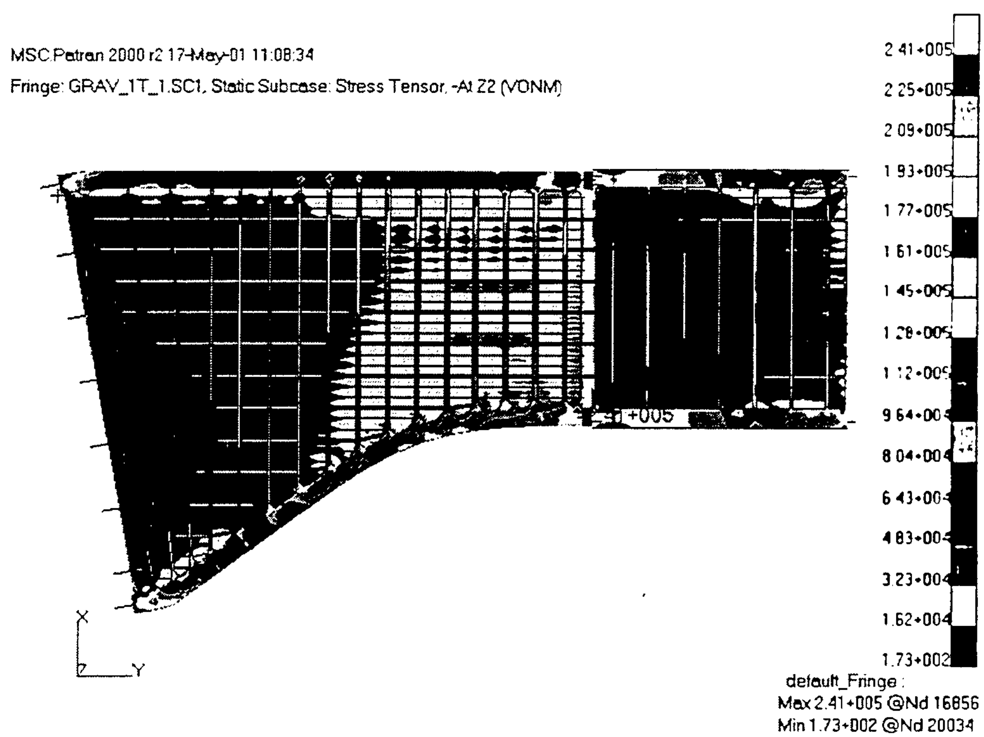

Figure 165. Cape H (bottom view) von Mises Stress Contour Plot, Max. Stress: 35.0 ksi (Inertia Loading, 1 Degree Twist, One Tank)

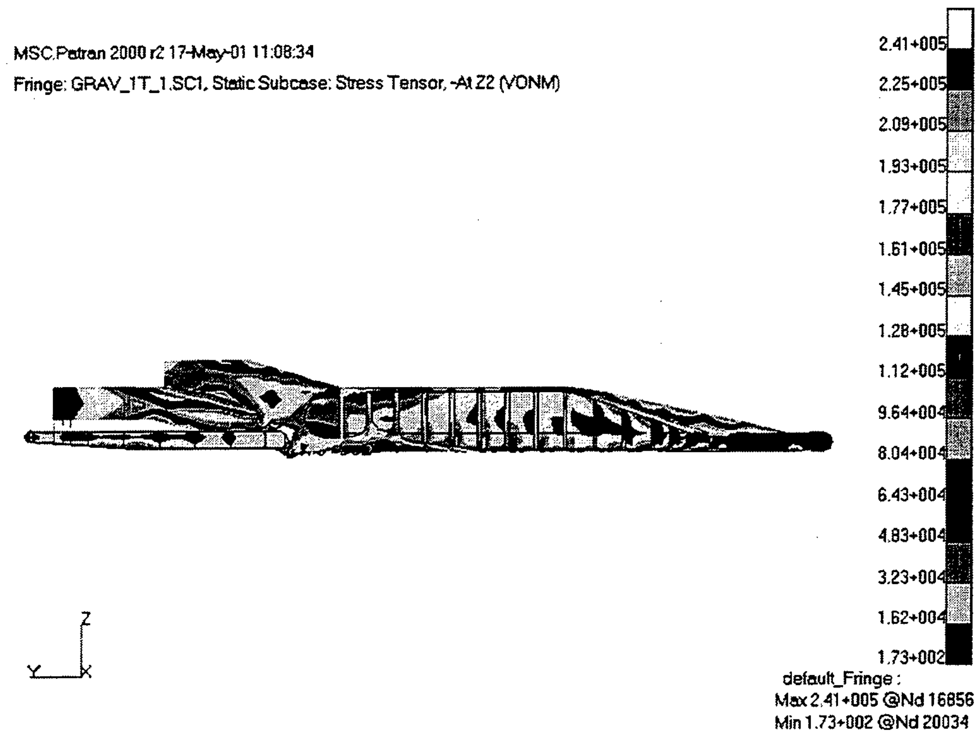

Figure 166. Cape H (left view) von Mises Stress Contour Plot, Max. Stress: 35.0 ksi (Inertia Loading, 1 Degree Twist, One Tank)

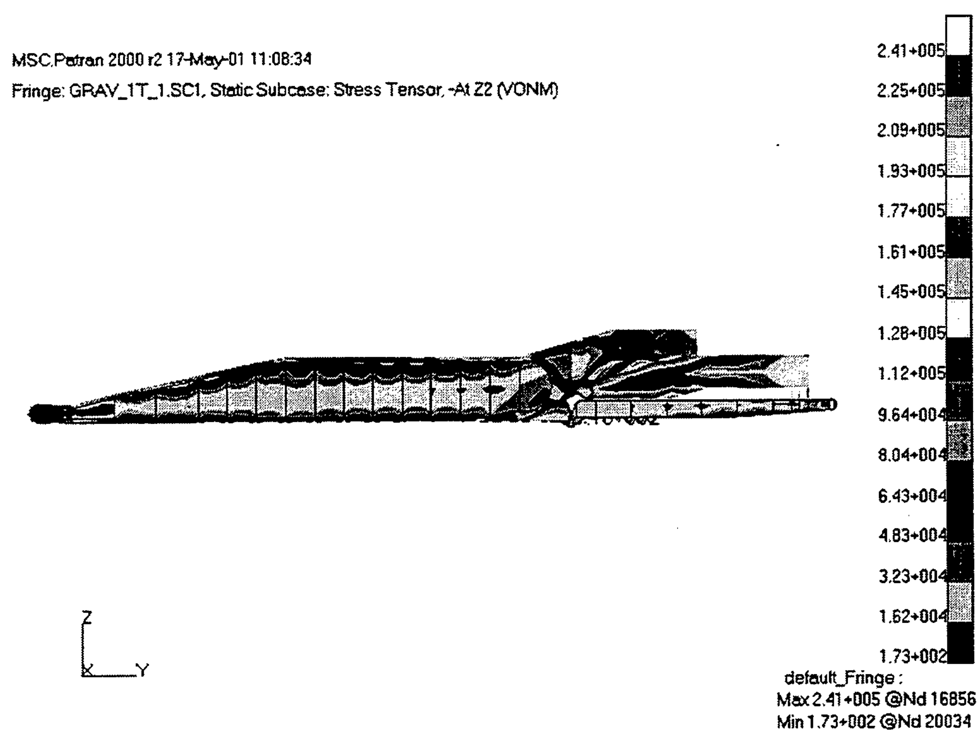

Figure 167. Cape H (right view) von Mises Stress Contour Plot, Max. Stress: 35.0 ksi (Inertia Loading, 1 Degree Twist, One Tank)

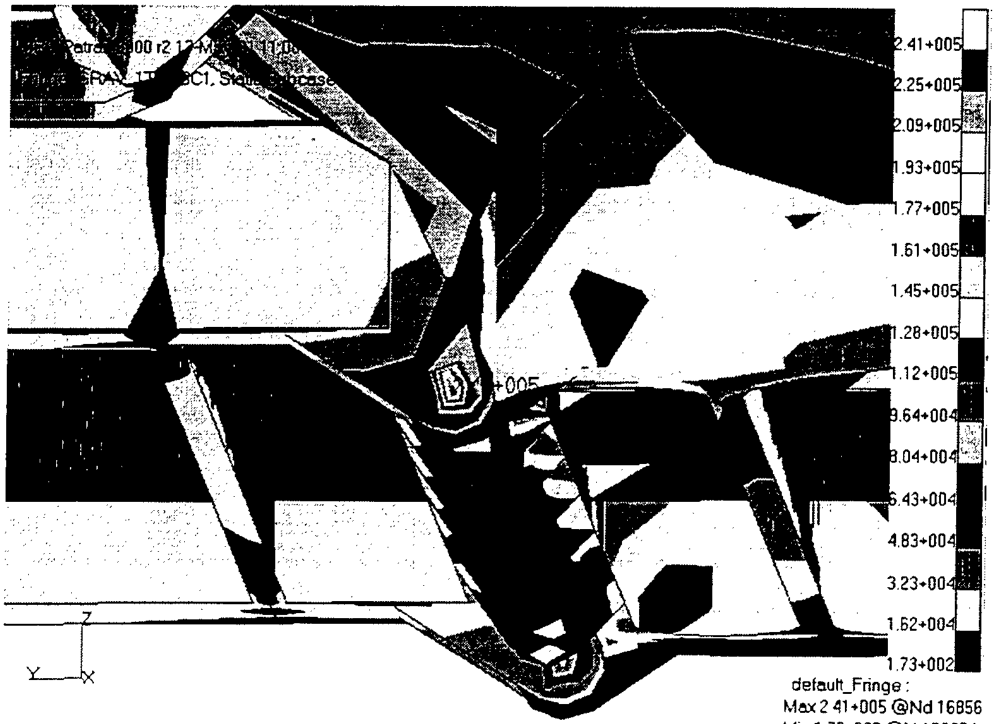

Figure 168. Cape H (close-up) von Mises Stress Contour Plot, Max. Stress: 35.0 ksi (Inertia Loading, 1 Degree Twist, One Tank)

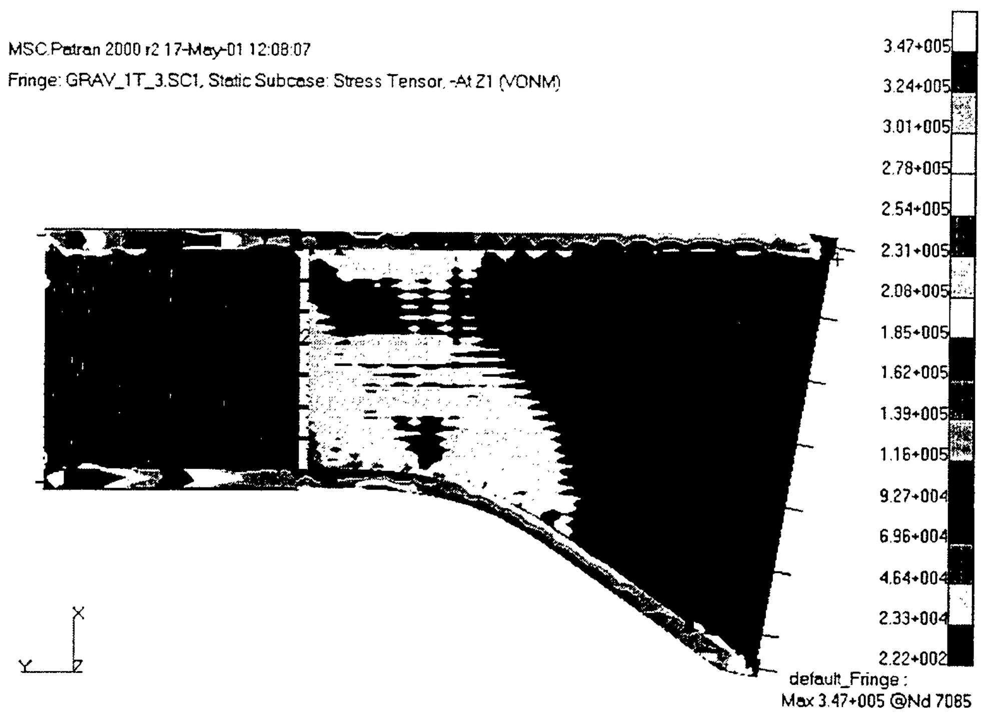

Figure 169. Cape H (top view) von Mises Stress Contour Plot, Max. Stress: 50.3 ksi (Inertia Loading, 3 Degree Twist, One Tank)

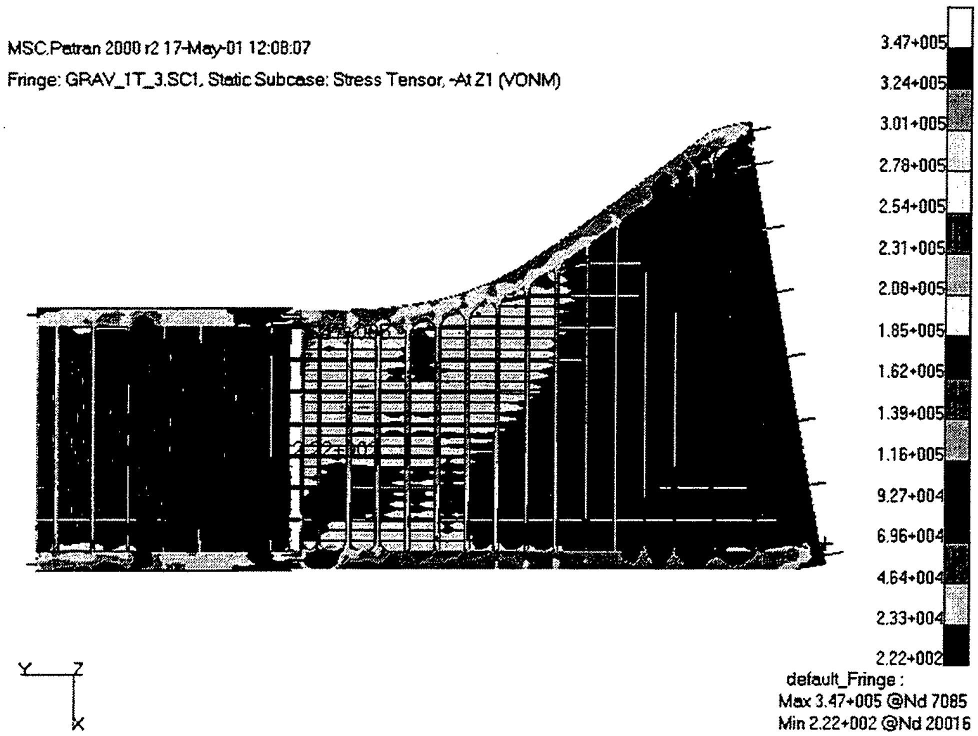

Figure 170. Cape H (bottom view) von Mises Stress Contour Plot, Max. Stress: 50.3 ksi (Inertia Loading, 3 Degree Twist, One Tank)

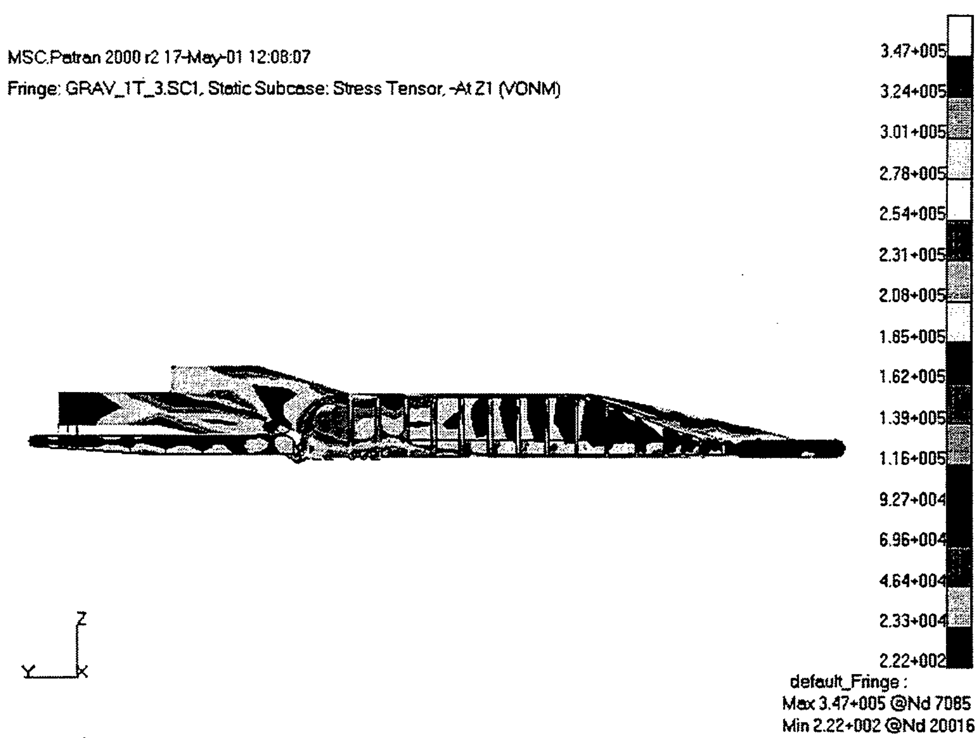

Figure 171. Cape H (left view) von Mises Stress Contour Plot, Max. Stress: 50.3 ksi (Inertia Loading, 3 Degree Twist, One Tank)

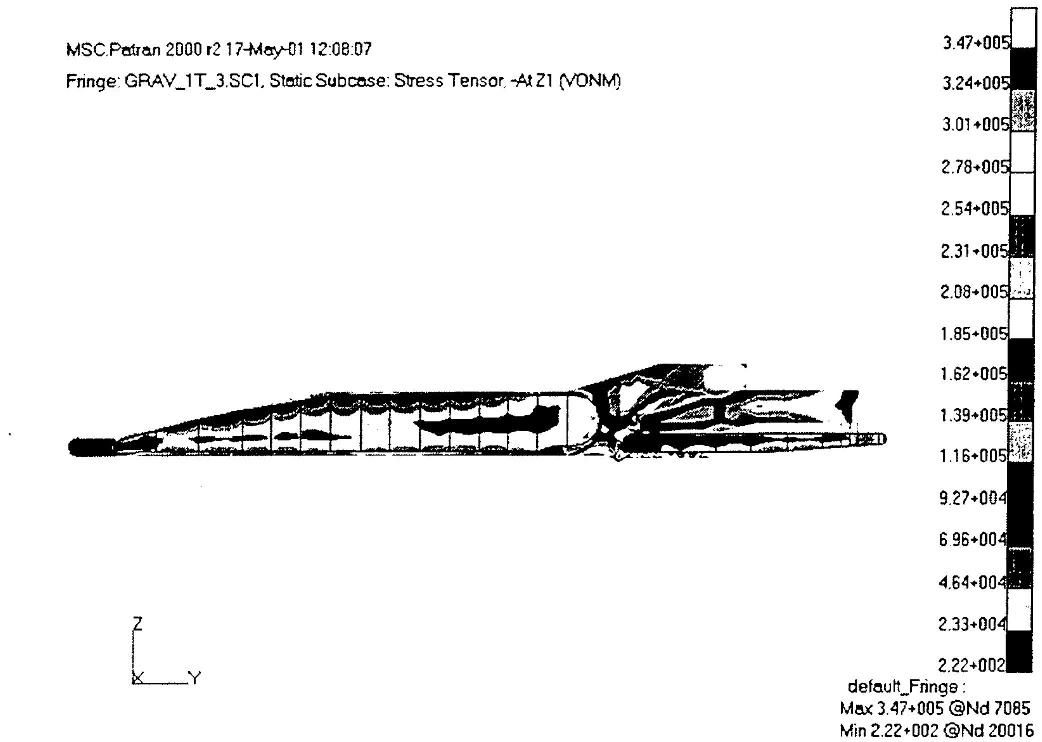

Figure 172. Cape H (right view) von Mises Stress Contour Plot, Max. Stress: 50.3 ksi (Inertia Loading, 3 Degree Twist, One Tank)

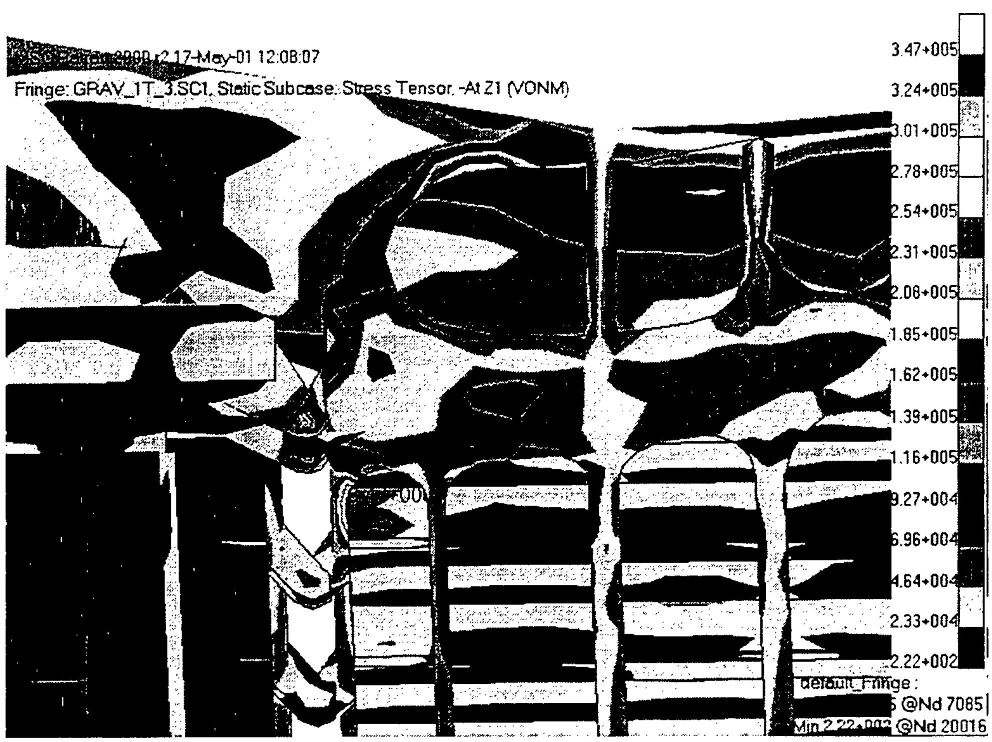

Figure 173. Cape H (close-up) von Mises Stress Contour Plot, Max. Stress: 50.3 ksi (Inertia Loading, 3 Degree Twist, One Tank)

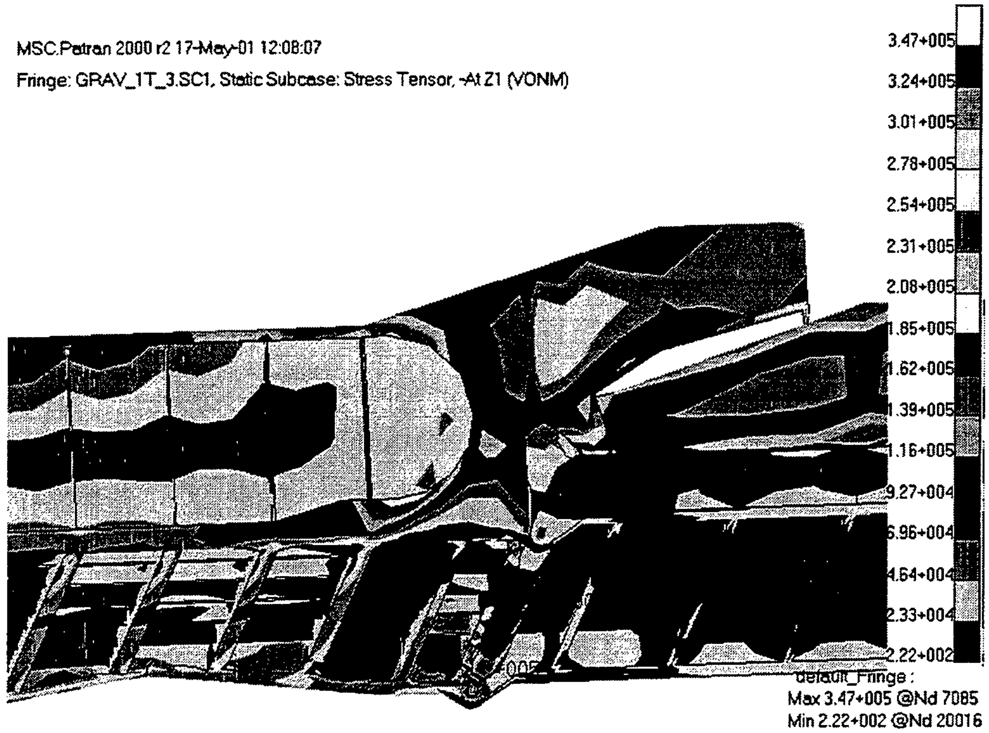

Figure 174. Cape H (close-up) von Mises Stress Contour Plot, Max. Stress: 50.3 ksi (Inertia Loading, 3 Degree Twist, One Tank)

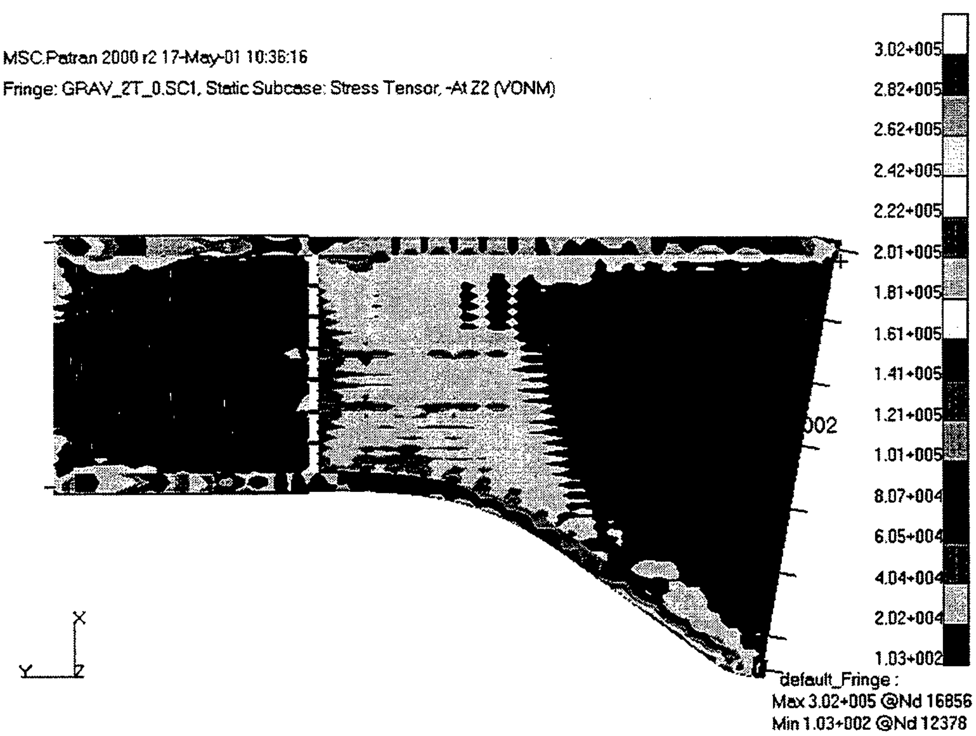

Figure 175. Cape H (top view) von Mises Stress Contour Plot, Max. Stress: 43.8 ksi (Inertia Loading, No Twist, Two Tanks)

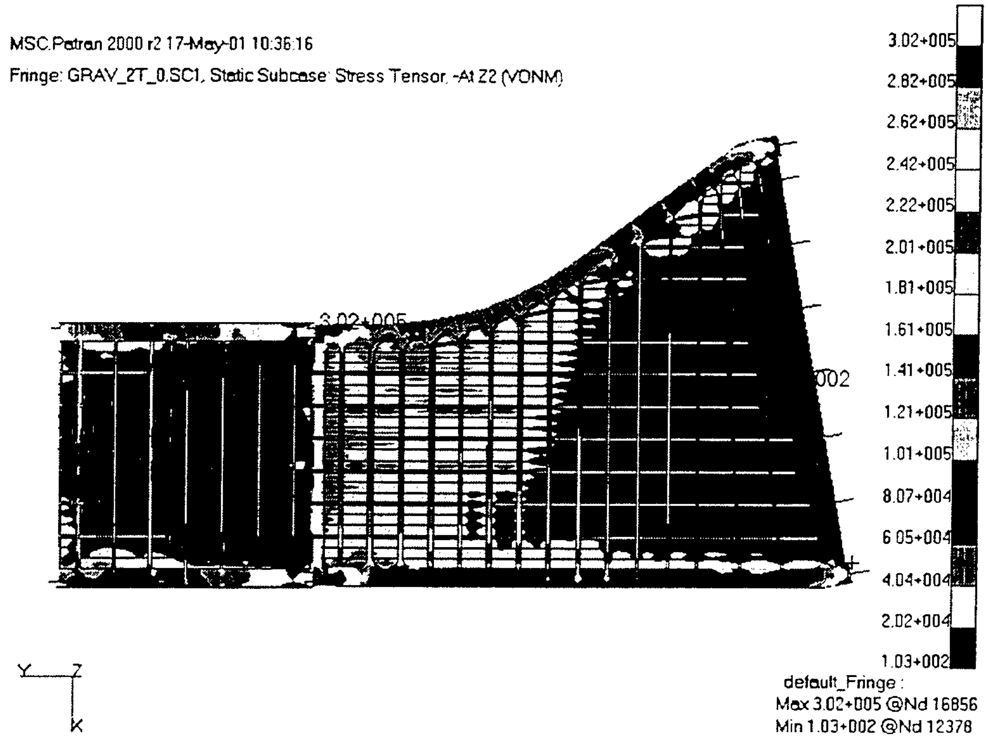

Figure 176. Cape H (bottom view) von Mises Stress Contour Plot, Max. Stress: 43.8 ksi (Inertia Loading, No Twist, Two Tanks)

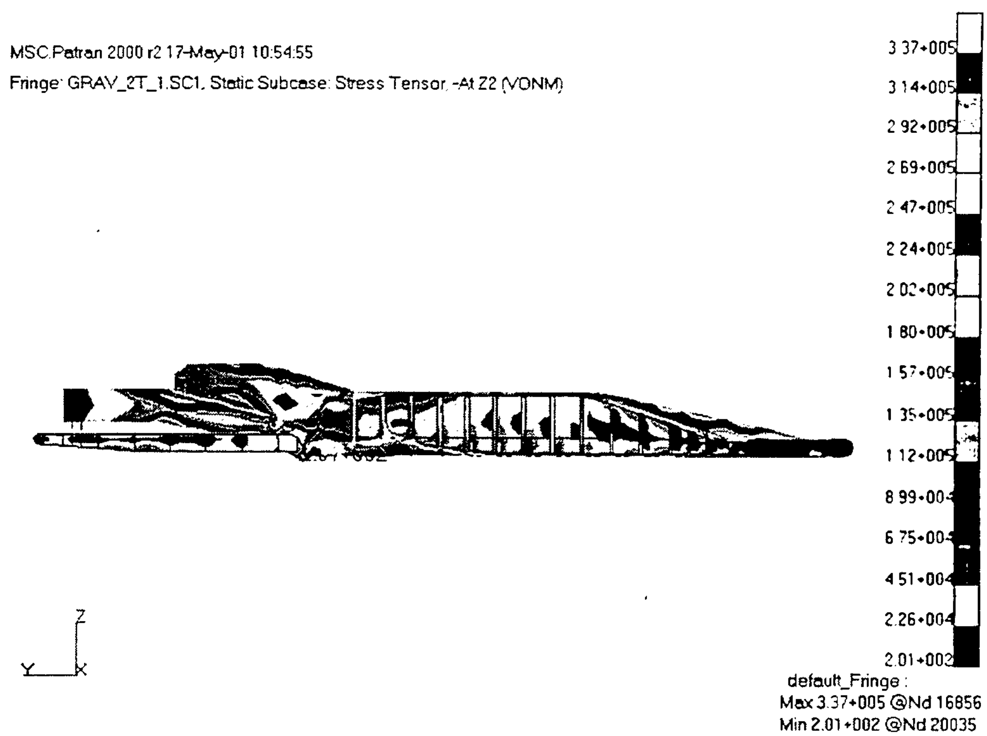

Figure 177. Cape H (left view) von Mises Stress Contour Plot, Max. Stress: 43.8 ksi (Inertia Loading, No Twist, Two Tanks)

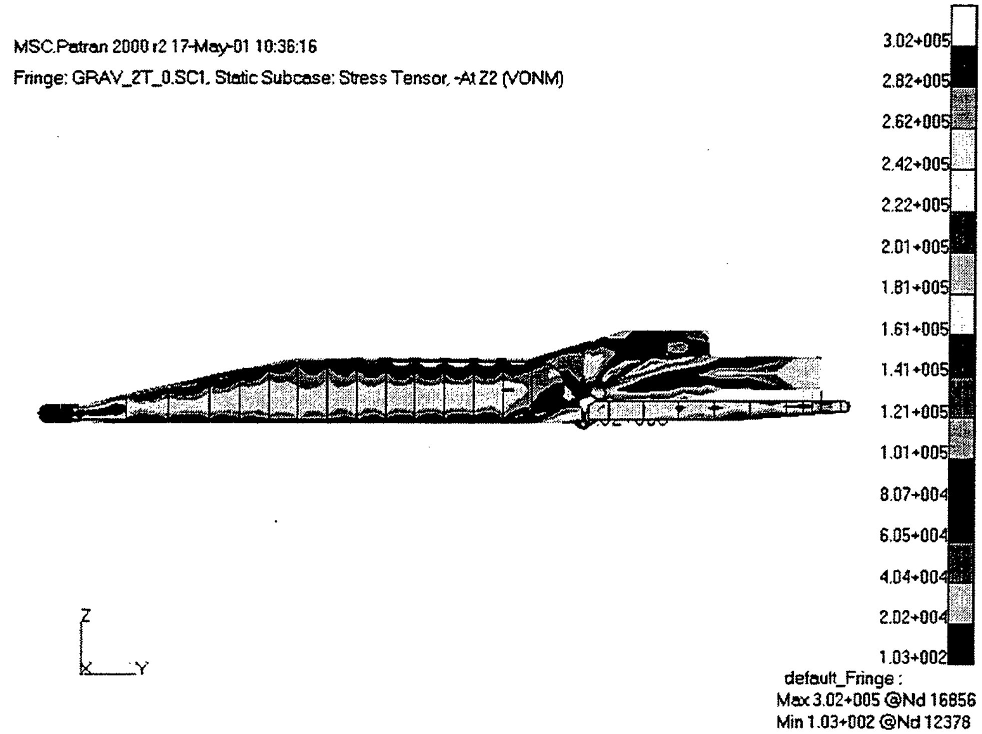

Figure 178. Cape H (right view) von Mises Stress Contour Plot, Max. Stress: 43.8 ksi (Inertia Loading, No Twist, Two Tanks)

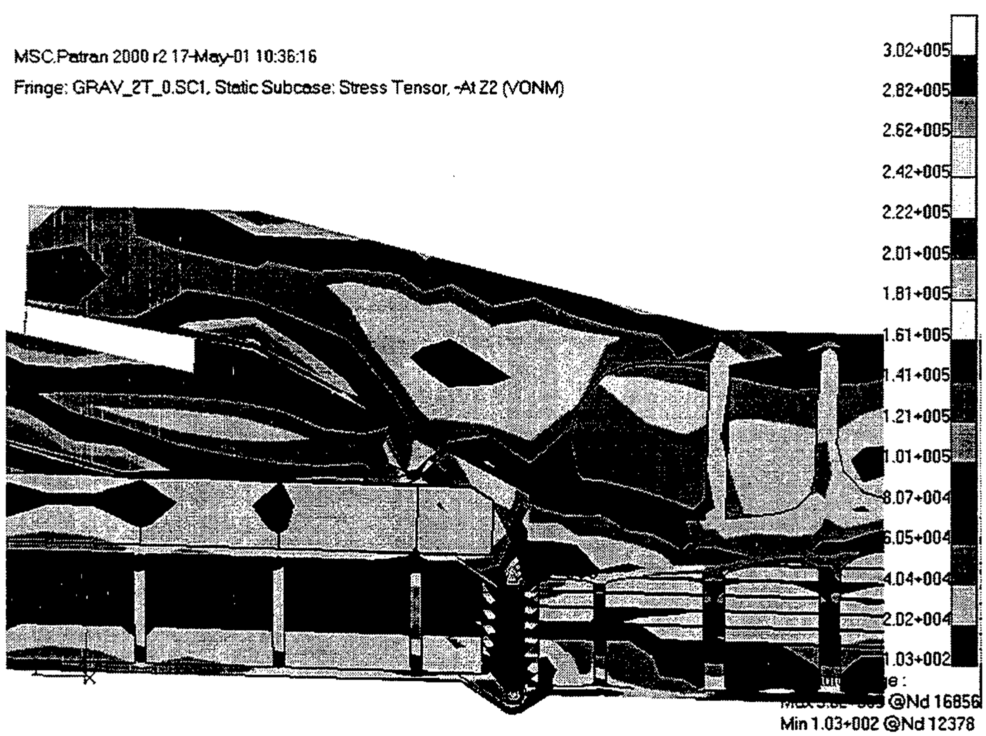

Figure 179. Cape H (close-up) von Mises Stress Contour Plot, Max. Stress: 43.8 ksi (Inertia Loading, No Twist, Two Tanks)

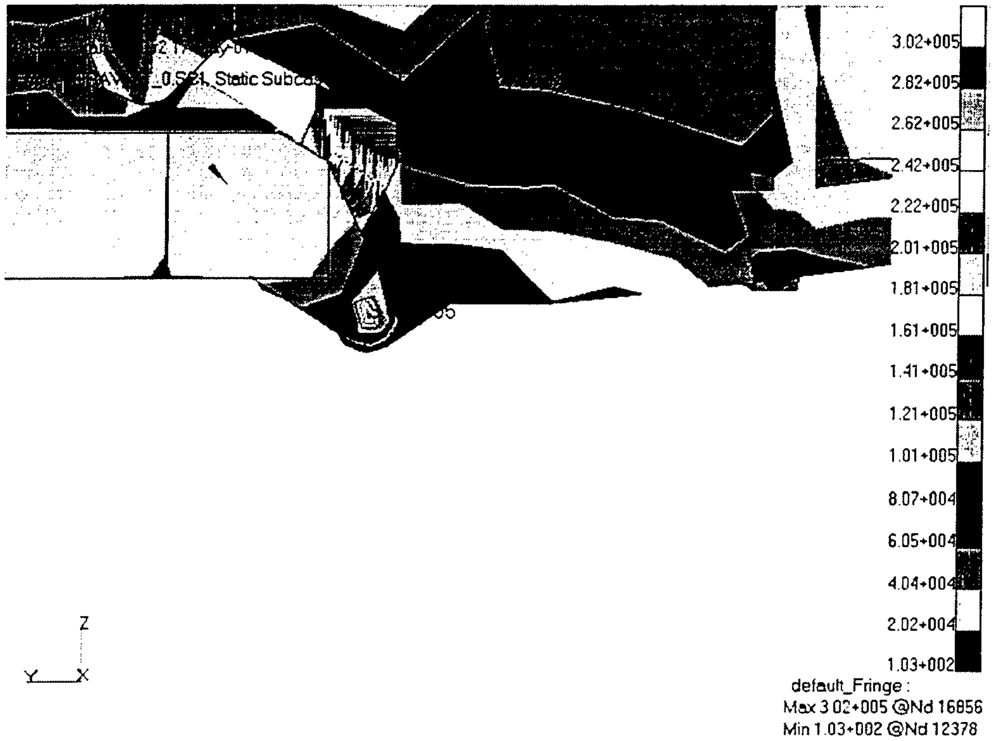

Figure 180. Cape H (close-up) von Mises Stress Contour Plot, Max. Stress: 43.8 ksi (Inertia Loading, No Twist, Two Tanks)

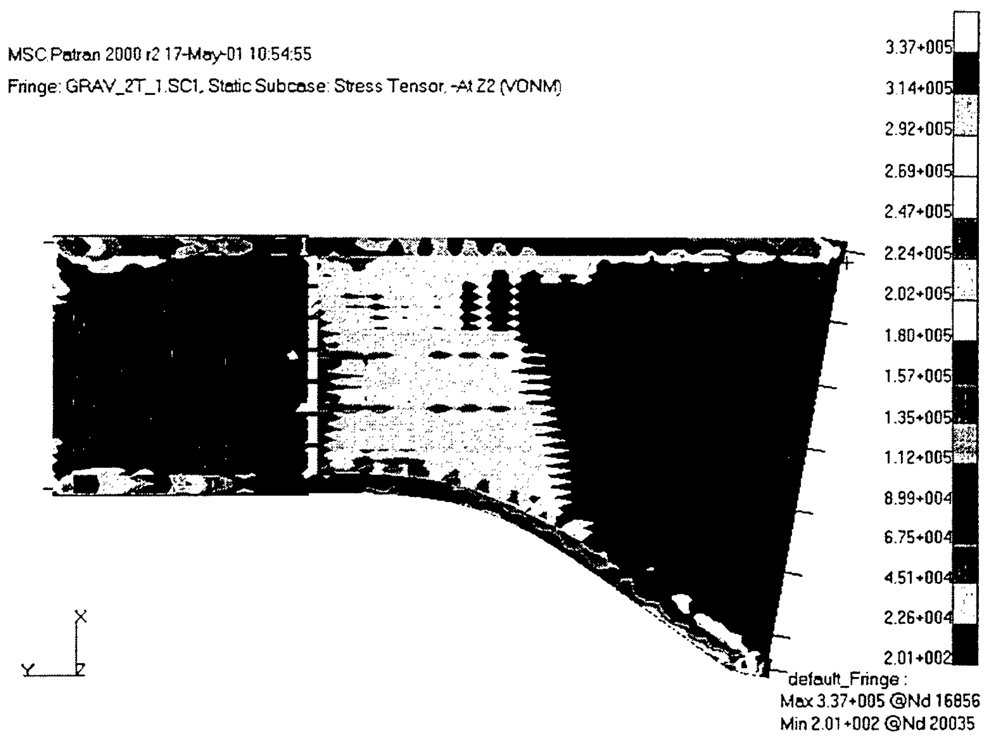

Figure 181. Cape H (top view) von Mises Stress Contour Plot, Max. Stress: 48.9 ksi (Inertia Loading, 1 Degree Twist, Two Tanks)

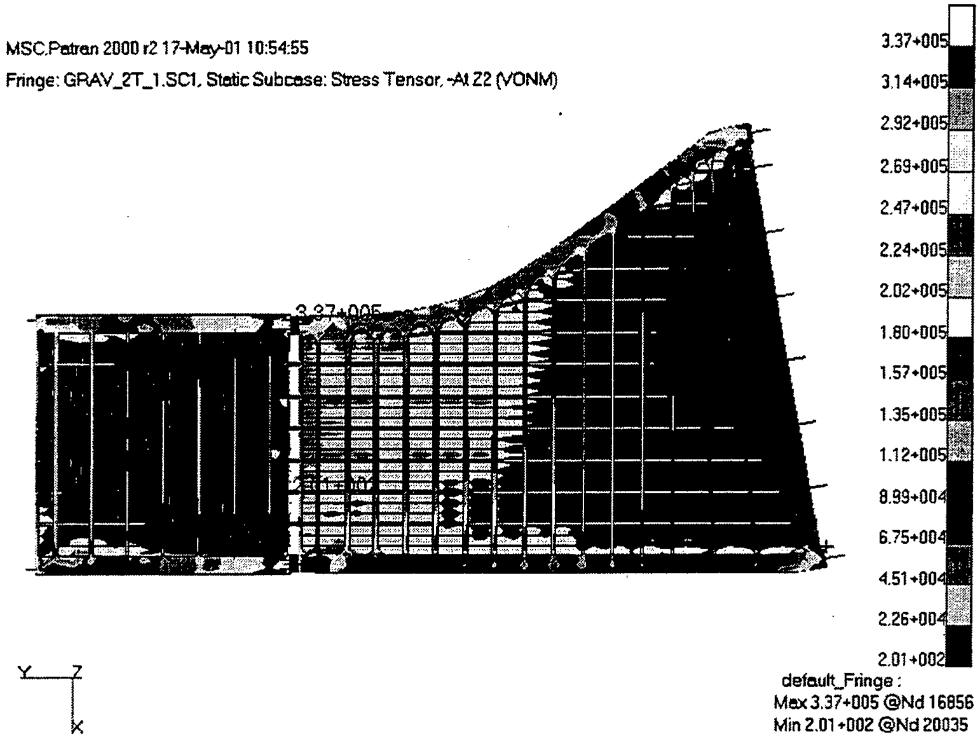

Figure 182. Cape H (bottom view) von Mises Stress Contour Plot, Max. Stress: 48.9 ksi (Inertia Loading, 1 Degree Twist, Two Tanks)

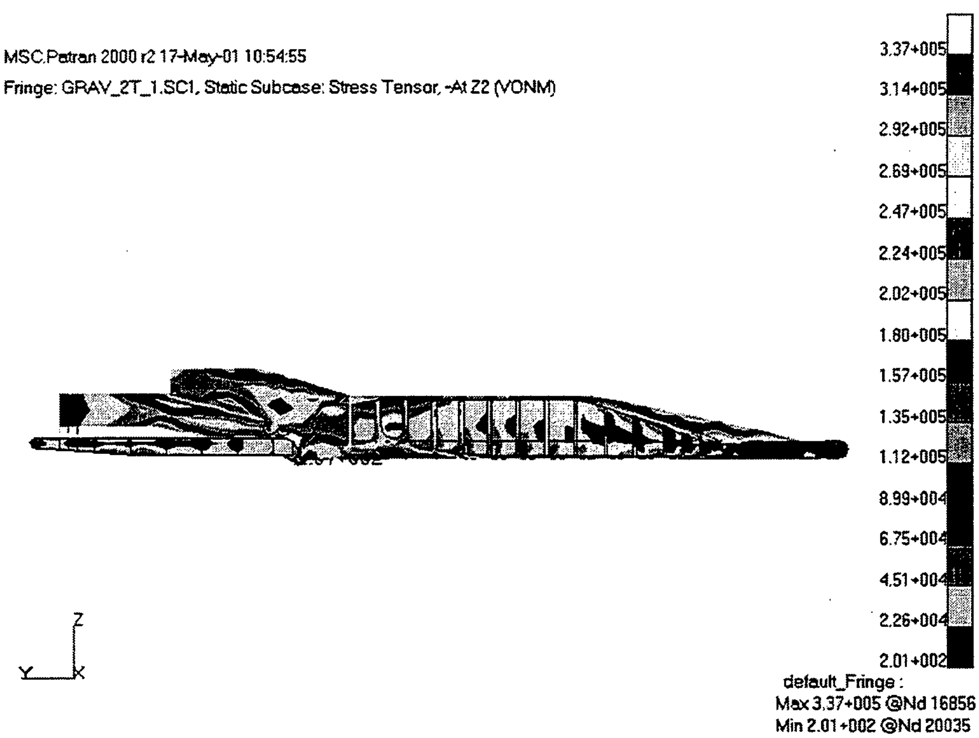

Figure 183. Cape H (left view) von Mises Stress Contour Plot, Max. Stress: 48.9 ksi (Inertia Loading, 1 Degree Twist, Two Tanks)

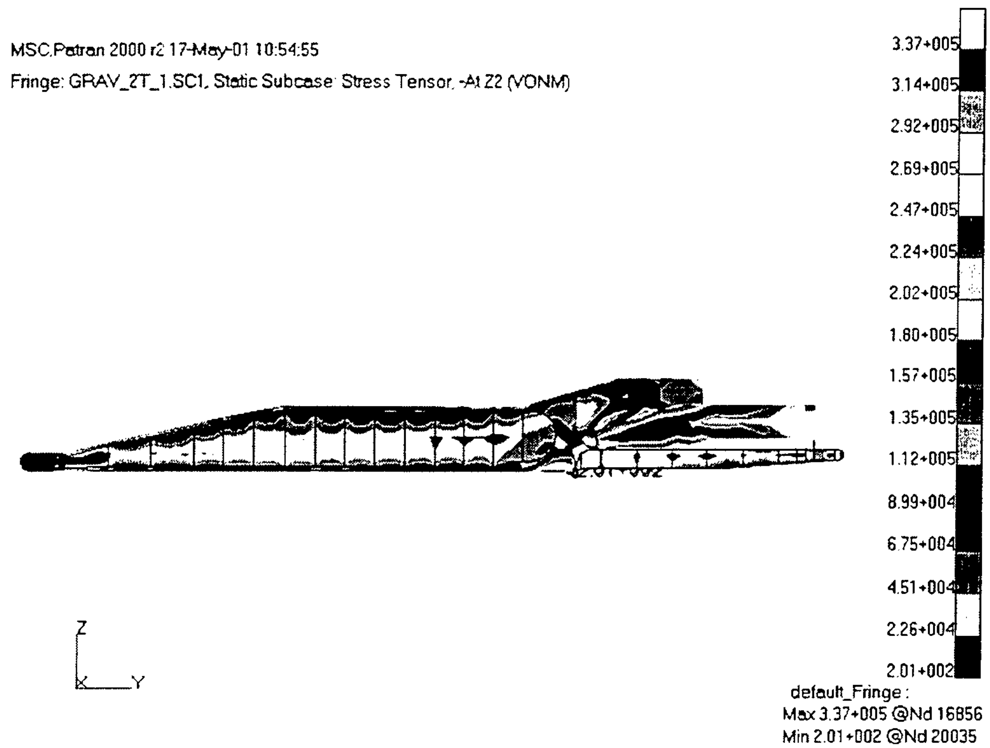

Figure 184. Cape H (right view) von Mises Stress Contour Plot, Max. Stress: 48.9 ksi (Inertia Loading, 1 Degree Twist, Two Tanks)

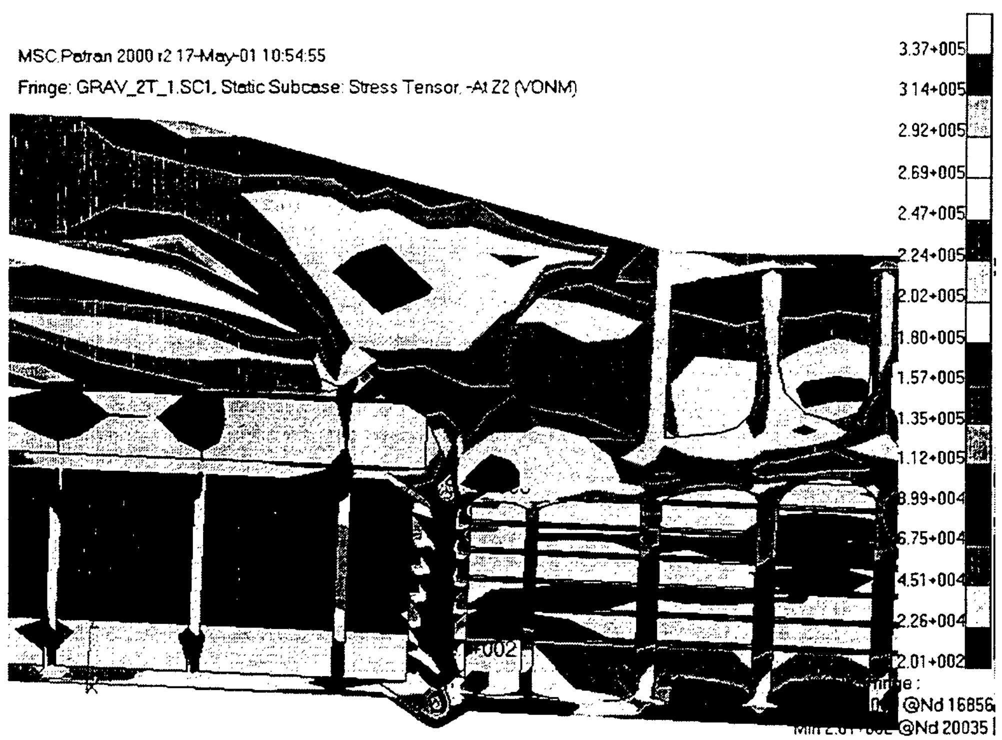

Figure 185. Cape H (close-up) von Mises Stress Contour Plot, Max. Stress: 48.9 ksi (Inertia Loading, 1 Degree Twist, Two Tanks)

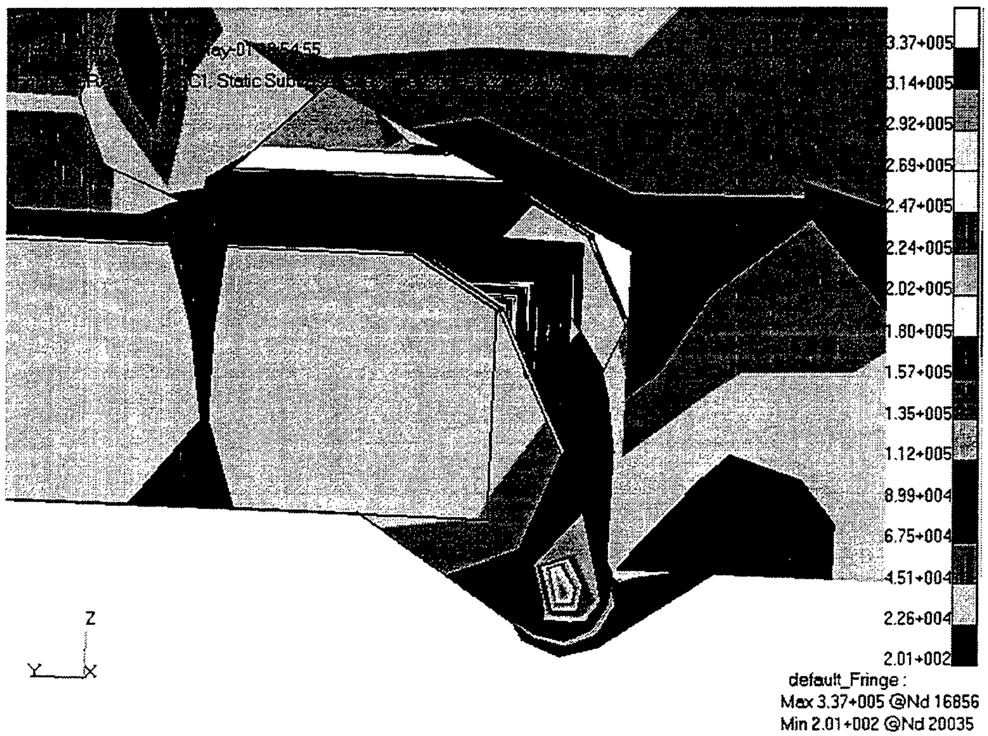

Figure 186. Cape H (close-up) von Mises Stress Contour Plot, Max. Stress: 48.9 ksi (Inertia Loading, 1 Degree Twist, Two Tanks)

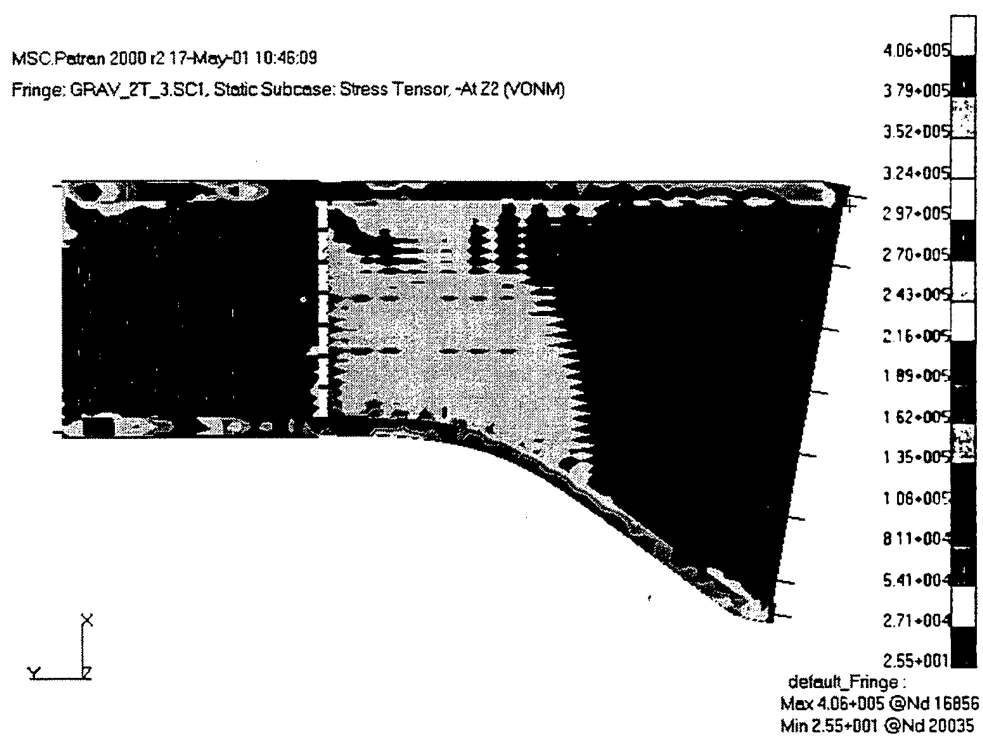

Figure 187. Cape H (top view) von Mises Stress Contour Plot, Max. Stress: 58.9 ksi (Inertia Loading, 3 Degree Twist, Two Tanks)

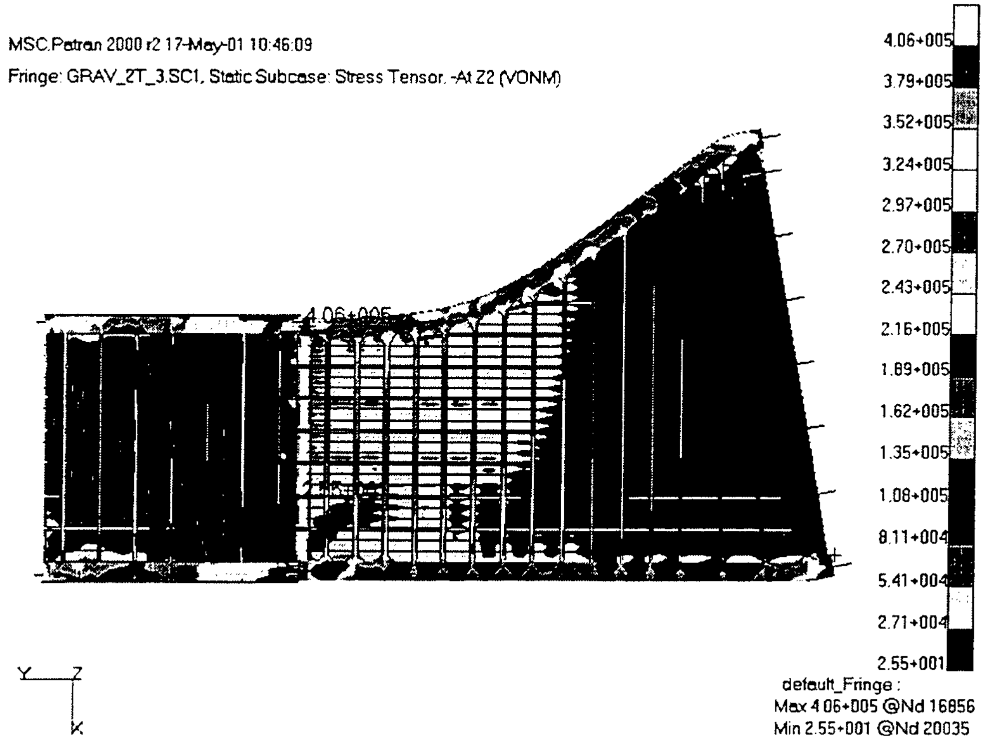

Figure 188. Cape H (bottom view) von Mises Stress Contour Plot, Max. Stress: 58.9 ksi (Inertia Loading, 3 Degree Twist, Two Tanks)

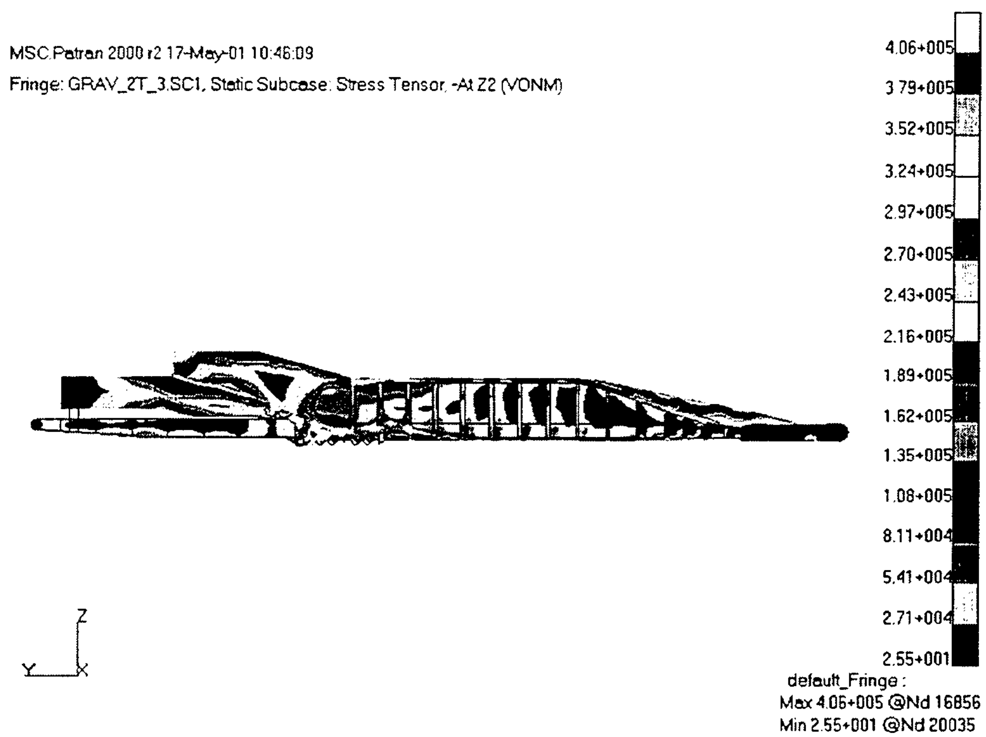

Figure 189. Cape H (left view) von Mises Stress Contour Plot, Max. Stress: 58.9 ksi (Inertia Loading, 3 Degree Twist, Two Tanks)

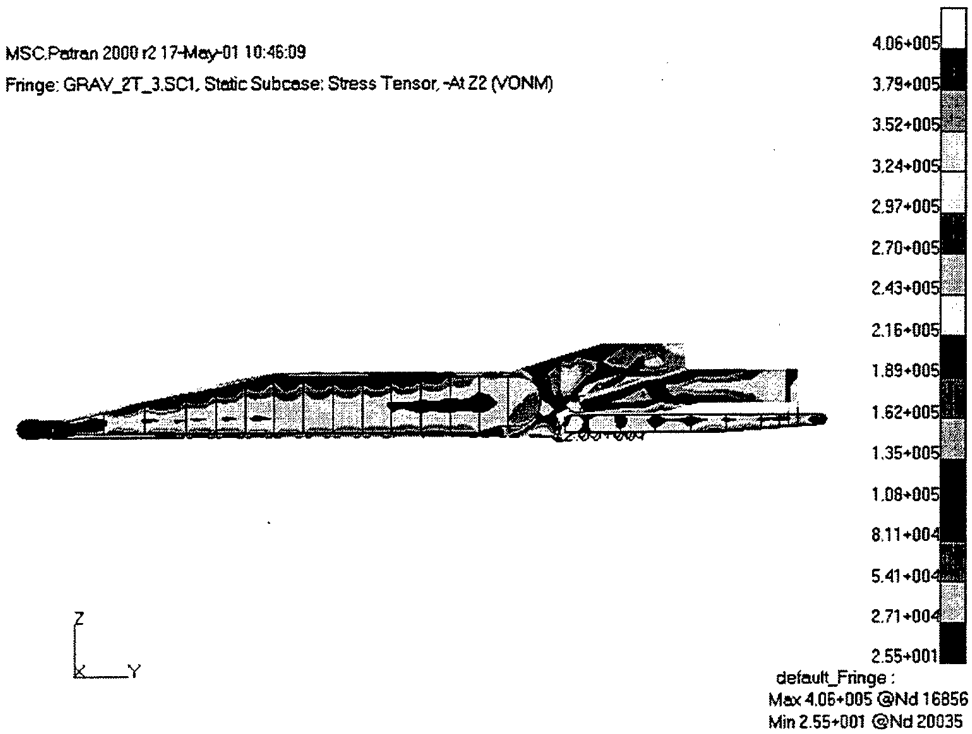

Figure 190. Cape H (right view) von Mises Stress Contour Plot, Max. Stress: 58.9 ksi (Inertia Loading, 3 Degree Twist, Two Tanks)

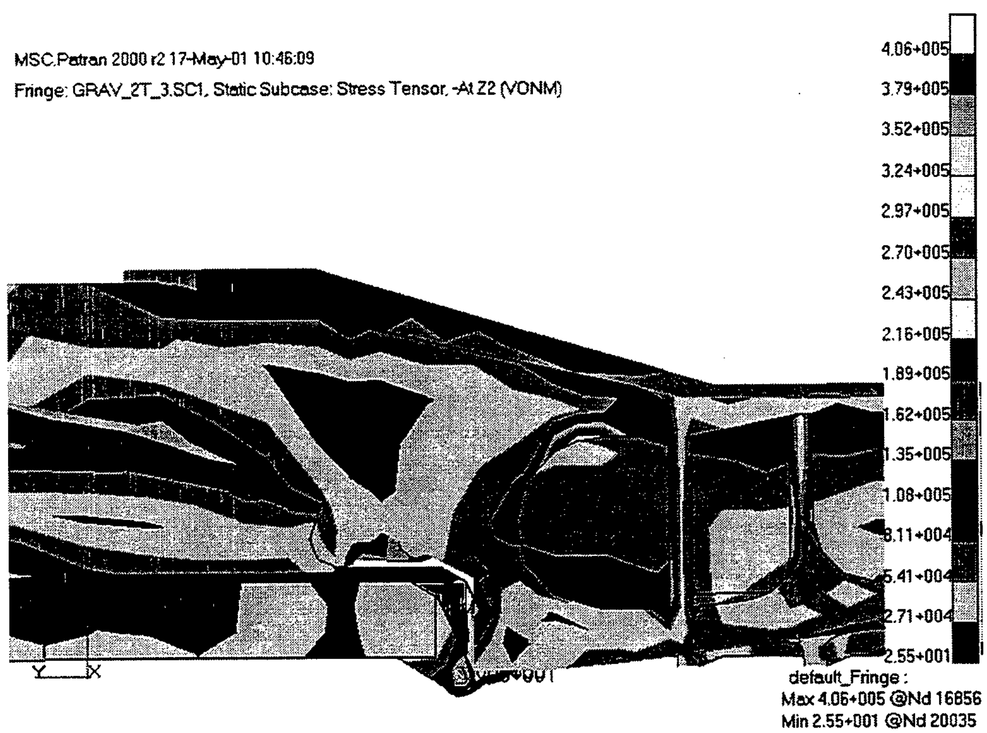

Figure 191. Cape H (close-up) von Mises Stress Contour Plot, Max. Stress: 58.9 ksi (Inertia Loading, 3 Degree Twist, Two Tanks)

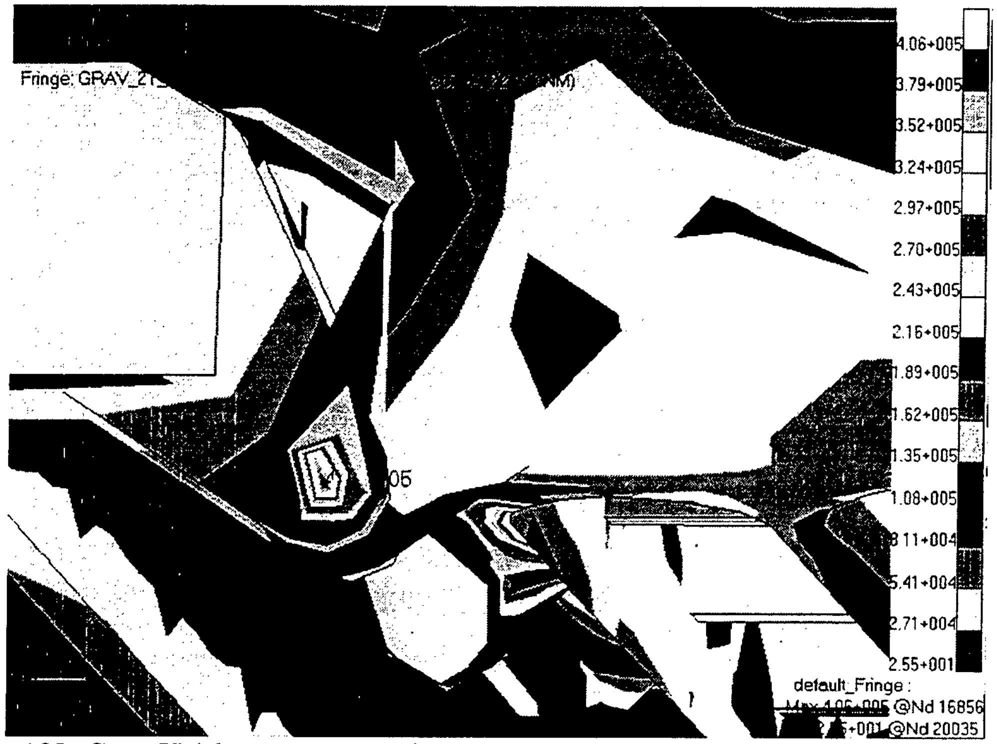

Figure 192. Cape H (close-up) von Mises Stress Contour Plot, Max. Stress: 58.9 ksi (Inertia Loading, 3 Degree Twist, Two Tanks)

C. EXPERIMENTAL MODAL ANALYSIS

1. Model-Scale Stern Ramp

Vibration testing was conducted on the model-scale ramp and the first four elastic modes were measured. The model-scale ramp was supported to enable the measurement of the normal modes with a free-free boundary condition. Figure 193 through 196 show the first four elastic modes.

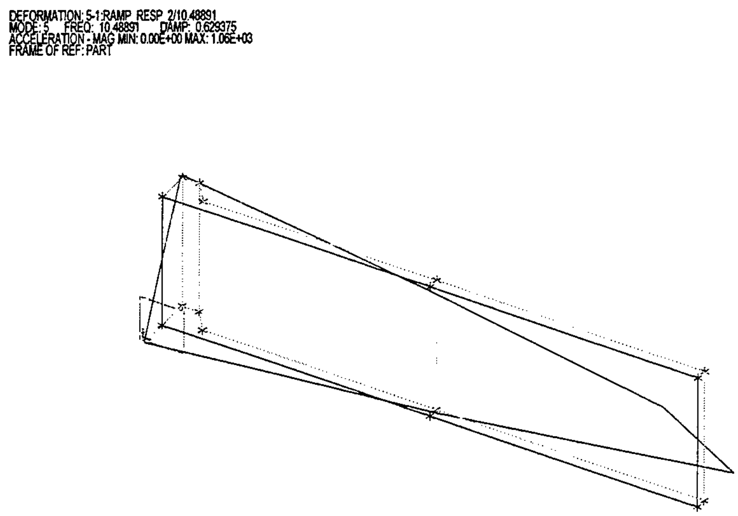

Figure 193. Model-Scale Ramp, Mode 1, Torsion

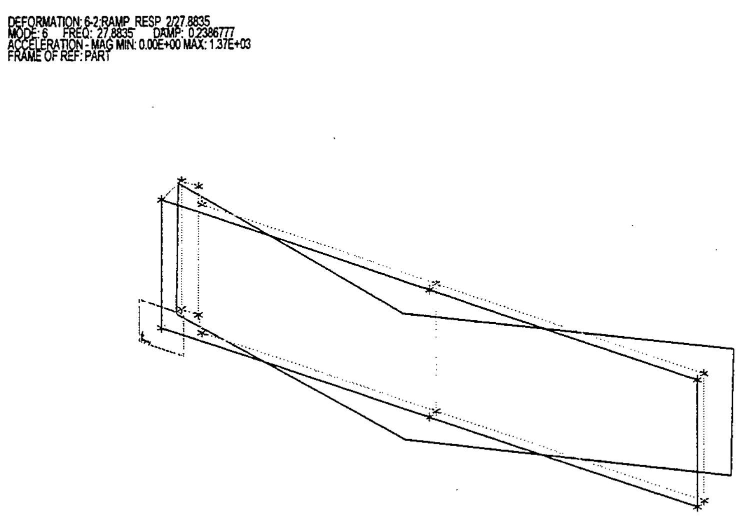

Figure 194. Model-Scale Ramp, Mode 2, Bending

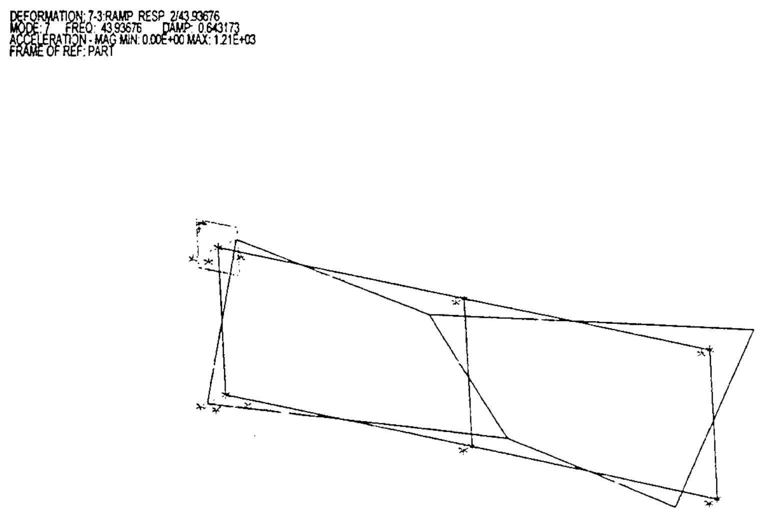

Figure 195. Model-Scale Ramp, Mode 3, Second Torsion

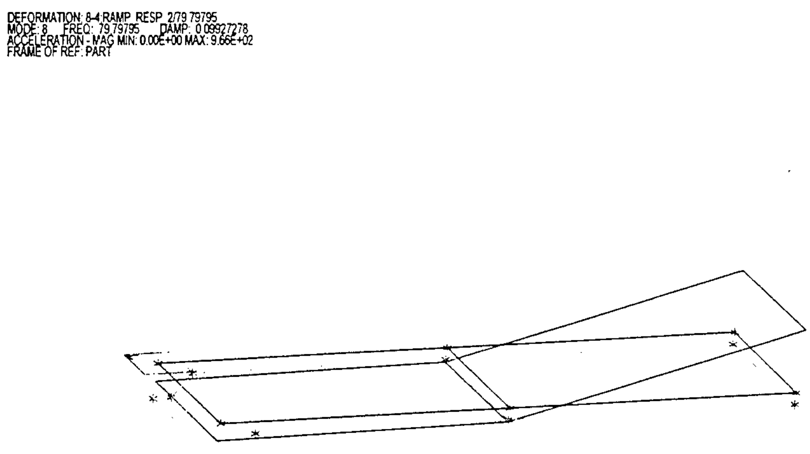

Figure 196. Model-Scale Ramp, Mode 4, Second Bending

Table 8 provides a summary comparison of the computational modal and experimental modal analysis of the model-scale stern ramp.

	Finite Element		Experimental	
Mode	Frequency (Hz)	Mode Shape	Frequency (Hz)	Mode Shape
1	12.46	1st Torsion	10.49	1st Torsion
2	27.23	1st Bending	27.88	1st Bending
3	45.13	2nd Torsion	43.94	2nd Torsion
4	76.38	2nd Bending	79.80	2nd Bending

Table 8. Comparison of Model-Scale Ramp Finite Element and Experimental Results

2. Model-Scale Stern Ramp Support

Vibration testing was conducted on the model-scale ramp support and all modes through 130 Hz were measured. The support was mounted to the deck in the position it will occupy for the constructed experimental test facility. Figure 197 shows the first elastic mode.

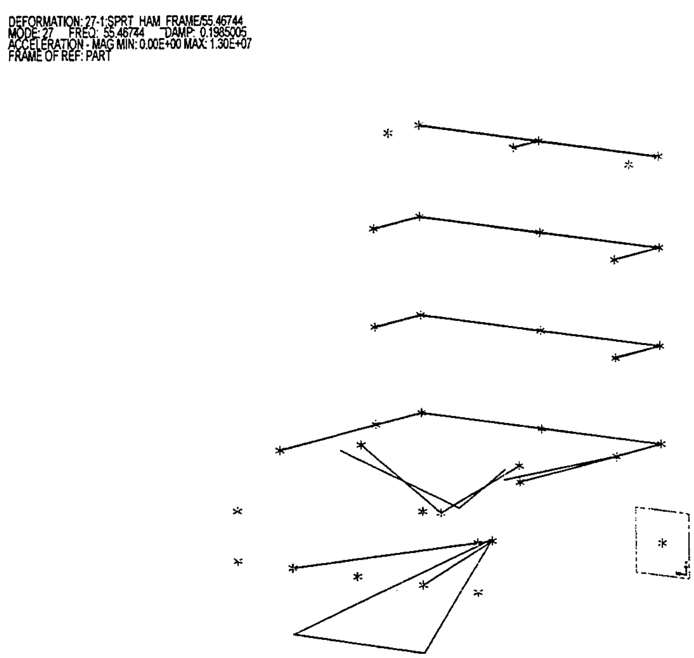

Figure 197. Model-Scale Ramp Support, Mode 1

Table 9 displays a comparison of the finite element results with the experimental results.

Mode	Finite Element Frequency (Hz)	Experimental Frequency (Hz)	Mode Shape Matches
1	51.31	55.47	Yes
2	71.44	67.02	No
3	72.109	68.73	No
4	93.04	78.34	No
5	96.97	88.63	No
6	102.99	107.65	No
7	119.53	122.20	Yes

Table 9. Comparison of Support Finite Element and Experimental Results

V. CONCLUSIONS AND RECOMMENDATIONS

A. CONCLUSIONS

The primary purpose of this thesis was to determine the suitability of the three full-scale stern ramp finite element model for inclusion in a coupled hydro-structural simulation model of the combined ship-ramp-RRDF. To assist in the determination, an ANSYS model of the LMSR stern ramp was obtained and nodal and elemental solutions were computed using ANSYS to compare with MSC/NASTRAN results. Four load cases were considered and are annotated as cases A through D. Load case A has gravity only as a load and cases B through D have gravity plus one, three and eight degrees of twist respectively. Tables 10 through 12 document these comparisons for no tank, one tank, and two tank configurations. All stress values are in pounds force per inch squared (psi) and are listed as peak {nominal}. Peak stress values are computed and nominal stresses are estimated.

Load Case	ANSYS Nodal	Peak Stress Location	ANSYS Elemental	Peak Stress Location	NASTRAN	Peak Stress Location
Case A	13,866 {7,711}	stbd hinge	32,331 {14,374}	stbd hinge	22,600 {9,090}	stbd hinge
Case B	17,511 {7,793}	top edge of first cavity on stbd side (section 1)	37,246 {16,562}	port hinge	25,600 {12,000}	port hinge
Case C	38,988 {21,668}	top edge of first cavity on stbd side (section 1)	47,935 {26,640}	port hinge	39,000 {18,000}	top edge of first cavity on stbd side (section 1)
Case E	92,995 {31,009}	top edge of first cavity on stbd side (section 1)	119,914 {66,640}	inside first cavity on port side (section 1)	99,800 {40,000}	inside first cavity on port side (section 1)

Table 10. LMSR ANSYS vs. NASTRAN Solution Comparison (No Tanks)

Load Case	ANSYS Nodal	Peak Stress Location	ANSYS Elemental	Peak Stress Location	NASTRAN	Peak Stress Location
Case A	26,804 {23,828}	stbd hinge	68,081 {37,833}	stbd hinge	46,600 {15,600}	stbd hinge
Case B	29,485 {26,211}	top edge of first cavity on stbd side (section 1)	72,592 {40,334}	port hinge	49,000 {19,700}	port hinge
Case C	50,959 {28,329}	top edge of first cavity on stbd side (section 1)	83,260 {46,271}	port hinge	56,000 {26,200}	port hinge
Case E	104,962 {69984}	top edge of first cavity on stbd side (section 1)	123,835 {82,563}	inside first cavity on port side (section 1)	108,000 {49,000}	inside first cavity on port side (section 1)

Table 11. LMSR ANSYS vs. NASTRAN Solution Comparison (One Tank)

Load Case	ANSYS Nodal	Peak Stress Location	ANSYS Elemental	Peak Stress Location	NASTRAN	Peak Stress Location
Case A	47,102 {26,183}	stbd hinge	110,389 {36,819}	stbd hinge	77,100 {25,800}	stbd hinge
Case B	45,526 {20,251}	port hinge	114,293 {50,809}	port hinge	78,900 {31,600}	port hinge
Case C	57,350 {38,250}	top edge of first cavity on stbd side (section 1)	124,981 {41,688}	port hinge	85,800 {34,400}	port hinge
Case D	111,349 {49,518}	top edge of first cavity on stbd side (section 1)	151,885 {67,521}	port hinge	111,000 {51,900}	top edge of first cavity on stbd side (section 1)

Table 12. LMSR ANSYS vs. NASTRAN Solution Comparison (Two Tanks)

As can be seen from the tables, the ANSYS nodal and elemental solutions bracket the MSC/NASTRAN results in all but case D with two tanks. Additionally, the disparity between the ANSYS nodal and elemental results indicates the LMSR model is not sufficiently refined. In particular, the hinge joints require updating. This is further

supported by the peak stress values being well above the yield for mild steel of 40,000 psi.

Tables 13 through 15 show a comparison of the linear static solutions of the three ramp designs. Again, three load cases were considered for no tank, one tank, and two tank configurations. As before, case A represents gravity only and cases B and C represent one degree and three degrees of twist. Eight degrees of twist was not used as the nominal stress estimations from the LMSR analysis predicted stresses well above yield.

Boundary Conditions and Loading	Cape T	Peak Stress Location	Cape H	Peak Stress Location	LMSR	Peak Stress Location
Case A	13,500 {9,035}	aft end of buttressing device port side	22,500 {13,500}	stbd hinge	22,600 {9,090}	stbd hinge
Case B	16,800 {8,950}	stbd side of lateral rib support (section 1)	23,700 {15,800}	stbd hinge of arm attached to section 2	25,600 {12,000}	port hinge
Case C	51,100 {20,450}	stbd side of lateral rib support (section 1)	43,900 {29,300}	bottom section 1, fwd port corner	39,000 {18,000}	top edge of first cavity on stbd side (section 1)

Table 13. Ramp Summary (No Tanks)

Boundary Conditions and Loading	Cape T	Peak Stress Location	Cape H	Peak Stress Location	LMSR	Peak Stress Location
Case A	49,900 {23,300}	lateral rib support (section 1)	31,900 {19,100}	stbd hinge of arm attached to section 2	46,600 {15,600}	stbd hinge
Case B	50,100 {23,300}	lateral rib support (section 1)	33,500 {22,300}	stbd hinge of arm attached to section 2	49,000 {19,700}	port hinge
Case C	70,300 {32,800}	port side of lateral rib support (section 1)	50,300 {30,200}	bottom section 1, fwd port corner	56,000 {26,200}	port hinge

Table 14. Ramp Summary (One Tanks)

Boundary Conditions and Loading	Cape T	Peak Stress Location	Cape H	Peak Stress Location	LMSR	Peak Stress Location
Case A	51,600 {24,100}	lateral rib support (section 1)	43,800 {23,400}	stbd hinge	77,100 {25,800}	stbd hinge
Case B	51,600 {24,100}	lateral rib support (section 1)	48,900 {26,100}	port hinge	78,900 {31,600}	port hinge
Case C	66,600 {31,000}	port side of lateral rib support (section 1)	51,300 {27,400}	port hinge	85,800 {34,400}	port hinge

Table 15. Ramp Summary (Two Tanks)

The high peak stresses predicted still indicate that all three ramp models are not sufficiently refined for accurate determination of stress levels; however, each of the designs may be used to ascertain the performance of passive isolation.

B. RECOMMENDATIONS

Because the three full-scale stern ramp finite element models can each be used in the simulation model, the two ramps most likely to be used for RORO operations at sea should be used in the simulation model. The Cape H stern ramp is much larger and

poses separate problems due to its size alone. The LMSR stern ramp was designed for sea state three capability and at this time seems to be the most likely candidate for at sea RORO application.

If the Cape H ramp design is to be used for at sea RORO operations, the Cape H finite element model should be modified to allow for normal modes analysis to determine if a pseudostatic response assumption is valid.

All three ramp models should be refined sufficiently to allow for more accurate stress level predictions. For the LMSR, Cape H, and Cape T designs, these refinements should be in the areas of high peak stress concentration.

Both finite element models for the model-scale stern ramp and support require additional updating. Specifically, both models should be modified to include parameters for accurate modeling of the weld joints.

Perform testing of materials used in the construction of both the model-scale stern ramp and support. This will ensure that the correct values for material modulus and density are included in the model rather than handbook values.

For the model-scale ramp support, update the finite element model to include the spring effects of the six fasteners used to mount the support to the deck. This will provide another parameter for updating the model.

Additional vibration analysis of the model-scale ramp and support must be conducted as the experimental test facility is completed.

THIS PAGE INTENTIONALLY LEFT BLANK

APPENDIX

A. COMPUTATIONAL LINEAR STATIC ANALYSIS

Static analyses require the solution of the following equation,

$$[K]\{u\} = \{p\} \tag{1}$$

where [K] is an (n x n) stiffness matrix, p(t) is an (n x 1) force vector, and u(t) is an (n x 1) vector of unknown displacement coordinates. Solution to equation (1) for large systems can be very difficult and computationally expensive as it involves the inversion of the stiffness matrix, [K]. The left and right hand sides of equation (1) are premultiplied by $[K]^{-1}$ yielding [Ref. 1],

$$\{u\} = [K]^{-1} \{p\} \tag{2}$$

Solution of equation (2) gives the physical displacements of the finite element model, {u}. MSC/NASTRAN conducts linear static analyses by the *displacement method.* [Ref. 2]

Each MSC/NASTRAN input file consists of several sections defining the type of analysis to be performed, boundary conditions, loads, material properties, element types, and grid point connectivity. MSC/NASTRAN will organize the input file for efficient processing and assemble the stiffness and mass matrices, [K] and [M]. The mass matrix in a static analysis is used to apply inertial or gravity loads to the structure. Specified constraints are applied to the stiffness matrix and appropriate rows and columns are eliminated through matrix partitioning. The load vector, {p}, is generated from parameters such as pressure loads on surfaces, enforced displacements, and inertia loads. The load vector is reduced to final form by application of restraints and elimination of the restrained components. The stiffness matrix, [K] is decomposed into

upper and lower triangular factors and solution for the independent displacements in {u} is accomplished for the reduced load vector {p} by means of forward and backward passes. Equations of constraint are applied to determine dependent grid point displacements. Knowledge of the displacement of the corners of an element allows the elemental strains and stresses to be determined based on the shape functions of the particular element. MSC/NASTRAN uses bilinear extrapolation to determine elemental stresses at the centroid and corners of each CQUAD4 element [Ref. 3]. A bilinear function is a special quadratic function that is linear in y for each x, and linear in x for each y.

B. COMPUTATIONAL MODAL ANALYSIS

The equations of motion for an n degree of freedom (DOF) undamped structure can be represented by the following matrix equation,

$$[M]\{\ddot{u}\} + [K]\{u\} = \{p(t)\}, \tag{3}$$

where [M] and [K] are (n x n) mass and stiffness matrices, p(t) in an (n x 1) force vector, and u(t) is an (n x 1) vector of unknown displacement coordinates. The natural frequencies of the system of equations represented by the homogeneous form of equation (3) can be determined by assuming the displacement response is harmonic,

$$\{u\} = \{U\}e^{i\omega t} \tag{4}$$

Equation (4) can be substituted into equation (3) leading to an nth order eigenvalue problem [Ref. 1],

$$([K] - \omega^2 [M])\{U\} = \{0\} \tag{5}$$

Equation (5) may also equivalently be written to form the structural eigenproblem [Ref. 4],

$$[K]\, \varphi_j = \lambda_j\, [M]\, \varphi_j\,,\ j = 1,\ldots,n \tag{6}$$

In equation (6) it is apparent that λ_j corresponds to ω_j^2 (the jth eigenvalue) and φ_j corresponds to U_j (the jth eigenvector). Damping may be included and the eigenvectors are unchanged provided damping is included in proportional form. A common method to solve equation (6) involves computing [L], the Cholesky factor of [K], provided [K] is positive definite. Substituting, $\mu_j = 1/\lambda_j$ in equation (6) yields,

$$[M]\, \varphi_j = \mu_j\, [K]\, \varphi_j \tag{7}$$

Finally, including the Cholesky factorization of [K] leads to,

$$[L]^{-1}\, [M]\, [L]^{-T}\, \psi_j = \mu_j\, \psi_j \tag{8}$$

The eigenvectors, φ_j, must be computed by using the transformation $\varphi_j = [L]^{-T} \psi_j$. If the model has rigid body modes, [K] is positive semidefinite and Cholesky decomposition is not possible. To efficiently solve such problems, MSC/NASTRAN employs a block Lanczos algorithm with shift points (σ) and equation (6) is adjusted as follows [Ref. 5],

$$[K - \sigma M]\, \varphi_j = (\lambda_j - \sigma)[M]\, \varphi_j\,,\; j = 1,\ldots,n \tag{9}$$

The values for the shift points are chosen by the software dependent on the user requested range of natural frequency interest and the nature of the finite element model.

C. EXPERIMENTAL MODAL ANALYSIS

Experimental modal analysis or vibration testing requires four components: a means to mount or support the structure to be tested; an excitation source; transducers to measure the vibration response and excitation input; and a method to record and analyze the data.

For a free-free vibration test, the structure should be supported at the nodal points of the first bending mode. The material used to support the structure should be of sufficient flexibility to minimize coupling of rigid body modes with elastic modes of the structure. If the response of an installed structure is desired, then vibration testing may be conducted with the structure restrained as if installed.

Two methods are commonly used to excite a structure. A shaker can be attached to the structure with a force input proportional to a specified input parameter, such as voltage, or an impact hammer with an attached force transducer may be used. The impact hammer imparts an approximate impulse to the structure with the intention of exciting all modes in the bandwidth of interest simultaneously and equally. Because the impact produced by the hammer in practice does not result in a perfect impulse, there exists a cut-off frequency above which modes are excited with very little energy. The cut-off frequency can be altered by using different mass hammers or changing the elasticity of the hammer tip. It is important that the frequency range of interest fall below the cut-off frequency.

Transducers are used to measure the vibration response of the excited structure and the excitation force. Transducers contain a piezoelectric material that generates an electric charge when undergoing strain. The electric charge can be converted to a

measurable voltage that is proportional to the applied strain. The applied strain is proportional to the excitation force or acceleration of the structure. Force transducers apply the excitation force directly to the piezoelectric material. Accelerometers differ in that a mass is attached to the structure through the piezoelectric material with the piezoelectric material acting as a stiff spring. The spring-mass system of the accelerometer should vibrate at frequencies well above the frequency range of interest.

Analyses of vibration tests are accomplished using a digital computer. The analog measured vibrations are converted to a digital signal by an analog to digital converter. Several sample intervals are averaged to reduce the effect of noise in the vibration measurements. The digital force and response functions are time domain signals. Fast Fourier transforms (FFT) of the force and response signals are performed by computer software to generate frequency domain functions. This leads to the frequency response function (FRF) as defined by the ratio of the response FFT to the force FFT. The FRFs can be viewed and used to determine the natural frequencies, mode shapes, and damping ratios of the structure tested. [Ref. 6]

D. MSC/NASTRAN INPUT FILES

```
INIT MASTER(S)
ASSIGN OUTPUT2 = 'LMSR_0T_1.op2', UNIT = 12
SOL 101
TIME 600
CEND
SEALL = ALL
SUPER = ALL
ECHO = NONE
MAXLINES = 999999999
SUBCASE 1
   SUBTITLE=GRAV_0T_1
   SPC = 1
   LOAD = 2
   DISPLACEMENT(SORT1,REAL)=ALL
   SPCFORCES(SORT1,REAL)=ALL
   STRESS(SORT1,REAL,VONMISES,BILIN)=ALL
BEGIN BULK
PARAM    POST    -1
PARAM,NOCOMPS,-1
PARAM   PRTMAXIM YES
PARAM   AUTOSPC  YES
PARAM   K6ROT    5.0
PARAM   GRDPNT   0
SPCD     2       5219    3       -5.04
SPC1     1       123     5243
SPC1     1       3       6481
SPC1     1       123     9961
SPC1     1       3       5219
GRAV     2       0       386.09  0.      0.      -1.
CELAS2   13953   2.4+7   9101    3       6786    3       0.      0.
CELAS2   13954   2.4+7   9106    3       6787    3       0.      0.
CELAS2   13955   2.4+7   9107    3       6788    3       0.      0.
CELAS2   13956   2.4+7   9105    3       6782    3       0.      0.
CELAS2   13957   2.4+7   9126    3       6799    3       0.      0.
CELAS2   13958   2.4+7   9131    3       6800    3       0.      0.
CELAS2   13960   2.4+7   9129    3       6801    3       0.      0.
CELAS2   13961   2.4+7   9127    3       6798    3       0.      0.
CELAS2   13962   2.4+7   5336    3       2320    3       0.      0.
CELAS2   13963   2.4+7   5338    3       2325    3       0.      0.
CELAS2   13964   2.4+7   5337    3       2324    3       0.      0.
CELAS2   13965   2.4+7   5332    3       1809    3       0.      0.
CELAS2   13966   2.4+7   5358    3       2332    3       0.      0.
CELAS2   13967   2.4+7   5360    3       2334    3       0.      0.
CELAS2   13968   2.4+7   5362    3       2333    3       0.      0.
CELAS2   13969   2.4+7   5357    3       1852    3       0.      0.
INCLUDE 'E:\LMSR\LMSR_BULK_DATA\LMSRbulk.dat'
ENDDATA
```

```
INIT MASTER(S)
ASSIGN OUTPUT2 = 'LMSR_1T_1.op2', UNIT = 12
SOL 101
TIME 600
CEND
SEALL = ALL
SUPER = ALL
ECHO = NONE
MAXLINES = 999999999
SUBCASE 1
   SUBTITLE=GRAV_1T_1
   SPC = 1
   LOAD = 2
   DISPLACEMENT(SORT1,REAL)=ALL
   SPCFORCES(SORT1,REAL)=ALL
   STRESS(SORT1,REAL,VONMISES,BILIN)=ALL
BEGIN BULK
PARAM    POST     -1
PARAM,NOCOMPS,-1
PARAM   PRTMAXIM YES
PARAM   AUTOSPC  YES
PARAM   K6ROT    5.0
PARAM   GRDPNT   0
SPCD     2       5219    3       -5.04
LOAD     2       1.      1.      3       1.      4
SPC1     1       123     5243
SPC1     1       3       6481
SPC1     1       123     9961
SPC1     1       3       5219
GRAV     3       0       386.09  0.      0.      -1.
PLOAD4   4       4957   -20.4   -20.4   -20.4   -20.4    THRU    4964
PLOAD4   4       5005   -20.4   -20.4   -20.4   -20.4    THRU    5012
PLOAD4   4       5053   -20.4   -20.4   -20.4   -20.4    THRU    5060
PLOAD4   4       12970  -20.4   -20.4   -20.4   -20.4    THRU    12977
PLOAD4   4       13026  -20.4   -20.4   -20.4   -20.4    THRU    13033
PLOAD4   4       13082  -20.4   -20.4   -20.4   -20.4    THRU    13089
CELAS2   13953   2.4+7   9101    3       6786    3       0.      0.
CELAS2   13954   2.4+7   9106    3       6787    3       0.      0.
CELAS2   13955   2.4+7   9107    3       6788    3       0.      0.
CELAS2   13956   2.4+7   9105    3       6782    3       0.      0.
CELAS2   13957   2.4+7   9126    3       6799    3       0.      0.
CELAS2   13958   2.4+7   9131    3       6800    3       0.      0.
CELAS2   13960   2.4+7   9129    3       6801    3       0.      0.
CELAS2   13961   2.4+7   9127    3       6798    3       0.      0.
CELAS2   13962   2.4+7   5336    3       2320    3       0.      0.
CELAS2   13963   2.4+7   5338    3       2325    3       0.      0.
CELAS2   13964   2.4+7   5337    3       2324    3       0.      0.
CELAS2   13965   2.4+7   5332    3       1809    3       0.      0.
CELAS2   13966   2.4+7   5358    3       2332    3       0.      0.
CELAS2   13967   2.4+7   5360    3       2334    3       0.      0.
CELAS2   13968   2.4+7   5362    3       2333    3       0.      0.
CELAS2   13969   2.4+7   5357    3       1852    3       0.      0.
INCLUDE 'E:\LMSR\LMSR_BULK_DATA\LMSRbulk.dat'
ENDDATA
```

```
INIT MASTER(S)
ASSIGN OUTPUT2 = 'LMSR_2T_1.op2', UNIT = 12
SOL 101
TIME 600
CEND
SEALL = ALL
SUPER = ALL
ECHO = NONE
MAXLINES = 999999999
SUBCASE 1
   SUBTITLE=GRAV_2T_1
   SPC = 1
   LOAD = 2
   DISPLACEMENT(SORT1,REAL)=ALL
   SPCFORCES(SORT1,REAL)=ALL
   STRESS(SORT1,REAL,VONMISES,BILIN)=ALL
BEGIN BULK
PARAM     POST     -1
PARAM,NOCOMPS,-1
PARAM    PRTMAXIM YES
PARAM    AUTOSPC  YES
PARAM    K6ROT    5.0
PARAM    GRDPNT   0
SPCD     2        5219     3       -5.04
LOAD     2        1.       1.       3       1.      4
SPC1     1        123      5243
SPC1     1        3        6481
SPC1     1        123      9961
SPC1     1        3        5219
GRAV     3        0        386.09  0.      0.      -1.
PLOAD4         4      4853    -20.4
PLOAD4         4      4854    -20.4
PLOAD4         4      4855    -20.4
PLOAD4         4      4856    -20.4
PLOAD4         4      4857    -20.4
PLOAD4         4      4858    -20.4
PLOAD4         4      4859    -20.4
PLOAD4         4      4860    -20.4
PLOAD4         4      4909    -20.4
PLOAD4         4      4910    -20.4
PLOAD4         4      4911    -20.4
PLOAD4         4      4912    -20.4
PLOAD4         4      4913    -20.4
PLOAD4         4      4914    -20.4
PLOAD4         4      4915    -20.4
PLOAD4         4      4916    -20.4
PLOAD4         4      4957    -20.4
PLOAD4         4      4958    -20.4
PLOAD4         4      4959    -20.4
PLOAD4         4      4960    -20.4
PLOAD4         4      4961    -20.4
PLOAD4         4      4962    -20.4
PLOAD4         4      4963    -20.4
PLOAD4         4      4964    -20.4
PLOAD4         4      5053    -20.4
PLOAD4         4      5054    -20.4
```

PLOAD4	4	5055	-20.4
PLOAD4	4	5056	-20.4
PLOAD4	4	5057	-20.4
PLOAD4	4	5058	-20.4
PLOAD4	4	5059	-20.4
PLOAD4	4	5060	-20.4
PLOAD4	4	5109	-20.4
PLOAD4	4	5110	-20.4
PLOAD4	4	5111	-20.4
PLOAD4	4	5112	-20.4
PLOAD4	4	5113	-20.4
PLOAD4	4	5114	-20.4
PLOAD4	4	5115	-20.4
PLOAD4	4	5116	-20.4
PLOAD4	4	5152	-20.4
PLOAD4	4	5153	-20.4
PLOAD4	4	5154	-20.4
PLOAD4	4	5155	-20.4
PLOAD4	4	5156	-20.4
PLOAD4	4	5157	-20.4
PLOAD4	4	5158	-20.4
PLOAD4	4	5159	-20.4
PLOAD4	4	9461	-20.4
PLOAD4	4	9462	-20.4
PLOAD4	4	9463	-20.4
PLOAD4	4	9464	-20.4
PLOAD4	4	9465	-20.4
PLOAD4	4	9466	-20.4
PLOAD4	4	9467	-20.4
PLOAD4	4	9468	-20.4
PLOAD4	4	9504	-20.4
PLOAD4	4	9505	-20.4
PLOAD4	4	9506	-20.4
PLOAD4	4	9507	-20.4
PLOAD4	4	9508	-20.4
PLOAD4	4	9509	-20.4
PLOAD4	4	9510	-20.4
PLOAD4	4	9511	-20.4
PLOAD4	4	12850	-20.4
PLOAD4	4	12851	-20.4
PLOAD4	4	12852	-20.4
PLOAD4	4	12853	-20.4
PLOAD4	4	12854	-20.4
PLOAD4	4	12855	-20.4
PLOAD4	4	12856	-20.4
PLOAD4	4	12857	-20.4
PLOAD4	4	12914	-20.4
PLOAD4	4	12915	-20.4
PLOAD4	4	12916	-20.4
PLOAD4	4	12917	-20.4
PLOAD4	4	12918	-20.4
PLOAD4	4	12919	-20.4
PLOAD4	4	12920	-20.4
PLOAD4	4	12921	-20.4
PLOAD4	4	12970	-20.4
PLOAD4	4	12971	-20.4

```
PLOAD4          4   12972   -20.4
PLOAD4          4   12973   -20.4
PLOAD4          4   12974   -20.4
PLOAD4          4   12975   -20.4
PLOAD4          4   12976   -20.4
PLOAD4          4   12977   -20.4
PLOAD4          4   13082   -20.4
PLOAD4          4   13083   -20.4
PLOAD4          4   13084   -20.4
PLOAD4          4   13085   -20.4
PLOAD4          4   13086   -20.4
PLOAD4          4   13087   -20.4
PLOAD4          4   13088   -20.4
PLOAD4          4   13089   -20.4
CELAS2  13953   2.4+7   9101    3       6786    3       0.      0.
CELAS2  13954   2.4+7   9106    3       6787    3       0.      0.
CELAS2  13955   2.4+7   9107    3       6788    3       0.      0.
CELAS2  13956   2.4+7   9105    3       6782    3       0.      0.
CELAS2  13957   2.4+7   9126    3       6799    3       0.      0.
CELAS2  13958   2.4+7   9131    3       6800    3       0.      0.
CELAS2  13960   2.4+7   9129    3       6801    3       0.      0.
CELAS2  13961   2.4+7   9127    3       6798    3       0.      0.
CELAS2  13962   2.4+7   5336    3       2320    3       0.      0.
CELAS2  13963   2.4+7   5338    3       2325    3       0.      0.
CELAS2  13964   2.4+7   5337    3       2324    3       0.      0.
CELAS2  13965   2.4+7   5332    3       1809    3       0.      0.
CELAS2  13966   2.4+7   5358    3       2332    3       0.      0.
CELAS2  13967   2.4+7   5360    3       2334    3       0.      0.
CELAS2  13968   2.4+7   5362    3       2333    3       0.      0.
CELAS2  13969   2.4+7   5357    3       1852    3       0.      0.
INCLUDE 'E:\LMSR\LMSR_BULK_DATA\LMSRbulk.dat'
ENDDATA
```

```
INIT MASTER(S)
ASSIGN OUTPUT2 = 'CT_0T_0.op2', UNIT = 12
SOL 101
TIME 600
CEND
SEALL = ALL
SUPER = ALL
ECHO = NONE
MAXLINES = 999999999
SUBCASE 1
   SUBTITLE=CT_0T_0
   SPC = 1
   LOAD = 2
   DISPLACEMENT(SORT1,REAL)=ALL
   SPCFORCES(SORT1,REAL)=ALL
   STRESS(SORT1,REAL,VONMISES,BILIN)=ALL
BEGIN BULK
PARAM    POST    -1
PARAM,NOCOMPS,-1
PARAM   PRTMAXIM YES
PARAM   GRDPNT    0
PARAM   K6ROT    5.0
PARAM   AUTOSPC  YES
SPC1     1       123     40288
SPC1     1       123     40289
SPC1     1       2       40769
SPC1     1       2       40805
GRAV     2       0       9.81    0.      -1.      0.
INCLUDE 'E:\CapeT\CT_STATIC\CT_STATIC_BULK.dat'
ENDDATA 1d86bebd
```

```
INIT MASTER(S)
ASSIGN OUTPUT2 = 'CT_1T_1.op2', UNIT = 12
SOL 101
TIME 600
CEND
SEALL = ALL
SUPER = ALL
ECHO = NONE
MAXLINES = 999999999
SUBCASE 1
   SUBTITLE=CT_1T_1
   SPC = 1
   LOAD = 2
   DISPLACEMENT(SORT1,REAL)=ALL
   SPCFORCES(SORT1,REAL)=ALL
   STRESS(SORT1,REAL,VONMISES,BILIN)=ALL
BEGIN BULK
PARAM     POST    -1
PARAM,NOCOMPS,-1
PARAM   PRTMAXIM YES
PARAM   GRDPNT    0
PARAM   K6ROT    5.0
PARAM   AUTOSPC  YES
LOAD     2       1.      1.      3       1.      4
SPCD     2       40769   2       -.13528
SPC1     1       123     40288
SPC1     1       123     40289
SPC1     1       2       40769
SPC1     1       2       40805
GRAV     3       0       9.81    0.      -1.     0.
PLOAD4   4       3370   -133069.
PLOAD4   4       3375   -133069.
PLOAD4   4       3380   -133069.
PLOAD4   4       3385   -133069.
PLOAD4   4       3390   -133069.
PLOAD4   4       3395   -133069.
PLOAD4   4       3400   -133069.
PLOAD4   4       3405   -133069.
PLOAD4   4       3410   -133069.
PLOAD4   4       3415   -133069.
PLOAD4   4       3420   -133069.
PLOAD4   4       3425   -133069.
PLOAD4   4       3430   -133069.
PLOAD4   4       3435   -133069.
PLOAD4   4       3440   -133069.
PLOAD4   4       3445   -133069.
PLOAD4   4       3450   -133069.
PLOAD4   4       3455   -133069.
PLOAD4   4       3460   -133069.
PLOAD4   4       3465   -133069.
PLOAD4   4       3470   -133069.
PLOAD4   4       3475   -133069.
PLOAD4   4       3480   -133069.
PLOAD4   4       3485   -133069.
PLOAD4   4       3490   -133069.
PLOAD4   4       3495   -133069.
```

PLOAD4	4	3500	-133069.		
PLOAD4	4	3505	-133069.		
PLOAD4	4	3510	-133069.		
PLOAD4	4	3515	-133069.		
PLOAD4	4	3520	-133069.		
PLOAD4	4	3525	-133069.		
PLOAD4	4	3530	-133069.		
PLOAD4	4	3535	-133069.		
PLOAD4	4	3637	-133069.	THRU	3639
PLOAD4	4	3642	-133069.	THRU	3644
PLOAD4	4	3647	-133069.	THRU	3649
PLOAD4	4	3652	-133069.	THRU	3654
PLOAD4	4	3657	-133069.	THRU	3659
PLOAD4	4	3662	-133069.	THRU	3664
PLOAD4	4	3667	-133069.	THRU	3669
PLOAD4	4	3672	-133069.	THRU	3674
PLOAD4	4	3677	-133069.	THRU	3679
PLOAD4	4	3682	-133069.	THRU	3684
PLOAD4	4	3687	-133069.	THRU	3689
PLOAD4	4	3692	-133069.	THRU	3694
PLOAD4	4	3792	-133069.	THRU	3794
PLOAD4	4	3797	-133069.	THRU	3799
PLOAD4	4	3802	-133069.	THRU	3804
PLOAD4	4	3807	-133069.	THRU	3809
PLOAD4	4	3812	-133069.	THRU	3814
PLOAD4	4	3817	-133069.	THRU	3819
PLOAD4	4	3822	-133069.	THRU	3824
PLOAD4	4	3827	-133069.	THRU	3829
PLOAD4	4	3832	-133069.	THRU	3834
PLOAD4	4	3837	-133069.	THRU	3839
PLOAD4	4	3842	-133069.	THRU	3844
PLOAD4	4	3847	-133069.	THRU	3849
PLOAD4	4	3852	-133069.	THRU	3854
PLOAD4	4	3857	-133069.	THRU	3859
PLOAD4	4	3862	-133069.	THRU	3864
PLOAD4	4	3867	-133069.	THRU	3869
PLOAD4	4	3872	-133069.	THRU	3874
PLOAD4	4	3877	-133069.	THRU	3879
PLOAD4	4	3882	-133069.	THRU	3884
PLOAD4	4	3887	-133069.	THRU	3889
PLOAD4	4	3892	-133069.	THRU	3894
PLOAD4	4	3897	-133069.	THRU	3899
PLOAD4	4	4430	133069.	THRU	4432
PLOAD4	4	4435	133069.	THRU	4437
PLOAD4	4	4440	133069.	THRU	4442
PLOAD4	4	4445	133069.	THRU	4447
PLOAD4	4	4450	133069.	THRU	4452
PLOAD4	4	4455	133069.	THRU	4457
PLOAD4	4	4460	133069.	THRU	4462
PLOAD4	4	4465	133069.	THRU	4467
PLOAD4	4	4470	133069.	THRU	4472
PLOAD4	4	4475	133069.	THRU	4477
PLOAD4	4	4480	133069.	THRU	4482
PLOAD4	4	4485	133069.	THRU	4487
PLOAD4	4	4490	133069.	THRU	4492
PLOAD4	4	4495	133069.	THRU	4497

PLOAD4	4	4500	133069.	THRU	4502
PLOAD4	4	4505	133069.	THRU	4507
PLOAD4	4	4510	133069.	THRU	4512
PLOAD4	4	4515	133069.	THRU	4517
PLOAD4	4	4520	133069.	THRU	4522
PLOAD4	4	4525	133069.	THRU	4527
PLOAD4	4	4530	133069.	THRU	4532
PLOAD4	4	4535	133069.	THRU	4537
PLOAD4	4	4544	133069.		
PLOAD4	4	4549	133069.		
PLOAD4	4	4554	133069.		
PLOAD4	4	4559	133069.		
PLOAD4	4	4564	133069.		
PLOAD4	4	4569	133069.		
PLOAD4	4	4574	133069.		
PLOAD4	4	4579	133069.		
PLOAD4	4	4584	133069.		
PLOAD4	4	4589	133069.		
PLOAD4	4	4594	133069.		
PLOAD4	4	4599	133069.		
PLOAD4	4	4699	133069.		
PLOAD4	4	4704	133069.		
PLOAD4	4	4709	133069.		
PLOAD4	4	4714	133069.		
PLOAD4	4	4719	133069.		
PLOAD4	4	4724	133069.		
PLOAD4	4	4729	133069.		
PLOAD4	4	4734	133069.		
PLOAD4	4	4739	133069.		
PLOAD4	4	4744	133069.		
PLOAD4	4	4749	133069.		
PLOAD4	4	4754	133069.		
PLOAD4	4	4759	133069.		
PLOAD4	4	4764	133069.		
PLOAD4	4	4769	133069.		
PLOAD4	4	4774	133069.		
PLOAD4	4	4779	133069.		
PLOAD4	4	4784	133069.		
PLOAD4	4	4789	133069.		
PLOAD4	4	4794	133069.		
PLOAD4	4	4799	133069.		
PLOAD4	4	4804	133069.		
PLOAD4	4	5093	133069.	THRU	5095
PLOAD4	4	5098	133069.	THRU	5100
PLOAD4	4	5103	133069.	THRU	5105
PLOAD4	4	5108	133069.	THRU	5110
PLOAD4	4	5113	133069.	THRU	5115
PLOAD4	4	5118	133069.	THRU	5120
PLOAD4	4	5123	133069.	THRU	5125
PLOAD4	4	5128	133069.	THRU	5130
PLOAD4	4	5133	133069.	THRU	5135
PLOAD4	4	5138	133069.	THRU	5140
PLOAD4	4	5143	133069.	THRU	5145
PLOAD4	4	5148	133069.	THRU	5150
PLOAD4	4	6632	-133069.		
PLOAD4	4	6757	-133069.	THRU	6759

```
PLOAD4   4        7085     133069.                                THRU    7087
PLOAD4   4        7094    -133069.
INCLUDE 'E:\CapeT\CT_STATIC\CT_STATIC_BULK.dat'
ENDDATA 1d86bebd
```

```
INIT MASTER(S)
ASSIGN OUTPUT2 = 'CT_2T_1.op2', UNIT = 12
SOL 101
TIME 600
CEND
SEALL = ALL
SUPER = ALL
ECHO = NONE
MAXLINES = 999999999
SUBCASE 1
   SUBTITLE=CT_2T_1
   SPC = 1
   LOAD = 2
   DISPLACEMENT(SORT1,REAL)=ALL
   SPCFORCES(SORT1,REAL)=ALL
   STRESS(SORT1,REAL,VONMISES,BILIN)=ALL
BEGIN BULK
PARAM     POST    -1
PARAM,NOCOMPS,-1
PARAM    PRTMAXIM YES
PARAM    GRDPNT    0
PARAM    K6ROT    5.0
PARAM    AUTOSPC  YES
LOAD     2        1.      1.      3       1.      4
SPCD     2        40769   2       -.13528
SPC1     1        123     40288
SPC1     1        123     40289
SPC1     1        2       40769
SPC1     1        2       40805
GRAV     3        0       9.81    0.      -1.     0.
PLOAD4   4        1988    133069. 133069. 133069. 133069.
PLOAD4   4        1993    133069. 133069. 133069. 133069.
PLOAD4   4        1998    133069. 133069. 133069. 133069.
PLOAD4   4        2003    133069. 133069. 133069. 133069.
PLOAD4   4        2139    133069. 133069. 133069. 133069. THRU    2141
PLOAD4   4        2144    133069. 133069. 133069. 133069. THRU    2146
PLOAD4   4        2149    133069. 133069. 133069. 133069. THRU    2151
PLOAD4   4        2154    133069. 133069. 133069. 133069. THRU    2156
PLOAD4   4        3370   -133069.-133069.-133069.-133069.
PLOAD4   4        3375   -133069.-133069.-133069.-133069.
PLOAD4   4        3380   -133069.-133069.-133069.-133069.
PLOAD4   4        3385   -133069.-133069.-133069.-133069.
PLOAD4   4        3390   -133069.-133069.-133069.-133069.
PLOAD4   4        3395   -133069.-133069.-133069.-133069.
PLOAD4   4        3400   -133069.-133069.-133069.-133069.
PLOAD4   4        3405   -133069.-133069.-133069.-133069.
PLOAD4   4        3410   -133069.-133069.-133069.-133069.
PLOAD4   4        3415   -133069.-133069.-133069.-133069.
PLOAD4   4        3792   -133069.-133069.-133069.-133069. THRU    3794
PLOAD4   4        3797   -133069.-133069.-133069.-133069. THRU    3799
PLOAD4   4        3802   -133069.-133069.-133069.-133069. THRU    3804
PLOAD4   4        3807   -133069.-133069.-133069.-133069. THRU    3809
PLOAD4   4        3812   -133069.-133069.-133069.-133069. THRU    3814
PLOAD4   4        3817   -133069.-133069.-133069.-133069. THRU    3819
PLOAD4   4        3822   -133069.-133069.-133069.-133069. THRU    3824
PLOAD4   4        3827   -133069.-133069.-133069.-133069. THRU    3829
```

PLOAD4	4	3832	-133069.	-133069.	-133069.	-133069.	THRU	3834
PLOAD4	4	3837	-133069.	-133069.	-133069.	-133069.	THRU	3839
PLOAD4	4	4430	133069.	133069.	133069.	133069.	THRU	4432
PLOAD4	4	4435	133069.	133069.	133069.	133069.	THRU	4437
PLOAD4	4	4440	133069.	133069.	133069.	133069.	THRU	4442
PLOAD4	4	4445	133069.	133069.	133069.	133069.	THRU	4447
PLOAD4	4	4450	133069.	133069.	133069.	133069.	THRU	4452
PLOAD4	4	4455	133069.	133069.	133069.	133069.	THRU	4457
PLOAD4	4	4460	133069.	133069.	133069.	133069.	THRU	4462
PLOAD4	4	4465	133069.	133069.	133069.	133069.	THRU	4467
PLOAD4	4	4470	133069.	133069.	133069.	133069.	THRU	4472
PLOAD4	4	4475	133069.	133069.	133069.	133069.	THRU	4477
PLOAD4	4	4544	133069.	133069.	133069.	133069.		
PLOAD4	4	4549	133069.	133069.	133069.	133069.		
PLOAD4	4	4554	133069.	133069.	133069.	133069.		
PLOAD4	4	4559	133069.	133069.	133069.	133069.		
PLOAD4	4	4564	133069.	133069.	133069.	133069.		
PLOAD4	4	4569	133069.	133069.	133069.	133069.		
PLOAD4	4	4574	133069.	133069.	133069.	133069.		
PLOAD4	4	4579	133069.	133069.	133069.	133069.		
PLOAD4	4	4584	133069.	133069.	133069.	133069.		
PLOAD4	4	4589	133069.	133069.	133069.	133069.		
PLOAD4	4	4594	133069.	133069.	133069.	133069.		
PLOAD4	4	4599	133069.	133069.	133069.	133069.		
PLOAD4	4	4604	133069.	133069.	133069.	133069.		
PLOAD4	4	4609	133069.	133069.	133069.	133069.		
PLOAD4	4	4614	133069.	133069.	133069.	133069.		
PLOAD4	4	4619	133069.	133069.	133069.	133069.		
PLOAD4	4	4624	133069.	133069.	133069.	133069.		
PLOAD4	4	4629	133069.	133069.	133069.	133069.		
PLOAD4	4	4634	133069.	133069.	133069.	133069.		
PLOAD4	4	4639	133069.	133069.	133069.	133069.		
PLOAD4	4	4644	133069.	133069.	133069.	133069.		
PLOAD4	4	4649	133069.	133069.	133069.	133069.		
PLOAD4	4	4654	133069.	133069.	133069.	133069.		
PLOAD4	4	4659	133069.	133069.	133069.	133069.		
PLOAD4	4	4664	133069.	133069.	133069.	133069.		
PLOAD4	4	4669	133069.	133069.	133069.	133069.		
PLOAD4	4	4674	133069.	133069.	133069.	133069.		
PLOAD4	4	4679	133069.	133069.	133069.	133069.		
PLOAD4	4	4684	133069.	133069.	133069.	133069.		
PLOAD4	4	4689	133069.	133069.	133069.	133069.		
PLOAD4	4	4694	133069.	133069.	133069.	133069.		
PLOAD4	4	4699	133069.	133069.	133069.	133069.		
PLOAD4	4	4704	133069.	133069.	133069.	133069.		
PLOAD4	4	4709	133069.	133069.	133069.	133069.		
PLOAD4	4	4714	133069.	133069.	133069.	133069.		
PLOAD4	4	4719	133069.	133069.	133069.	133069.		
PLOAD4	4	4724	133069.	133069.	133069.	133069.		
PLOAD4	4	4729	133069.	133069.	133069.	133069.		
PLOAD4	4	4734	133069.	133069.	133069.	133069.		
PLOAD4	4	4739	133069.	133069.	133069.	133069.		
PLOAD4	4	4744	133069.	133069.	133069.	133069.		
PLOAD4	4	5093	133069.	133069.	133069.	133069.	THRU	5095
PLOAD4	4	5098	133069.	133069.	133069.	133069.	THRU	5100
PLOAD4	4	5103	133069.	133069.	133069.	133069.	THRU	5105

PLOAD4	4	5108	133069.	133069.	133069.	133069.	THRU	5110
PLOAD4	4	5113	133069.	133069.	133069.	133069.	THRU	5115
PLOAD4	4	5118	133069.	133069.	133069.	133069.	THRU	5120
PLOAD4	4	5123	133069.	133069.	133069.	133069.	THRU	5125
PLOAD4	4	5128	133069.	133069.	133069.	133069.	THRU	5130
PLOAD4	4	5133	133069.	133069.	133069.	133069.	THRU	5135
PLOAD4	4	5138	133069.	133069.	133069.	133069.	THRU	5140
PLOAD4	4	5143	133069.	133069.	133069.	133069.	THRU	5145
PLOAD4	4	5148	133069.	133069.	133069.	133069.	THRU	5150
PLOAD4	4	5153	133069.	133069.	133069.	133069.	THRU	5155
PLOAD4	4	5158	133069.	133069.	133069.	133069.	THRU	5160
PLOAD4	4	5163	133069.	133069.	133069.	133069.	THRU	5165
PLOAD4	4	5168	133069.	133069.	133069.	133069.	THRU	5170
PLOAD4	4	5173	133069.	133069.	133069.	133069.	THRU	5175
PLOAD4	4	5178	133069.	133069.	133069.	133069.	THRU	5180
PLOAD4	4	5183	133069.	133069.	133069.	133069.	THRU	5185
PLOAD4	4	5188	133069.	133069.	133069.	133069.	THRU	5190
PLOAD4	4	5193	133069.	133069.	133069.	133069.	THRU	5195
PLOAD4	4	5198	133069.	133069.	133069.	133069.	THRU	5200
PLOAD4	4	5203	133069.	133069.	133069.	133069.	THRU	5205
PLOAD4	4	5208	133069.	133069.	133069.	133069.	THRU	5210
PLOAD4	4	5213	133069.	133069.	133069.	133069.	THRU	5215
PLOAD4	4	5218	133069.	133069.	133069.	133069.	THRU	5220
PLOAD4	4	5223	133069.	133069.	133069.	133069.	THRU	5225
PLOAD4	4	5228	133069.	133069.	133069.	133069.	THRU	5230
PLOAD4	4	5233	133069.	133069.	133069.	133069.	THRU	5235
PLOAD4	4	5238	133069.	133069.	133069.	133069.	THRU	5240
PLOAD4	4	5243	133069.	133069.	133069.	133069.	THRU	5245
PLOAD4	4	6632	-133069.	-133069.	-133069.	-133069.		
PLOAD4	4	6633	133069.	133069.	133069.	133069.	THRU	6637
PLOAD4	4	6692	133069.	133069.	133069.	133069.	THRU	6694
PLOAD4	4	6697	133069.	133069.	133069.	133069.	THRU	6699
PLOAD4	4	6702	133069.	133069.	133069.	133069.	THRU	6704
PLOAD4	4	6707	133069.	133069.	133069.	133069.	THRU	6709
PLOAD4	4	6712	133069.	133069.	133069.	133069.	THRU	6714
PLOAD4	4	6717	133069.	133069.	133069.	133069.	THRU	6719
PLOAD4	4	6722	133069.	133069.	133069.	133069.	THRU	6724
PLOAD4	4	6727	133069.	133069.	133069.	133069.	THRU	6729
PLOAD4	4	6732	133069.	133069.	133069.	133069.	THRU	6734
PLOAD4	4	6737	133069.	133069.	133069.	133069.	THRU	6739
PLOAD4	4	6742	133069.	133069.	133069.	133069.	THRU	6744
PLOAD4	4	6747	133069.	133069.	133069.	133069.	THRU	6749
PLOAD4	4	6752	133069.	133069.	133069.	133069.	THRU	6754
PLOAD4	4	6757	-133069.	-133069.	-133069.	-133069.	THRU	6759
PLOAD4	4	7009	133069.	133069.	133069.	133069.	THRU	7011
PLOAD4	4	7030	133069.	133069.	133069.	133069.	THRU	7032
PLOAD4	4	7035	133069.	133069.	133069.	133069.	THRU	7037
PLOAD4	4	7040	133069.	133069.	133069.	133069.	THRU	7042
PLOAD4	4	7045	133069.	133069.	133069.	133069.	THRU	7047
PLOAD4	4	7050	133069.	133069.	133069.	133069.	THRU	7052
PLOAD4	4	7055	133069.	133069.	133069.	133069.	THRU	7057
PLOAD4	4	7060	133069.	133069.	133069.	133069.	THRU	7062
PLOAD4	4	7065	133069.	133069.	133069.	133069.	THRU	7067
PLOAD4	4	7070	133069.	133069.	133069.	133069.	THRU	7072
PLOAD4	4	7075	133069.	133069.	133069.	133069.	THRU	7077
PLOAD4	4	7080	133069.	133069.	133069.	133069.	THRU	7082

PLOAD4	4	7085	133069.	133069.	133069.	133069.	THRU	7087
PLOAD4	4	7094	-133069.	-133069.	-133069.	-133069.		
PLOAD4	4	7107	-133069.	-133069.	-133069.	-133069.	THRU	7109
PLOAD4	4	32507	-133069.	-133069.	-133069.	-133069.	THRU	32516
PLOAD4	4	32536	-133069.	-133069.	-133069.	-133069.	THRU	32545
PLOAD4	4	32565	-133069.	-133069.	-133069.	-133069.	THRU	32574
PLOAD4	4	32594	-133069.	-133069.	-133069.	-133069.	THRU	32603
PLOAD4	4	33029	-133069.	-133069.	-133069.	-133069.	THRU	33038
PLOAD4	4	33058	-133069.	-133069.	-133069.	-133069.	THRU	33067
PLOAD4	4	33087	-133069.	-133069.	-133069.	-133069.	THRU	33096
PLOAD4	4	33116	-133069.	-133069.	-133069.	-133069.	THRU	33125
PLOAD4	4	34884	-133069.	-133069.	-133069.	-133069.	THRU	34895
PLOAD4	4	34938	-133069.	-133069.	-133069.	-133069.	THRU	34949
PLOAD4	4	45450	-133069.	-133069.	-133069.	-133069.		
PLOAD4	4	45457	-133069.	-133069.	-133069.	-133069.	THRU	45459
PLOAD4	4	45470	-133069.	-133069.	-133069.	-133069.	THRU	45472
PLOAD4	4	45479	-133069.	-133069.	-133069.	-133069.		
PLOAD4	4	2606	133069.	133069.	133069.	133069.	THRU	2608
PLOAD4	4	2611	133069.	133069.	133069.	133069.	THRU	2613
PLOAD4	4	2616	133069.	133069.	133069.	133069.	THRU	2618
PLOAD4	4	2621	133069.	133069.	133069.	133069.	THRU	2623
PLOAD4	4	2759	133069.	133069.	133069.	133069.		
PLOAD4	4	2764	133069.	133069.	133069.	133069.		
PLOAD4	4	2769	133069.	133069.	133069.	133069.		
PLOAD4	4	2774	133069.	133069.	133069.	133069.		
PLOAD4	4	3480	-133069.	-133069.	-133069.	-133069.		
PLOAD4	4	3485	-133069.	-133069.	-133069.	-133069.		
PLOAD4	4	3490	-133069.	-133069.	-133069.	-133069.		
PLOAD4	4	3495	-133069.	-133069.	-133069.	-133069.		
PLOAD4	4	3500	-133069.	-133069.	-133069.	-133069.		
PLOAD4	4	3505	-133069.	-133069.	-133069.	-133069.		
PLOAD4	4	3510	-133069.	-133069.	-133069.	-133069.		
PLOAD4	4	3515	-133069.	-133069.	-133069.	-133069.		
PLOAD4	4	3520	-133069.	-133069.	-133069.	-133069.		
PLOAD4	4	3525	-133069.	-133069.	-133069.	-133069.		
PLOAD4	4	3530	-133069.	-133069.	-133069.	-133069.		
PLOAD4	4	3535	-133069.	-133069.	-133069.	-133069.		
PLOAD4	4	3540	133069.	133069.	133069.	133069.		
PLOAD4	4	3545	133069.	133069.	133069.	133069.		
PLOAD4	4	3550	133069.	133069.	133069.	133069.		
PLOAD4	4	3555	133069.	133069.	133069.	133069.		
PLOAD4	4	3560	133069.	133069.	133069.	133069.		
PLOAD4	4	3565	133069.	133069.	133069.	133069.		
PLOAD4	4	3570	133069.	133069.	133069.	133069.		
PLOAD4	4	3575	133069.	133069.	133069.	133069.		
PLOAD4	4	3580	133069.	133069.	133069.	133069.		
PLOAD4	4	3585	133069.	133069.	133069.	133069.		
PLOAD4	4	3590	133069.	133069.	133069.	133069.		
PLOAD4	4	3595	133069.	133069.	133069.	133069.		
PLOAD4	4	3600	133069.	133069.	133069.	133069.		
PLOAD4	4	3605	133069.	133069.	133069.	133069.		
PLOAD4	4	3610	133069.	133069.	133069.	133069.		
PLOAD4	4	3615	133069.	133069.	133069.	133069.		
PLOAD4	4	3620	133069.	133069.	133069.	133069.		
PLOAD4	4	3625	133069.	133069.	133069.	133069.		
PLOAD4	4	3630	133069.	133069.	133069.	133069.		

```
PLOAD4   4        3637    -133069.-133069.-133069.-133069. THRU     3639
PLOAD4   4        3642    -133069.-133069.-133069.-133069. THRU     3644
PLOAD4   4        3647    -133069.-133069.-133069.-133069. THRU     3649
PLOAD4   4        3652    -133069.-133069.-133069.-133069. THRU     3654
PLOAD4   4        3657    -133069.-133069.-133069.-133069. THRU     3659
PLOAD4   4        3662    -133069.-133069.-133069.-133069. THRU     3664
PLOAD4   4        3667    -133069.-133069.-133069.-133069. THRU     3669
PLOAD4   4        3672    -133069.-133069.-133069.-133069. THRU     3674
PLOAD4   4        3677    -133069.-133069.-133069.-133069. THRU     3679
PLOAD4   4        3682    -133069.-133069.-133069.-133069. THRU     3684
PLOAD4   4        3687    -133069.-133069.-133069.-133069. THRU     3689
PLOAD4   4        3692    -133069.-133069.-133069.-133069. THRU     3694
PLOAD4   4        3697     133069. 133069. 133069. 133069. THRU     3699
PLOAD4   4        3702     133069. 133069. 133069. 133069. THRU     3704
PLOAD4   4        3707     133069. 133069. 133069. 133069. THRU     3709
PLOAD4   4        3712     133069. 133069. 133069. 133069. THRU     3714
PLOAD4   4        3717     133069. 133069. 133069. 133069. THRU     3719
PLOAD4   4        3722     133069. 133069. 133069. 133069. THRU     3724
PLOAD4   4        3727     133069. 133069. 133069. 133069. THRU     3729
PLOAD4   4        3732     133069. 133069. 133069. 133069. THRU     3734
PLOAD4   4        3737     133069. 133069. 133069. 133069. THRU     3739
PLOAD4   4        3742     133069. 133069. 133069. 133069. THRU     3744
PLOAD4   4        3747     133069. 133069. 133069. 133069. THRU     3749
PLOAD4   4        3752     133069. 133069. 133069. 133069. THRU     3754
PLOAD4   4        3757     133069. 133069. 133069. 133069. THRU     3759
PLOAD4   4        3762     133069. 133069. 133069. 133069. THRU     3764
PLOAD4   4        3767     133069. 133069. 133069. 133069. THRU     3769
PLOAD4   4        3772     133069. 133069. 133069. 133069. THRU     3774
PLOAD4   4        3777     133069. 133069. 133069. 133069. THRU     3779
PLOAD4   4        3782     133069. 133069. 133069. 133069. THRU     3784
PLOAD4   4        3787     133069. 133069. 133069. 133069. THRU     3789
INCLUDE 'E:\CapeT\CT_STATIC\CT_STATIC_BULK.dat'
ENDDATA 1d86bebd
```

```
INIT MASTER(S)
ASSIGN OUTPUT2 = 'CH_0T_1_new.op2', UNIT = 12
SOL 101
TIME 600
CEND
SEALL = ALL
SUPER = ALL
TITLE = MSC.Nastran job created on 09-May-01 at 14:36:17
ECHO = NONE
MAXLINES = 999999999
SUBCASE 1
   SUBTITLE=GRAV_0T_1
   SPC = 1
   LOAD = 2
   DISPLACEMENT(SORT1,REAL)=ALL
   SPCFORCES(SORT1,REAL)=ALL
   STRESS(SORT1,REAL,VONMISES,BILIN)=ALL
BEGIN BULK
PARAM    POST    -1
PARAM,NOCOMPS,-1
PARAM   PRTMAXIM YES
PARAM   AUTOSPC  YES
PARAM   GRDPNT  0
PARAM   K6ROT   5.0
SPCD    2       16942   3       -236.73
SPC1    1       123     13757
SPC1    1       3       16942
SPC1    1       3       19491
SPC1    1       123     19494
SPC1    1       123     19503
SPC1    1       123     19513
SPC1    1       123     19519
SPC1    1       123     19531
SPC1    1       123     19540
SPC1    1       123     20463
GRAV    2       0       9807.   0.      0.      -1.
PELAS   19      1.7+10
CELAS1  20953   19      15487   3       15693   3
CELAS1  20954   19      15488   3       15692   3
CELAS1  20955   19      19552   3       15694   3
CELAS1  20956   19      14619   3       14695   3
CELAS1  20957   19      14623   3       14700   3
CELAS1  20958   19      14622   3       14699   3
CELAS1  20959   19      14621   3       14698   3
CELAS1  20964   19      15631   3       204     3
CELAS1  20965   19      14657   3       16982   3
CELAS1  22003   19      20215   3       20144   3
CELAS1  22004   19      20218   3       20147   3
CELAS1  22175   19      20263   3       20357   3
CELAS1  22176   19      20286   3       20328   3
INCLUDE 'E:\CapeH\CH_BULK_DATA\CH_NEW_BULK.DAT'
ENDDATA 18e5ef82
```

```
INIT MASTER(S)
ASSIGN OUTPUT2 = 'CH_1T_1_new.op2', UNIT = 12
SOL 101
TIME 600
CEND
SEALL = ALL
SUPER = ALL
TITLE = MSC.Nastran job created on 09-May-01 at 14:36:17
ECHO = NONE
MAXLINES = 999999999
SUBCASE 1
   SUBTITLE=GRAV_1T_1
   SPC = 1
   LOAD = 2
   DISPLACEMENT(SORT1,REAL)=ALL
   SPCFORCES(SORT1,REAL)=ALL
   STRESS(SORT1,REAL,VONMISES,BILIN)=ALL
BEGIN BULK
PARAM    POST    -1
PARAM,NOCOMPS,-1
PARAM   PRTMAXIM YES
PARAM   AUTOSPC  YES
PARAM   GRDPNT   0
PARAM   K6ROT    5.0
LOAD     2       1.      1.      3       1.      4
SPCD     2       16942   3       -236.73
SPC1     1       123     13757
SPC1     1       3       16942
SPC1     1       3       19491
SPC1     1       123     19494
SPC1     1       123     19503
SPC1     1       123     19513
SPC1     1       123     19519
SPC1     1       123     19531
SPC1     1       123     19540
SPC1     1       123     20463
GRAV     3       0       9807.   0.      0.      -1.
PLOAD4   4       11962   137.    137.    137.    137.    THRU    11973
PLOAD4   4       12028   137.    137.    137.    137.    THRU    12033
PLOAD4   4       12665   137.    137.    137.    137.    THRU    12670
PLOAD4   4       12689   137.    137.    137.    137.    THRU    12694
PLOAD4   4       12759   137.    137.    137.    137.    THRU    12764
PELAS    19      1.7+10
CELAS1   20953   19      15487   3       15693   3
CELAS1   20954   19      15488   3       15692   3
CELAS1   20955   19      19552   3       15694   3
CELAS1   20956   19      14619   3       14695   3
CELAS1   20957   19      14623   3       14700   3
CELAS1   20958   19      14622   3       14699   3
CELAS1   20959   19      14621   3       14698   3
CELAS1   20964   19      15631   3       204     3
CELAS1   20965   19      14657   3       16982   3
CELAS1   22003   19      20215   3       20144   3
CELAS1   22004   19      20218   3       20147   3
CELAS1   22175   19      20263   3       20357   3
CELAS1   22176   19      20286   3       20328   3
```

```
INCLUDE 'E:\CapeH\CH_BULK_DATA\CH_NEW_BULK.DAT'
ENDDATA 18e5ef82
```

```
INIT MASTER(S)
ASSIGN OUTPUT2 = 'CH_2T_1_new.op2', UNIT = 12
SOL 101
TIME 600
CEND
SEALL = ALL
SUPER = ALL
TITLE = MSC.Nastran job created on 09-May-01 at 14:36:17
ECHO = NONE
MAXLINES = 999999999
SUBCASE 1
   SUBTITLE=GRAV_2T_1
   SPC = 1
   LOAD = 2
   DISPLACEMENT(SORT1,REAL)=ALL
   SPCFORCES(SORT1,REAL)=ALL
   STRESS(SORT1,REAL,VONMISES,BILIN)=ALL
BEGIN BULK
PARAM    POST    -1
PARAM,NOCOMPS,-1
PARAM   PRTMAXIM YES
PARAM   AUTOSPC  YES
PARAM   GRDPNT   0
PARAM   K6ROT    5.0
LOAD     2       1.      1.      3       1.      4
SPCD     2       16942   3       -236.73
SPC1     1       123     13757
SPC1     1       3       16942
SPC1     1       3       19491
SPC1     1       123     19494
SPC1     1       123     19503
SPC1     1       123     19513
SPC1     1       123     19519
SPC1     1       123     19531
SPC1     1       123     19540
SPC1     1       123     20463
GRAV     3       0       9807.   0.      0.      -1.
PLOAD4   4       2530    137.                                    THRU    2536
PLOAD4   4       11766   137.                                    THRU    11775
PLOAD4   4       11962   137.                                    THRU    11967
PLOAD4   4       12028   137.                                    THRU    12039
PLOAD4   4       12076   137.                                    THRU    12081
PLOAD4   4       12527   137.                                    THRU    12536
PLOAD4   4       12665   137.                                    THRU    12670
PLOAD4   4       12759   137.                                    THRU    12764
PLOAD4   4       12859   137.                                    THRU    12864
PLOAD4   4       12943   137.                                    THRU    12948
PLOAD4   4       20811   137.                                    THRU    20818
PELAS    19      1.7+10
CELAS1   20953   19      15487   3       15693   3
CELAS1   20954   19      15488   3       15692   3
CELAS1   20955   19      19552   3       15694   3
CELAS1   20956   19      14619   3       14695   3
CELAS1   20957   19      14623   3       14700   3
CELAS1   20958   19      14622   3       14699   3
CELAS1   20959   19      14621   3       14698   3
```

```
CELAS1   20964   19        15631   3        204        3
CELAS1   20965   19        14657   3        16982      3
CELAS1   22003   19        20215   3        20144      3
CELAS1   22004   19        20218   3        20147      3
CELAS1   22175   19        20263   3        20357      3
CELAS1   22176   19        20286   3        20328      3
INCLUDE 'E:\CapeH\CH_BULK_DATA\CH_NEW_BULK.DAT'
ENDDATA 18e5ef82
```

LIST OF REFERENCES

1. R. Craig, "Structural Dynamics An Introduction To Computer Methods", John Wiley & Sons, Inc., New York (1981)

2. John P Caffrey and John M. Lee, "MSC/NASTRAN Linear Static Analysis", The MacNeal-Schwendler Corporation, Los Angeles (1994)

3. MSC/NASTRAN, "NASTRAN Theoretical Manual", The MacNeal-Schwendler Corporation, Los Angeles (1972)

4. M. I. Frishwell and J. E. Mottershead, "Finite Element Model Updating in Structural Dynamics", Kluwer Academic Publishers, Dordrecht, The Netherlands (1996)

5. Roger G. Grimes, John G. Lewis, and Horst D. Simon, "A Shifted Block Lanczos Algorithm For Solving Sparse Symmetric Generalized Eigenproblems", *SIAM J. Matrix Anal. Appl.,* Vol. 15, No. 1, pp. 000-000, January 1994

6. D. J. Ewins, "Modal Testing Theory and Practice", John Wiley & Sons, Inc., New York (1992)

THIS PAGE INTENTIONALLY LEFT BLANK

INITIAL DISTRIBUTION LIST

No. Copies

1. Defense Technical Information Center 2
   8725 John J. Kingman Road, Ste 0944
   Ft. Belvoir, VA 22060-6218

2. Dudley Knox Library 2
   Naval Postgraduate School
   411 Dyer Road
   Monterey, CA 93943-5101

3. Professor Joshua H. Gordis, Code ME/GO 1
   Department of Mechanical Engineering
   Naval Postgraduate School
   Monterey, CA 93943

4. Engineering and Technology Curricular Office (Code 34) 1
   Naval Postgraduate School
   Monterey, CA 93943

5. Department of Mechanical Engineering 1
   Naval Postgraduate School
   Monterey, CA 93943

6. Professor Fotis A. Papoulias, Code ME/PA 1
   Department of Mechanical Engineering
   Naval Postgraduate School
   Monterey, CA 93943

7. LT James E. Buckley 2
   2340 Springbrook Road
   Medford, OR 97504

8. Jason Chang 1
   Code 282
   Naval Surface Warfare Center-Carderock Division
   9500 MacArthur Blvd
   Building 17W Room 223
   West Bethesda, MD 20817-5700

9. Mr. Frank Leban 1
Code 2820
Naval Surface Warfare Center-Carderock Division
9500 MacArthur Blvd
Building 17W Room 223
West Bethesda, MD 20817-5700

10. John J McMullen Associates, Inc. 1
Edgewood Towne Center Office, Suite 400
1789 South Braddock Ave.
Pittsburgh PA 15218
Attn: Mr. John Chen